

**R-08-88**

# **Site engineering report Laxemar**

## **Guidelines for underground design Step D2**

Svensk Kärnbränslehantering AB

September 2009

**Svensk Kärnbränslehantering AB**

Swedish Nuclear Fuel  
and Waste Management Co

Box 250, SE-101 24 Stockholm  
Phone +46 8 459 84 00



ISSN 1402-3091

SKB R-08-88

# **Site engineering report Laxemar**

## **Guidelines for underground design Step D2**

Svensk Kärnbränslehantering AB

September 2009

# Summary

The design and construction of an underground nuclear waste repository (final repository facility) must consider the site conditions that may impact the long-term safety of a repository. Many of the constraints that are needed to ensure the safe performance of a final repository facility with respect to radionuclide containment are unique for the repository. The main purpose of this Site Engineering Report is to provide an overall framework for the designers responsible for the underground design and layout that meets both the operational requirements for such an underground facility and the long-term safety requirements related to nuclear-waste containment. The foundation for the development of this framework is the site descriptive model.

The Site Engineering Report builds on the extensive surface based site investigations carried out at the Laxemar site and the interpretation and evaluation of the data that are given in the site descriptive model. However, because the site descriptive model serves the needs of many users, and especially those of safety assessment, not all the information contained in site descriptive model is needed for engineering design and layout purposes. The information obtained from the site investigation phase and contained in site descriptive model for Laxemar must be in sufficient detail to enable SKB to: (1) develop a functional design and layout for the facility, (2) conduct a safety assessment for the site and identify the possible environmental impact of the final repository and its extent, and (3) develop an excavation strategy.

For the purpose of this report the final repository facility is divided into three functional areas that are referred to as: (1) repository access, including the access ramp and shafts, (2) Central Area, and (3) deposition areas, including the deposition tunnels and deposition holes. Each of these areas has different design constraints and requirements. For design Step D2, the geological constraints and engineering guidelines provided in this Site Engineering Report cover the site adaptation of the final repository facility with respect to: (1) deformation zones and rock mass conditions at depth, (2) parameters that affect the depth and areal size of the repository, and (3) description of ground conditions for assessment of constructability. The design process for the final repository facility must be in agreement with the European standard for construction, Eurocode, and in particular the standard for geotechnical design, EN 1997-1:2004, Section 2.7, which will be implemented in Sweden in 2009. This allows for the application of the Observational Method in underground design and construction. The Observational Method is a risk-based approach to underground design and construction.

The inherent complexity and variability in the geological setting prohibits a complete picture of the ground structure and quality to be obtained before the facility is excavated. Thus during design, statistical methods will be required to evaluate the sensitivity of the design to this variability and for quantifying project risks.

There are several general engineering guidelines that should be considered in laying out the repository:

1. The Elevation of the repository should be at or below 500 m.
2. The deposition holes should be located in sparsely fractured or massive rock.
3. The Central Area can be located in any rock mass suitable for constructing large caverns.
4. The access tunnels and shafts should be located to minimise the potential for large groundwater inflows.
5. Layouts for tunnel and shaft access should be oriented such that the intersection lengths with major water bearing zones are as short as practical.
6. A respect distance of 100 m is required for major deformation zones with a trace length at ground surface greater than 3 km.
7. The repository layout should minimise stress concentrations on the boundary of the underground excavations (deposition holes and deposition tunnels), unless it can be shown that such stress concentrations do not cause spalling.

In addition to the general guidelines given above there are several issues which need special consideration when designing the repository layout. These are highlighted below.

- The most significant challenge for the Laxemar site is finding a suitable volume of rock for the repository. Because of the number of deformation zones and their associated respect distance the footprint area available for the deposition tunnels is limited. Moreover the lithology is expected to be heterogeneous.
- The heterogeneity of a rock panel between deformation zones that is identified as suitable for deposition holes is expected to be significant. The lithological variability implies significantly varying mechanical and thermal properties, and probably also hydraulic properties. As a result, the loss of deposition positions due to this heterogeneity may be significant.
- Experience from the construction of the Äspö HRL clearly showed that NW-SE fractures were the dominant conductive fractures with inflows at 450 m depth of several 10 s of litres per minute. Should the same fracture set occur at Laxemar at depth, the deposition tunnels should be oriented to minimise the impact of these conductive fractures, i.e. the tunnels should be oriented approximately perpendicular to these fractures: However in order to avoid spalling deposition tunnels should be aligned to maximum horizontal stress, which means almost parallel to these highly conductive fractures.
- Given the spatial variability of the conductive fractures and number of deformation zones the designer should consider that grouting of the access tunnels and shafts will be required on a routine basis. Grouting of the deposition tunnels is not expected to be routinely required unless the conductive NW-SE steeply dipping fractures are encountered.
- The intersection of the deposition tunnels with the access tunnels will require special design attention, particularly the transition from the access tunnel to the deposition tunnel. Experience from Äspö HRL and elsewhere suggests that this portion of the intersection will need support, regardless of rock mass quality and ground type.

# Contents

<b>1</b>	<b>Purpose and scope</b>	7
1.1	Background	7
1.2	Objectives	8
1.3	Long-term safety and Design	9
1.4	Design strategy and Observational Method	10
1.5	Design methodology	11
1.6	Terminology	13
1.7	Report structure	14
<b>2</b>	<b>General site conditions and rock properties</b>	15
2.1	Rock type and intact rock properties	16
2.1.1	Rock Type	16
2.1.2	Bedrock temperature and thermal properties	16
2.1.3	Strength and deformability properties	20
2.1.4	Rock mass deformation properties	20
2.2	Deformation zones	22
2.2.1	Description	22
2.2.2	Mechanical properties of deformation zones	24
2.3	Fractures and fracture domains	25
2.3.1	Mechanical properties of fractures	26
2.3.2	Strength and deformation properties of fractured rock	28
2.4	In-Situ Stress	29
2.5	Hydraulic properties	30
2.5.1	Deterministically modelled deformation zones – HCDs	30
2.5.2	Minor deformation zones (MDZ)	31
2.5.3	Hydraulic Rock mass Domains	33
2.6	Groundwater composition	37
2.7	Summary	37
<b>3</b>	<b>Overview of tunnelling experiences from the Oskarshamn area</b>	39
3.1	Steeply dipping highly conductive fractures	39
3.2	Distribution of water-bearing structures	41
3.3	Stress conditions	41
3.4	Summary	43
<b>4</b>	<b>Ground types and behaviour, rock support and grouting</b>	45
4.1	Variability and uncertainty in key parameters	45
4.2	Ground types	45
4.3	Ground behaviour	51
4.4	Support types	51
4.5	Grouting	52
4.6	Monitoring and documenting the performance of underground excavations	52
<b>5</b>	<b>Repository access</b>	55
5.1	Location	55
5.2	General rock mass conditions	57
5.3	Passages of water-bearing fractures	57
5.3.1	Shafts	57
5.3.2	Access ramp	58
5.4	Summary	58
<b>6</b>	<b>Central Area</b>	59
6.1	Constraints	59
6.2	General rock mass conditions	59
6.3	Summary	59

<b>7</b>	<b>Deposition areas</b>	61
7.1	General rock mass conditions	61
7.2	Deformation zones and respect distances	62
7.3	Deposition tunnel and deposition hole spacing	63
7.4	Spalling in tunnels and deposition holes	63
7.5	Deposition tunnel alignment	63
7.6	Loss of deposition-hole positions	64
7.7	Summary	64
<b>8</b>	<b>Repository depth</b>	65
8.1	In-situ temperature	65
8.2	Fracture frequency	67
8.3	Hydrogeological considerations	67
8.4	Spalling considerations	67
8.5	Available space – site adaptation	67
8.6	Construction costs and environmental impact	68
8.7	Other considerations	68
8.8	Recommended repository depth	68
<b>9</b>	<b>Summary of Layout/design issues for D2</b>	69
<b>10</b>	<b>References</b>	71
<b>Appendix A</b>	Thermal dimensioning of the Canister spacing	73
<b>Appendix B</b>	Properties of deformation zones modelled to intersect the local model volume at –400 to –600 m masl	83

# 1 Purpose and scope

The design and construction of a nuclear waste repository at depths of 400 to 700 m may appear similar to the development of an underground mine. However, unlike an underground mine, which typically lasts from 10 to 100 years for the purpose of mineral extraction, the design of a nuclear waste facility must consider the site conditions that may impact the long-term safety of a repository. Many of the constraints that are needed to ensure the safe performance of a repository with respect to radionuclide containment are unique for the Final Repository. The design of such an underground facility cannot be simply based on traditional empirical rules that have been developed from previous underground projects.

The main purpose of this Site Engineering Report (SER) is to provide an overall framework for the designers responsible for the underground design and layout that meets both the operational requirements for such an underground facility and the long-term safety requirements related to nuclear-waste containment. This is done by presenting a rationale and guidelines for the design that are focused on constructing a repository. These guidelines also incorporate the operational and safety assessment issues that may impact construction and facility layout.

## 1.1 Background

The overall purpose of the Final Repository is to isolate the spent fuel so that unacceptable quantities of radionuclide do not migrate to the biosphere. The design of the Final Repository must address a number of considerations related to the project objective not faced in traditional mining or civil engineering underground projects. This involves the characterisation of a large volume of rock, assessment of thermal effects, the construction of underground openings that meet strict quality control requirements, and the need to consider an extremely long design life. The major tasks for the underground design for the Final Repository are described in the UDP/D2 /SKB 2007/ and are summarised below:

- Outline a design for the site, considering site adaptation, functional requirements and step-wise development in parallel to operation of the Final Repository.
- Examine the feasibility for grouting, and estimate the required grout quantities.
- Establish the rock support required and estimate the support quantities.
- Perform a technical risk analysis of the potential hazard(s) for the project that are considered in the design process, and propose measures to reduce the risk from these hazards within the next design step.

A Site Descriptive Model (SDM) in the context of the Final Repository refers to the integration and interpretation of multidisciplinary data to develop a geoscientific description of a site /Munier et al. 2003/. The early stages of the Site Descriptive Model for the Laxemar site has been provided by /SKB 2005/ and updated in /SKB 2006b/. These reports provide the detailed geoscientific description of the site based on the Initial Site Investigation (ISI) phase of the Final Repository. Based on the results of these previous investigations a programme for the Complete Site Investigations (CSI) was proposed /SKB 2006c/ and the CSI phase is reported in /SKB 2009/. Running in parallel with the Site Investigation Phase is the design and layout of the repository. The preliminary layouts were given in D1 /Janson et al. 2006/. As demonstrated during design Step D1, there was a need to extract the data contained in the site descriptive model into parameters that are required for the design and layout. This Site Engineering Report (SER) is focused on this task.

The information obtained from the Complete Site Investigation Phase and contained in the Site Descriptive Model (SDM) must be in sufficient detail to enable SKB to:

1. Develop a functional design and layout for the facility
2. Conduct a safety assessment for the site, and
3. Identify the possible environmental impact of the final repository and its extent
4. Develop an excavation strategy.

For the purpose of this report the Final Repository is divided into three functional areas that are referred to as:

1. **Repository Access**, including the access ramps and shafts
2. **Central Area**,
3. **Deposition areas**, including the deposition tunnels and deposition holes.

Each of these areas will have different design constraints and requirements, and hence the discussion of these functional areas has been separated in this report. Figure 1-1 provides a general overview of these functional areas.

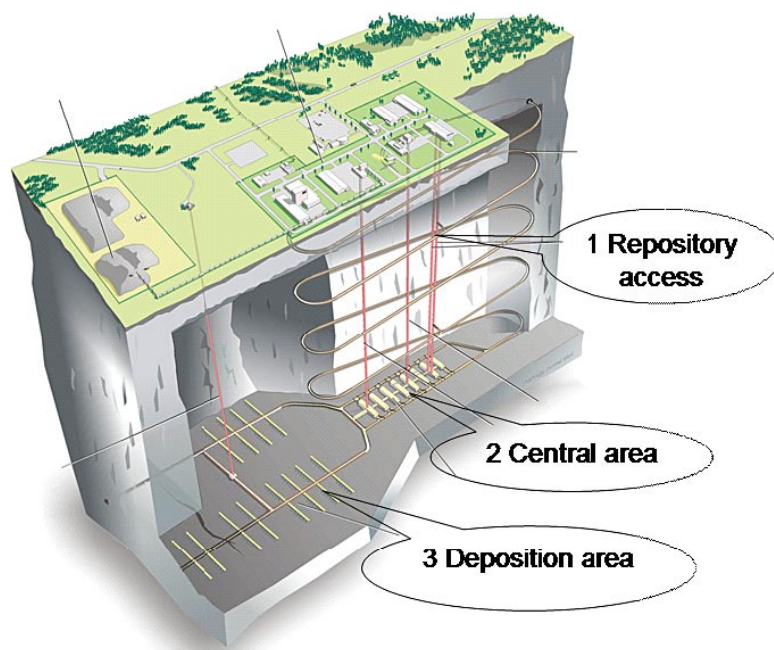
## 1.2 Objectives

The Site Engineering Report builds on the extensive surface based site investigations carried out at the Laxemar site and the interpretation and evaluation of these data that are given in the SDM-Site /SKB 2009/. However, because SDM-Site serves the needs of many users, and especially those of safety assessment, not all the information contained in SDM-Site is needed for engineering design and layout purposes.

Figure 1-2 illustrates the role of this report which was to extract the relevant information and parameters/values from SDM-Site and summarise them in a format suitable for developing a ground engineering model. Parameters that are recommended in this report for engineering purposes are based on the SDM-Site Laxemar and in some cases these parameters may be modified to reflect modern engineering practice. Geological conditions that may constrain the layout from the safety assessment point of view are also provided.

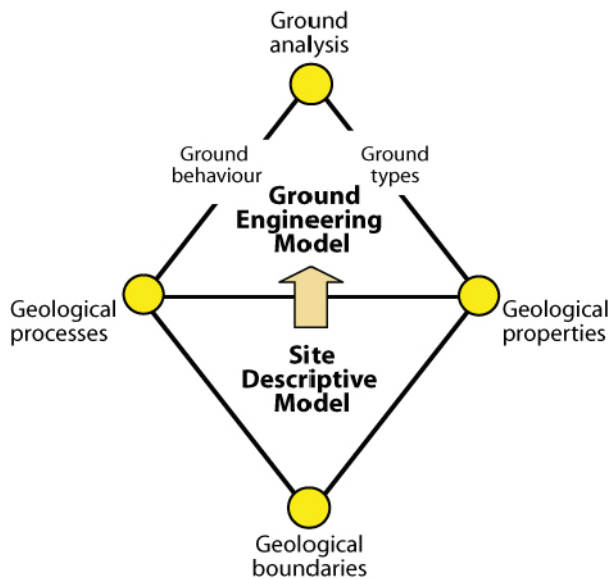
The main users of the Site Engineering Report will be the engineers responsible for the repository design and layout during various design stages. As such the major objectives of the Site Engineering report are to:

1. Present an engineering description of the rock mass for the design of the underground openings associated with the deep geological repository.
2. Derive and present site specific requirements and constraints on the design related to long-term safety.



*Figure 1-1. General three dimensional overview of the repository layout showing the major functional areas.*





**Figure 1-2.** Illustration of the interface (Site Engineering Report – represented by the arrow) between the Site Descriptive Model (SDM) and the Ground Engineering Model. The Site Engineering Report translates and summarises the relevant information contained in the SDM into numbers/values that are used in the analyses to develop the Ground Engineering Model.

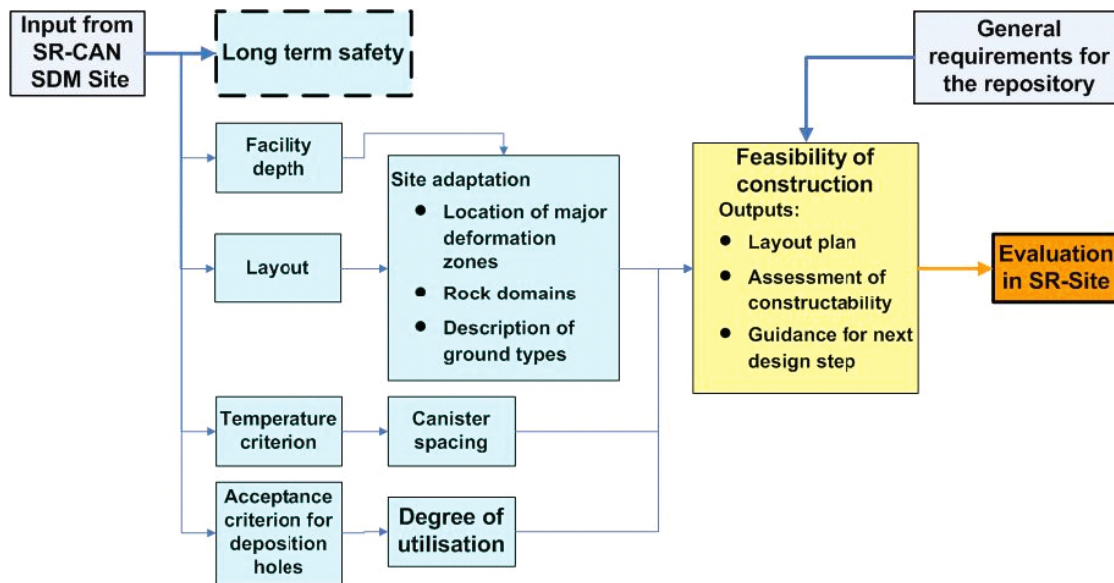
3. Establish geological engineering parameters for the rock mass that should be used in the repository design and layout, for design step D2.
4. Highlight issues that require special attention during the repository design and layout.
5. Establish a procedure for dealing with uncertainties and potential hazards in some elements of the design process.

### 1.3 Long-term safety and Design

The long-term safety is assessed using site specific data including the layout of the facility. As a consequence, long-term safety requirements can impact the design of the underground openings and the layout of the facility. For design Step D2, the geological constraints and engineering guidelines provided in SER cover the site adaptation of the Final Repository with respect to: (1) unsuitable deformation zones and rock mass conditions at depth, (2) parameters that affect the depth and areal size of the Repository, and, (3) description of ground conditions for assessment of constructability. The final design will be optimised for these restrictions.

Figure 1-3 provides an overview of the main content of this Site Engineering Report. The input for this report comes from Laxemar site descriptive model /SKB 2009/, as well as from the main conclusions from the preliminary Safety Assessment (SR-Can) /SKB 2006a/ carried out for the site. The major long-term safety elements considered in this Site Engineering Report and shown in Figure 1-3 are:

- Facility depth which is determined and justified in Chapter 8.
- Constraints for the layout which are discussed in Chapter 7. These constraints identify deformation zones that require a respect distance and specific site conditions that should be considered in the design, such as recommended alignment of the deposition tunnels, and the distribution of ground types within each functional area.
- Chapter 7 also deals with the site conditions that affect the areal size of the Final Repository. The areal size is a function of the recommended deposition tunnel and canister spacings which are dependent upon the thermal properties of the rock (lithological) domains.
- The design tasks in accordance with /SKB 2007/ are based on the input from this report and the input from the general requirements on the Final Repository. The output from the design will be audited by the final Safety Assessment prior to the application for siting of the Final Repository.



**Figure 1-3.** Overview of main deliverables from the Laxemar Site Engineering Report with respect to long-term safety (blue) and major outputs from design (yellow) to Safety Assessment (red).

## 1.4 Design strategy and Observational Method

One of the design methodologies used in underground design and construction to address the uncertainty and variability in the geological setting and ground structure interaction is the Observational Method. The Observational Method is a risk-based approach to underground design and construction that employs adaptive management, including advanced monitoring and measurement techniques, to substantially reduce costs while protecting capital investment, human health, and the environment. Development of the Observational Method in geo-engineering is generally attributed to /Casagrande 1965/, /Peck 1969/ who initially outlined the essential elements of the methodology and /Stille 1986/ who described the adaptation of the method in Sweden under the name “Active Design”.

As outlined in Underground Design Premises report UDP/D2 /SKB 2007/, in underground engineering there are some major aspects that must be addressed during the design phase. The repository design must be safe, economically feasible and meet the requirements from long term safety based on a realistic estimate of the expected ground conditions and their potential behaviour as a result of the excavation. The design process using the Observational Method has several steps and is constantly updated during each step, as more information becomes available. During the design steps, the inherent complexity and variability in the geological setting prohibits a complete picture of the ground structure and quality to be obtained before the facility is excavated. Thus during design, statistical methods may be used to evaluate the sensitivity of the design to the variability as well as the quality of the existing data. This is most important during the early stages of design when trying to quantify project risks and cost estimates. As new data are acquired during subsequent investigations the site descriptive model will be updated and the parameter distributions refined.

The SKB design strategy is outlined in Section 5.7 of the UDP/D2 /SKB 2007/. SKB plans to carry out the design process for the Final Repository project in agreement with the European standard for construction, Eurocode, and in particular the standard for geotechnical design, Section 2.7 in EN 1997-1:2004, which will be implemented in Sweden in 2009. This allows for the application of the Observational Method in underground design and construction. /SKB 2007/ presents how the Observational Method should be applied in design step D2 and an overview of the design in relation to the Observational Method is given in Table 1-1. The scope of the design tasks in design step D2 will be primarily limited to the following five requirements of the Observational Method stated in Eurocode EN 1997-1:2004, Section 2.7:

1. Establish acceptable limits of behaviour.
2. Assess the range of possible behaviour and show that there is an acceptable probability that the actual behaviour will be within the acceptable limits.

**Table 1-1. Design documents in an iterative design process, focus on SKB design step D2.**

Design Documents	General content	SKB document corresponding to design document
Background documents	Description of rock domain distribution and properties, deformation zones, fracture domains and hydrogeology conditions in the focused volume.	Site description of Laxemar at completion of the site investigation phase (SDM-Site Laxemar) /SKB 2009/.
Engineering characterisation and classification documents	The rock mass is divided into separate ground types that meet the objectives of SER. The description of the ground types considers geological conditions, rock mechanics, hydrogeology, hydro geochemistry and thermal issues.	Site Engineering Report Laxemar Guidelines for Underground Design Step D2 ( <i>this report</i> ). Construction and engineering experiences are compiled in CECR. /SKB R-07-66, Carlsson and Christiansson 2007/.
Design documents for excavation, rock support, grouting	Description of possible construction-, support- and grouting solutions.  Assessment of the rock mass response to the excavation based on the proposed support and grouting measures.	The design works for this preliminary design shall be described in the Underground Design Premises (UDP) D2 /SKB 2007/. The design methodology is summarised in Chapter 5. Chapters 7–10 describe the design studies in this Design step.
Control programme	Outline which parameters that may be monitored and observed during construction. Such parameters should relate to the critical issues described in the design documents.	This is handled on a general level in design step D2, cf. Chapter 10 in /SKB 2007/.

The procedures in the Observational Method that address the construction phase will be regarded in future design steps

3. Develop a plan for monitoring the behaviour, which will reveal whether the actual behaviour lies within the acceptable limits. The monitoring shall make this clear at a sufficiently early stage, and with sufficiently short intervals to allow contingency actions to be undertaken successfully.
4. the response time of the monitoring and the procedures for analysing the results shall be sufficiently rapid in relation to the possible evolution of the system.
5. Develop a contingency plan which may be adopted if the monitoring reveals behaviour outside acceptable limits.

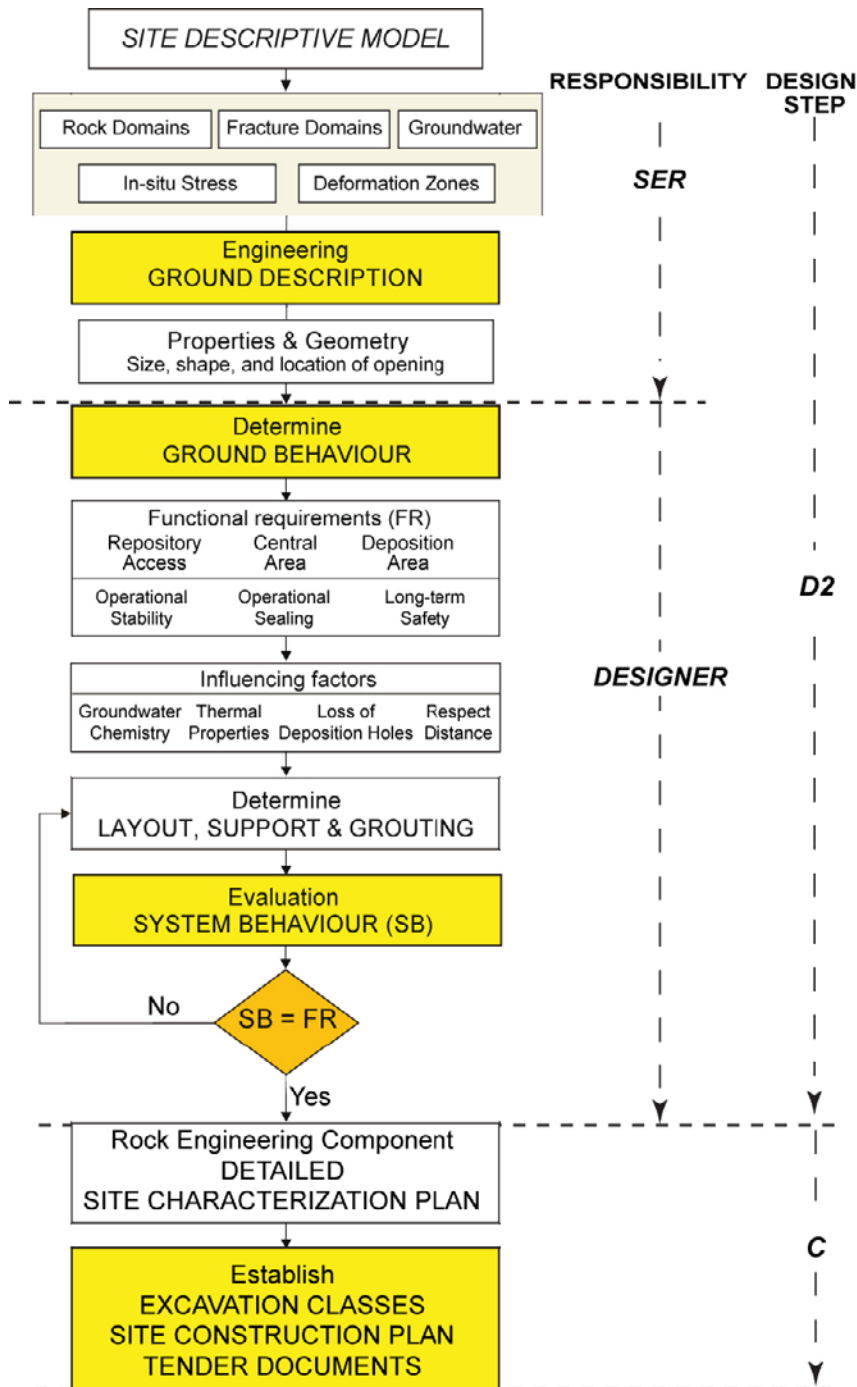
The Observational Method has several caveats. One must be able to define an action plan for every possible adverse condition based on current site understanding. The method cannot be used if a predictive model for the behaviour cannot be developed, i.e. one must be able to establish a model that can calculate the parameters that will subsequently be monitored during construction. This is not a trivial problem as often we can measure what we cannot calculate and vice versa. This means that the monitoring plan must be chosen very carefully with a good understanding of the significance to the problem.

The construction of the access shafts and tunnels will rely on the Observational Method and the method will also be used to ensure that the facility layout will meet the requirements of the safety analysis. For example, the Observational Method will be used to decide the orientation and location of the deposition tunnels, and to locate the deposition holes in suitable rock conditions. A requirement with the Observational Method is the ongoing underground characterisation and associated modelling that will go hand-in-hand with choosing the final layout for the facility. Hence it is important to consider the Observational Method as a key component of all stages of design and to identify those key parameters that can be used for monitoring during the design steps.

This report is limited to preliminary assessments of the first two requirements of the Observational Method as stated in Section 2.7 in Eurocode EN 1997-1:2004.

## 1.5 Design methodology

A general flow chart for the design of the layout and the various underground openings for this design step is outlined in Figure 1-4. A detailed description of the approach outlined in the flow chart to underground design is given by /Palmström and Stille 2006/ and additional background information for Figure 1-4 is given by /Goricki 2003/.



**Figure 1-4.** Flow Chart for the design of underground openings associated with the nuclear waste repository. Modified from /Schubert and Goricki 2004/.

The site descriptive model provides the detailed geoscientific description of the site obtained from the Complete Site Investigation phase /SKB 2001/ and /Munier et al. 2003/. The primary purpose of this site descriptive model is to provide data for the design of the facility site and for Safety Assessment. The SER has extracted the relevant data from the Laxemar site descriptive model /SKB 2009/ that pertains to the design of underground openings and repository layout and integrated it with the construction experiences from the nearby Äspö hard rock laboratory facilities to develop the underground design guidelines contained in this report for Design Step D2. The SER also includes current engineering practice for the design and construction of underground openings in hard rock. As shown in Figure 1-4 the first phase of the underground design is to develop an engineering description of the rock mass (Engineering Ground Description) based on the site descriptive model. This description considers the rock domains (based on intact rock properties), fracture domains, major deformation zones, ground water conditions and in situ

stress conditions, obtained from the SDM, and incorporates parameters that are required to provide an engineering description of the rock mass. The product of this description is an account of the ground types (GT) which will be encountered during construction. The number of ground types is project and site specific, and depends on the design step, as well as on the complexity of the geological conditions. The ground types used for design step D2 are described in Chapter 4 of this report.

The second step in Figure 1-4 (Determine Ground Behaviour) involves evaluation of the potential ground behaviour considering each ground type. The ground behaviour must be evaluated for the underground opening in each of the functional areas without considering the effect of support, or the benefit of any modifications including the excavation method and/or sequence, and support or other auxiliary measures. The ground behaviour must also consider the influencing factors, as well as the relative orientation of relevant discontinuities to the excavation, groundwater conditions and/or in situ stresses.

The final step in Figure 1-4 (Evaluation System Behaviour) requires an assessment of the System Behaviour, i.e. the interaction between the ground behaviour and construction measures. After the Ground Types and the ground behaviour have been determined, appropriate construction methods (excavation sequence, support methods, and auxiliary measures such as grouting) are determined. The system behaviour can be assessed using analytical methods, numerical methods, and/or comparative studies, based on experience from previous similar projects. For example it may be acceptable to use the Construction Experience Compilation Report /Carlsson and Christiansson 2007/ for the existing facilities at or near the site, such as the Äspö Hard Rock Laboratory, to evaluate the system behaviour for the Access Area at this stage of the design. The analysis of the system behaviour should assess the range of possible behaviour and show that there is an acceptable probability that the actual behaviour will be within the acceptable limits in terms of:

- Stability of underground openings.
- Repository design requirements, i.e. that the layout complies with constraints imposed by respect distance, loss of deposition holes, canister spacing and the required number of deposition holes.
- Acceptable seepage limits.

All analyses used to assess the system behaviour should be documented in a way, that is traceable and auditable in accordance with Underground Design Premises D2 /SKB 2007/.

In Figure 1-4 there is a final stage in the design process called Detailed Site Characterisation and the requirement to develop Excavation classes, Site Construction Plan and Tender Documents. This and the next step are included in the design activities (inside the yellow box in Figure 1-3). The Excavation Classes are defined based on the evaluation of the support, excavation and grouting requirements. The distribution of the expected ground behaviour and the excavation classes in the repository provides the basis for establishing the construction plan and tender documents. This stage of the design is not described in this SER and would take place during Design Step C /SKB 2007/.

## 1.6 Terminology

The site descriptive model may use terms that are not generally used in underground engineering or have restricted definitions. A brief summary of these terms, taken from /SKB 2009/, is provided below.

- **Candidate area:** The candidate area refers to the area at the ground surface that was recognised as suitable for a site investigation, following the feasibility study work /SKB 2000/. The extension at depth is referred to as candidate volume.
- **Rock unit (RU):** A rock unit is defined in the single-hole geological interpretation on the basis of the composition, grain size and inferred relative age of the dominant rock type. Other geological features including the degree of bedrock homogeneity, and the degree and style of ductile deformation also help to define and distinguish some rock units. N.B. Defined rock units differ between boreholes.
- **Rock domain (RD):** A rock domain refers to a rock volume in which rock units that show specifically similar composition, grain size, degree of bedrock homogeneity, and degree and style of ductile deformation have been combined and distinguished from each other. The term rock domain is used in the 3D geometric modelling work and different rock domains at Laxemar are referred to as RSMxxx.

- **Deformation zone (DZ):** Employed as a general notation of an essentially 2D structure characterised by ductile or brittle deformation, or a combination of the two. Those deformation zones which are possible to correlate between the associated surface expression (lineament with a length > 1,000 m) and an interpreted borehole intercept, or alternatively between one or more borehole intercepts, or exhibit an interpreted true thickness > 10 m are modelled deterministically, and are thus explicitly accounted for in the 3D RVS model. Deformation zones at Laxemar that are correlated to surface are denoted ZSM followed by two to eight letters or digits. An indication of the orientation of the zone is included in the identification code. Other deterministic deformation zones are denoted KLXxx\_DZxx (the digits corresponding respectively to the borehole ID and the DZ ID from Extended Single hole interpretation).
- **Fracture domain:** A fracture domain is a rock volume outside deformation zones in which rock units show similar fracture intensity characteristics. Fracture domains at Laxemar are denoted FSMxx.
- **Hydraulic domains:** the bedrock was divided into 3 hydraulic domains which are 1) HRD (hydraulic rock mass domain) which represents the fracture domains between the deterministic deformation zones, 2) HCD (hydraulic conductor domain) which represents deterministic deformation zones and 3) HSD (hydraulic soil domain) which represents the overburden. The division in hydraulic domains represents the basis for hydrogeological modelling.

There are also additional terms that are used in the description of the bedrock characteristics:

- **Discrete fracture network (DFN).** The fracturing in the bedrock is described on the basis of a standardised statistical procedure, which provides orientation, size distribution and spatial distributions for the fractures within defined fracture domains. Both open and sealed fractures are used to establish the DFN /SKB 2009/. Two DFN models are developed, one based only on geological data and one which is coupled to the hydrogeological characteristics of the bedrock.
- **Sealed fracture network** is used to denote a high frequency and complex network of sealed fractures associated with deformation zones.

Table 1-2 presents the terminology for brittle structures based on trace length and thickness that is used to describe the Laxemar bedrock geology /Andersson et al. 2000/.

## 1.7 Report structure

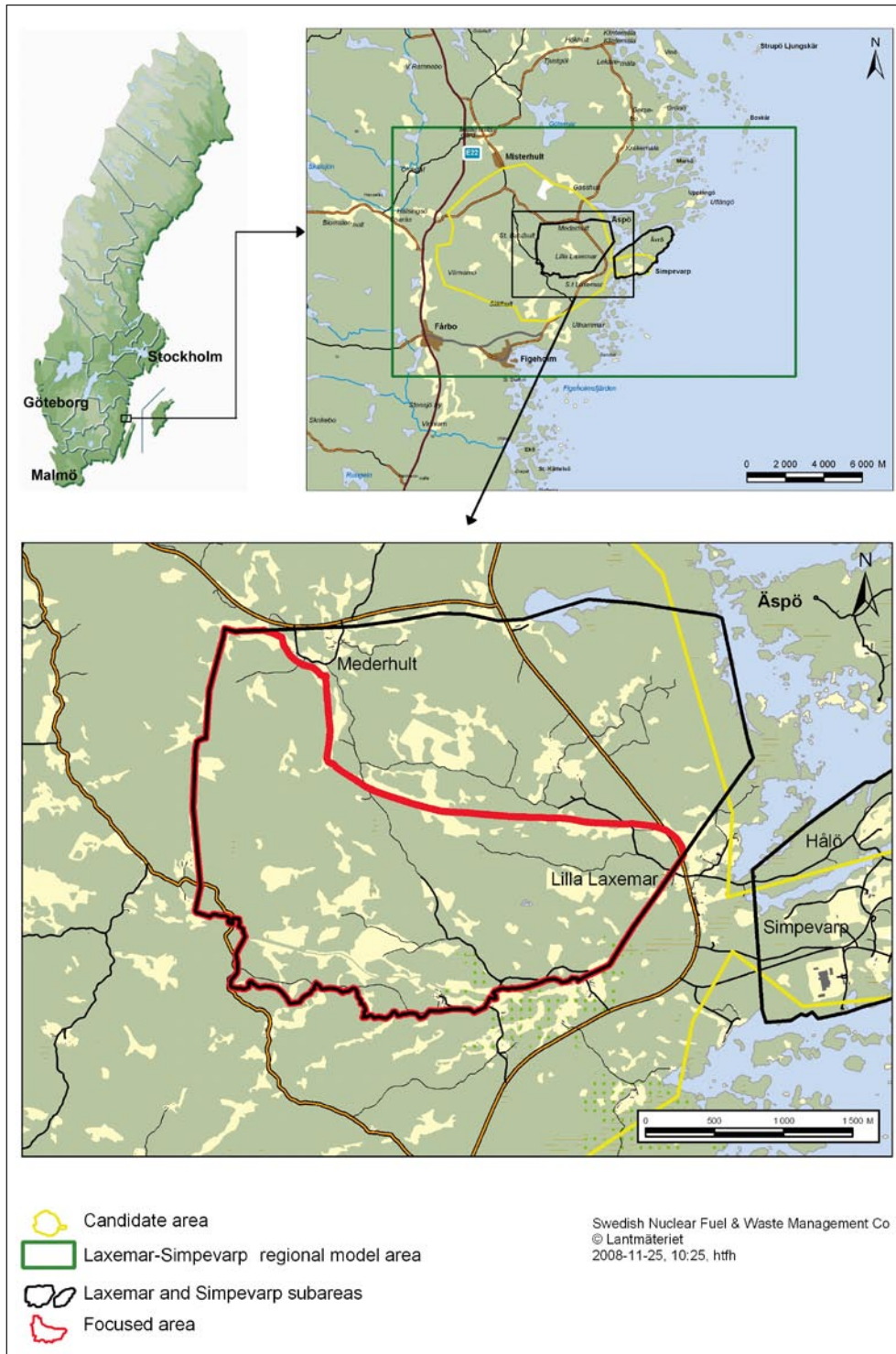
This report is organised into 9 chapters. Chapter 1 contains an overview of the design strategy for the layout and design of the underground openings for design step D2. Chapter 2 presents a synthesis of the site descriptive model as it pertains to the ground descriptions needed for the underground design. Chapter 3 summarises the relevant construction experience from the Oskarshamn nuclear power plant and the Äspö Hard Rock Laboratory. Chapter 4 provides the designer with the relevant parameters required for the underground design. Chapters 5, 6 and 7 describe the conditions that are likely to be encountered in the Access, Central and Deposition functional areas, respectively. Chapter 8 provides a summary of the factors that influenced the selection of the repository depth. Chapter 9 provides a summary of major issues that should be considered in the layout in design step D2.

**Table 1-2. Classification and naming of the geological structures used to describe the brittle structures in bedrock (length and width measurements are approximate) /Andersson et al. 2000/. The equivalent engineering term is also provided.**

Terminology	Length	Width	Engineering description
Regional deformation zone	> 10 km	> 100 m	Regional shear zone or fault
Local major deformation zone	1 km–10 km	5 m–100 m	Major shear zone or fault
Local minor deformation zone	10 m–1 km	0.1–5 m	Shear zone or fault
Fracture (open/closed)	< 10 m	< 0.1 m	Discontinuity or joint

## 2 General site conditions and rock properties

The Simpevarp candidate area is located in the municipality of Oskarshamn, about 300 km south of Stockholm. The Simpevarp candidate area is divided into two parts, the Simpevarp subarea, concentrated on the Simpevarp Peninsula and the Laxemar subarea located on the mainland west of the Simpevarp Peninsula, see Figure 2-1, /SKB 2009/.



**Figure 2-1.** Overview of the Laxemar-Simpevarp regional model area (upper right). Simpevarp and Laxemar subareas are shown in black and the focused area in red /SKB 2009/.

Based on preliminary safety assessment on Laxemar 1.2 and Simpevarp 1.2, and in order to restrain the investigations in the volumes of rock that were judged to be most suitable to host the repository, an early decision was taken to select Laxemar for continued site investigations /SKB 2006c/. Moreover within the Laxemar subarea a focused area has been defined /SKB 2005/. Hence in this report description of general site conditions and rock properties are therefore most often restricted to the focused area.

The Laxemar subarea is relatively flat with a gentle dip towards the east. The Laxemar subarea is characterised by a mildly uneven topography at a relatively low altitude, but with marked both short and longer valleys/topographical depressions. The most elevated areas are located at c. 50 metres above current sea level. The whole area is located below the highest coastline associated with the last glaciation, and the area has emerged from the Baltic Sea during the last 11,000 years /SKB 2009/.

## 2.1 Rock type and intact rock properties

The distribution of rock types reveals important aspect of the homogeneity of the site. Furthermore, the chemical composition of these rock types directly affects the ore potential as well as thermal and rock mechanics properties. In the SDM-Site for Laxemar /SKB 2009/, the rock type is described in the context of rock domains, defined based on composition, grain size and homogeneity, and inferred degree of ductile deformation.

### 2.1.1 Rock Type

According to the Laxemar site description /SKB 2009/, the majority of the rocks at the present day erosional level in south-eastern Sweden were formed during a period of intense igneous activity c. 1.86–1.65 Ma ago. The dominant rocks have granitic, granodioritic, monzodioritic and gabbroic composition. This generation of igneous rocks belong to the so-called Transscandinavian Igneous Belt (TIB). Locally, fine- to medium-grained granite dykes and minor massifs, and also pegmatite occur frequently. Though volumetrically subordinate, these rocks constitute essential lithological inhomogeneities in parts of the bedrock. North-south trending dolerite dykes are also present but constitute a very subordinate lithological component in the bedrock /SKB 2009/.

The bedrock of interest for a planned repository is geologically relatively homogeneous and dominated by a rock with low quartz content, associated with fairly low thermal conductivity and moderate uniaxial compressive strength (UCS). The area of interest for a planned repository is bounded by subvertical deformation zones /SKB 2009/.

The distribution of rock types in the Laxemar local model area is illustrated in Figure 2-2.

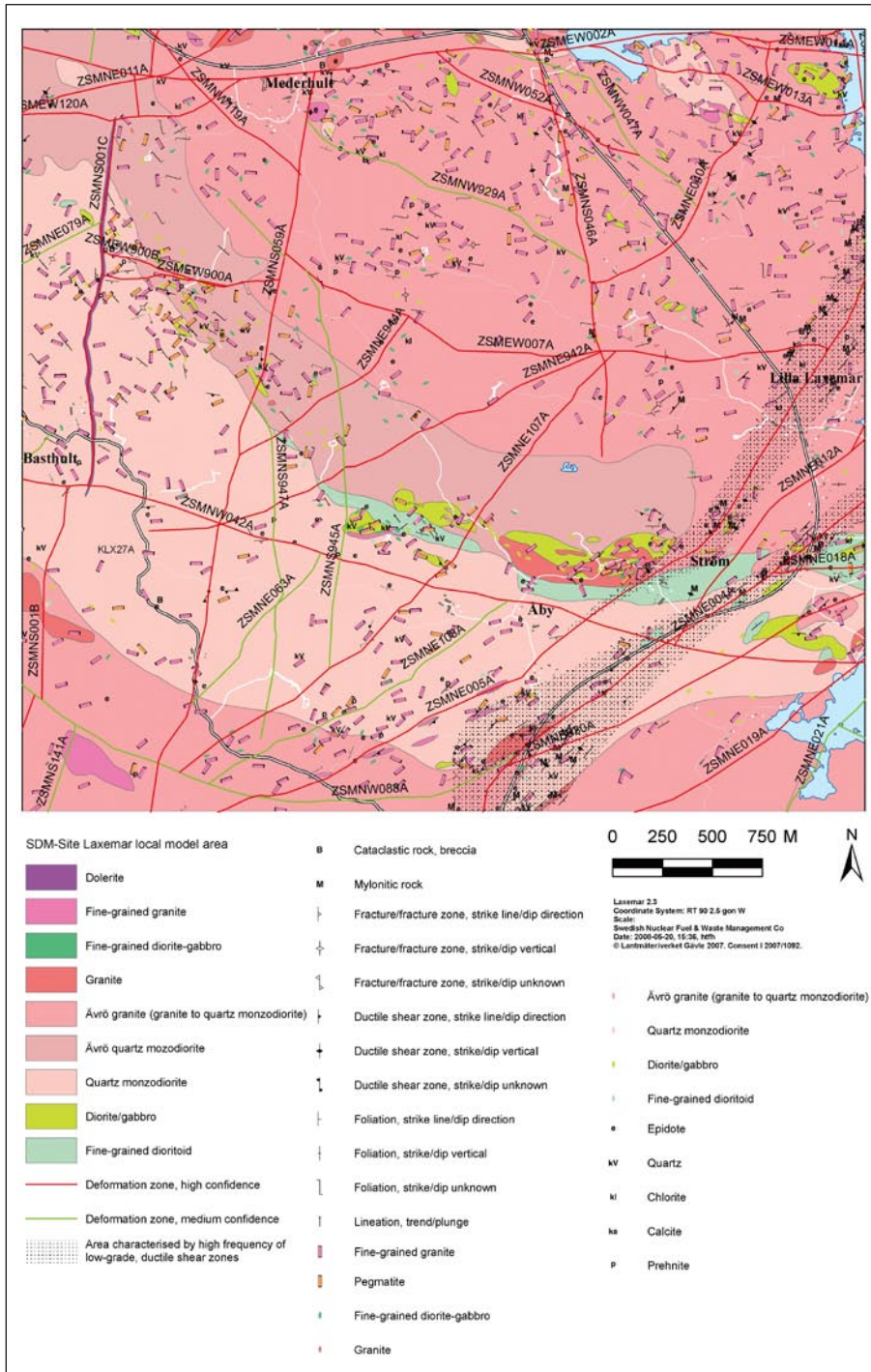
In total thirteen rock domains are defined in the local model volume /SKB 2009/. The RSMBA03 domain only occurs at depth in the lower part of the model volume. It is based on a mixture of Ävrö granite and fine-grained dioritoid in borehole KLX02. The geometry of the RSMM01 domain combined with RSMD01, RSMP01, RSMP02, RSMB05 and RSMB06 domains in the focused volume is displayed in Figure 2-4. The RSMD01 domain in combination with the RSMP01 and RSMP02 domains are shown in Figure 2-5. A description of the dominant rock domains RSMD01, RSMM01 and RSMA01 is given in the sections below. The distribution of rock types by rock domain is provided in Table 2-1.

### 2.1.2 Bedrock temperature and thermal properties

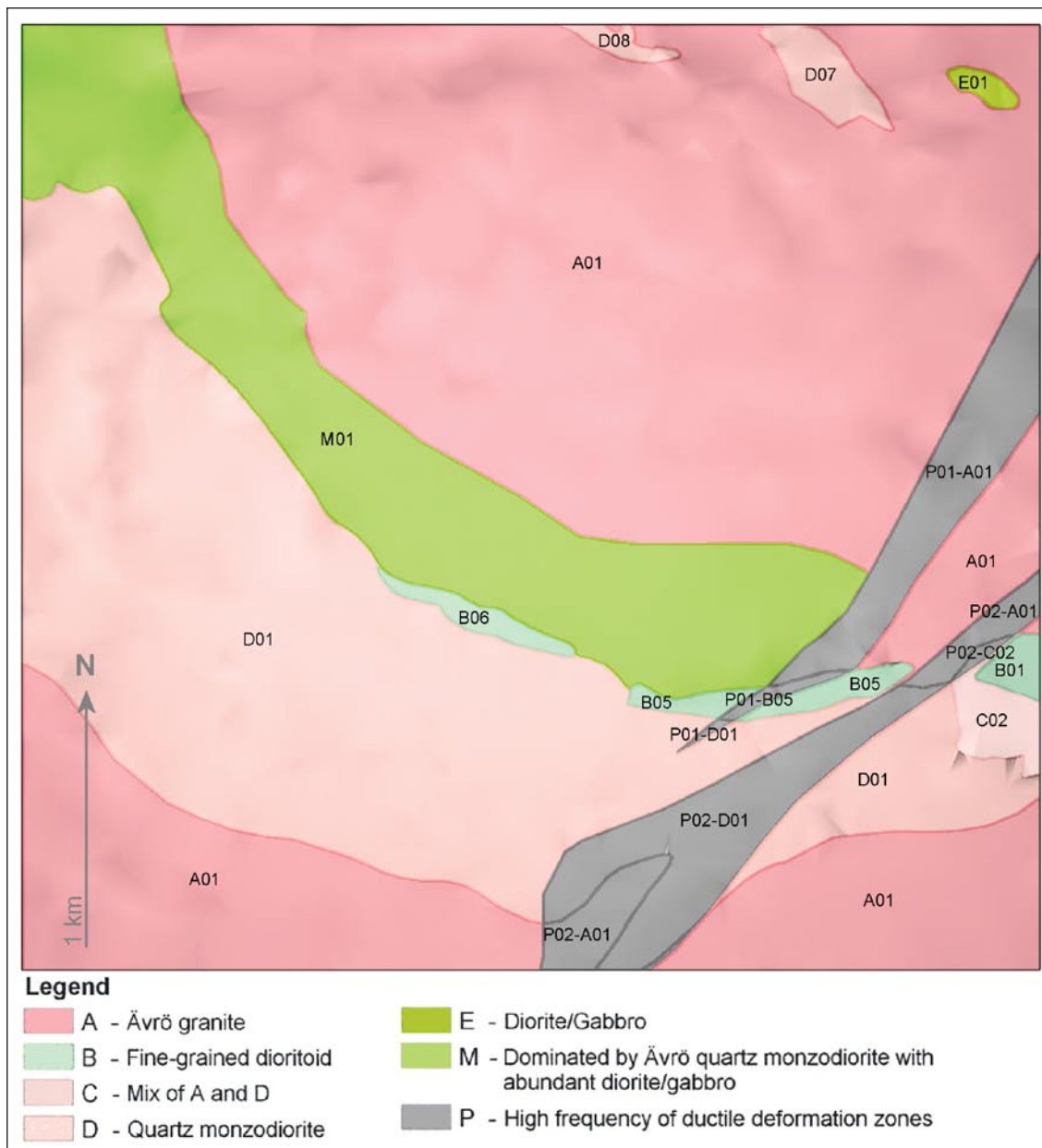
The in situ temperatures have been measured in various boreholes to depths of 1,000 m. The temperature variability between boreholes at the same depth was significant and was partly related to high uncertainties in the data. The reliability of the measured data has been assessed based on measurement techniques criteria and the mean rock mass temperatures at the depth(s) for the repository were evaluated on “approved” boreholes /Sundberg et al. 2008/. The evaluated mean temperature is provided in Table 2-2 for different depths.

The thermal properties, i.e. thermal conductivity and heat capacity, of the rock are closely related to rock type, since these properties depend on the mineral composition, and especially the quartz content.

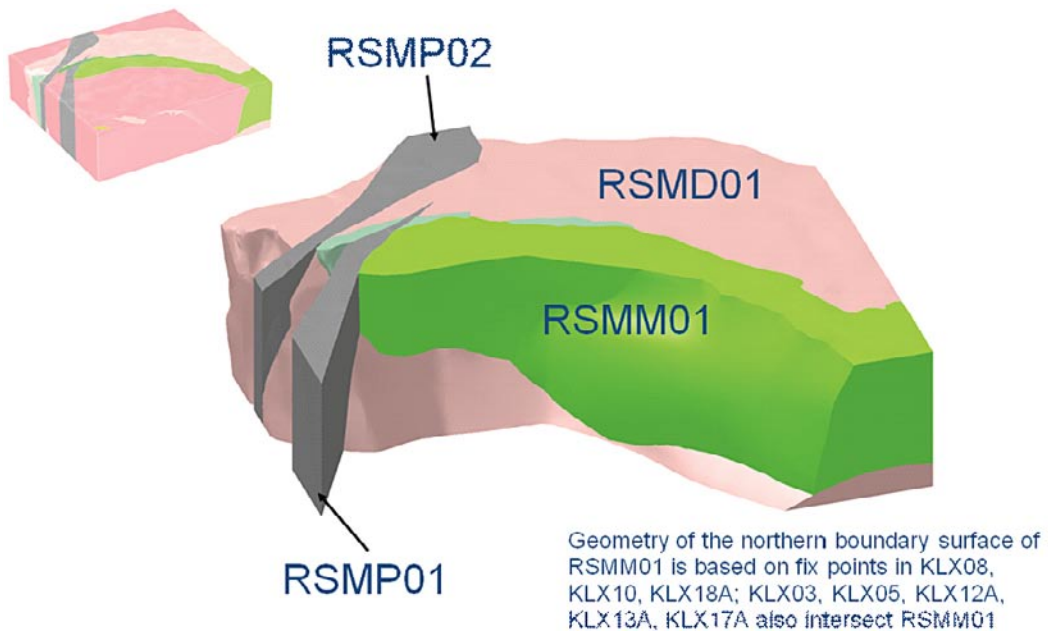




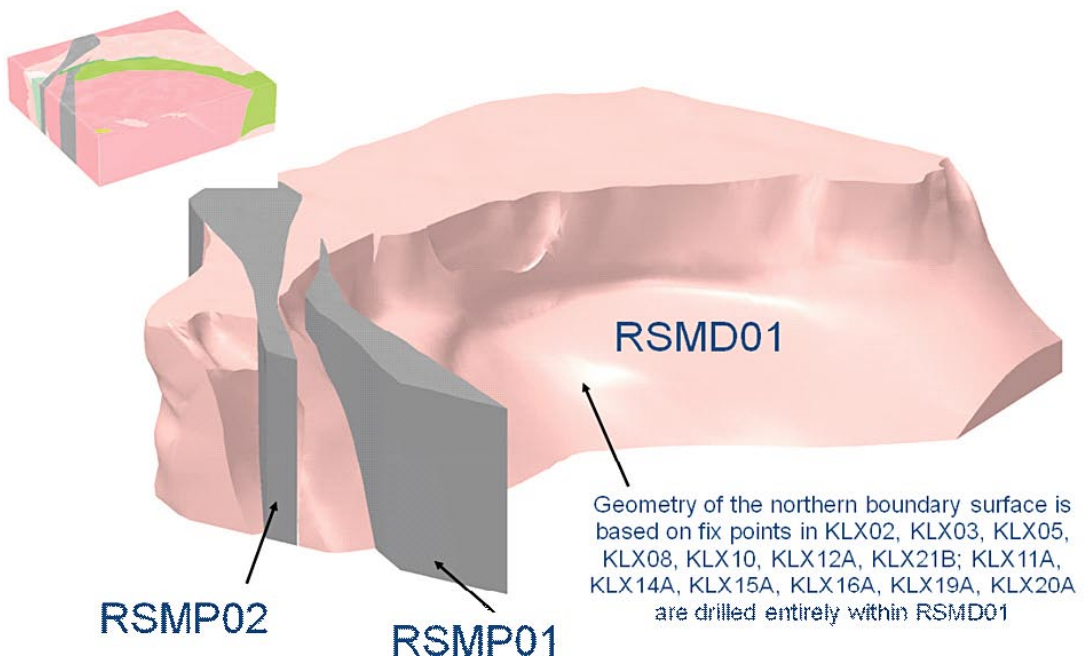
**Figure 2-2.** Bedrock geological map showing the rock type distribution in the Laxemar local model area /SKB 2009/.



**Figure 2-3.** Two-dimensional model at the surface for rock domains in the Laxemar local model area. For reasons of simplicity, the prefix RSM has been excluded in the denomination of the rock domains /SKB 2009/.



**Figure 2-4.** View of the RSMM01 domain combined with RSMD01, RSMP01, RSMP02, RSMB05 and RSMB06 /SKB 2009/. View to the south.



**Figure 2-5.** View of the RSMD01 and intersecting RSMP01 and RSMP02 domains /SKB 2009/. View to the south-southwest.

**Table 2-1. Proportions of rock type occurrence in the three largest rock domains in Laxemar. Compiled from /Hakami et al. 2008/.**

Occurrence of Rock type (SKB rock code)	Rock Domain		
	RSMA01 [%]	RSMD01 [%]	RSMM01 [%]
Ävrö granodiorite (501056)	62	0.5	24
Ävrö quartz monzodiorite (501046)	22	0.6	43
Oxidised Ävrö quartz monzodiorite (501046)	4	–	7
Quartz monzodiorite (501036)	3	80	0.4
Oxidised quartz monzodiorite (501036)	–	8	–
Diorite-gabbro (501033)	0.2	0.1	16
Fine-grained granite (511058)	3	5	5
Fine-grained dioritoid (501030)	3	0.3	0.4
Fine-grained diorite-gabbro (505102) <sup>1)</sup>	2	2	2
Granite (501058) <sup>1)</sup>	1	0.4	2
Pegmatite (501061) <sup>1)</sup>	0.3	1	0.5
Dolerite (501027) <sup>1)</sup>	–	2	–

<sup>1)</sup> Not included in rock mechanics description.

**Table 2-2. Mean temperature at different vertical depths from the ground surface from /SKB 2009/.**

	400 m	500 m	600 m
Mean Temperature (°C)	13.3	14.8	16.3

The higher the quartz content the higher the thermal conductivity. The thermal conductivity of the rock type has been assessed from direct measurements and by calculations based on mineral composition from modal analyses. At this stage the thermal modelling strategy has been significantly modified compared to the previous versions. The conceptual model developed in the strategy /Back and Sundberg 2007/ simulates the spatial variability of thermal conductivity in terms of lithological and mineralogical heterogeneities, and also provides an explanation for anisotropy of thermal properties. The main result of the modelling is a set of realisations describing the spatial distribution of thermal properties in the 2 m scale for each of the three rock domains RSMA01, RSMM01 and RSMD01. Table 2-3 provides the thermal conductivity for these three rock domains. The values provided in this table are valid at temperature of 20°C. With increasing temperature the thermal conductivity of the dominant rock type decreases by 0.1–10%/100°C temperature increase.

### 2.1.3 Strength and deformability properties

Rock type also directly affects the strength and deformability properties of the intact rock. The results for the dominant rock types at Laxemar are provided in Table 2-4. The rock is quite stiff and the strength high, but properties exhibit fairly large spread. A great spread in the distribution for fine-grained dioritoid can be noted, probably due to spatial variations in rock type characteristics /Hakami et al. 2008/. For quartz monzodiorite (501036) and Ävrö quartz monzodiorite (501046), the mechanical and deformability properties of the oxidised rock were determined separately because all the properties of oxidised rock are lower than for corresponding unaltered rock, except for the Poisson's ratio. For the oxidised parts of these two rock types, the mean properties in Table 2-4 should be adjusted by the reduction factors given in footnotes of the same table.

### 2.1.4 Rock mass deformation properties

It is well known that the deformation properties of a rock mass are a function of scale. The deformation properties of the intact rock measured in laboratory samples are given in Table 2-4. It must be remembered that these laboratory values are representative of the relatively homogeneous rock free of any micro or macro flaws. These values should not be used when modelling tunnel scale or repository scale problems. Scaling of the laboratory values to the tunnel scale or repository scale is problematic and there are no guidelines established for such scaling procedures. /Hoek and Diederichs 2006/ established a correlation between the Geological Strength Index (GSI) and rock mass modulus.

**Table 2-3. Thermal conductivity for different rock domains in Laxemar, upscaled at 5 m scale /SKB 2009/. Based on simulations at the 2 m scale.**

Statistical parameter	Domain RSMA01	Domain RSMM01	Domain RSMD01
Mean, W/(m·K)	2.93	2.65	2.76
Standard deviation, W/(m·K)	0.29	0.32	0.17
0.1-percentile, W/(m·K)	2.16	2.11	2.41
1-percentile, W/(m·K)	2.27	2.19	2.48
2.5-percentile, W/(m·K)	2.34	2.23	2.50

**Table 2-4. Intact laboratory strength and deformation properties for different rock types for the SDM-Site Laxemar /Hakami et al. 2008/.**

Parameter	501030	501033	501036	501046	501056	511058
	Fine-grained dioritoid	Diorite/ gabbro	Quartz monzodiorite – Unaltered	Ävrö quartz monzodiorite – Unaltered	Ävrö granodiorite	Fine-grained granite
	Mean/stdev Min – Max Uncertainty	Mean/stdev Min – Max Uncertainty	Mean/stdev Min – Max Uncertainty	Mean/stdev Min – Max Uncertainty	Mean/stdev Min – Max Uncertainty	Mean/stdev Min – Max Uncertainty
Uniaxial compressive strength, UCS (MPa)	239/72 100–360 ±16%	225/20 200–270 ±5%	186 <sup>1)</sup> /30 110–240 ±5%	167 <sup>1)</sup> /11 140–190 ±3%	198/19 150–240 ±3%	280/45 210–350 ±11%
Crack initiation stress, $\sigma_{ci}$ (MPa)	122/53 48–190 ±28%	130/14 105–155 ±6%	104 <sup>2)</sup> /22 52–130 ±7%	88 <sup>2)</sup> /19 50–110 ±9%	104/16 70–135 ±5%	148/20 110–180 ±9%
$\sigma_{ci}/UCS$ <sup>3)</sup> (%)	52.4	57.3	56.0	52.8	52.8	52.6
Indirect tensile strength (MPa)	19/2.5 14–24 ±5%	16/1 15–17 ±4%	16.5 <sup>4)</sup> /3.0 10–23 ±4%	13 <sup>4)</sup> /1.3 10–16 ±4%	13/1.5 10–16 ±3%	–
Young's modulus (GPa)	80/8 70–97 ±5%	80/6 70–92 ±4%	76 <sup>5)</sup> /6.5 63–83 ±3%	71 <sup>5)</sup> /4 63–80 ±3%	72/5.5 60–83 ±3%	74/2.5 70–79 ±3%
Poisson's ratio (–)	0.26/0.05 0.17–0.33 ±3%	0.33/0.03 0.30–0.39 ±5%	0.29 <sup>6)</sup> /0.03 0.20–0.33 ±4%	0.28 <sup>6)</sup> /0.06 0.16–0.33 ±9%	0.25/0.05 0.15–0.34 ±7%	0.28/0.03 0.22–0.32 ±8%
Cohesion (MPa)	33/7 19–47 ±10%	30 <sup>7)</sup>	26 <sup>1)</sup> /3.5 19–33 ±4%	24 <sup>1)</sup> /1.5 21–27 ±2.5%	24/2 20–28 ±2.5%	–
Friction angle (°)	53/0.8 51–54 ±1%	60 <sup>7)</sup>	56 <sup>8)</sup> /0.3 56–57 ±0.2%	55 <sup>8)</sup> /0.3 55–56 ±0.2%	60/0.3 59–60 ±0.2%	–

- 1) For oxidised rock: mean uniaxial compressive strength and cohesion reduced by 7%.
- 2) For oxidised rock: mean crack initiation stress reduced by 8%.
- 3) From Best fit linear correlation curve shown in Figure 3-10 in /Hakami et al. 2008/. Crack initiation and UCS are correlated.
- 4) For oxidised rock: mean tensile strength reduced by 20%.
- 5) For oxidised rock: mean Young's modulus reduced by 14%.
- 6) For oxidised rock: mean Poisson's ratio increased by 8%.
- 7) Purely estimated valued used by the theoretical modelling.
- 8) For oxidised rock: no reduction of the friction angle applies.

While this method is a significant improvement over the RMR and Q correlations there is still an issue when the GSI values are greater than 80. This issue arises because as the GSI value approaches 100 the rock mass modulus approaches the modulus of the intact laboratory value. /Jackson and Lau 1990/ carried out a series of uniaxial compressive tests on Lac du Bonnet granite to investigate the effect of scale on the tangent Young's modulus determined at about 50% of the peak uniaxial strength. They showed using samples that varied in diameter from 38 mm to 300 mm that the laboratory Young's modulus of Lac du Bonnet granite decreased by approximately 12% as the scale of the laboratory samples increased from 50 mm diameter samples to 200 mm diameter. When one considers the effect of sealed fractures and sparse open fractures, this reduction by 12% may not be sufficient to account for these more compliant large scale features in the massive rock at repository level.

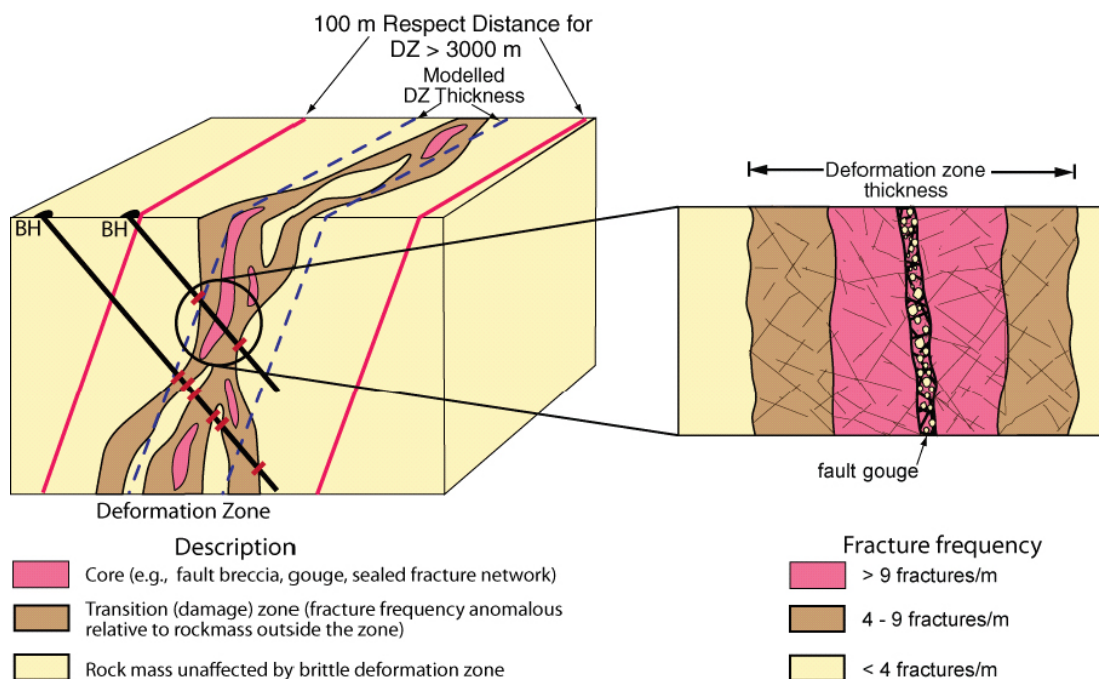
## 2.2 Deformation zones

Deformation zones and frequency and properties of fractures in the bedrock affect the possible layout and location of the repository, the mechanical stability and the groundwater flow. These can affect both the construction (rock stability and water inflow) and operation (water inflow) of the facility, and the safety assessment for the site (respect distances to deformation zones with a trace length at ground surface greater than 3,000 m). It is therefore essential to have a clearly defined geometry and description of the deformation zones. Figure 2-6 defines a “generic” deformation zone using the generally accepted division of zones into undeformed host rock, transition or damage zone, and fault core, e.g. /Caine et al. 1996/ and /Munier et al. 2003/.

### 2.2.1 Description

The bedrock in the Simpevarp candidate area has been exposed to a series of tectonic events that have involved shifts in the direction and magnitude of compressional forces exerted on the rock mass. The majority of the regional and local major deformation zones that have been deterministically modelled in Laxemar, although dominated by polyphase brittle deformation, show signs of having been originally formed during ductile conditions/SKB 2009/. One deformation zone within the local model volume (ZSMEW007A-C) is characteristic by means of a completely brittle origin.

The similarity between the orientation of both the large and small scale, ductile and brittle structures, strongly suggest that the ductile anisotropy that developed during the waning stages of the Svevokarelian orogeny has strongly influenced the orientation of brittle structures during the geological evolution. Furthermore, the similarity between the orientation of the fractures outside and inside deformation zones suggests that the deformation zones themselves may have controlled the fracturing in the bedrock in the Laxemar local model volume.



**Note:**

The modelled DZ thickness is based on an average thickness when more than one borehole intersection occurs.

The “fixed-point” of the DZ is located using the fault core or if the core is absent the zone with the greatest fracture frequency.

**Figure 2-6.** Definition of deformation zone, modelled deformation zone thickness and deformation zone Respect Distance. Within the focused volume at Laxemar fault gouge is seldom found and the core is primarily composed of a sealed fracture network. Modified from /Figure 5-29 in SKB 2009/ and /Figure 4-2 in Munier et al. 2003/.

A special group of deformation zones, interpreted from the borehole investigations, have not been correlated with any surface lineament, reflection seismic reflector or neighbouring boreholes. Where such deformation zones have an interpreted true thickness of 10 m or more, they have eventually been modelled deterministically. Such deformation zones have been assigned circular disk geometry with a surface area equivalent to a 1,000 m·1,000 m square /SKB 2009/.

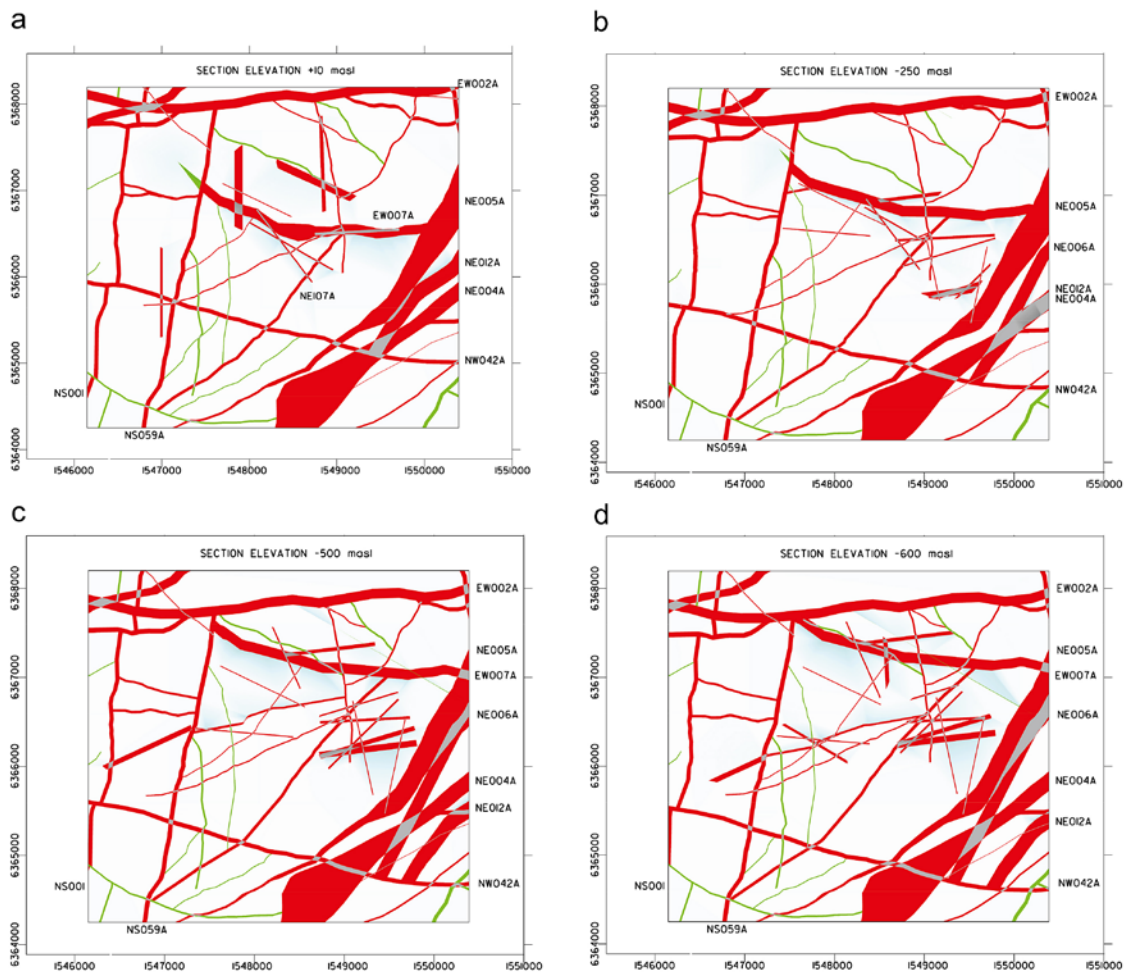
Deformation zones were modelled deterministically inside the local model volume /Wahlgren et al. 2008/. Vertical and steeply dipping deformation zones dominate the picture and comprise 48 zones whereas a further 12 zones are gently dipping. All deformation zones that were modelled deterministically within the local model are presented in plan view at different depths in Figure 2-7.

Five sets of deformation zones can be distinguished at the Laxemar site;

- Northeast-southwest.
- North-south.
- West-east to northwest-southeast sub vertical to moderate dip to the south.
- West-east to northwest-southeast moderate dip to the north.
- Gently dipping.

An overview of the deterministically modelled deformation zones within the local model volume displayed at four different depths is shown in Figure 2-7.

The deterministic modelling work addresses zones that have a trace length at the surface longer than 1,000 m /SKB 2009/.



**Figure 2-7.** All deformation zones in horizontal section at four different depths within the local model. a) Section elevation +10 m. b) Section elevation -250 m. c) Section elevation -500 m. d) Section elevation -600 m /SKB 2009/.

A conceptual geometric model for a brittle deformation zone at Laxemar is presented in Figure 2-6. The deformation zones are subdivided into a transition zone and a fault core. The transition zone, which ranges from a few metres up to a few hundred metres in Laxemar, contains a fracture frequency and commonly also an alteration that is anomalous with respect to that observed in the host rock. If the deformation zone includes a core its thickness may vary from a few centimetres up to a few metres. The fault core is normally composed of a high frequency of fractures and some crushed sections in combination with rock alteration.

Calcite and chlorite are common in deformation zones, and their frequency of occurrence follows the variation of fracture frequency /Wahlgren et al. 2008/. The relative frequency of clay minerals is generally higher in deformation zones than in fractures outside of deformation zones. Hematite is occasionally frequent in open fractures in deformation zones.

At the scale of local major and regional deformation zones there are no zones which are solely ductile. Many zones have a ductile origin but all show clear signs of brittle reactivation. One single zone, ZSMEW007A, which has been investigated by a number of boreholes, is the only zone that is solely brittle with no evidence of an earlier ductile phase.

The character and kinematics of the deformation zones have been studied in detail by /Viola and Venvik Ganerød 2007/. A more extensive overall study of all the available kinematic data across Laxemar and Simpevarp is currently underway. All the evidence to date shows the brittle history of Laxemar to be complex, involving a series of reactivation events.

The division between minor deformation zones and local major deformation zones is set at an associated surface lineament trace length of 1,000 m. A Laxemar specific, hypothetical thickness-length relationship based on deterministic deformation zones suggests that a zone with a true thickness > 10 m has a length > 1,000 m. All possible deformation zones that have been identified in a single borehole (i.e. through ESHI) and have an estimated thickness ≤ 10 m are termed possible minor deformation zones (MDZ). Possible minor deformation zones are not modelled deterministically in RVS, but are handled statistically in the GeoDFN modelling.

Red staining caused by a fine-grained dissemination of hematite can be found associated with a majority of the deformation zones. Crushed zones are mapped separately during the drill core mapping, and represent often sections characterised by increased hydraulic conductivity.

## 2.2.2 Mechanical properties of deformation zones

The location and extent of the major deformation zones at Laxemar are known with reasonable confidence for preliminary design purposes. From the construction experience at Oskarshamn Nuclear Power plants, CLAB Facility, and Äspö Hard Rock Laboratory, the strength, i.e. plastic yielding or squeezing, of these deformation zones does not significantly inhibit the construction of tunnels through these features. What can impact the construction is water inflows and ravelling of blocks. Typically these zones are characterised by several fracture orientation sets and an increase in fracture frequency, which implies that blocky ground may be locally encountered. The Oskarshamn Construction Experience and Compilation Report /Carlsson and Christiansson 2007/ documents the tunnelling conditions encountered when passing the NE1 deformation zone during the construction of the access ramp for the Hard Rock Laboratory. In /Glamheden et al. 2007/ the mechanical properties of a major deformation zone at the Forsmark Site have been back-calculated. The back-calculated geomechanical properties of this deformation zone are provided in Table 2-5.

**Table 2-5. Summary of geomechanical parameters for major deformation zones using the geometric definitions in Figure 2-6 from /Glamheden et al. 2007/.**

Property	Host Rock	Transition Zone	Core
Young's Modulus (GPa)	45	32	2.7
Poisson's ratio	0.36	0.43	0.43
Tensile Strength (MPa)	0.3	0.1	0.1
Cohesion (MPa)	5	4	2
Friction Angle	65	51	37



The properties provided in this table are assumed to represent geomechanical properties of major deformation zones. A deformation zone may have three distinct sections: (1) central core, (2) a transition zone and (3) adjacent host rock as described in Figure 2-6. The parameters in Table 2-5 are provided for each section but should be treated cautiously. At the present time the mechanical properties are not corrected for deformation zone orientation. The experience in Sweden and elsewhere is that these deformation zones have large undulations and may vary significantly in thickness and properties. Should the design identify that these deformation zones could have a significant impact on the facility a parametric study may be required.

## 2.3 Fractures and fracture domains

Smaller deformation zones (trace length shorter than 1,000 m) and fractures in the rock mass are not covered by the deterministic deformation zone model. They are handled in a statistical way through discrete fracture network (DFN) models. The geological DFN model is developed from data based on fracture observations in the boreholes, mapped fractures at outcrop and from interpretation of lineaments. The DFN captures both open and sealed fractures.

Analysis of fracture data in boreholes at Laxemar indicate that the rock mass between deformation zones in the whole model area can be mainly described by 4 fracture sets:

- NS striking, subvertical (the oldest fracture set).
- ENE-WSW striking, subvertical.
- WNW-ESE striking, subvertical.
- Subhorizontal to moderately dipping, generally striking N-S to NNW.

Fracture domains were defined in order to better describe spatial variability of fracturing in the model volume. They are used to describe volumes with similar properties in terms of fracture intensity and orientation. The identification of the fracture domains in Laxemar is mainly steered by the location of major deformation zones and the relative intensity of fracture sets. Six separate fracture domains were distinguished within the local model volume, namely FSM\_C (central), FSM\_W (west), FSM\_N (north), FSM-S (south), FSM\_EW007 (closer to deformation zone ZSMEW007) and FSM\_NE005 (closer to ZSMNE005). Figure 2-8 shows a top view of the three-dimensional image of the fracture domain model with the deterministic deformations zones in the local model area. The same fracture domains are used in the rock mechanics description for rock mass properties. The fracture domains that will host the facility are described below.

**Fracture domain FSM\_C** is located in the central part of the volume in focus for the planned repository. It is delimited in the south and west by 2 major deformation zones, respectively ZSMNW042A and ZSMNS059A, and in the eastern and northern edges by fracture domains FSM\_EW007 and FSM\_NE005 (Figure 2-8). This fracture domain is dominated by N-S striking sealed fractures, in a similar way as in FSM\_W, and open WNW striking fractures (Figure 2-9 and Figure 2-10). The bedrock in this domain can be described as medium fractured rock including a mixture of crystalline rocks. In the northern part the main rock type is Ävrö quartz monzodiorite and in the south of this fracture domain the dominating rock type is quartz monzodiorite.

**Fracture domain FSM\_EW007** is a volume of rock that extends ca 250 m south and 100 m north of the deformation zone PZSNEW007A (Figure 2-8). Both fracture intensity and orientation have been interpreted to be affected by the deformation zone. This domain features a reduced intensity of both N-S striking fractures and open subhorizontally dipping fractures (Figure 2-9 and Figure 2-10). In this domain most open fractures appear to belong to the WNW set (Figure 2-10). The main rock type in FSM\_EW007 is Ävrö granodiorite, but there is a mixture with other rock types to some minor extent.

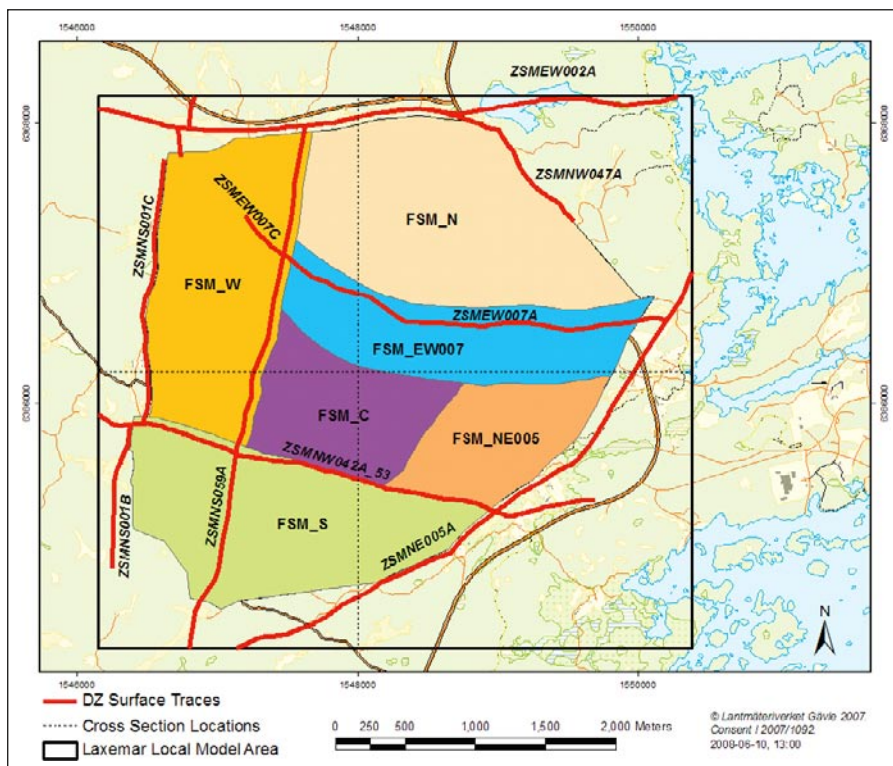
**Fracture domain FSM\_NE005** represents a volume of rock bounded at the eastern edge by the regional deformation zone ZSMNE005 and by ZSMNE107A in the west. The southern part of FSM\_NE005 makes up the footwall of ZSMNW042A (Figure 2-8). This domain is characterised by a significant increase of the relative intensity of N-S striking sealed fractures (Figure 2-9 and Figure 2-10), relative to the rest of the Laxemar local model area. The delimitation of the fracture domain to the south is the most uncertain due to paucity of data south of ZSMNW042A.

**Fracture domain FSM\_W** is delimited by four regional deformation zones, ZSMNS001C, ZSMNS059A, ZSMNW042A, and ZSMEW002A (Figure 2-8). It is characterised by a relative intensity increase of N-S striking sub-vertical as well as sub-horizontal fractures, (Figure 2-9 and Figure 2-10). The ENE fracture set is relatively subdued in intensity when compared to the rest of the Laxemar local model volume. Fundamentally this fracture domain represents a crustal block isolated by the major ENE and N-S sinistral tectonic structures.

The fracture frequency for the different fracture sets in the fracture domains is given in Table 2-6. The fracture intensity for the 4 orientation sets previously defined is provided in Table 2-7 for the fracture domains inside the focused volume.

### 2.3.1 Mechanical properties of fractures

The discrete fractures (commonly referred to as joints or discontinuities in underground engineering) within the fracture domains are classed as open and sealed. An extensive laboratory testing program has been carried out to characterise the mechanical behaviour of the discrete open fractures. These fractures were selected from core samples and were tested using direct shear tests. The tests were carried out at three normal stress levels (0.5, 5, 20 MPa) and hence the shear stiffness models vary with the normal stress. The results are valid for all fracture orientation and are summarised in Table 2-8. Note that the model may be considered valid only for the frequently occurring smaller fractures of the population and may not necessarily represent the main hydraulic conductors in the rock between the deformation zones /SKB 2009/.



**Figure 2-8.** Surface projection of SDM-Site Laxemar fracture domains (FSM\_x) and bounding deformation zones (ZSM\_x) in Laxemar (from /La Pointe et al. 2008/). The black box represents the limits of the Laxemar local model, while the colored polygons represent the surface limits of the fracture domains.

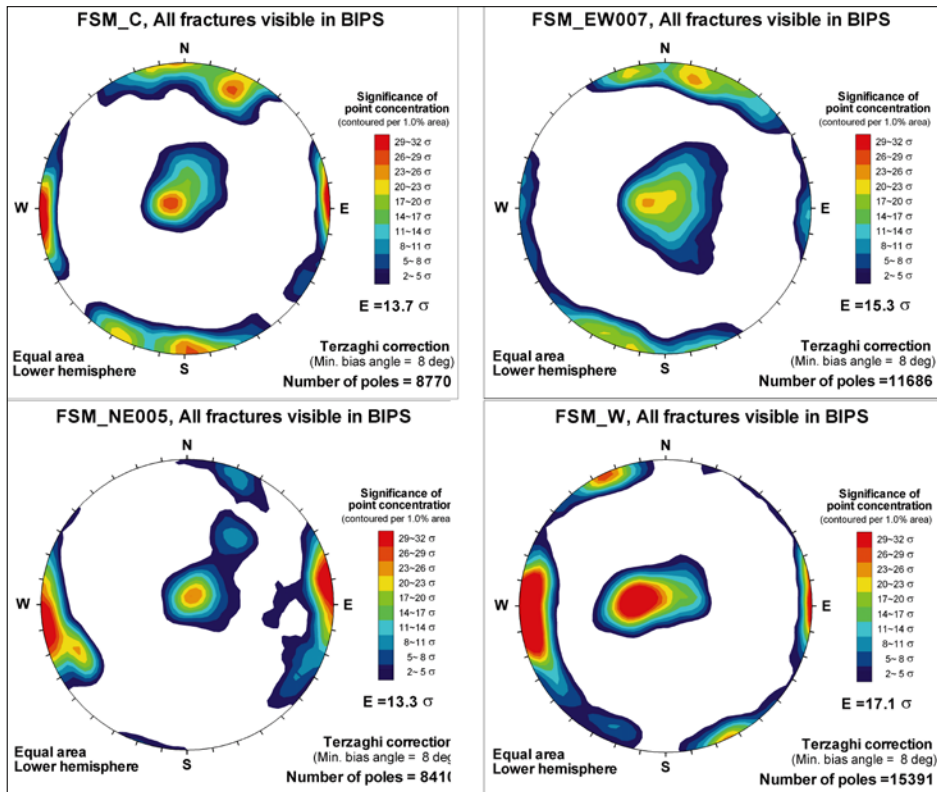


Figure 2-9. Stereographic projection (equal area, lower hemisphere) of poles to fracture planes in the different fracture domains in the focused volume. From /Wahlgren et al. 2008/. All fractures visible in BIPS are plotted.

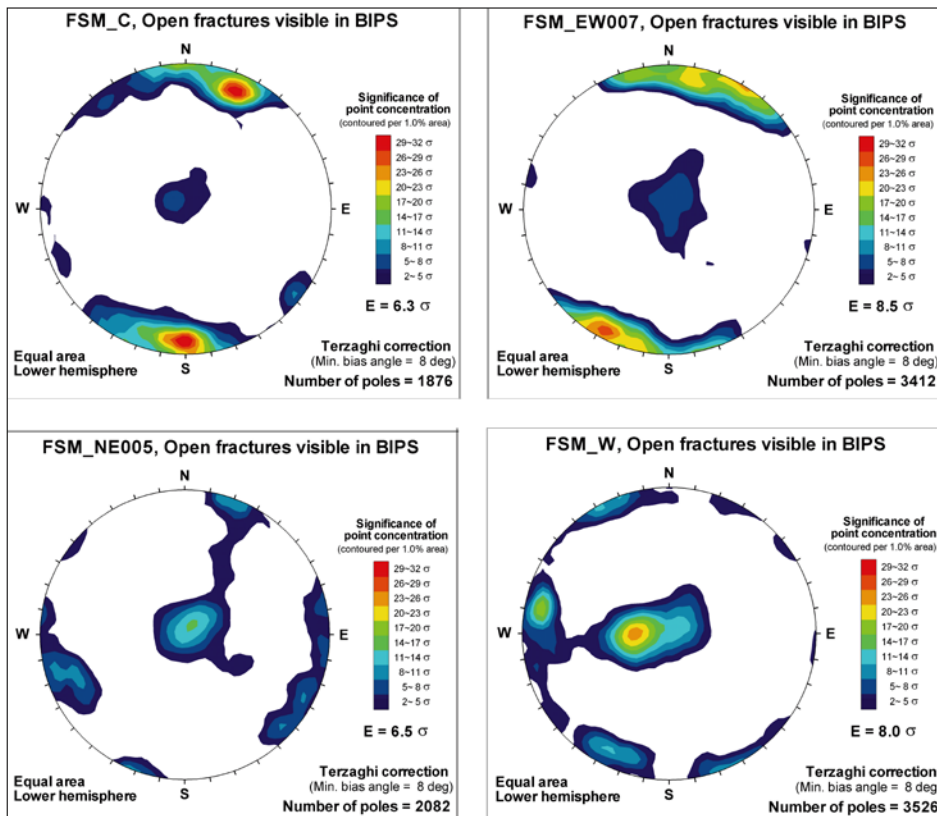


Figure 2-10. Stereographic projection (equal area, lower hemisphere) of poles to fracture planes in the different fracture domains in the focused volume. From /Wahlgren et al. 2008/. Only open fractures visible in BIPS are plotted.

**Table 2-6. Fracture frequency ( $P_{10}$ ) in the different fracture domains in the focused volume.**

$P_{10}$ (1/m)	Open fractures	Open + sealed fractures	All fractures <sup>(1)</sup>
FSM_C	1,17	4,65	7,46
FSM_EW007	1,78	5,98	10,28
FSM_NE005	1,40	5,15	9,62
FSM_W	1,35	5,06	7,42

(1) All mapped fractures inclusive partly open, sealed networks outside of deformation zones and fractures in crush.

**Table 2-7. Fracture intensity ( $P_{32}$ ) for the different fracture orientation sets in the fracture domains in the focused volume, from /La Pointe et al. 2008/.**

$P_{32}$ ( $m^2/m^3$ )	WNW	NS	ENE	SH
FSM_C	2.53	2.33	1.72	2.66
FSM_EW007	2.9	2.96	1.98	4.42
FSM_NE005	2.37	4.3	1.6	3.17
FSM_W	1.97	3.6	1.6	3.4

Note: it is important to remember that the  $P_{32}$  values are conditioned to a given size-intensity model, and that varying the size-intensity model impacts on the fracture intensity.

**Table 2-8. Summary of models for strength and deformation of fractures for SDM-Site Laxemar. The parameters are described as truncated normal distributions /SKB 2009/.**

Parameter <sup>1</sup>	Minimum	Mean	Maximum	Standard deviation
Normal stiffness $K_N$ (MPa/mm)	72	721	4,003	655 <sup>2</sup>
Shear stiffness $K_{SS}$ (MPa/mm)	11	26	49	9
Dilatancy angle, at 5 MPa (°)	2.5	8.3	15.4	2.9
Peak friction angle (°)	28.5	36.6	45.4	3.2
Peak cohesion (MPa)	0.3	0.9	2.5	0.4

<sup>1</sup> Note that this is only a selection of numbers and that all values are shown in Table 4-9 in /Hakami et al. 2008/.

<sup>2</sup> The distribution is much skewed towards high values, and thus the St. dev. is high compared to the mean.

### 2.3.2 Strength and deformation properties of fractured rock

The strength and deformation of the fractured rock mass has been evaluated using empirical approaches such as  $Q$ , RMR and GSI. A comparison of the  $Q$  and RMR values for the fracture domains outside deterministic deformation zones are provided in Table 2-9. The mean  $Q$  values in FSM\_C, FSM\_W and FSM\_NE005 class the rock mass as “Very good”. Similarly the mean RMR values class the same fracture domains as “Very Good (81–100)” /Bieniawski 1989/. Fracture domains N and EW007 are “good rock” quality rock according to the same classification. This table highlights the good quality of the rock mass in the focused volume.

The  $Q$  and RMR values were converted to strength and deformation properties of the fractured rock mass using traditional empirical approaches such as GSI. In addition, an independent assessment of the fractured rock strength was carried out using a numerical approach. The results of both approaches were harmonised. Table 2-10 provides estimated values for the strength and deformation characteristics of the fractured rock mass.

**Table 2-9. Estimated Q and RMR values of the rock mass in the fracture domains outside the deformation zones (Table 5-1 in /Hakami et al. 2008/).**

Fracture domain <sup>1</sup>	FSM_C	FSM_W	FSM_N	FSM_EW007	FSM_NE005
	Mean/std. dev. Min-max	Mean/std. dev. Min-max	Mean/std. dev. Min-max	Mean/std. dev. Min-max	Mean/std. dev. Min-max
Q <sup>2</sup>	53.5 6.9–704	87.0 11.4–87.0	17.6 3.4–150	29.7 0.9–528	75.7 3.5–264
RMR	82.0/3.6 68.9–90.9	83.2/1.8 70.5–83.8	77.0/5.5 66.2–87.9	77.7/5.1 63.0–88.7	82.5/6.5 60.2–90.0

- 1) The Rock Mass properties in the domains do not include the effects of MDZ. MDZ properties are described separately.  
2) For Q, the most frequent value is reported instead of the average.

**Table 2-10. Strength and deformation properties of the rock mass outside deformation zones in the two groups of fracture domains /SKB 2009/.**

Properties of the rock mass	FSM_C, FSM_W and FSM_NE005	FSM_N and FSM_EW007
	Mean/std. dev. Min-max <i>Uncertainty of mean</i>	Mean/std. dev. Min-max <i>Uncertainty of mean</i>
Deformation	59/12	50/14
Modulus [GPa]	35–83 ±3%	22–78 ±3%
Poisson's ratio [-]	0.3/0.04 0.22–0.34 ±10%	0.3/0.03 0.24–0.36 ±10%
Uniaxial compressive strength (Hoek&Brown) [MPa]	51/14 23–79 ±14%	42/12 18–66 ±14%
Tensile strength (Hoek&Brown) [MPa]	1 0–8 <sup>2)</sup> 0.5–5 <sup>3)</sup>	0.5 0.2–1.5 <sup>2)</sup> 0–2.5 <sup>3)</sup>
Friction angle <sup>4)</sup> [°]	43/3 37–49 ±3%	42/2.5 37–47 ±3%
Cohesion <sup>4)</sup> [MPa]	18/2.5 13–23 ±7%	17/2 13–21 ±7%

- 1) The rock mass properties in the domains do not include the effects of DZ and MDZ, see text.  
2) Minimum and maximum expected tensile strength (no Stand. dev given due to uncertainty in distribution).  
3) The mean tensile strength is expected in this range, which describes the uncertainty.  
4) For confinement stress between 10 and 30 MPa.

## 2.4 In-Situ Stress

Direct stress measurements have been performed using both overcoring and/or hydraulic stress measurements methods in several boreholes. Note that both methods have only been used in one borehole in the focused area (KLX12). The estimated stress gradients based on those results are given in Table 2-11. These stress gradients are similar to the stress magnitudes and orientations found at Äspö see /Ask 2006/. The model is only applicable to the focused volume, i.e. the three fracture domains effectively bounded by the main deformation zones ZSMNS001C, ZSMNE005A, ZSMNW042 and fracture domain FSM\_EW007. The stress magnitudes and orientation suggest that the minimum horizontal stress is approximately the same as the vertical stress suggesting a strike-slip geological regime.

**Table 2-11. Stress model for domains FSM\_C, FSM\_W, FSM\_NE005, at 400–700 m depth. The stress magnitude is modelled as a function of vertical depth, z /SKB 2009/.**

Parameter	Most likely value (mean value)	Estimated uncertainty (in mean value)	Upper limit at 400 m depth	Local stress variability (st. dev. of a normal dist. around the local mean value)
<b>Magnitude</b>				
Major horizontal stress, $\sigma_H$	$0.039z + 3$ MPa	$\pm 20\%$	31–34 MPa <sup>1)</sup>	12%
Minor horizontal stress, $\sigma_h$	$0.022z + 1$ MPa	$\pm 20\%$		13%
Vertical stress, $\sigma_v$	$0.027z$ MPa	$\pm 3\%$		15%
<b>Orientation</b>				
Major horizontal stress trend, $\sigma_H$	$135^\circ$	$\pm 15^\circ$		$\pm 15^\circ$

1) Depending on the dominating rock type, lower value in RSMM01 and higher in RSMD01.

To evaluate the possibility of elevated stress magnitudes at the repository depth, the stresses are provided as uncertainty spans on the mean value at three different depths in Table 2-12. These magnitudes can be used to provide a “Maximum Stress Model” that should only be used in assessing the risks associated with spalling for the depth range given in Table 2-12. When combining the stress magnitudes in Table 2-12 for probability analyses, the ratio of maximum to minimum horizontal stress should be constrained between 2.5 and 4.5.

## 2.5 Hydraulic properties

The bedrock is divided into 3 hydraulic domains which are:

- HCD (Hydraulic Conductor Domain) represents deformation zones,
- HRD (Hydraulic Rock mass Domain) represents the fracture domains between the deformation zones and
- HSD (Hydraulic Soil Domain) represents the overburden.

The systems approach constitutes the basis for the conceptual modelling, the site investigations and the numerical simulations carried out in support of the SDM.

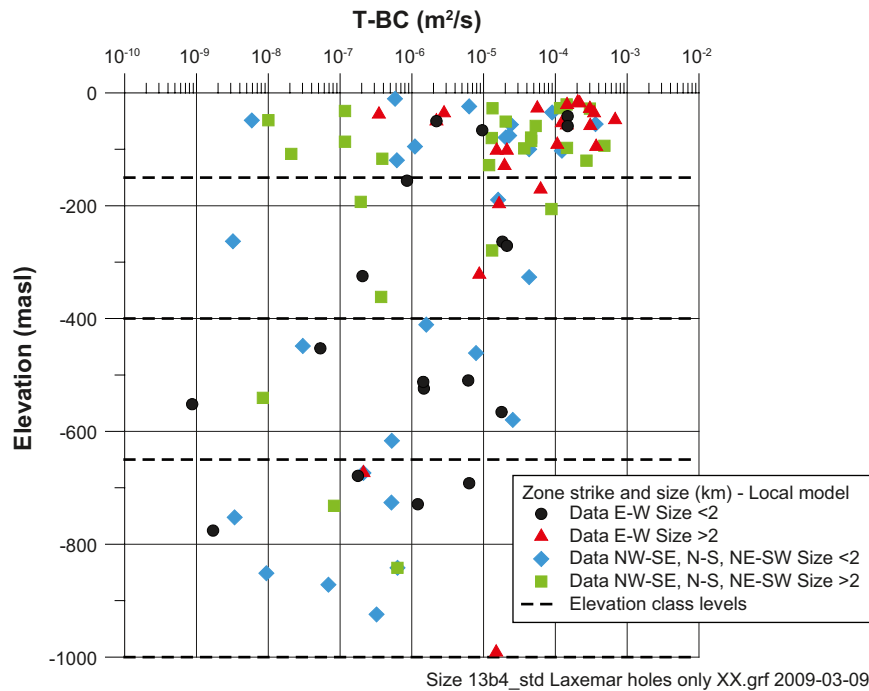
### 2.5.1 Deterministically modelled deformation zones – HCDs

The geometry of the HCDs of the hydrogeological model essentially coincides with the deformation zones (DZ) modelled deterministically in the SDM-Site Laxemar DZ model. Hydraulic information is available for a large number of these deformation zones, but not all.

Deformation zones transmissivities as a function of orientation and size of DZ are presented in Figure 2-11. Few gently dipping deformation zones have been identified in the local model and their transmissivity (both magnitude and variation) does not seem to differ much from other HCD.

**Table 2-12. Stress model for domains FSM\_C, FSM\_W, FSM\_NE005 /SKB 2009/. The stress magnitudes and orientations are here given as uncertainty span for the mean stress values at three different depths (cf. Table 2-11).**

Depth	400 m	500 m	600 m
<b>Magnitude, MPa</b>			
Major horizontal stress, $\sigma_H$	14.9–22.3	18.0–27.0	21.1–31.7
Minor horizontal stress, $\sigma_h$	7.8–11.8	9.6–14.6	11.4–17.0
Vertical stress, $\sigma_v$	10.5–11.1	13.2–14.0	15.7–16.7
<b>Orientation</b>			
Major horizontal stress trend, $\sigma_H$	$120^\circ$ – $150^\circ$	$120^\circ$ – $150^\circ$	$120^\circ$ – $150^\circ$



**Figure 2-11.** Deformation zone transmissivity ( $T$ ) related to deformation zone orientations in the horizontal plane and size, versus elevation /Rhén et al. 2008/.

Figure 2-12 shows clearly evident depth trends in the transmissivity data, both overall, and for the identified groups, that spans 5 orders of magnitude from  $10^{-3}$  to  $10^{-8}$   $m^2/s$  near the surface, to  $10^{-5}$  to  $10^{-9}$   $m^2/s$  at a depth of  $-500$  m. A slightly increased transmissivity is seen for orientation set EW compared with the NW-SE, NS and NE-SW sets. This is in part explained by the notably increased transmissivity of deformation zone ZSMEW007A foremost.

Figure 2-12 also shows that the transmissivity seems to increase with the HCD size, but the variation is great.

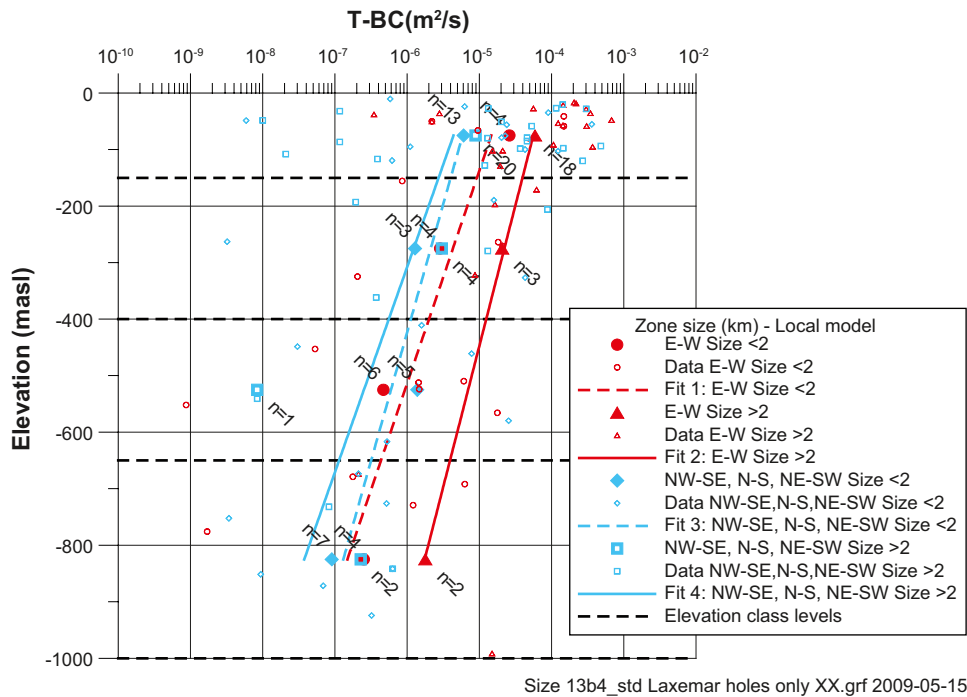
It should be noted that within the local model the number of boreholes intercept with deformation zones below  $-150$  m is limited thus making the depth trend uncertain.

However Figure 2-13 illustrates the significant variability of transmissivity within a HCD. Increased transmissivity is often related to an increased intensity of flowing fractures in the deformation zone. Estimated transmissivity for deterministic deformation zones as well as its estimated variation towards depth are presented in detail in /Rhén et al. 2008/.

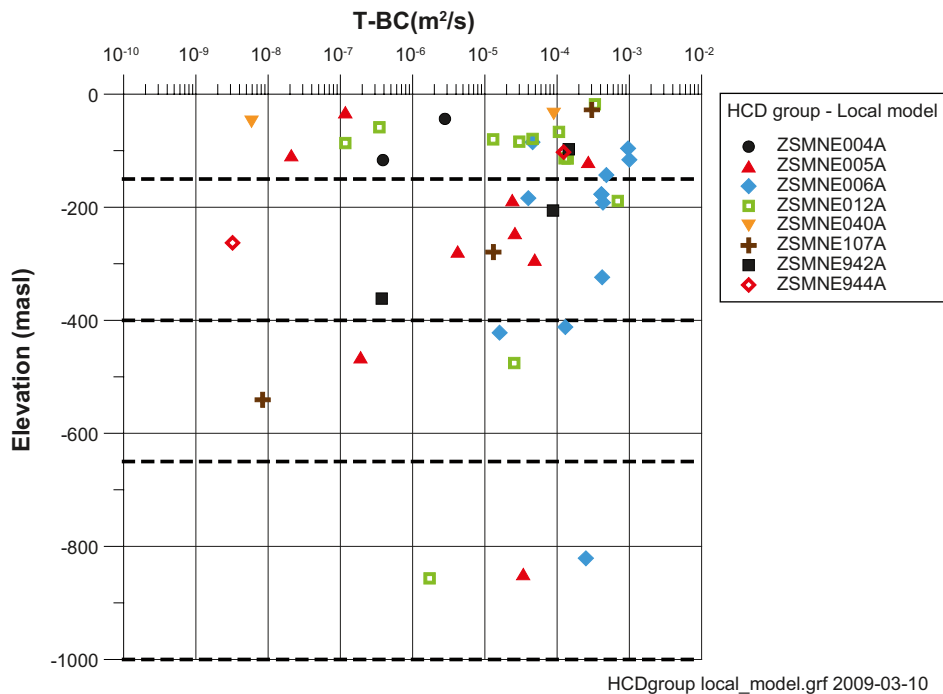
The existence of dolerite dykes as hydraulic barriers have been proven by cross-hole test results. However it is highly uncertain if they are barriers over long distances. Larger dykes have been identified in conjunction with deformation zones ZSMNS001C, ZSMNS059A, klx\_19\_dz5-8). The core of the dykes has a low hydraulic conductivity whereas the flanking contacts that are more fractured seem to be more conductive.

### 2.5.2 Minor deformation zones (MDZ)

Deformation zones interpreted from the geological extended single-hole interpretation that are not deterministically modelled are systematically considered as minor deformation zones (MDZ). These features are integrated in the hydrogeological DFN developed to model the hydraulic rock domains. However as the thickness of these features is not negligible (range of 1–10 m according to /Rhén et al. 2008/), a more detailed analysis of the hydraulic character and spatial distribution of flowing single fractures within a MDZ is of interest for grouting purposes.



**Figure 2-12.** Deformation zone transmissivity ( $T$ ) related to deformation zone orientations in the horizontal plane and size, versus elevation. Data points and statistics. For each depth interval the number of observations ( $n$ ), geometric mean  $T$  (Mean), 95% confidence limits for mean  $\log_{10}(T)$  (vertical bars on horizontal line) and  $\pm 1$  standard deviation  $\log_{10}(T)$  (entire horizontal line) are plotted. The line is fitted to the 4 Geometric mean values of the respective depth interval /Rhen et al. 2008/.



**Figure 2-13.** HCD transmissivity ( $T$ ) versus elevation: Transmissivity for HCDs with more than 1 borehole intercept plotted /Rhen et al. 2008/.



According to /Rhén et al. 2008/, about 60% of the MDZs can be expected to have a conductive feature with a transmissivity  $T > 10^{-9} \text{ m}^2/\text{s}$ , i.e. the MDZ are usually hydraulically significant features. Their total transmissivity seems to increase in relation to the number of flowing fractures within the MDZ. The total transmissivity (sum over the apparent thickness) of a MDZ decreases weakly with depth, but the confidence limits do nearly not support this depth dependency, see Figure 2-14. However, on average, one can expect that the total transmissivity of a MDZ decreases by depth as the frequency of MDZ without PFL-f features increase by depth.

### 2.5.3 Hydraulic Rock mass Domains

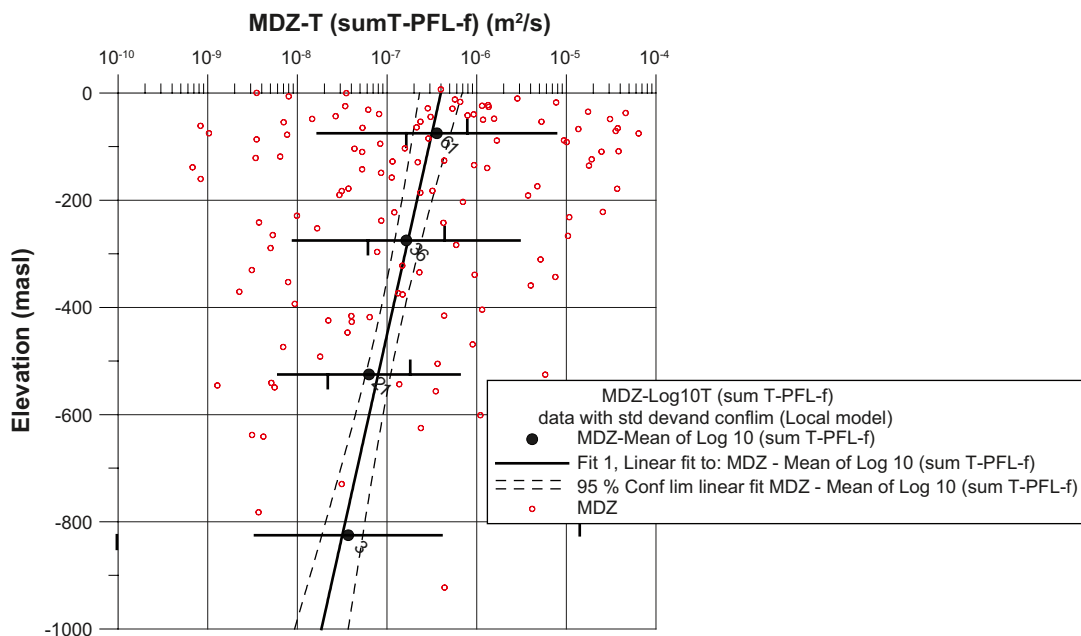
The HRD coincide with the fracture domains defined by geologists, except that hydraulic data provided arguments for combining FSM\_C, FSM\_NE005 and FSM\_S into one single hydraulic rock mass domain named HRD\_C, see Figure 2-15 and Figure 2-16. Other hydraulic rock mass domains are HRD\_N (coinciding with fracture domain FSM\_N), HRD\_EW007 (coinciding with fracture domain FSM\_EW007), HRD\_W (coinciding with fracture domain FSM\_W).

Detailed analysis of conductive fracture frequency and transmissivity data in primarily HRD\_C and HRD\_W entailed definition of the depth zones 1 to -150 m, -150 to -400 m, -400 to -650 m, and  $< -650 \text{ m}$ . The site descriptive model provides hydraulic properties for the hydraulic rock domains as a function of depth (Table 2-13).

The flowing fracture frequency and mean hydraulic conductivity (expressed as  $\Sigma T/L$ ) decrease monotonously with depth in hydraulic rock domains HRD\_W and HRD\_C. In HRD\_EW007 the trend is not as constant but at depth the mean hydraulic conductivity is almost insignificant.

#### Upper 150 m

The upper 150 m of rock generally have quite high frequency of connected and conductive fractures. In the three HRDs the linear frequency of flowing fractures is between 0.5 to 0.82  $\text{m}^{-1}$ , and the mean hydraulic conductivity is between 2 and  $3 \cdot 10^{-7} \text{ m/s}$ , see Table 2-13.



**Figure 2-14.** Total transmissivity (sum of T-PFL-f) of a MDZ versus elevation. For elevation intervals following parts are plotted: mean  $\log_{10}(T(\text{sum T-PFL-f}))$  (or  $\text{std } \log_{10}(T(\text{sum T-PFL-f}))$ ), confidence limits for mean  $\log_{10}(T(\text{sum T-PFL-f}))$  (vertical bars on horizontal line) and  $\pm 1$  standard deviation of mean  $\log_{10}(T(\text{sum T-PFL-f}))$ , (entire horizontal line). Curves are fitted to the 4 mean (or 4 standard deviation values) and the confidence intervals for fitted lines are shown. The mean and standard deviation is based on the number of samples shown near the mean value. Confidence intervals for fitted lines are shown for lines fitted to the 4 interval means (or std). From /Rhén et al. 2008/.

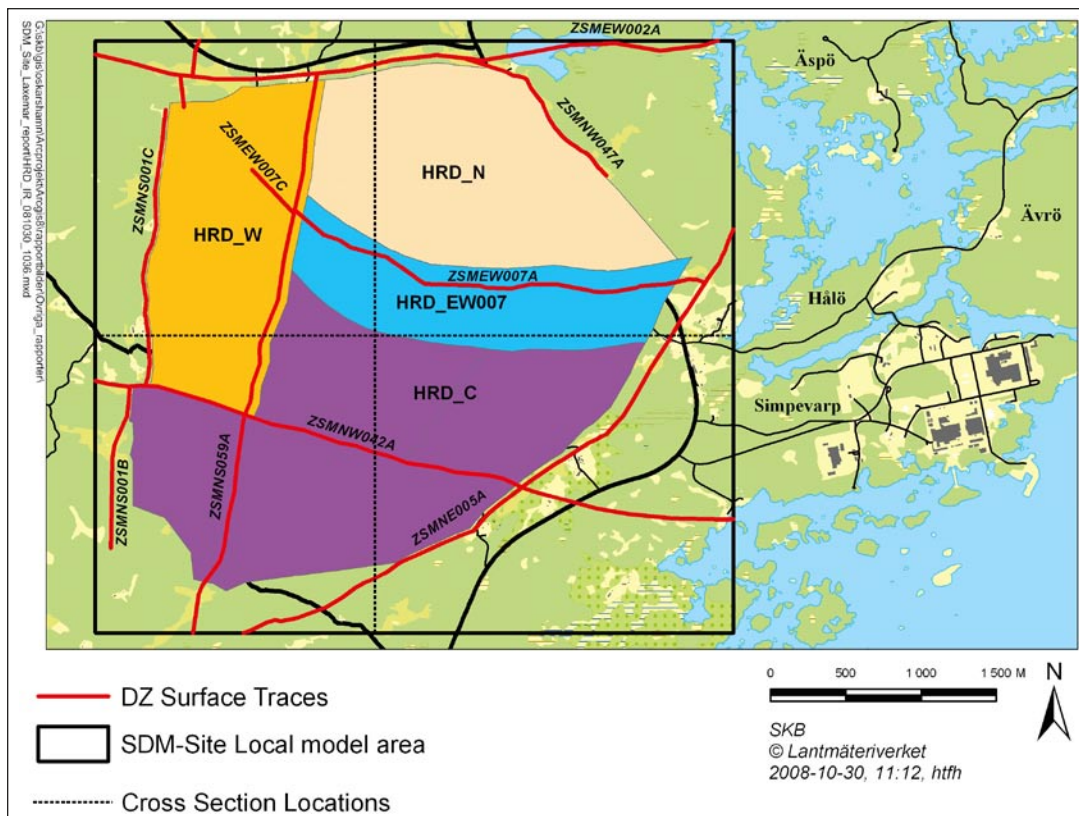


Figure 2-15. Illustration of the Hydraulic Rock Domains /SKB 2009/.

Table 2-13. Summary of flowing fracture transmissivity statistics for the different HRD.  $P_{10,PFL}$  denotes the linear fracture frequency [ $m^{-1}$ ], T denotes transmissivity [ $m^2/s$ ]. Compiled from Tables 9-12 and 9-13 in /Rhén et al. 2008/.

HRD	$\Sigma$ BH Length (m)	No. of flowing Features	Flowing feature frequency ( $P_{10,PFL}$ ) (corrected)	$\Sigma T/L$ (m/s)	Min T ( $m^2/s$ )	Max T ( $m^2/s$ )	Mean LogT	SD logT
<b>HRD_C</b>								
50–150	741	236	0.564	2.1E-07	3.9E-10	3.8E-05	-7.5	1.1
150–400	1,451	122	0.164	2.4E-08	3.7E-10	1.2E-05	-7.9	1.1
400–650	1,655	68	0.107	3.4E-09	3.3E-10	1.1E-06	-8.1	0.9
650–1,000	1,384	8	0.008	5.5E-10	1.5E-09	4.4E-07	-7.6	0.8
<b>HRD_W</b>								
50–150	1,282	379	0.499	2.8E-07	3.7E-10	4.6E-05	-7.5	1.0
150–400	904	33	0.078	2.9E-08	1.1E-09	1.0E-05	-7.9	1.2
400–650	677	23	0.060	2.8E-08	6.7E-10	9.2E-05	-7.5	1.4
650–1,000	272	1	0.005	1.4E-11	3.7E-09	3.7E-09	-8.4	N/A
<b>HRD_EW007</b>								
50–150	279	107	0.816	3.1E-07	4.4E-10	3.2E-05	-7.4	1.2
150–400	1,001	241	0.550	1.2E-07	3.1E-10	3.7E-05	-7.5	0.9
400–650	843	72	0.225	1.2E-08	7.9E-10	1.8E-06	-7.6	0.7
650–1,000	213	1	0.000	0	0	0	N/A	N/A

### Between 150 m and 400 m

The flowing fracture frequency as well as the average hydraulic conductivity decreases significantly in HRD\_C and HRD\_W below 150 m, see Table 2-13. However this table enhances differences in the geometry of the connected network between these 2 hydraulic rock domains. Meanwhile the mean hydraulic conductivity is almost similar at this depth interval, the flowing fracture frequency is much lower in HRD\_W, meaning that there are fewer but highly conductive features compared to HRD\_C.

In HRD\_EW007 the flowing fracture frequency is still significant compared to the other hydraulic domains and the mean hydraulic conductivity is still in the same range as in the upper 150 m of rock, which means that there are quite many connected conductive fractures in this depth interval.

**Between 400 m and 650 m**

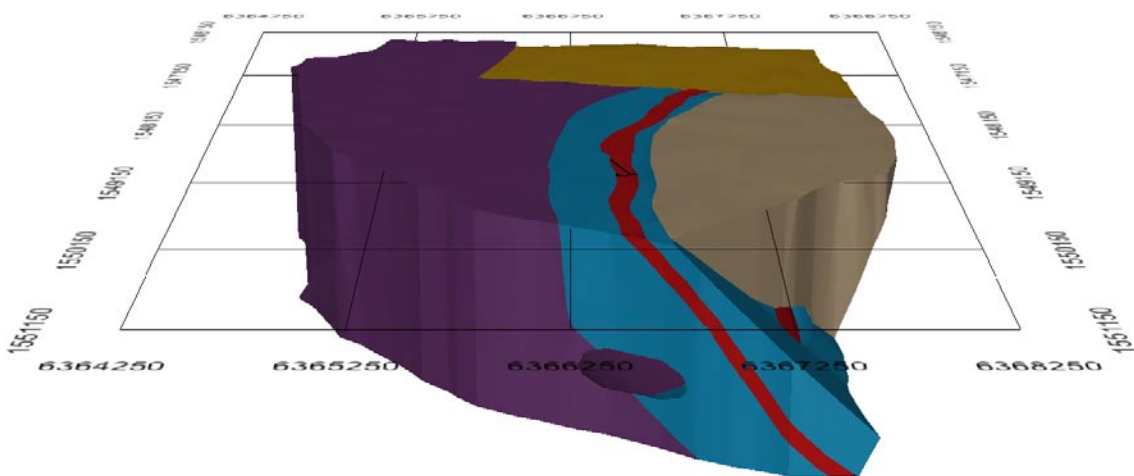
Below 400 m both flowing fracture frequency and average hydraulic conductivity are lower. The low frequency of flowing fractures ( $< 0.005 \text{ m}^{-1}$ ) and low mean hydraulic conductivity in the order of  $1.4 \cdot 10^{-11} \text{ m/s}$  or less in both HRD\_W and HRD\_EW007 suggest that the rock mass between deterministic deformation zones approaches the permeability of the intact rock.

**Below 650 m**

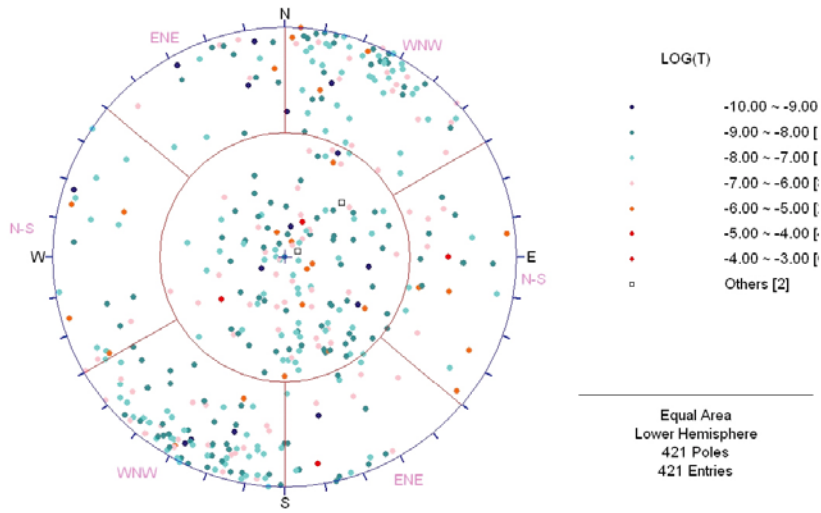
Below 650 m there are few conductive features. No flowing features are recorded in HRD\_EW007 below 650 m. However, data from these depths are relatively scarce, making the statistics uncertain and the occurrence of low transmissive fractures in this depth interval cannot be excluded.

It should also be noted that the flowing fracture frequency could be used to estimate the number of flowing features along a certain tunnel distance. At least approximately this number follows a Poisson distribution with mean  $\text{Dist} \cdot P_{10\text{PFL}}$ . There is a strong consistent theme for most of the hydraulic rock domains (and subordinate fracture domains) that PFL-f features is the WNW set, and with SH usually as the secondary set, see Figure 2-17. However, for FSM\_W, the dominant set for PFL-f features is the SH set.

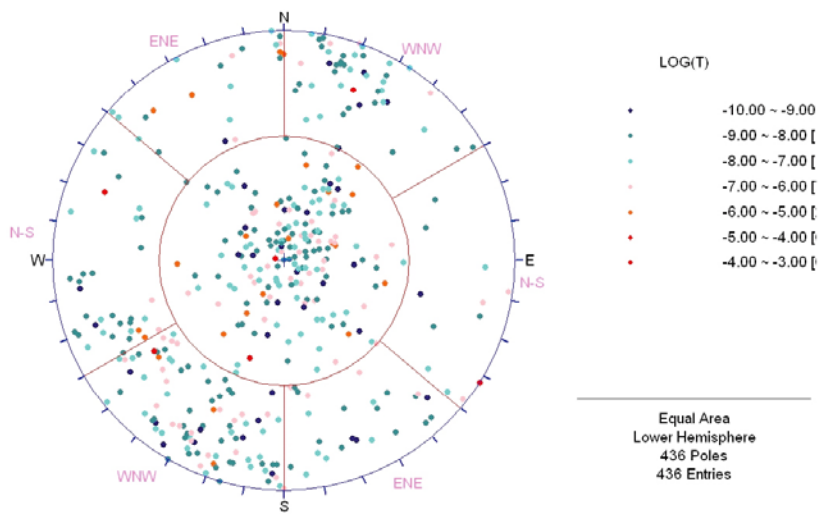
Using this basic data a hydrogeological discrete fracture network (DFN) model is developed. These models are primarily developed for use in safety assessment, but are also essential for estimating the inflow distribution to deposition holes – and thus for estimating loss of canister positions. In addition to the discrete fracture network model part of the SDM, an equivalent continuous porous medium model (ECPM) was developed in order to estimate total inflow in simulated deposition holes or tunnel sections. These results are significant input to the ground engineering model. Realisations of water-bearing fractures described by the hydrogeological DFN model have been simulated in accordance to the methodology described in /Stigsson 2009/. The simulations reflect the conditions between 400 and 650 m depth. Sampling of transmissivities along 20 m and 100 m long horizontal scan lines in the main orientation of deposition tunnels ( $130^\circ$ ), as well as 8 m vertical scanlines has been carried out and are presented in respectively Table 2-14, Table 2-15 and Table 2-16 for 3 hydraulic rock domains HRD\_C, HRD\_W and HRD\_EW007. Results are given for the DFN-model assuming only a statistical correlation between fracture size and transmissivity (correlated) /Stigsson 2009/, which is judged to give a more realistic model for prediction of groutability.



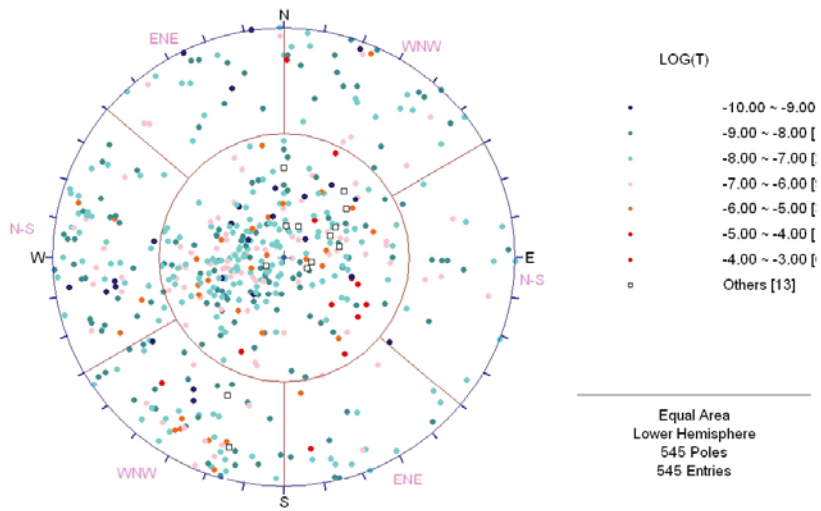
**Figure 2-16.** Illustration of the SDM Site Laxemar Hydraulic Rock Domain Model, 3D view looking westward /SKB 2009/.



a) FSM\_EW007



b) HRD\_C



c) FSM\_W

Figure 2-17. Orientation of flowing fractures in hydraulic rock domains a) HRD\_EW007, b) HRD\_C and c) HRD\_W.

## 2.6 Groundwater composition

Explorative analyses of measured groundwater chemistry data and hydrogeochemical modelling have been used to evaluate the hydrogeochemical conditions at the site in terms of the origin of the groundwater and the processes that control the water composition.

The major groundwater feature is that the groundwater composition is mainly a result of transport (mixing) of groundwaters of different origins. The major groundwater characteristics are summarised in Figure 2-18.

## 2.7 Summary

In this section a summary of the rock mass descriptions and properties have been provided based on the SDM-Site Laxemar and related documents. In all cases the source of the data used to produce parameter values associated with that description have been provided. In Chapter 4 these data provide the basic input that was used to establish the ground engineering description.

**Table 2-14. Tabulated numbers of 20 m horizontal sections with total transmissivity in the given intervals. Compiled from /Stigsson 2009/.**

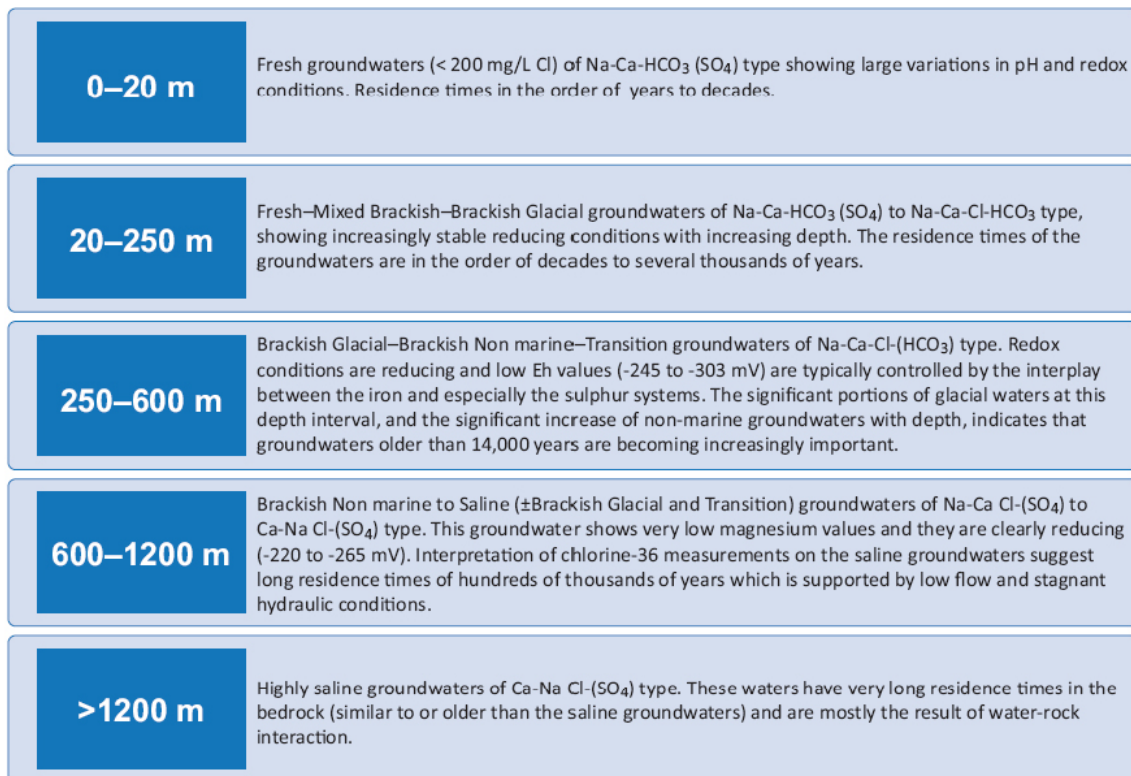
	model	$< 4 \cdot 10^{-9}$	$4 \cdot 10^{-9} - 3 \cdot 10^{-8}$	$3 \cdot 10^{-8} - 2 \cdot 10^{-7}$	$2 \cdot 10^{-7} - 5 \cdot 10^{-7}$	$5 \cdot 10^{-7} - 1 \cdot 10^{-6}$	$> 1 \cdot 10^{-6}$
HRD_C	corr	0.39	0.13	0.29	0.11	0.05	0.03
HRD_W	corr	0.58	0.07	0.19	0.06	0.03	0.07
HRD_EW007	corr	0.09	0.02	0.12	0.26	0.32	0.19

**Table 2-15. Tabulated numbers of 100 m horizontal sections with total transmissivity in the given intervals. Compiled from /Stigsson 2009/.**

	model	$< 4 \cdot 10^{-9}$	$4 \cdot 10^{-9} - 3 \cdot 10^{-8}$	$3 \cdot 10^{-8} - 2 \cdot 10^{-7}$	$2 \cdot 10^{-7} - 5 \cdot 10^{-7}$	$5 \cdot 10^{-7} - 1 \cdot 10^{-6}$	$> 1 \cdot 10^{-6}$
HRD_C	corr	0.02	0.02	0.18	0.28	0.26	0.24
HRD_W	corr	0.10	0.04	0.21	0.19	0.13	0.33
HRD_EW007	corr	0.000	0.000	0.002	0.002	0.017	0.979

**Table 2-16 Tabulated numbers of 8 m vertical sections with total transmissivity in the given intervals. Compiled from /Stigsson 2009/.**

	model	$< 4 \cdot 10^{-9}$	$4 \cdot 10^{-9} - 3 \cdot 10^{-8}$	$3 \cdot 10^{-8} - 2 \cdot 10^{-7}$	$2 \cdot 10^{-7} - 5 \cdot 10^{-7}$	$5 \cdot 10^{-7} - 1 \cdot 10^{-6}$	$> 1 \cdot 10^{-6}$
HRD_C	corr	0.69	0.07	0.11	0.06	0.03	0.04
HRD_W	corr	0.77	0.02	0.06	0.03	0.03	0.09
HRD_EW007	corr	0.38	0.06	0.28	0.20	0.07	0.01



**Figure 2-18.** Major groundwater characteristics and their applicable depth intervals. Note that the above depth intervals differs slightly from the depth zones introduced by hydrogeology, see Section 2.5 /SKB 2009/.

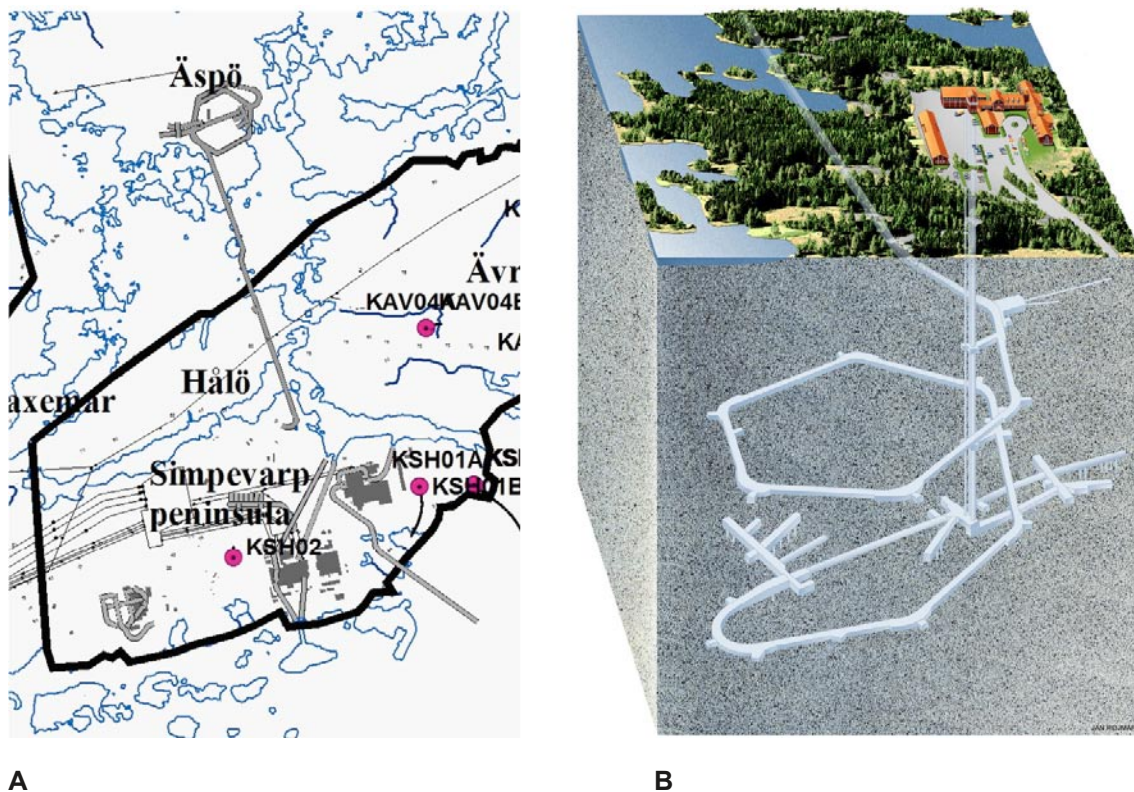
### 3 Overview of tunnelling experiences from the Oskarshamn area

/Carlsson and Christiansson 2007/ summarised the underground construction experiences from the Simpevarp area and Äspö Hard Rock Laboratory (HRL). These experiences cover projects with excavations down to 460 m depth (Figure 3-1). Tunnels for intake and discharge of the cooling water for the nuclear power plants were excavated at shallow depths across the Simpevarp peninsula at two locations. To the southwest of the peninsula two caverns were constructed for the Central Intermediate Storage of Spent Fuel (Clab). There is also a facility for intermediate storage of operational waste (BFA) located close to Clab. The largest depth excavated for these facilities was approximately 50 m. The underground works include a total excavated volume of 405,000 m<sup>3</sup> rock and more than 4 km of tunnels.

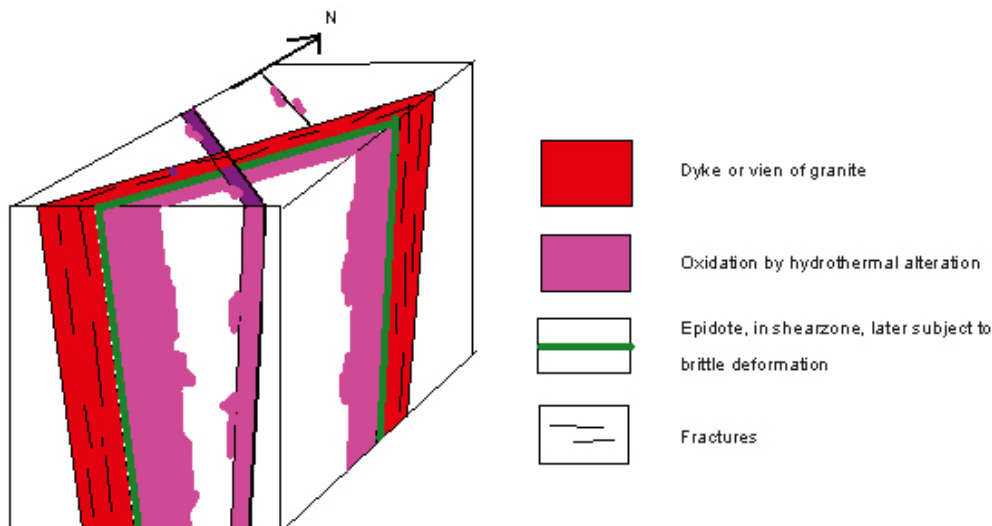
The access portal to the Äspö HRL is located on the Simpevarp peninsula. The access tunnel/ramp was at 200 m depth when it reached the Äspö island, where a spiral ramp was used to access the research area located at a depth of 400–450 m. The total length of the tunnel/ramps is approximately 4 km. In addition, the Äspö HRL also consists of a drill-and-blast access shaft and two raise-bored ventilation shafts.

#### 3.1 Steeply dipping highly conductive fractures

There were no significant grouting problems reported from the construction of the underground facilities in the Simpevarp peninsula. Water was observed in several joint sets during construction. It was reported that the N-S to NE-SW, steeply dipping fractures associated with the granitic veins tended to be more water-bearing, (Figure 3-2). Gently dipping fractures in the superficial rock mass were also reported to have a tendency to cause seepage into the underground openings.



**Figure 3-1.** Overview of the underground facilities in the Oskarshamn area. A) Plan view of the underground facilities at Äspö HRL, Clab and tunnels for nuclear power stations. B) Isometric view of Äspö HRL to a depth of 460 m.



**Figure 3-2.** Simplified illustration of the structure of the partly water-bearing steeply dipping granitic dykes observed in for example the Clab facility /Carlsson and Christiansson 2007/.

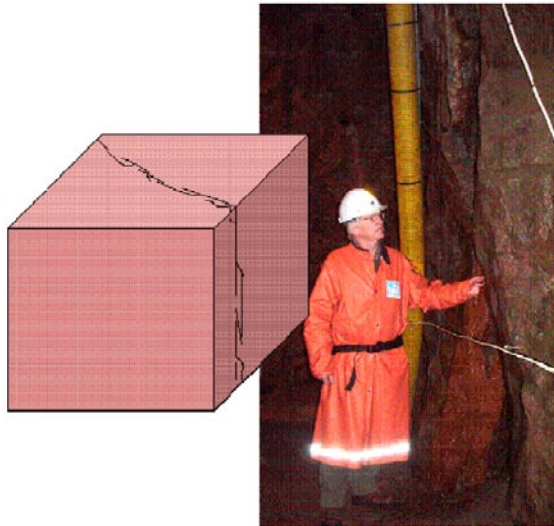
Records from systematic grouting are only available from the second cavern construction of Clab that was completed in 2000. The cavern is approximately 115 m long with a cross sectional area of approximately 700 m<sup>2</sup>. The excavation was carried out with one central tunnel with side slashing for the gallery, and four benches. Systematic probing and pre-grouting was carried out for all excavation sequences. In total, 19,600 litres of normal cement grout was used, and the resulting seepage to the Clab2 cavern was measured at 7–8 l/min at the end of the construction period. The total seepage to the rest of the facility (access tunnels and the Clab1 cavern) was 40 l/min. The total inflow to the facility increased slightly after construction of the second cavern.

The access ramp for the Äspö HRL encountered a highly transmissive deformation zone, NE1 at a depth of approximately 170 m. A drilling program determined that the structure could be characterised as a 8 m thick core with highly fractured and crushed, partly altered rock, surrounded by 15 m transition zones on either side of the core. The core was composed of granite, mylonite and fault gauge. Prior to grouting, transmissivity values ranging from 4–5 10<sup>-4</sup> m<sup>2</sup>/s were recorded in the cored boreholes penetrating the zone. The estimated mean hydraulic conductivity was 8.8 10<sup>-4</sup> m/s for the core and 1.8 10<sup>-4</sup> m/s for the transition zones.

The water-bearing fractures observed at below 400 m depth at the Äspö HRL are primarily observed in the NW-SE steeply dipping joint set, even though other fracture sets are present. This fracture set is very rough with a large undulation, wave length and amplitude can be > 1 m respectively 20–30 cm. Water flow along these fractures frequently occurs in channels as can be observed in many sections of the TBM tunnel. It is common to find splays and parallel fractures within short distances along this fracture set (see Figure 3-3). Fracture statistics for the NW-SE joint set show a bimodal distribution in orientation that varies by approximately 20°. It is likely that this bimodal distribution for the orientation is caused by the large undulations and the multiple fractures that are often encountered. For example in Figure 3-3 there are some 4–5 parallel fractures at the location of the person's left hand, but only 30 cm above this point there is only one single fracture. This heterogeneity within short distances causes uncertainties in interpreting borehole orientation observations.

The grouting conducted at the Äspö HRL was not optimised for construction purposes as there were restrictions on the grout spread. The main purpose of the grouting was to minimise the impact of the construction on the natural hydraulic and hydrogeochemical conditions. In general, probing was done at the tunnel phase every fourth round. Grouting was carried out selectively in the boreholes that yielded the most water. Pressures and volumes were normally restricted. This was also the approach used during the passage of the highly conductive NE1.





**Figure 3-3.** Photo along a NW-SE trending, steeply dipping fracture at the 450 m level in the Äspö HRL /Carlsson and Christiansson 2007/. The surface closest to the yellow pipe is also a fracture surface. Notice the red stain at the lower part, caused by precipitation of iron oxide.

### 3.2 Distribution of water-bearing structures

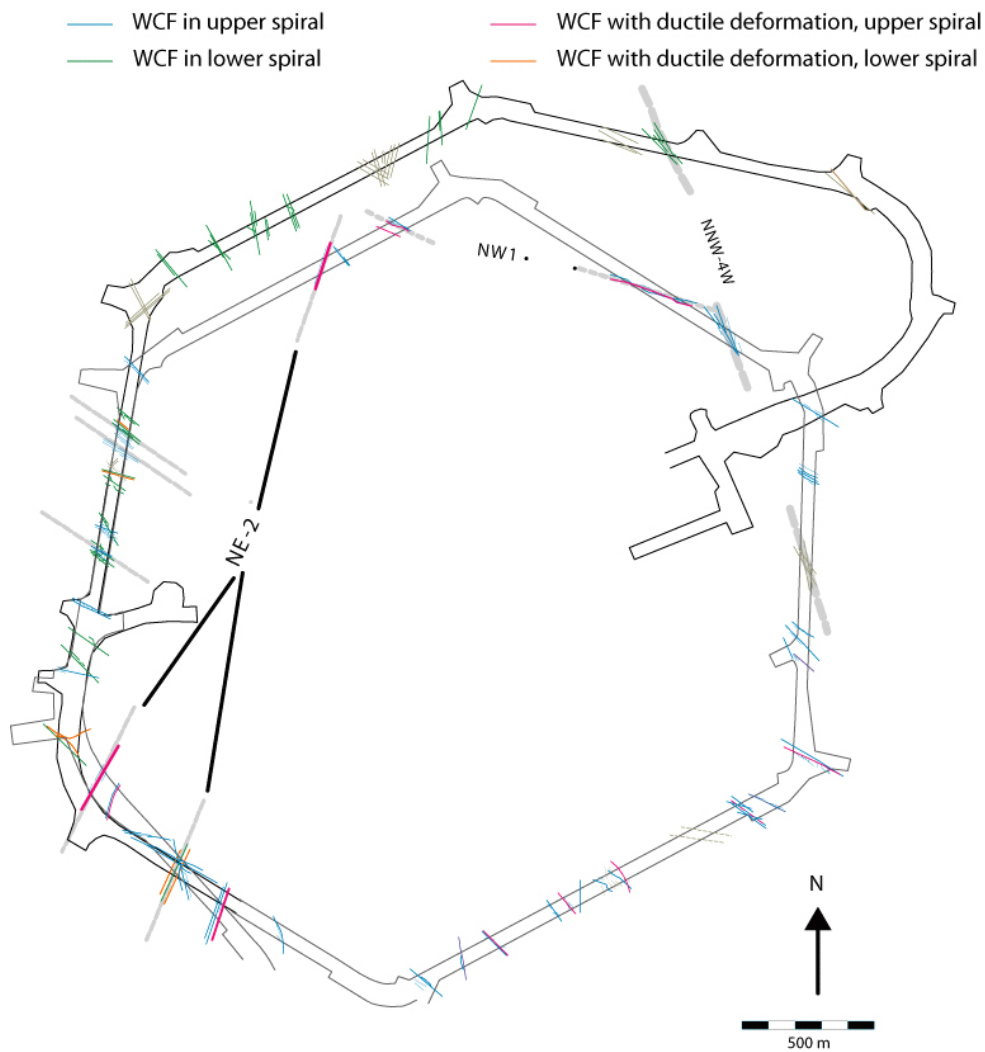
There is an extensive documentation of the distribution of water-bearing fractures from the Äspö HRL. The characterisation of new experimental areas at approximately 450 m level illustrates the water-bearing capacity of individual fractures encountered in cored holes (normally 76 mm). In two examples where exploration boreholes for new tunnels were drilled approximately perpendicular to the major horizontal stress and the NW-SE water-bearing fractures, 100 m long boreholes produced between 20 and 150 l/min. In the investigations for the APSE tunnel a 90 m long borehole recorded a total inflow of 80 l/min /Emmelin et al. 2004/. Flow log measurements with the Posiva flow log (PFL) recorded 25 seeping sections, ranging from 0.02 to 27 l/min (note: the PFL cannot detect flows exceeding 5 l/min. Larger flows are estimated based on records during drilling). The inflows > 2 l/min were located at borehole intervals between 47.7–51.8 m, 57–58.2 m and 65.6 m.

In a recent investigation campaign for a tunnel oriented perpendicular to the NW-SE joint set at the 450 m level, the observed frequency of the NW-SE joint set was > 2 fractures/m. However, significant water conductive sections only occurred at depths of 18.4–20.7 m and 54.5–54.7 m. These borehole observations agree well with the observations of seepage in the TBM tunnel, were it is very easy to observe individual fractures.

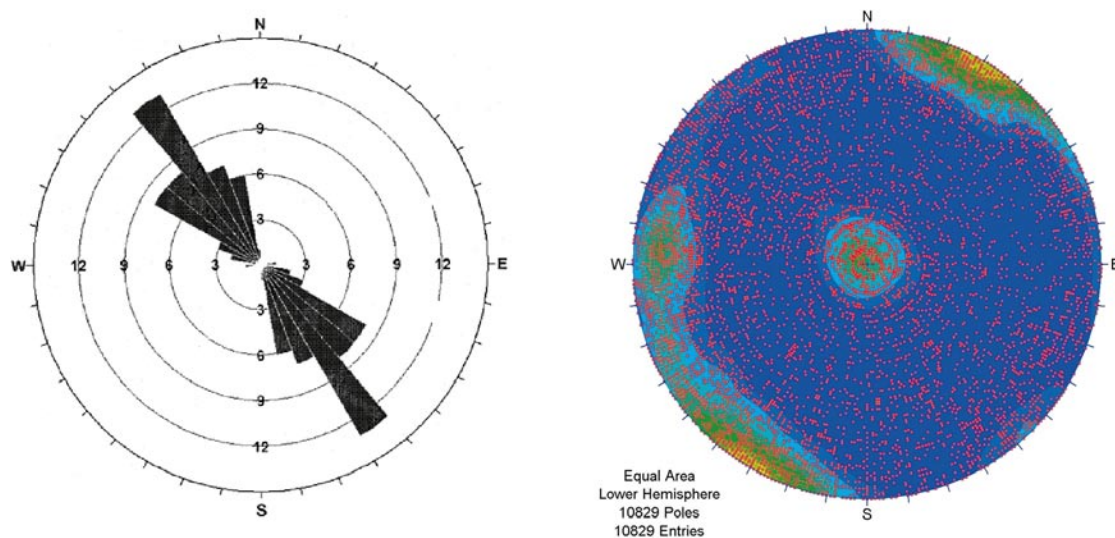
A general summary of the occurrence of dominant flowing features at Äspö HRL was given in /Berglund et al. 2003/, see Figure 3-4. As can be seen in Figure 3-4 the dominant inflows encountered in the spiral ramp were associated with NW-SE fractures. However, some inflows were also observed along the NE-SW trending structures. These NE-SW structures are generally minor deformation zones often associated with ductile mylonite that were reactivated and subject to brittle fracturing (Figure 3-2). Both the NE-SW trending structures, and also gently dipping fractures can provide hydraulic connectivity within the rock mass between the dominant steeply dipping NW-SE structures.

### 3.3 Stress conditions

In-situ stress measurements were carried out prior to construction of the Clab facility and the Äspö HRL. In addition, extensive characterisation of the state of stress was carried out for different projects at the Äspö HRL within 420 to 500 m depth. Summary of the stress orientations found at Äspö HRL is given in Figure 3-5. The variability in the stress orientation can be locally affected by the dominant orientation of the steeply dipping NW-SE trending fracture set.



**Figure 3-4.** Water-conducting features (WCF) in the tunnel section 1,500 to 2,450 (FCC database). Top view of Äspö HRL. Fault planes with ductile deformation in wall rock adjacent to the WCF are highlighted with different colour. WCF not in the FCC database are shown with grey lines (see text for explanation). Grey hatched lines denote structures tentatively possible to connect /Berglund et al. 2003/.



**Figure 3-5.** Orientation of maximum principal stress 380–500 m /Makurat et al. 2002/ (left) and poles of all mapped fractures in the HRL tunnels and outside deformation zones /Carlsson and Christiansson 2007/ (right).

The stress magnitude at the 450 m level is in the order of 30 MPa for the maximum horizontal stress and close to the weight of the overburden (12–13 MPa) for the minimum horizontal and vertical stress. The stress magnitudes have not caused any problems related to tunnel stability during construction and operation of the Äspö HRL. Large areas of the facility are only supported with spot bolting to enable access and studies of the geological conditions. Scaling of tunnel walls and ceiling is sufficient to keep the facility safe /Andersson and Söderhäll 2001/. The support for the larger openings, such as the assembly hall for the TBM and the lower sump and pump station, was changed to systematic rock bolts approximately 6–7 years after construction was completed. In both cases the tunnels are much higher than wide which resulted in stress relaxation of the high sidewalls.

### **3.4 Summary**

Construction of the underground excavations in the Simpevarp area, to depth of 450 m were carried out using traditional techniques for hard rock tunnelling. Stability of the underground excavations was achieved using traditional support methods including rock bolts and reinforced shotcrete. Spalling was not encountered in any of the underground excavations. The inflows to these excavations were controlled using cement-based grouts. The NW-SE oriented fracture set was frequently associated with these inflows.

## 4 Ground types and behaviour, rock support and grouting

To apply the design methodology described by /Palmström and Stille 2006/ and outlined in Figure 1-4 in Design Step D2 the ground types (GT) and anticipated ground behaviour (GB) must be defined. In addition to the ground types and behaviour, design step D2 will also require an estimate of ground support and grouting quantities.

To facilitate estimates for the ground support, support types (ST) are defined. These support types are based on the extensive underground construction experience in the Oskarshamn area /Carlsson and Christiansson 2007/ particularly the construction and operation of the Äspö Hard Rock Laboratory. Likewise, grouting types (GRT) are also defined based on the construction experience at Äspö and elsewhere. Because grouting technology has advanced significantly since the construction of the Äspö HRL, the grouting types have been modified to incorporate those changes.

The description in this chapter should be used by the designer for design step D2.

### 4.1 Variability and uncertainty in key parameters

To assess the system behaviour, values must be assigned to key parameters that will be used in this assessment. There is no doubt that uncertainty and spatial variability exists in these values. The values assigned to each parameter are based on the data provided in the SDM- Laxemar /SKB 2009/ as well as the engineering judgement of the authors of this report. To establish the system behaviour the designer is provided with what is judged to be the most likely value and a deterministic design based on this value may be adequate in most cases. However, in keeping with the philosophy of the Observational Method, a range of values that represent conceivable worst case conditions may also be provided. The range in values is provided when it is judged that a change in this value may significantly impact the design. For example, the in-situ stress magnitudes are difficult to estimate and can significantly impact the ground behaviour. Hence minimum and maximum stress values are provided in addition to the most likely value so that the impact in the range of values can be fully assessed. For such situations a probability based approach may be required to explore the likely outcome. Probability functions are usually not known for many of the design parameters and for such cases a triangular distribution may be assumed, truncated by a minimum and maximum value.

### 4.2 Ground types

The division of the rock mass into ground types starts with a description of the basic geology and proceeds by defining key geotechnical parameters for each ground type. The key values of each parameter and their distributions or ranges are based on the information provided in Chapter 2, the SDM-Site Laxemar /SKB 2009/ and on the authors engineering judgment. The four Ground Types that have been defined for Design Step D2 are presented in Table 4-1, and their properties are given in the forms following Table 4-1. Table 4-2 provides an estimate of the expected distribution of ground types to be encountered in the deformation zones and the fracture domains in the focused volume.

GT1 represents the good quality rock mass suitable for the placement of deposition holes. The parameters used to describe the rock mass properties for GT1 were compiled from the SDM-Site Laxemar /SKB 2009/ using the values provided for both intact rock and fractures. These properties were taken from laboratory tests but were scaled to the tunnel dimensions. As a result the properties, particularly the fracture stiffness, values have been reduced from the values provided in Table 2-5.

GT2 represents the blocky rock conditions that are likely to be encountered in either rock type. The mechanical and strength properties for this ground type are slightly reduced from those in GT1 and reflect the properties in the SDM-Site Laxemar /SKB 2009/ that are assigned to fracture domains see Table 2-9.

**Table 4-1. Summary of the four ground types for Design Step D2.**


Ground type	Description
GT1	Sparsely fractured, isotropic rock mass.
GT2	Blocky rock mass. Moderately fractured rock contains fractures and hair cracks, but the blocks between joints are intimately interlocked.
GT3	Minor deformation zone, moderately fractured rock, fractures may be altered and the fracture frequency may be locally increased
GT4	Major deformation zone, containing crush rock, strong hydrothermal alteration, cataclasite and gouge


**Table 4-2. Summary of expected distribution of ground types in the focused volume.**


Description	Distribution of Ground Type (%)			
	GT1	GT2	GT3	GT4
<b>Specified deformation zones and corresponding respect distances</b>				
ZSMNE107A	0	30	30	40
ZSMNS059A	0	70	30	0
Respect distance to ZSMNE107A, ZSMNE042A	0	70	30	0
Respect distance to ZSMNS059A	0	80	20	0
Respect distance to ZSMEW007A	0	70	30	0
<b>Other deformation zones</b>				
Gently dipping deformation zones (< 30°)	0	80	10	10
Steeply dipping deformation zones	20	50	30	0
<b>Fracture domains</b>				
FSM_W	80	20		
FSM_C	70	30		
FSM_NE005	70	30		
FSM_EW007	60	30	10	

GT3 represents the minor deformation zones. The mechanical and strength properties of this ground type have been parameterised on the basis of the information provided by SDM-Site Laxemar /SKB 2009/, including results from empirical approaches.

GT4 represents the major deformation zones. The mechanical and strength properties of this ground type have been taken from /Glamheden et al. 2007/. It is very difficult to determine mechanical and strength properties from borehole data for such large scale highly heterogeneous features. The values taken from /Glamheden et al. 2007/ were back-calculated from measured deformations and hence represent a tunnel scale best estimates see Table 2-5.

Ground Type: GT1- Sparsely fractured crystalline rock				
<b>Description</b>	<i>Lithology:</i> Any rock type in Laxemar Subarea			
<b>Indicators</b>	<i>Fracture/anisotropy:</i>	Sparsely fractured/isotropic		
	<i>Block Size:</i>	> 1.5 m		
	<i>Joint persistence:</i>	Low		
	<i>Large scale hydraulic conductivity</i>	Approaches that of intact rock 1 10 <sup>-12</sup> to 1 10 <sup>-10</sup> m/s		
<b>Intact Rock – Lab</b>	<i>UCS, Crack Initiation, Tensile Strength, Young’s Modulus, Poisson’s ratio</i> <i>Obtain mean values from Table 2-4</i>			
<b>Joints</b>	Cohesion = 0.5 MPa		Friction angle = 34°, dilation angle = 10°	
	Normal Stiffness = 500 MPa/mm		Shear stiffness = 100 MPa/mm	
	Infilling: Precipitates of low-temperature minerals such as calcite and chlorite occurs commonly			
<b>Thermal</b>	See Table 2-3 for thermal properties			
<b>Unsupported behaviour indicators</b>	<i>Stress:</i> Far-field maximum stress < 0.15 UCS, Gravity controlled block failure may occur locally Maximum tangential stress on boundary of opening > 110 MPa, Local spalling should be expected.			
	<i>Structure:</i> Persistent joints are expected to be open and water bearing.			
	<i>Water:</i> Inflows can occur as minor seepage along individual joints. T < 10 <sup>-8</sup> m <sup>2</sup> /s			
<b>Tunnel scale properties (Empirical systems)</b>	<i>GSI</i> = 85–95	<i>RMR</i> = 85–95	<i>Q</i> = > 100	<i>Em</i> = 55 GPa, <i>v</i> = 0.23
	Hoek-Brown: UCS = Lab mean value, <i>m</i> <sub>i</sub> = 30, <i>m</i> <sub>b</sub> = 20.254, <i>s</i> = 0.2946, <i>D</i> = 0			
	Mohr-Coulomb: Cohesion = 20 MPa, Friction angle = 55°, Tensile strength = 4 MPa			
<b>Photo or sketch</b>				
		Example of good wall quality in a 5-m-diameter tunnel excavated by drill and-blast in massive to sparsely fracture rock mass. Note the half-barrels on the perimeter profile.		
<b>Uncertainties</b>	Secondary horizontal jointing, frequency and dependency on depth			

Ground Type: GT2- Blocky rock mass			
<b>Description</b>	<i>Lithology:</i> Any rock type within Laxemar Subarea		
<b>Indicators</b>	<i>Fracture/anisotropy:</i>	Blocky rock mass, 2 to 3 joint sets and 1 random set	
	<i>Block Size:</i>	0.5 < between > 1.5 m	
	<i>Joint persistence:</i>	Low to moderate	
	<i>Large scale hydraulic conductivity</i>	Blocky rock: 1 10 <sup>-10</sup> to 1 10 <sup>-9</sup> m/s	
<b>Intact Rock – Lab</b>	<i>UCS, Crack Initiation, Tensile Strength, Young's Modulus, Poisson's ratio</i> Obtain mean values from Table 2-4		
<b>Joints</b>	Cohesion = 0.5 MPa	Friction angle = 34°, dilation angle = 10°	
	Normal Stiffness = 500 MPa/mm	Shear stiffness = 100 MPa/mm	
	Infilling: Precipitates of low-temperature such as calcite, chlorite and laumontite occurs commonly. Open fractures may occur		
<b>Unsupported behaviour indicators</b>	<i>Stress:</i> Far-field maximum stress < 0.15 UCS, Gravity controlled block failure may occur locally Maximum tangential stress on boundary of opening > 100 MPa, Local spalling should be expected.		
	<i>Structure:</i> Joints can cluster to form minor sub-horizontal deformation zones of limited extent		
	<i>Water:</i> Inflows can occur as minor seepage along individual joints. $T < 10^{-8}$ m <sup>2</sup> /s Along steeply dipping minor deformation zones inflow occurs occasionally $T < 10^{-7}$ m <sup>2</sup> /s Along minor deformation zones inflows can be significant $T \geq 10^{-5}$ m <sup>2</sup> /s		
<b>Tunnel scale properties (Empirical systems)</b>	GSI = 80–90	RMR = 80–90	Q = 40–100
	Em = 50 GPa, $\nu = 0.3$		
	Hoek-Brown: UCS = Lab mean value, $m_i = 30$ , $m_b = 17.55$ , $s = 0.189$ , $D = 0$		
Mohr-Coulomb: Cohesion = 15 MPa, Friction angle = 55°, Tensile strength = 2 MPa			
<b>Photo or sketch</b>			
		Example of the sidewall quality observed in a drill-and-blast tunnel in a blocky rock mass.	
<b>Uncertainties</b>	Secondary horizontal jointing, frequency and depth dependency		

<b>Ground Type: GT3 – Minor Deformation zone (&lt; 1,000 m)</b>			
<b>Description</b>	<i>Lithology:</i> Any rock type within Laxemar Subarea		
<b>Indicators</b>	<i>Fracture/anisotropy:</i>	Blocky rock mass with flowing fractures	
	<i>Block Size:</i>	0.5 < between > 1.5 m	
	<i>Joint persistence:</i>	Moderate to high	
	<i>Large scale hydraulic conductivity</i>	Minor deformation zones: $1 \cdot 10^{-8}$ to $1 \cdot 10^{-5}$ m/s	
<b>Intact Rock (Estimated)</b>	<i>UCS, Crack Initiation, Tensile Strength, Young's Modulus, Poisson's ratio</i> <i>Obtain from Table 2-4</i>		
<b>Joints</b>	Cohesion = 0.5 MPa		Friction angle = 34°, dilation angle = 10°
	Normal Stiffness = 100 MPa/mm		Shear stiffness = 30 MPa/mm
	Infilling: Calcite, chlorite, prehnite, clay minerals		
<b>Unsupported behaviour indicators</b>	<i>Stress:</i> Far-field maximum stress < 0.15 UCS, Gravity controlled block failure may occur locally Maximum tangential stress on boundary of opening > 80 MPa, Spalling/crushing should be expected.		
	<i>Structure:</i> System of sealed fractures that may be susceptible to blast induced damage		
	<i>Water:</i> Inflows can occur as minor seepage along individual joints. $T < 10^{-7}$ m <sup>2</sup> /s		
<b>Tunnel scale properties (Empirical systems)</b>	<i>GSI</i> = 75–85	<i>RMR</i> = 75–85	<i>Q</i> = 10–40
	<i>Em</i> = 35 GPa, $\nu$ = 0.3		
	Hoek-Brown: UCS = Lab mean value, $m_i$ = 25, $m_b$ = 12.239, $s$ = 0.1084, $D$ = 0		
Mohr-Coulomb: Cohesion = 10 MPa, Friction angle = 45°, Tensile strength = 1.3 MPa			
<b>Photo or sketch</b>			
			
<b>Uncertainties</b>	Concentrated fracturing may lead to zones which are relatively weak with open fractures.		



Ground Type: GT4 – Major deformation zone (> 3,000 m)			
<b>Description</b>	<i>Lithology:</i> Any Rock Type within Laxemar Subarea		
<b>Indicators</b>	<i>Fracture/anisotropy:</i>	Major Deformation Zone – no core	
	<i>Block Size:</i>	dm < between > 1 m	
	<i>Joint persistence:</i>	Continuous	
	<i>Large scale hydraulic conductivity</i>	1 10 <sup>-8</sup> to 1 10 <sup>-5</sup> m/s	
<b>Intact Rock (Estimated)</b>	<i>UCS, Crack Initiation, Tensile Strength, Young's Modulus, Poisson's ratio</i> Obtain from Table 2-4		
<b>Joints</b>	Cohesion = 0.5 MPa	Friction angle = 34°, dilation angle = 10°	
	Normal Stiffness = 100 MPa/mm	Shear stiffness = 25 MPa/mm	
	Infilling: Joints likely to have clay coating		
<b>Unsupported behaviour indicators</b>	<i>Stress:</i> Far-field maximum stress < 0.15 UCS, Gravity controlled block failure may occur locally Maximum tangential stress on boundary of opening > 80 MPa, Spalling/crushing should be expected.		
	<i>Structure:</i> System of sealed and open fractures that may be susceptible to blast induced damage		
	<i>Water:</i> Inflows can be large if open fracture encountered. T ≥ 10 <sup>-4</sup> m <sup>2</sup> /s		
<b>Tunnel scale properties (Empirical systems)</b>	GSI = 70–80	RMR = 70–80	Q = 4–20
	Em = 35 GPa, ν = 0.3		
	Hoek-Brown: UCS = Lab mean value, mi = 25, mb = 12.239, s = 0.1084, D = 0		
Mohr-Coulomb: Cohesion = 4 MPa, Friction angle = 45°, Tensile strength = 1. MPa			
<b>Photo or sketch</b>			
<p>Example of a slickensided surface. Chlorite, calcite and clay minerals coat the surface.</p>			
<b>Uncertainties</b>			

### 4.3 Ground behaviour

/Palmström and Stille 2006/ provide three general categories of ground behaviour commonly observed in hard rocks (see Table 4-3) and /Martin 2005/ provides a detailed description of the hard rock behaviour referred to as stress-induced spalling. The categories of ground behaviour given in Table 4-3 should be used to assess the overall system behaviour.

### 4.4 Support types

The support types are based on modern construction practice in the Scandinavian shield. For this design step D2, 5 tunnel support types (ST1 through ST5) and 1 cavern support type (STC) are provided (Table 4-4). The bolt type, spacing and length, and shotcrete thickness are not provided as part of the support types that decision remains with the designer when all the functional requirements and influence factors are considered.

**Table 4-3. General categories for ground behaviour (GB). Modified from /Palmström and Stille 2006/.**

GB1	Gravity driven, mostly discontinuity controlled failures (block falls), where pre-existing fragments or blocks in the roof and sidewalls become free to move once the excavation is made.
GB2	Stress induced, gravity assisted failures caused by overstressing, i.e. the stresses developed in the ground exceeding the local strength of the material. These failures may occur in two main forms, namely:
GB2A	– as spalling, buckling or rock burst in brittle materials, i.e. massive brittle rocks;
GB2B	– as plastic deformation, creep, or squeezing in materials having ductile or deformable properties, i.e. massive, soft/ductile rocks or particulate materials (soils and heavy jointed rocks).
GB3	Water pressure; an important load to consider in design especially in heterogeneous rock conditions.
GB3A	– Groundwater initiated failures may cause flowing ground in particulate materials exposed to large quantities of water, and trigger unstable conditions (e.g. swelling, slaking, etc) in some rocks containing special minerals. Water may also dissolve minerals like calcite in limestone.
GB3B	– Water may also influence block falls, as it may lower the shear strength of unfavourable joint surfaces, especially those with a soft filling or coating.

**Table 4-4. Summary of support types to be used in Design Step D2.**

Support Type	Description
ST1	Spot bolts, Example: Ground Type 1, Ground Behaviour 1
ST2	Systematic bolting, Ground Types 1 and 2 Example: Ground Behaviour 1 and Ground Behaviour 2A
ST3	Systematic bolting plus wire mesh Example: Ground Types 1 and 2 Example: Ground Behaviour 1
ST4	Systematic bolting plus fibre-reinforced shotcrete Example: Ground Types 1, 2 and 3 Example: Ground Behaviour 1 and 2B
ST5	Concrete Lining Example: Ground Type 4 Example: Ground Behaviour 3
Caverns	Systematic bolting plus fibre-reinforced shotcrete
STC	All Ground Types suitable for Central Area Caverns Example: Ground Behaviour 1 and 2

## 4.5 Grouting

The need for construction grouting at Laxemar will vary significantly as the hydraulic properties of the rock mass shows considerable spatial variability. Construction experiences from the Äspö HRL confirms the spatial variability to depths of 450 m /Carlsson and Christiansson 2007/.

For the current design step D2, 3 grouting types (GRT1 through GRT3) are provided and this number is considered sufficient to meet the design requirements (Table 4-5). The parameters that define each grouting type, e.g., number of holes, spacing, number of stages, and the type of grouting material are not provided. Those parameters must be chosen by the designer. The grouting requirements at Laxemar will vary depending on the rock domain being traversed by the underground excavations and the functional requirements. Excavations for the access ramps and shafts are expected to encounter a wide range of hydrogeological conditions and hence extensive grouting may be required locally to meet the seepage requirements.

The hydrogeological conditions expected in each of the functional areas are described in Table 4-6. Based on this information the designer must evaluate if the predicted inflows exceed the seepage restrictions. If grouting must be carried out, the designer must specify the parameters for the grouting type that will achieve the required seepage. The seepage limits are specified in the Design Premises Document for D2. The methodology that should be used to estimate the grout quantities required to meet the seepage limits is given in /Emmelin et al. 2007/.

The grout hole lengths, number of holes, spacing, pressures, and grouting material are not provided as part of the grouting types, that decision remains with the designer when all the functional requirements and influence factors are considered.

## 4.6 Monitoring and documenting the performance of underground excavations

In Section 1.4 it was noted that the Observational Method should be used as a key component in the design of the underground excavations. As listed in Section 1.3, one of the steps in the Observational Method is to develop a monitoring plan which can be used to assess whether the actual ground system behaviour lies within the acceptable limits of the predicted behaviour. By monitoring the key elements of the system, the observed system behaviour during construction can be compared with the predicted system behaviour. In order to make this assessment a monitoring and documentation plan will be required. The basic elements of that monitoring/documenting plan are described below and are focused on providing the designers with sufficient information to make the assessment. For design stage D2, the Designer should propose a monitoring plan for each functional area. These plans should address the uncertainty in the design assumptions, particularly where the consequences of this uncertainty may significantly impact the design and/or performance of the project /SKB 2007/. Prior to the start of any excavation an assessment will be made of the adequacy of available geological and geotechnical information to predict the underground system behaviour. It is anticipated that cored probe-hole drilling will be required for all excavations and that this information will form the bases for the predicted system behaviour following the general flow chart logic given in Figure 1-4. Once the excavation commences the following steps should be carried out and will form the bases for assessing the underground system behaviour during construction:

**Table 4-5 Summary of grouting types to be used in Design Step D2.**

Grouting Type	Description
GRT1	Discrete fracture grouting
GRT2	Systematic tunnel grouting
GRT3	Control of large inflows and high pressure

**Table 4-6. Transmissivity of individual fractures and their distribution with depth determined from PFL-f measurements (based on the tables and text provided in Section 2.5).**

Depth (m)	Transmissivity (m <sup>2</sup> /s) of individual water bearing fractures (in log scale) min, mean, max, StDev.	Water bearing Fracture frequency fractures/m
<b>HRD_C</b>		
50–150 m	min = -9.4, mean = -7.5 max = -4.4, StDev = 1.1	0.564/m
150–400 m	min = -9.4, mean = -7.9 max = -4.9, StDev = 1.1	0.164/m
400–650 m	min = -9.5, mean = -8.1 max = -6.0, StDev = 0.9	0.107/m
650–1,000 m	min = -8.8, mean = -7.6 max = -6.4, StDev = 0.8	0.008/m
<b>HRD_W</b>		
50–150 m	min = -9.4, mean = -7.5 max = -4.33, StDev = 1.0	0.499/m
150–400 m	min = -7.6, mean = -7.9 max = -5, StDev = 1.2	0.078/m
400–650 m	min = -9.2, mean = -7.5 max = -4.0, StDev = 1.4	0.060/m
650–1,000 m	min = -8.4, mean = -8.4 max = -8.4, StDev = N/A	0.005/m
<b>HRD_EW07</b>		
50–150 m	min = -9.4, mean = -7.4 max = -4.5, StDev = 1.2	0.816/m
150–400 m	min = -9.5, mean = -7.5 max = -4.4, StDev = 0.9	0.550/m
400–650 m	min = -9.1, mean = -7.6 max = -5.7, StDev = 0.7	0.225/m
650–1,000 m	min = N/A, mean = N/A max = N/A, StDev = N/A	0.000/m

**1. Determine the ground type encountered**

Geological documentation during construction must record sufficient information that the ground types can be readily established. The three-dimensional spatial description of the excavated profile, lithology, open fractures and inflows should be documented.

**2. Determine the actual ground type Behaviour**

The types of anticipated ground behaviour are listed in Table 4-2. The observations during excavation, must document the ground behaviours encountered and their spatial location.

**3. Determine the adequacy of the support type**

Prior to the start of construction, support classes will be determined and specified in the baseline construction plan. Documentation during construction must adequately record the support types used in the support classes and their spatial locations. The adequacy of the support types must be assessed in a formal manner. For example convergence measurements should be carried out and used to aid in assessing the adequacy of the support type. Even if no support type is specified convergence monitoring should be carried out to show that support is not required, i.e. the ground behaviour is elastic.

**4. Determine the adequacy of the grouting type**

Grouting classes will be determined and specified in the baseline construction plan. Documentation during construction must adequately record the grout types used and their spatial locations. Monitoring of tunnel inflows must be carried out to demonstrate that the grout type is effective in meeting the specified seepage requirements. Monitoring of tunnel inflows will also be required in areas where no grouting is specified to ensure that the specified seepage limits are met. In addition to monitoring the seepage, the chemistry of the inflows should also be monitored. This will be used to aid in evaluating the support types for long-term performance.

## 5. **Verification of system behaviour**

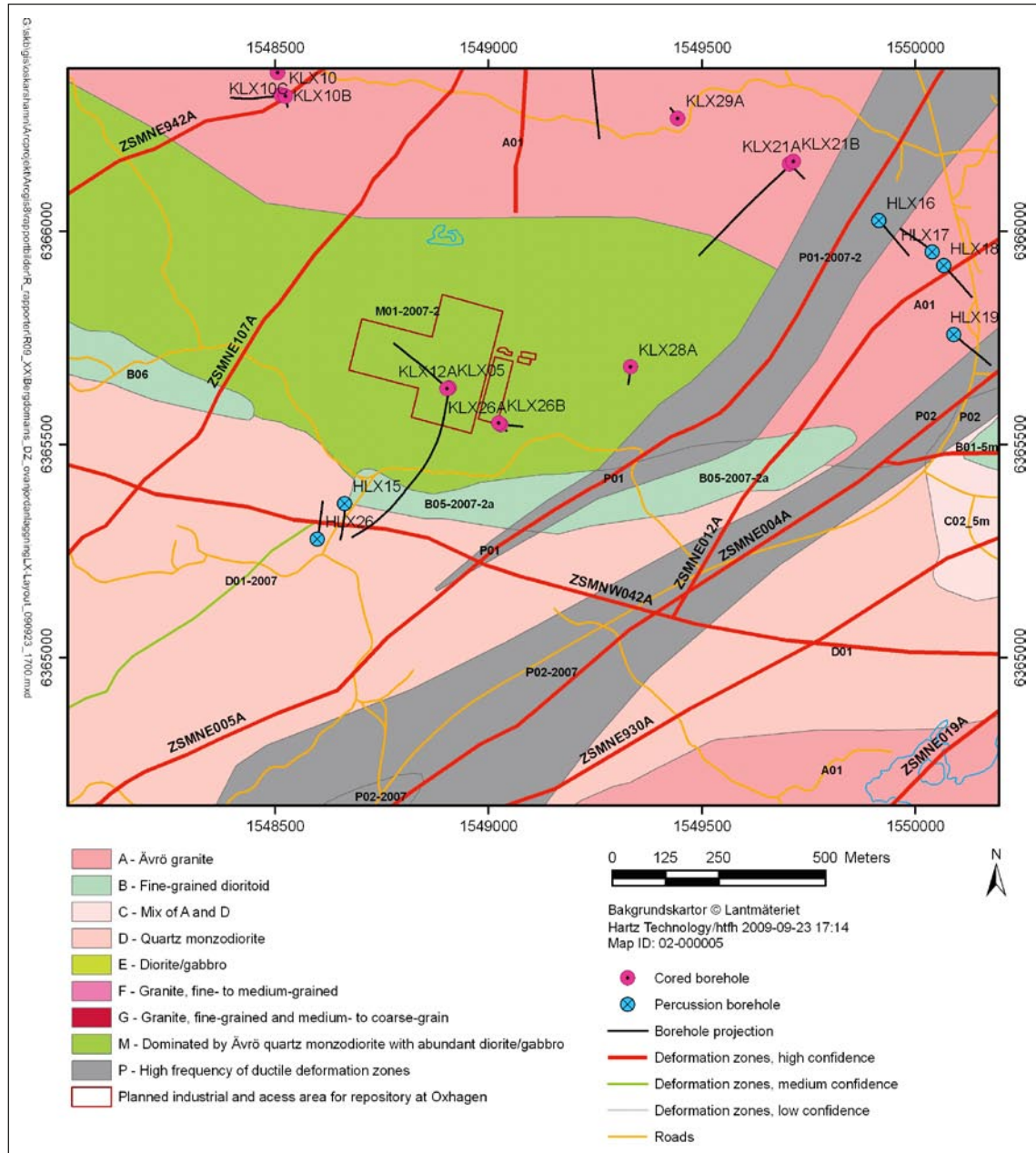
When differences between the observed and predicted system behaviour occur, the parameters and criteria used have to be reviewed. When the displacements, support utilisation or grout takes are higher than predicted, a detailed investigation into the reasons for the different system behaviour has to be carried out, and if required the design may be modified or the basis for support and/or grouting classes must be changed. In case the system behaviour is better than expected, the reasons for this difference must also be analyzed, and the findings used to update future predictions.

The frequency of a formal evaluation of the system behaviour will depend on the complexity of the geological environment. At Laxemar it is anticipated that the formal evaluation of the system behaviour will be carried out for each of the functional areas and for each of the ground types in these functional areas. In addition the intersection of minor and major deformation zones will also require a formal evaluation. It should be noted that in addition to the monitoring elements described above there may be additional monitoring required as part of the detailed site characterisation program and as part of the contractor's method statements and QA/QC related to the construction works. Those monitoring requirements are not considered part of the Observational Method for underground design. For example, the in-situ stress is an essential parameter needed for the evaluation of the system behaviour. In-situ stress will be one of the parameters measured as part of the detailed site characterisation program prior to and during construction and is therefore not considered a parameter for construction monitoring.

# 5 Repository access

## 5.1 Location

The proposed location of the surface facilities is illustrated in Figure 5-1. The main access to the repository will be arranged via vertical shafts and an inclined ramp. Based on the preliminary layout the main access area will be located in the area of drill sites KLX05A–KLX12A and KLX26, i.e. in fracture domain FSM\_NE005. The rock domain at the ground surface at this location is rock domain M, which is dominated by Ävrö quartz-monzodiorite.



**Figure 5-1.** Schematic illustration of the planned industrial and access area for a repository at site Oxhagen in Laxemar (red squares).

Figure 5-2 represents a three dimensional view of the regional model volume with the disposition of the three main rock domains for the repository access, i.e. RSMRSMM01 and RSMD01. Figure 5-3 illustrates the variation with depth of the geometry of rock domain RSMD01. As seen in this figure, rock domain RSMM01 does not extend down to the bottom of the model and the facility will encounter more of the rock domain RSMD01 at depth.

Figure 5-4 represents the fracture domains encountered from surface to depth in the local model volume. With regards to the planned location of the facility this figure illustrates that the facility at surface will be mostly located in FSM\_EW007. However at depth the facility will be mostly located in FSM\_C.

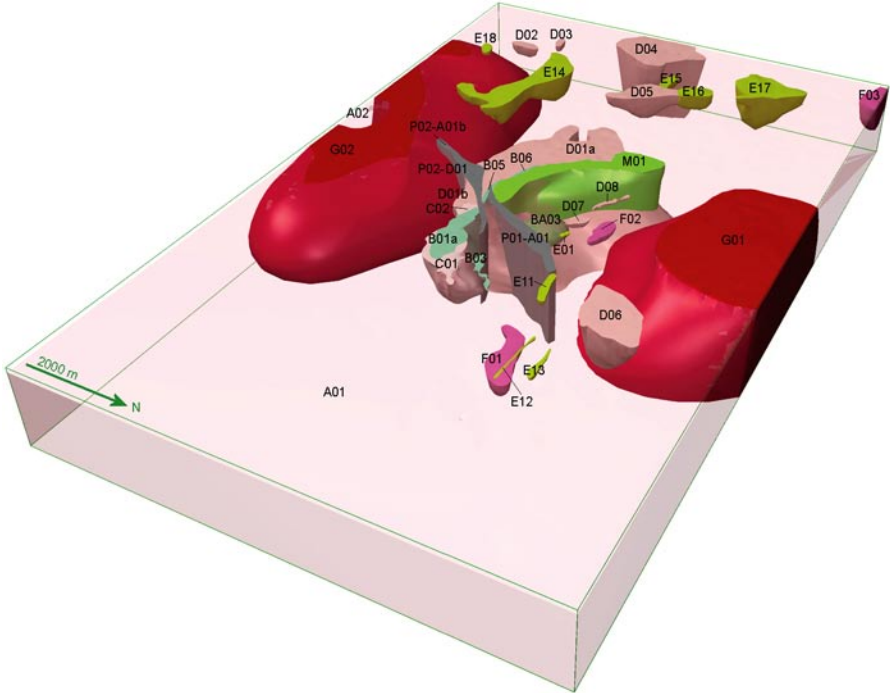


Figure 5-2. Three dimensional model for rock domains in the regional model volume /Wahlgren et al. 2008/.

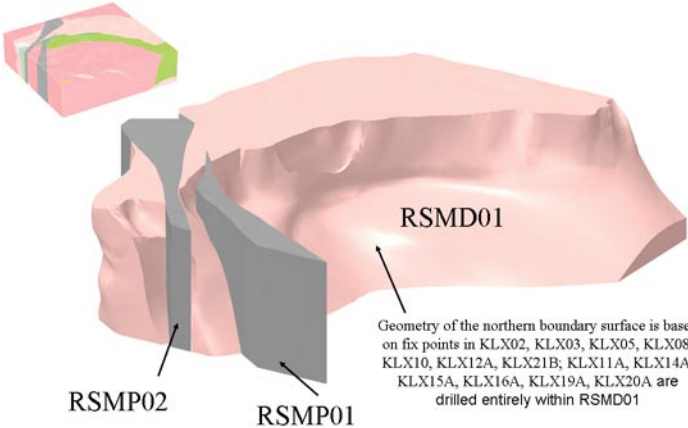


Figure 5-3. View of the northern boundary of RSMD01 (when removing RSM01). View to the south-southwest /Wahlgren et al. 2008/.

## Fracture domain model



**Figure 5-4.** 2D vertical N-S section of the conceptual model for fracture domains in the local model volume /SKB 2009/.

## 5.2 General rock mass conditions

The rock conditions outside of deformation zones at near surface do not differ significantly from that expected at repository depth. In the uppermost near surface (5–10 m) the bedrock might be more altered and fractured, thus being more conductive. The hydraulic conductivity is expected to decrease both in surrounding rock and deformation zones in the upper 100–200 m of the bedrock. This is correlated to a decrease in the number of flowing features. In the focused area most flowing fractures are striking NW and subvertical.

## 5.3 Passages of water-bearing fractures

Water-bearing fractures may occur in all Ground Types but are likely decreasing in frequency and transmissivity with depth. Gently dipping water-bearing fractures should be anticipated within the uppermost 150–200 m, while steeply dipping conductive fractures are likely to occur at any depth. For example inflows greater than 10 l/min were encountered along individual fractures in the rock mass outside deformation zones during construction of the Äspö HRL to depths of 460 m /Carlsson and Christiansson 2007/. Excavations for shafts and for the access ramp should be prepared for variable hydraulic conditions even although the overall rock mass hydraulic conductivity may decrease with depth.

Table 5-1 provides the estimated thickness and hydraulic conductivity for the deterministic deformation zones that might intersect the facility access and/or shafts.

### 5.3.1 Shafts

Shafts may penetrate transmissive gently and subvertical dipping structures ( $T \geq 10^{-7} \text{ m}^2/\text{s}$ ) which will need to be grouted before the shaft excavation commences. Large inflows and increasing water pressure with depth must be anticipated and its impact minimised. The rock support for these transmissive structures must be designed to withstand hydrostatic water pressures unless adequate drainage is provided.

**Table 5-1. Estimated thickness and hydraulic conductivity for deformation zones in the local model which might intersect the facility. The thickness and hydraulic properties of the deformation zones are compiled from data presented in /Rhén et al. 2008, respectively Table A3-1 and Table A6-4/.**

Deformation zone	Thickness in CF model (m)	Hydraulic conductivity K (m/s) for depth interval (m, RHB 70)				
		0 to –100	–100 to –200	–200 to –300	–300 to –400	–400 to –500
Klx11_dz11	20	2.83E-07	1.71E-07	1.03E-07	6.24E-08	3.77E-08
ZSMNE107A	35	1.48E-06	8.25E-07	4.59E-07	2.55E-07	1.42E-07



For the selected shaft locations, and the different type of shafts, the designer should evaluate the need for lining of shafts. For shafts which are designed to be fully lined, adequate temporary support must be provided to allow installation of the permanent lining.

### 5.3.2 Access ramp

The ramp may intersect transmissive gently and subvertical dipping structures ( $T \geq 10^{-7} \text{ m}^2/\text{s}$ ). Large inflows and increasing water pressure with depth should be anticipated and its impact must be minimised. Large water flows together with high water pressures will require sealing and support measures with adequate efficiency for a safe and timely excavation progress.

The layout of the ramp geometry should be optimised with respect to the geometry of the transmissive structures. Excavation of a ramp-leg more or less parallel to a water-bearing zone will require advanced sealing/grouting and support techniques. This may also have a major impact on construction schedule and costs. Penetration of these transmissive fractures zones at as favourable an angle as possible should be a major target.

## 5.4 Summary

The ground conditions anticipated for the underground openings associated with the Repository Access are summarised in Table 5-2. It should be realised that this summary represents the general conditions anticipated and must be evaluated in Design Step D2.

**Table 5-2. Summary of the ground conditions anticipated for the Repository Access.**

Access	Ground Type	Behaviour Type	Support Type	Grouting Type
0–200 m	All	GB1, GB3	ST1,ST2,ST4	GRT2 & GRT3
200–400 m	GT1b, GT2, GT3	GB1, GB3	ST1, ST2, ST4	GRT1 & GRT2
400–600 m	GT1b, GT2	GB1, GB3	ST1 to ST4	GRT1 to GRT3
> 600 m	GT1b, GT2	GB1, GB2B, GB3	ST1 to ST4	GRT1 to GRT3
Minor Deformation Zones	GT3	All	ST4 & ST5	All

## 6 Central Area

The Central Area is composed of a series of caverns of various dimensions, located at approximately the same depth as the deposition tunnels (Figure 6-1). The location of the Central Area is dependent on both suitable rock conditions and environmental and functional issues related to the siting of the surface facilities.

### 6.1 Constraints

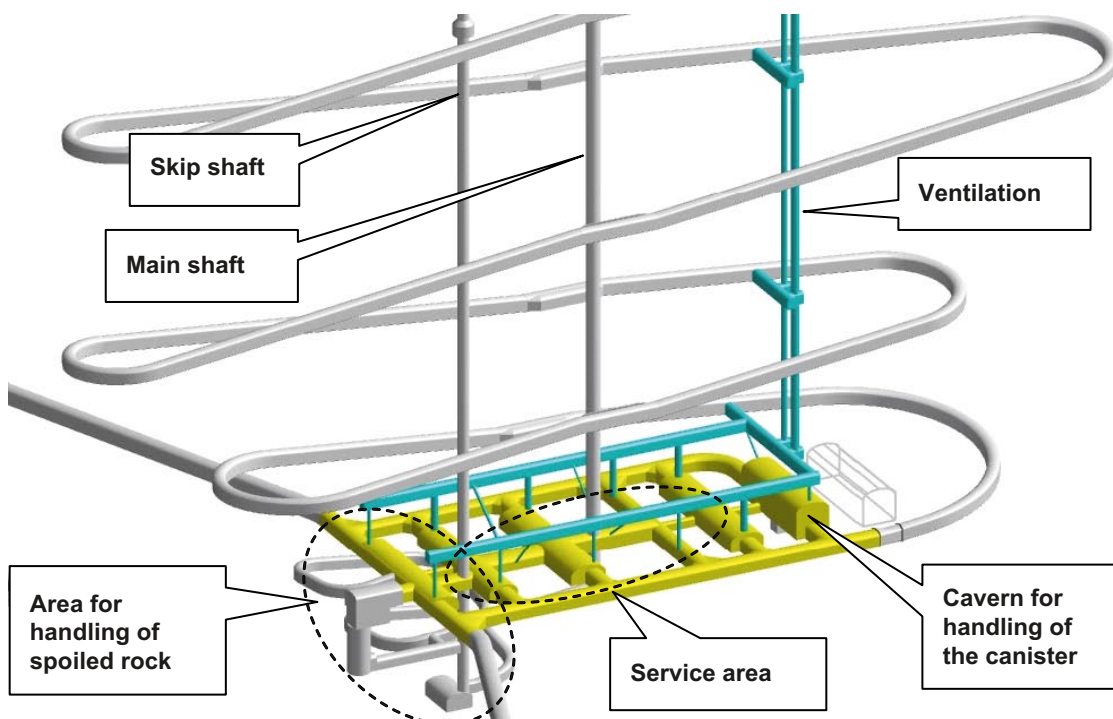
If spalling of the rock mass is anticipated the caverns should be oriented to reduce unfavourable stress concentrations. The spacing of the caverns may need to be adjusted should spalling be an issue. The layout of the caverns should also be optimised with respect to the geometry of the transmissive structures.

### 6.2 General rock mass conditions

It is anticipated that the caverns for the Central Area will be constructed in Ground Type 1 and/or 2. The support may be required for the walls as well as the roof and may require special construction sequencing depending on the cavern size.

### 6.3 Summary

The ground conditions anticipated for the underground openings associated with the Central Area are summarised below. It should be realised that this summary represents the general conditions anticipated and must be evaluated in Design Step D2.



*Figure 6-1. Simplified layout of the Central Area (in yellow).*

**Table 6-1. Summary of the ground conditions anticipated for the Central Area.**

	<b>Ground Type</b>	<b>Behaviour Type</b>	<b>Support Type</b>	<b>Grouting Type</b>
Central Area				
400–600 m	GT1b, GT2	GB1, GB2A	STC	GRT1, GRT2
> 600 m	GT1b, GT2	GB1, GB2A	STC	GRT1 to GRT3
Minor Deformation Zones	GT2 & GT3	GB1, GB2	STC	GRT2, GRT3

## 7 Deposition areas

### 7.1 General rock mass conditions

The deposition areas will be located in the rock mass considered to have the lowest fracture frequency and to be the most homogenous. At Laxemar the deposition areas will be located in Ground Type 1 where the ground behaviour GB1 and/or GB2 is expected. Preliminary information indicates that such conditions could be expected within rock domain RSMA01 which is dominated by quartz monzodiorite and within rock domain RSMD01, dominated by Ävrö granite. The access to the area for the repository is however constrained by deformation zones some of which are longer than 3 km, and thus shall require a respect distance of 100 m /Munier and Hökmark 2004/.

The area is cross-cut by dykes. Northeast-southwest trending dykes of fine-grained granite are sometimes found associated with old ductile deformation (mylonite) that was reactivated by brittle fracturing. This fracturing is more or less well healed by the granitic intrusion. A north-south trending set of mafic dykes also intersect the area. In some cases, the contact of the mafic dykes with the host rock is crushed and hydraulically conductive. However, in the case of the deformation zones ZSMNS001A and ZSMNS059A, the dykes are very solid and may even form a barrier for ground water flow.

Table 7-1 provides the estimated thickness and hydraulic conductivity for the deterministic deformation zones identified in the local model and which intersect the deposition areas.

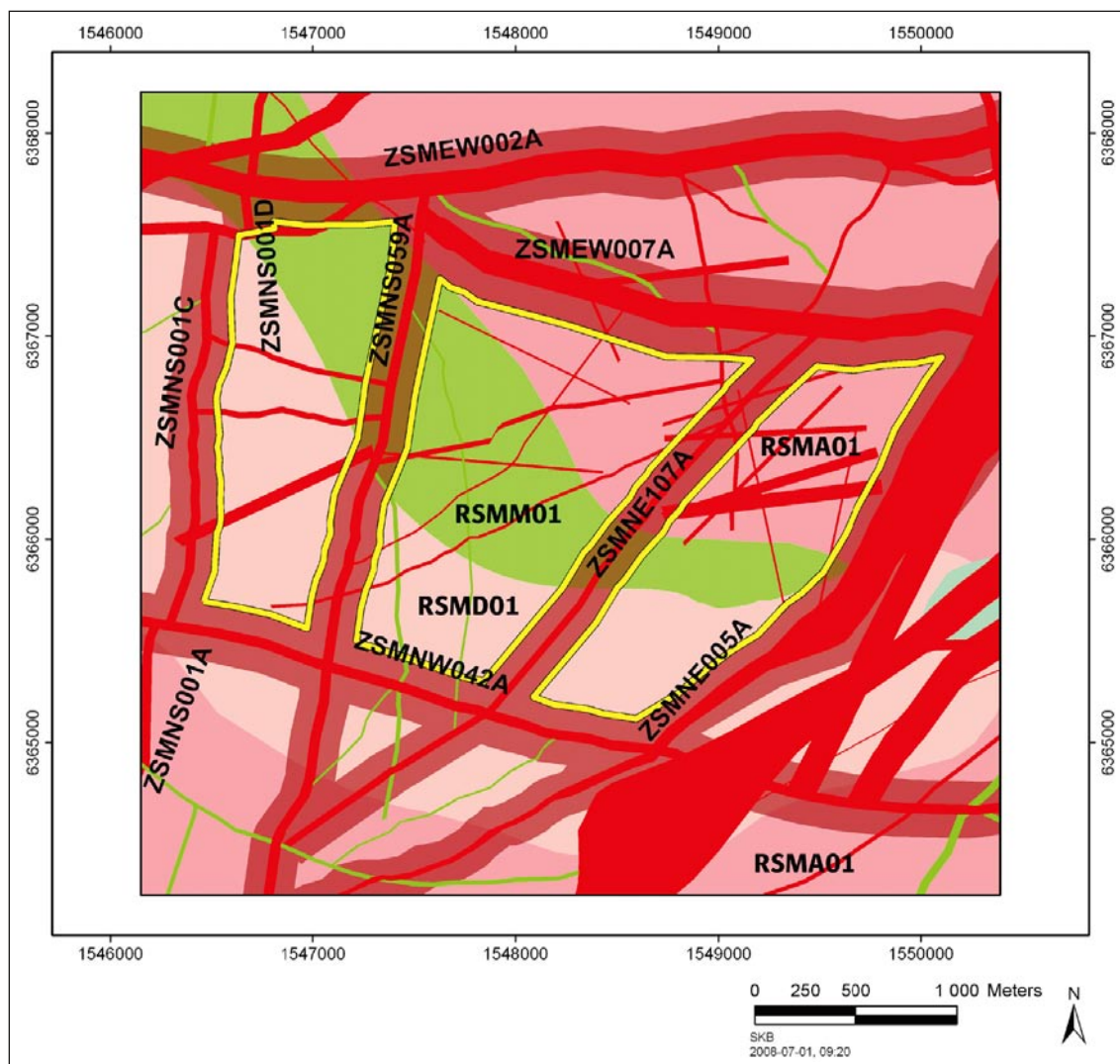
**Table 7-1. Estimated thickness and hydraulic conductivity for the deterministic deformation zones that might intersect the facility at repository depth. The thickness and hydraulic properties of the deformation zones are compiled from data presented in /Rhén et al. 2008, respectively Table A3-1 and Table A6-4/.**

Deformation zone	Thickness in CF model (m)	Hydraulic conductivity K (m/s) for depth interval (m RHB 70)
		-500 to -600
klx04_dz6b	14	3.25E-08
klx07_dz10	10	4.56E-08
klx07_dz11	30	1.52E-08
klx07_dz12	47	9.69E-09
klx07_dz13	10	4.56E-08
klx07_dz7	30	1.52E-08
klx07_dz9	10	4.56E-08
klx08_dz6	10	4.56E-08
klx11_dz11	20	2.28E-08
klx18_dz9	10	4.56E-08
klx19_dz5-8_dolerite	45	9.11E-08
klx21b_dz10-12	10	4.56E-08
zsmew120a	50	1.74E-08
zsmew900a	25	1.82E-08
zsmew900b	25	1.82E-08
zsmew946a	10	1.73E-08
zsmne040a	20	2.28E-08
zsmne107a	35	7.88E-08
zsmne942a	15	8.75E-08
zsmne944a	10	4.56E-08
zsmns046a	20	1.38E-07
zsmns059a	50	2.12E-07
zsmns945a	10	2.76E-07
zsmns947a	20	2.28E-08

## 7.2 Deformation zones and respect distances

The focused volume is constrained by deformation zones that are large enough to potentially require respect distance: ZSMEW007A at north, ZSMNE005A at east, ZSMNW042A at south and ZSMNS001C at west. Moreover 2 deformation zones that also are large enough to potentially require respect distance are modelled through the focused volume: ZSMNS059A, and ZSMNE107A. The resulting geometry of available deposition areas is illustrated in Figure 7-1. The three dimensional geometric coordinates that define the respect distance are defined by SKB and provided to the designer in a digital three dimensional model (RVS).

Deformation zones that are shorter than 3 km are not expected to pose any stability issues for the deposition tunnels. However, such zones may not be suitable for placing deposition holes and may increase the loss of deposition holes (see Section 7.6 for a discussion on the loss of deposition holes).



**Figure 7-1.** Plan view at the 500 m depth. The rock domain RSMA01 is dominated by quartz monzodiorite, the rock domain RSMM01 is a mixed domain dominated by quartz monzodiorite, Ävrö granite and diorite-gabbro, and finally the rock domain RSMD01 is dominated by Ävrö granite. The deformation zones with high confidence of existence are marked in bright red and related respect distances in dark red. Deformation zones with medium confidence of existence are marked with green /SKB 2009/. The areas outlined in yellow indicate the candidate deposition areas.

### 7.3 Deposition tunnel and deposition hole spacing

The minimum distance between deposition tunnels and between deposition holes should in design step D2 be determined with respect to the highest permissible temperature in the buffer. For Design Step D2, the minimum centre-to-centre spacing for the deposition tunnels should be 40 m and the optimisation of minimum centre-to-centre spacing for deposition holes with consideration to geology is discussed and presented in Appendix A. Table 7-2 provides the calculated spacing between canisters for the different rock domains.

### 7.4 Spalling in tunnels and deposition holes

In general, stress magnitudes tend to increase with depth. Because spalling is a function of the stress magnitudes relative to the rock strength, it is generally assumed that the potential for spalling also increases with depth, assuming the rock strength remains constant. A complete description of spalling and the methodology used to assess the potential for spalling is given in /Martin 2005/. For design stage D2, the potential for spalling must be assessed using stress domains given in Table 2-11, including the most likely and mean value, as well as the estimated uncertainty. /Martin 2005/ showed that when the factor of safety for assessing the potential for spalling was less than 1.25, the probability for spalling increased to significant levels. In other words the minimum and maximum magnitude values as given in Table 2-12 should be used for estimating the potential for spalling for design stage D2 when the most likely magnitudes in Table 2-12 give factors of safety less than 1.25.

If the risk for potential for spalling is judged to be significant using the methodology given in /Martin 2005/ three dimensional elastic stress analyses may be required, especially for deposition holes and tunnel intersections. At the intersection of the deposition tunnel with the transport tunnel three dimensional elastic stress analyses will also be required to assess the potential for spalling.

### 7.5 Deposition tunnel alignment

The deposition tunnels should be aligned with the direction of the maximum horizontal stress to reduce the tangential stress on the boundary of the deposition tunnels and minimise the risk for spalling. /Martin 2005/ showed that the risk for spalling in the deposition tunnels could be significantly reduced if not eliminated by orienting the deposition tunnels parallel to the maximum horizontal stress. At Laxemar, the orientation of the maximum horizontal stress is Azimuth  $135 \pm 15$  degree. As shown in /Martin 2005/, if the depositions tunnels are aligned within  $\pm 45^\circ$  of the trend of the maximum horizontal stress, the risk of spalling will be significantly reduced.

NW-SE steeply dipping fractures are interpreted as potentially highly transmissive in Laxemar (see Section 2-4). Experience from Äspö HRL indicates that the prominent transmissive sub-vertical fracture set at depth is aligned with the maximum horizontal stress (see Section 3). As is often the case, the designer must balance the need to reduce the risk for spalling with the need for intersecting these sub-vertical fractures at a large angle.

**Table 7-2. Calculated spacing between canisters at 500 m depth (14.8°C initial temperature) and 40 m tunnel spacing in the rock domains.**

Domain	Threshold	Canister cc distance (m)
RSMD01	96.3°C	8.1
RSMM01	96.1°C	10.6
RSMA01	96.1°C	9.0

## 7.6 Loss of deposition-hole positions

The design premises document /SKB 2007/ identified preliminary criteria to be used for assessing the degree-of-utilisation to ensure that the repository is large enough to host 6,000 canisters. The bases for rejecting a potential deposition position are briefly outlined below.

1. During a future earthquake, the deposition hole may be sheared so much that it can harm the canister. This could occur if the canister is intersected by a fracture, or minor deformation zone, of a radius larger than 75 m.
2. In order to avoid piping erosion of the buffer, only deposition holes with limited inflows can be used. The acceptable inflow criteria into a deposition holes is 0.1 l/min and 5 l/min for 300 m of deposition tunnel length, and for all other openings 10 l/min per 100 m tunnel length /SKB 2007/.
3. Spalling in the deposition hole due to excavation-induced stresses should be minimised. Stress analyses that utilises the minimum and maximum, as well as the most likely value should be carried out to assess the spalling potential.
4. Placing a deposition hole in rock with a very low thermal conductivity, i.e. amphibolite.

Due to the inherent uncertainty in the spatial distribution of the fracturing in the rock mass described in the site descriptive model, the layout cannot a priori identify which actual deposition positions would be rejected. Therefore the designer should assess the gross-capacity of the layout within the focused volume (Figure 7-1).

## 7.7 Summary

The ground conditions anticipated for the underground openings associated with the Deposition areas are summarised below in Table 7-3. It should be realised that this summary represents the general conditions anticipated and that these must be evaluated in Design Step D2. It is anticipated that the deposition holes should be located in Ground Type 1.

**Table 7-3. Summary of the ground conditions anticipated for the Deposition areas.**

	Ground Type	Behaviour Type	Support Type	Grouting Type
Deposition areas				
450–600 m	GT1, GT2	GB1, GB2A	ST1, ST2,ST3	GRT1
> 600 m		GB2A		
Minor Deformation Zones	GT2 & GT3	GB1, GB2	ST2,ST3,ST4	GRT2

## 8 Repository depth

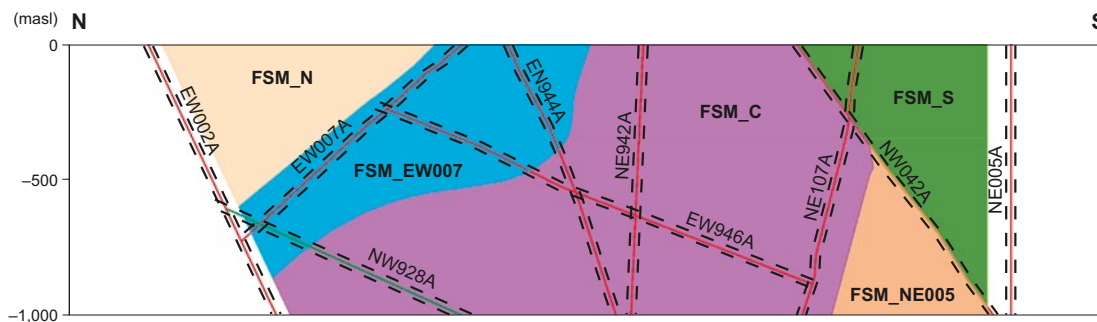
In /SKB 2006b/ it was suggested that a repository in typical Scandinavian shield could be safely constructed at a depth interval between 400–700 m. The general site conditions at Laxemar are illustrated in Figure 8-1. As illustrated in Figure 8-1 the frequency of connected open fractures decrease significantly at least below 500 m. At this depth range there are also several site specific factors related to long-term safety that must also be considered when selecting the repository depth. An overview of these factors is provided in Table 8-1 and Section 13.6.8 in /SKB 2006b/ describes the role each factor can play in the depth selection. The depth of the repository must, in general, balance the safety requirements for the repository and the constructability of the underground excavations required for the deposition tunnels and deposition holes. The safety requirements are largely influenced by the hydrogeology of the site, i.e. frequency and occurrence of conductive fractures with depth while the constructability is mainly related to rock mechanics issues, i.e. stability of the deposition holes prior to emplacement.

The designers must also consider the practical requirements for inclining the tunnels for drainage purposes. This will result in approximately 25–30 m difference in elevation from the highest point of the repository to the lowest point. At this stage of the design flexibility in the depth selection is required to ensure that both the operational and performance-related requirements are satisfied.

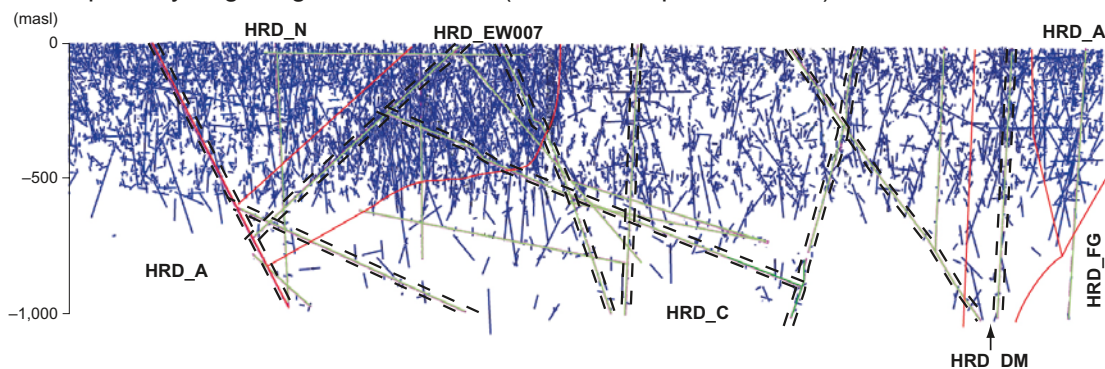
### 8.1 In-situ temperature

The in situ temperature at 400-, 500- and 600-m depths is given in Table 2-2 and the gradient over this depth interval ranges from 1.2 to 1.5°C/100 m /Sundberg et al. 2008/. Based on sensitivity analyses for thermal dimensioning (see appendix A), the expected range in canister spacing with depth is illustrated in Figure 8-2. Rock domain RSMM01 (Domain M) shows the largest canister spacing increase, approximately 1.0 m between 500-m and 600-m depth.

Fracture domain model



Conceptual hydrogeological DFN model (connected open fractures)

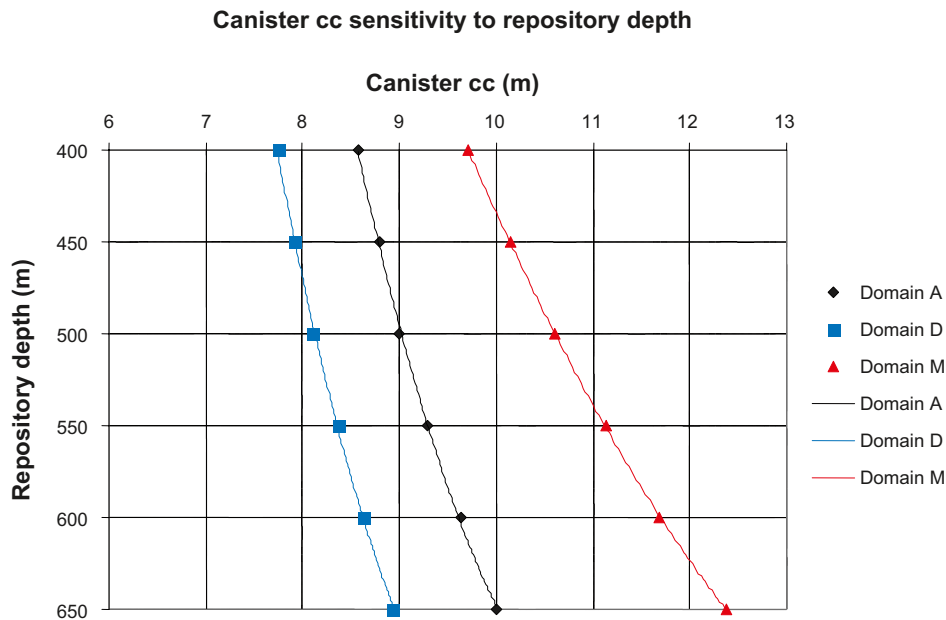


**Figure 8-1.** Illustration of the general rock mass characteristics at Laxemar, highlighting the fracture domains and their correlation with hydrogeology /from SKB 2009/.



**Table 8-1. Engineering and safety factors considered for the recommendation of repository depth. NB: Up and down refers to the relative position of the repository.**

Engineering factors	Safety factors
<b>Initial temperature</b> Up: lower in situ temperature favorable for canister spacing	<b>Initial temperature</b> Considered in design, no direct effect
<b>Water inflow, grouting efforts</b> Up: lower groundwater pressure favorable. Down – if hydraulic conductivity decreases with depth	<b>Salinity and upconing</b> Up: possibly lower inflow to facility <b>Groundwater pressure</b> Up: marginal importance
<b>Rock stability, rock stress</b> Positioning above a tentative triggering depth where stress conditions may be unfavorable for tunneling	<b>Rock stress</b> Positioning above a tentative triggering depth where stress conditions may be unfavorable for long term effects around the deposition holes
<b>Available space, layout adaptation – 3D structural model</b> Undecided, site specific	<b>3D structural model – layout adaptation, degree of utilisation</b> Site specific – fracturing, thermal properties, hydraulic properties, stability
<b>Degree of utilisation – fracturing, thermal properties, inflow, stability</b> Site specific	<b>Length and transport resistance of travel paths</b> Down: longer paths generally favorable
<b>Environment (short term)</b> Up: less excavated rock volume, less inflow (drawdown)	<b>Fracture frequency and Transmissivity</b> Undecided, site specific
<b>Time and cost</b> Up: shorter access shafts and ramp	<b>Inadvertent human intrusion</b> Down: lower risk of intrusion, difficult to quantify
<b>Design of underground openings</b> Not affected	<b>Freezing</b> Down: reduces risk associated to permafrost <b>Surface erosion</b> No importance



**Figure 8-2. Canister spacing sensitivity to repository depth for the Laxemar temperature gradient (1.5°C/100 m).**

## 8.2 Fracture frequency

Fracture intensity as a function of orientation set and fracture domain does vary with depth, but the variability could not be linked to any observed geological or tectonic criteria, and was not consistent. This means that the analysis of fracture intensity as a function of depth did not show any systematic decrease or increase in fracture intensity with depth in a given fracture domain, or across the Laxemar local model volume as a whole /SKB 2009/.

However the hydrogeological modelling shows a significant decrease of flowing fractures especially below 400 m in the hydraulic domains. It might be speculative, but the notion that the hydraulic data indicate an upper hydraulic domain down to approximately 400 m and a different hydraulic domain with lower transmissivity under that depth may indicate a decrease in the fracture frequency below 400 m. Hence, the fracture frequency cannot be considered to have a significant influence on the proposed depth of the repository at this stage.

The orientations of the observed fracture sets at the Clab and Äspö HRL facilities are given in /Carlsson and Christiansson 2007/. In general, based on the observations from the Äspö HRL, steeply dipping NW-SE and NE-SW fractures as well as gently dipping fractures are dominant. In addition, steeply dipping, N-S to NE-SW trending fractured zones associated with fine grained granitic dykes occur within the Simpevarp peninsula. /Stanfors et al. 1997/ noted a decrease in fracture frequency below a depth of approximately 400 m in the Äspö HRL both in the tunnel and in boreholes drilled for the surface. This was interpreted to be explained by an increasing homogeneity of the rock below ~ 400 m depth.

## 8.3 Hydrogeological considerations

According to Table 2-13 the frequency of transmissive fractures decreases significantly from surface to depth. The flowing fracture frequency is between 0.1 and 0.2 fractures/m in the 400–650 m interval, and exhibits significant spatial variability between the different hydraulic domains. There is no general trend of decrease in the frequency of transmissive fractures in the depth interval –400 to –650 m. Thus, from a hydrogeological point of view there is no advantage of going deep within this depth interval.

The flowing fracture frequency appears to become very low below 650 m depth. This is however based on limited amount of data and establishing the repository at these depths would imply increased engineering challenges.

## 8.4 Spalling considerations

In general, stress magnitudes tend to increase with depth. Because stress induced spalling is a function of the stress magnitudes relative to the rock strength, it is generally assumed that the potential for spalling also increases with depth, assuming the rock strength remains constant. The stress conditions at the site are given in Section 2.4 and the strength of the intact rock is provided in Section 2.1.3. With consideration to the stress model given in Table 2-12 the horizontal stress magnitudes seem to increase quite significantly with depth thus increasing the risk for excavation-induced spalling in the deposition holes.

Spalling in the deposition tunnels is not considered to be an issue provided the tunnels are aligned parallel or sub-parallel ( $\pm 30^\circ$ ) to the maximum horizontal stress (c.  $135^\circ$  Azimuth).

## 8.5 Available space – site adaptation

The repository layout in Laxemar is strongly constrained by the geometry of deterministically modelled deformation zones that are large enough to potentially require respect distance and by the lithological domains. The lithological domains at Laxemar appear to have significantly different mechanical, thermal properties and also hydraulic properties.

The available space increases slightly with depth. However, the required canister spacing is also increasing with depth (Figure 8-2).

## **8.6 Construction costs and environmental impact**

Both the construction cost and the environmental impact is a function of the repository depth. The deeper the excavation, the larger the repository footprint due to increasing in situ temperature with depth, and hence the greater the impact. As illustrated by Figure 8-2 an increase in depth by 50 m will require an increase in canister spacing of approximately 0.2 m (and even more in rock domain M). The difference in canister spacing and required total length of deposition tunnels must be explored by the designer in an early stage of design D2. The impact of different options for site adaptation and choice of facility depth should be evaluated in consultation with the Design Coordinator.

## **8.7 Other considerations**

Other safety factors from Table 8-1 are discussed in /SKB 2006a/ and considered to have less importance on repository depth selection.

## **8.8 Recommended repository depth**

The hydraulic properties of the rock mass are judged to be the most important parameter from long term safety point of view. Between the 400 m and 650 m depth, there is no statistically significant change in the frequency of water conducting fractures. Below 650 m depth, the frequency of water conducting fractures is very low but this is based on relatively few and sparsely distributed data.

The available space for canister positions increases with depth, but the required canister spacing also increases because of the increase in rock temperature. The construction and operational cost will also increase with increased facility depth.

Within the target depth of 400 to 650 m, the repository elevation of 500 m is judged to provide a reasonable balance of canister spacing with available space, and frequency of water bearing fractures. The roof of the repository should not extend above Elevation 500 m.

## 9 Summary of Layout/design issues for D2

The design step D2 is a preliminary design and the focus described in /SKB 2007/ pertains to the design issues and not the construction issues. The outcome of design step D2 will provide input to design step C where the construction issues will be addressed in more detail, at least for the access routes such as shafts and ramp.

There are several general engineering guidelines that should be considered in laying out the repository:

1. The deposition holes should be located in Ground Type GT1.
2. The Central Area can be located in any rock mass suitable for constructing large caverns.
3. The access tunnels and shafts should be located to minimise the potential for large groundwater inflows.
4. Layouts for tunnel and shaft access should be oriented such that the intersection lengths with major water-bearing zones are as short as practical.
5. Deformation zones with a trace length at ground surface greater than 3,000 m require respect distance of 100 m where deposition holes should not be located. This respect distance is measured perpendicular from the transition zone boundary and a model of these zones and their respect distances is provided by SKB.
6. The repository depth and layout should minimise stress concentrations on the boundary of the underground excavations (deposition holes and deposition tunnels), unless it can be shown that such stress concentrations do not cause spalling.

In addition to the general guidelines given above there are several issues which need special consideration when designing the repository layout. These are highlighted below.

### ***Issue: Repository layout***

The most significant challenge for the Laxemar site is finding a suitable volume of rock for the repository.

### **Large deformation zones**

Because of the number of deformation zones and their associated respect distance the footprint area available for the deposition tunnels is limited. Two options should be evaluated by the designer: (1) a single level repository broken into panels, and (2) a two-level repository. Option 1 will require long access tunnels and a large footprint area. Option 2 will require a smaller footprint area but access will be required on two levels separated by approximately 100 m.

### **Thermal dimensioning**

The thermal properties of the rock in the focused volume must also be considered. The heterogeneity of a rock panel between deformation zones that is identified as suitable for deposition holes is expected to be significant. Depending on the geometry of the layout less conductive rock types can be encountered with depth, thus leading to larger distances between canisters. Moreover as temperature increases with depth, option (1) as described above will also require larger spacing between canisters in order not to override the maximum temperature in the buffer.

### ***Issue: Highly transmissive fractures***

#### **Deposition tunnels**

This issue has an impact on the orientation of the deposition tunnels. Experience from the construction of the Äspo HRL clearly showed that NW-SE fractures were the dominant transmissive fractures with inflows of several 10 s of litres per minute at the 450 m depth. Should the same fracture set

occur at Laxemar at depth, the deposition tunnels should be oriented to minimise the impact of these transmissive fractures, i.e. the tunnels should be oriented approximately perpendicular to these fractures. However this implies orienting the tunnel more or less perpendicular to the maximum horizontal stress which has a major impact on spalling risk.

### **Deposition areas**

At this stage, the occurrence at repository depth of fractures with a relatively high transmissivity cannot be ruled out. These fractures should not intersect deposition holes as they will impact the repository layout.

### **Issue: Grouting**

Given the spatial variability of the transmissive fractures and number of deformation zones the designer should consider that grouting of the access tunnels and shafts will be required on a routine basis. Grouting of the deposition tunnels is not expected to be routinely required unless the transmissive NW-SE steeply dipping fractures are encountered.

## 10 References

SKB's (Svensk Kärnbränslehantering AB) publications can be found at [www.skb.se/publications](http://www.skb.se/publications).

**Andersson J, Ström A, Svemar C, Almén K-A, Ericsson L-O, 2000.** What requirements does the KBS-3 repository make on the host rock? Geoscientific suitability indicators and criteria for siting and site evaluation. SKB TR-00-12, Svensk Kärnbränslehantering AB.

**Andersson C, Söderhäll J, 2001.** Rock mechanical conditions at the Äspö HRL – A study of the correlation between geology, tunnel maintenance and tunnel shape. SKB R-01-53, Svensk Kärnbränslehantering AB.

**Ask D, 2006.** New developments in the Integrated Stress Determination Method and their application to rock stress data at the Äspö HRL, Sweden. *Int. J. Rock Mech. and Min. Sci.*, 43, 107–126.

**Back P-E, Sundberg J, 2007.** Thermal site descriptive model. A strategy for the model development during site investigations – version 2. SKB R-07-42, Svensk Kärnbränslehantering AB.

**Berglund J, Curtis P, Eliasson T, Olsson T, Starzec P, Tullborg E-L, 2003.** Äspö Hard Rock Laboratory. Update of the geological model 2002. SKB International Progress Report IPR-03-34, Svensk Kärnbränslehantering AB.

**Bieniawski Z T, 1989.** Engineering rock mass classification. Wiley, New York.

**Caine J S, Evans J P, Forster C B, 1996.** Fault zone architecture and permeability structure. *Geology* 24 (11), 1025–1028.

**Carlsson A, Christiansson R, 2007.** Construction experiences from underground works at Oskarshamn. SKB R-07-66, Svensk Kärnbränslehantering AB.

**Casagrande A, 1965.** Role of the Calculated Risk in Earthwork and Foundation Engineering. *Proceedings of the American Society of Civil Engineers* 91(SM4):1–40.

**Emmelin A, Eriksson M, Fransson A, 2004.** Characterisation, design and execution of two grouting fans at 450 m level, Äspö HRL. SKB R-04-58, Svensk Kärnbränslehantering AB.

**Emmelin A, Brantberger M, Eriksson M, Gustafson G, Stille H, 2007.** Rock grouting – Current competence and development for the final repository. SKB R-07-30, Svensk Kärnbränslehantering AB.

**Glamheden R, Hansen L M, Fredriksson A, Bergkvist L, Markström I, Elfström M, 2007.** Mechanical modeling of the Singö deformation zone – Site descriptive modeling Forsmark Stage 2.1. SKB R-07-06, Svensk Kärnbränslehantering AB.

**Goricki A, 2003.** Classification of rock mass behaviour based on a hierarchical rock mass characterisation for the design of underground structures. PhD Thesis submitted to Department of Civil Engineering, Graz University of Technology, Austria.

**Hakami E, Fredriksson A, Lanaro F, Wrafter J, 2008.** Rock mechanics Laxemar. Site descriptive modelling SDM-Site Laxemar. R-08-57, Svensk Kärnbränslehantering AB.

**Hoek E, Diederichs M S, 2006.** Empirical estimation of rock mass modulus. *Int. J. Rock Mech. and Min. Sci.*, 43, 203–215.

**Jackson R, Lau J S O, 1990.** The effect of specimen size on the mechanical properties of Lac du Bonnet grey granite. In *Proc. 1st. Int. Workshop on Scale Effects in Rock Masses*, Loen, Norway, (Edited by da Cunha, A. P.) A. A. Balkema, Rotterdam, 1990, 165–174.

**Janson T, Magnusson J, Bergvall M, Olsson R, Cuisiat F, Skurtveit E, Grimstad E, 2006.** Final repository for spent nuclear fuel – Underground design Laxemar Layout D1. SKB R-06-36, Svensk Kärnbränslehantering AB.

**La Pointe P, Fox A, Hermanson J, Öhman J, 2008.** Geological discrete fracture network model for the Laxemar site. Site descriptive modelling SDM-Site Laxemar. SKB R-08-55, Svensk Kärnbränslehantering AB.

**Makurat A, Löset F, Wold Hagen A, Tunbridge L, Kveldsvik V, Grimstad E, 2002.** Äspö HRL. A descriptive rock mechanics model for the 380–500 m model. SKB R-02-11, Svensk Kärnbränslehantering AB.

- Martin C D, 2005.** Preliminary assessment of potential underground stability (wedge and spalling) at Forsmark, Simpevarp and Laxemar sites. SKB R-05-71, Svensk Kärnbränslehantering AB.
- Munier R, Stanfors R, Milnes A G, Hermanson J, Triumf C-A, 2003.** Geological Site Descriptive Model – A strategy for the model development during site investigations. SKB R-03-07, Svensk Kärnbränslehantering AB.
- Munier R, Hökmark H, 2004.** Respect distances – Rationale and means of computation SKB R-04-17, Svensk Kärnbränslehantering AB.
- Palmström A, Stille H, 2006.** Ground behaviour and rock engineering tools for underground excavations. *Tunnelling and Underground Space Technology* (2006), doi:10.1016/j.tust.2006.03.006.
- Peck R B, 1969.** Ninth Rankine Lecture: Advantages and limitations of the observational method in applied soil mechanics *Geotechnique*, 19:171–187.
- Rhén I, Forsmark T, Hartley L, Jackson P, Roberts D, Swan D, Gylling B, 2008.** Hydrogeological conceptualisation and parameterisation, Site descriptive modelling SDM-Site Laxemar. SKB R-08-78, Svensk Kärnbränslehantering AB.
- Schubert W, Goricki A, 2004.** Probabilistic assessment of rock mass behaviour as basis for stability analyses of tunnels. In *Proceedings of the Rock Mechanics Meeting*, Stockholm, Sweden, March 2004, pp. 1–20 (Published by SvBeFo, Swedish Rock Engineering Research).
- SKB, 2000.** What requirements does the repository have on the host rock? SKB TR-00-12, Svensk Kärnbränslehantering AB.
- SKB, 2001.** Site investigations – Investigation methods and general execution programme. SKB TR-01-29, Svensk Kärnbränslehantering AB.
- SKB, 2005.** Platsundersökning Oskarshamn. Utvärdering av platsdata inför fokusering av de fortsatta undersökningarna inom delområde Laxemar. SKB P-05-264, Svensk Kärnbränslehantering AB.
- SKB, 2006a.** Preliminary Site description, Laxemar subarea – version 1.2. SKB R-06-10, Svensk Kärnbränslehantering AB.
- SKB, 2006b.** Long-term safety for KBS-3 repositories at Forsmark and Laxemar – a first evaluation, Main Report of the SR-Can project. SKB TR-06-09, Svensk Kärnbränslehantering AB.
- SKB, 2006c.** Preliminary site description Laxemar stage 2.1. Feedback for completion of the site investigation including input from safety assessment and repository engineering. SKB R-06-110, Svensk Kärnbränslehantering AB.
- SKB, 2007.** Final repository facility. Underground Design Premises/D2. SKB R-07-33, Svensk Kärnbränslehantering AB.
- SKB, 2009.** Site description of Laxemar at completion of the site investigation phase (SDM-Site Laxemar). SKB TR-09-01, Svensk Kärnbränslehantering AB.
- Stanfors R, Olsson P, Stille H, 1997.** Äspö HRL – Geoscientific evaluation 1997/3. Results from pre-investigations and detailed site characterization. Comparison of predictions and observations. Geology and mechanical stability. SKB TR 97-04, Svensk Kärnbränslehantering AB.
- Stigsson M, 2009.** Statistics of modelled conductive fractures based on Laxemar and Forsmark Site descriptive model data. R-09-48, Svensk Kärnbränslehantering AB.
- Stille H, 1986.** Experiences of design of large caverns in Sweden. *Proceedings Int. Conf. On Large Rock Caverns*, Helsinki, pp 231–241, Pergamon Oxford.
- Sundberg J, Wrafter J, Back P-E, Rosén L, 2008.** Thermal properties Laxemar. Site descriptive modelling SDM-Site Laxemar. SKB R-08-61, Svensk Kärnbränslehantering AB.
- Viola G, Venvik Ganerød G, 2007.** Oskarshamn site investigation. Structural analysis of brittle deformation zones in the Simpevarp-Laxemar area, Oskarshamn, southeast Sweden. SKB P-07-41, Svensk Kärnbränslehantering AB.
- Wahlgren C-H, Curtis P, Hermanson J, Forssberg O, Öhman J, Fox A, La Pointe P, Drake H, Triumf C-A, Mattsson H, Thunehed H, Juhlin C, 2008.** Geology Laxemar. Site descriptive modelling. SDM-Site Laxemar. SKB R-08-54, Svensk Kärnbränslehantering AB.

## Thermal dimensioning of the Canister spacing

### A1 Introduction

In order to meet the temperature requirements on the bentonite buffer, calculation of cc distance between canisters have been performed for Domain RSMD01, RSMM01 and RSMA01 in Laxemar. The strategy for thermal dimensioning of the layout of the repository is described in /Hökmark et al. 2009/. The calculations have been performed on the basis of the following pre-requirements:

1. Maximum allowed peak temperature in the bentonite buffer in all deposition holes; 100°C.
2. Maximum thermal power in the canister; 1,700 W.
3. Distance between deposition tunnels; 40 m.
4. Distance between deposition holes;  $\geq 6$  m.
5. No optimizing of the layout is performed.

The requirements mean that the necessary cc distance for the canister with the lowest thermal conductivity in the rock mass, will be dimensioning for **all** canisters. The calculation method is summarised as follows:

- An uncertainty margin to the 100°C threshold is determined, see Section A5.
- An "approximate value" (guess value) of canister spacing is determined preliminarily from the lower tail of the distribution of thermal conductivities in the rock mass at the 5 m scale /Sundberg et al. 2008/ and nomographic chart assuming homogenous conditions /Hökmark et al. 2009/, see Section A6.
- Canister spacing is calculated with the numerical solution described in /Hökmark et al. 2009/ on the basis of data from the "worst case" thermal property realisations from the stochastic modelling in the 2 m scale of thermal properties in each rock domain /Sundberg et al. 2008/.

### A2 Summary of results

The results of the calculations for a repository at 500 m depth are summarised in Table A-1. The threshold is calculated as: 100° – margin (as estimated in Table A-5).

### A3 Implementation – Numerical calculation

In the thermal site descriptive model /Sundberg et al. 2008/, stochastic modelling of the spatial thermal conductivity in the rock mass have been performed. For the different domains, 1,000 realisations have been performed. Each realisation contains 125,000 cells at 2 m scale ( $2 \cdot 2 \cdot 2 = 8 \text{ m}^3$ ). The simulation volume is consequently 100·100·100 m. In Laxemar there are no obvious relationships between thermal conductivity and heat capacity. In Laxemar the heat capacity has been modelled based on the TRC-distribution in each domain together with a statistical distribution model for heat capacity for each TRC /Sundberg et al. 2008/. A code identifying the actual TRC is also connected to each cell. Domain RSMM01 and RSMD01 have been subdivided into thermal subdomains.

The realisations are used as input to a numerical calculation model with a deposition tunnel and 9 canisters, described in /Hökmark et al. 2009/. The realisations are in a local coordinate system due to considerations made in the thermal modelling /Sundberg et al. 2008/. In the numerical model, data is collected from each cell in the realisation and transformed into the coordinate system for the numerical

**Table A-1 Calculated spacing between canisters at 500 m depth (14.8°C initial temperature) and 40 m tunnel spacing in the different rock domains in the Laxemar area.**

Domain	Threshold	Canister cc distance
RSMD01	96.3°C	8.1 m
RSMM01	96.1°C	10.6 m
RSMA01	96.1°C	9.0 m



model. In the numerical model, the origin is at the centre of the central canister (half the height of canister 5) with the x-axis parallel to the deposition tunnel. The deposition tunnel is positioned in the designed direction with respect to the potential anisotropy in the geology. However, in the present calculations in Laxemar the tunnel direction is irrelevant since anisotropy have not been modelled (RSMM01, RSMA01) or the foliation plane is subhorizontal (RSMD01). In a pre-processing step, the realisations are ranked in an expected order, from the realisation with the lowest thermal conductivity in a weight volume around each canister, to the realisation with the highest thermal conductivity (the weighted thermal conductivity also includes the tunnel backfill). Numerical calculations are made for a number of realisations, normally the ones with the highest ranking, i.e. the lowest weighted thermal conductivity. The two outermost canisters on each side are ignored due to possible boundary effects, which mean that only canisters 3–7 are considered /Hökmark et al. 2009/.

The methodology implies that all relevant scales for the spatial variability of the thermal conductivity are considered. Also the anisotropy in the geology is taken into account. The model also makes it possible to simulate temperature dependency in the thermal properties. This has been done for all three rock domains.

## A4 Data

In Table A-2 input data to the numerical model is presented.

**Table A-2. Description of input data to numerical model. The thermal realisations are described in /Sundberg et al. 2008/.**

Description	Value	Comment
Temperature at 500 m depth, °C	14.8	/Sundberg et al. 2008/
Temperature gradient, °C/m	0.015	/Sundberg et al. 2008/
Tunnel spacing, m	40	
Tunnel direction, °	0	Tunnel direction is 135° but is irrelevant since geological anisotropi has not been modelled or is subhorizontal
Thermal conductivity of tunnel backfill, W/(m·K)	0.7	
Thermal conductivity of bentonite, W/(m·K)	1	
Gap coefficient	16	/Hökmark et al. 2009/
Effective thermal conductivity of bentonite and gap in radial direction from canister, W/(m·K)		Calculated from gap coefficient and conductivity of bentonite /Hökmark et al. 2009/
Thermal conductivity of canister, W/(m·K)	30	
Size of realisation, m <sup>3</sup>	100·100·100	1,000,000 m <sup>3</sup>
Cell size in realisation file, m <sup>3</sup>	2·2·2	
Thermal realisations dA	SKB's model database	File name: addsim_std_dA_2m.out
Number of realisations	1,000	
Thermal realisations dD	SKB's model database	File name: geomerge_std_dD_2m.out
Number of realisations	1,000	
Thermal realisations dM	SKB's model database	File name: addsim_std_dM_2m.out
Number of realisations	1,000	
Temperature dependence in thermal properties	See report	/Sundberg et al. 2008/
Transformation parameters realisations		all rock domains /Sundberg et al. 2008/
$\alpha_1$ (trend-90°)	0°	
$\beta_1$ (plunge)	0°	
$\alpha_2$ (strike-90°+90°)	0°	
$\beta_2$ (dip)	0°	

## A5 Temperature margin

The uncertainties relevant to the dimensioning issue are listed and discussed in /Hökmark et al. 2009/ and applied to the Laxemar rock domains in Table A-3 and Table A-4. The rock thermal conductivity has an influence on the margin and is typically 2.0 W/(m·K) for low conductivity rock in domains RSMM01 and RSMA01 and 2.5 W/(m·K) for domain RSMD01.

The temperature margin is 3.7°C for domain RSMD01 and 3.9°C for domain RSMM01 and RSMA01 for the numerical solution in order to establish definitive spacing (Table A-5). The temperature threshold used in the numerical calculations is **96.3°C** (100°–3.7°C) for domain RSMD01 and **96.1°C** for domain RSMM01 and RSMA01. The temperature margin for the analytical solution in order to establish a guess (start) value is determined to approximately two degrees higher; approximately 5.7°–6°C.

## A6 Results

### Guess value – canister spacing

An "approximate value" (guess value) of canister spacing is determined. The guess values for the spacing between canisters are based on low percentiles for the thermal conductivity distribution in 5 m scale in the different rock domains /Sundberg et al. 2008/, see Table A-6 . The guess values are approximated from nomographic chart of the analytical solution in /Hökmark et al. 2009/, see Figure A-1. Note that the nomographic chart is based on a slightly overestimated value of the heat capacity. For the purpose of establishing spacing guess values this is of no importance. The temperature at 500 m depth and the margin for the analytical solution 5.7–6°C above are also used as input. The guess values for the spacing in Table A-6 vary between 8 and 11 m for the different domains and percentiles. For the same domain the guess value vary within 0.5 to 1 m for the different percentiles.

### Spacing between canisters – Domain RSMD01

The guess value based on the 0.1 percentile for canister spacing is too large. Through iterative calculations with the numerical model the canister spacing is set to 8.1 m in order to fulfil the temperature threshold (96.3°C). The calculation results presented in Table A-7 show that all canisters in domain RSMD01 fulfil the temperature criterion if the spacing is set at 8.1 m.

**Table A-3. Local solution. Modified from /Hökmark et al. 2009/ with site specific data.**

$\Delta T_{\text{tot}}$ , difference between rock wall temperature and maximum bentonite temperature		Rock conductivity		Comment
		2.0 W/(m·K)	2.5 W/(m·K)	
		Domain RSMM01 and RSMA01	Domain RSMD01	
	Uncertainties related to:	Margin		
U1	Geometry of air-filled canister/bentonite slot and variations in barrier conductivity	2.7°C	3°C	The influence can be interpolated from /Hökmark et al. 2009/.
U2-	Moisture redistribution in barrier	0.2°C	0.2°C	
U3	Spalling	0.1°C	0.1°C	
U4	Vertical variation of rock conductivity along deposition hole	0.25°C	0.25°C	
U5	Vertical distribution of heat generation in the canisters	0.2°C	0.2°C	
<b>Sum <math>\Delta T_{\text{tot}}</math></b>		<b>3.45°C</b>	<b>3.75°C</b>	

**Table A-4. Uncertainties in numerically calculated rock wall temperature. Modified from /Hökmark et al. 2009/ with site specific data.**

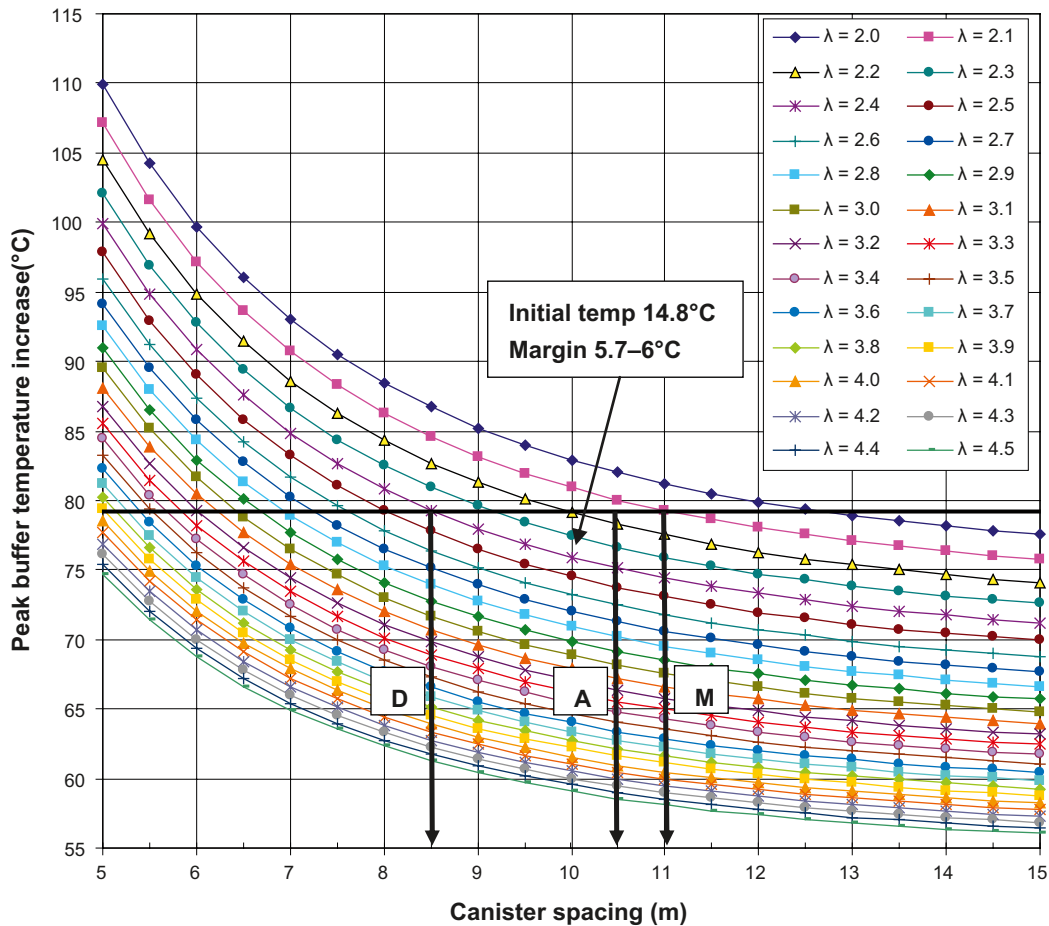
$T_{wall}$	Rock wall temperature at canister mid-height at the time of buffer temperature peak	Rock conductivity		Comment
		2.0 W/(m·K)	2.5 W/(m·K)	
		Domain RSMM01 and RSMA01	Domain RSMD01	
	<b>Uncertainties related to:</b>	<b>Margin</b>		
U6	Anisotropy within rocktype	0.3°C	0°C	The anisotropy factor is 15% but the orientation of foliation (see /Sundberg et al. 2008/ Section 3.8) is more favourable compared to worst case in /Hökmark et al. 2009/. RSMD01 has subhorizontal dip and RSMM01 and RSMA01 have variable or moderate dip of foliation plane. The temperature effect is approximated from /Hökmark et al. 2009/.
U7	Bias in thermal properties	1.0°C	0.8°C	Interpolated from /Hökmark et al. 2009/
U8	Site model	0.1°C	0.1°C	In /Sundberg et al. 2008/ uncertainty estimated to less than 1% in the lower tail
U9	Initial temperature	0.35°C	0.35°C	Variability between lowest and highest temperature is approx. 0.1°C, see also /Hökmark et al. 2009/
U10	Temperature dependence	0°C	0°C	Included in numerical calculation, data from /Sundberg et al. 2008/
U11	Pressure dependence	-0.2°C	-0.2°C	
U12	Tunnel backfill	0°C	0°C	Accounted for in calculations
U12	Strategy uncertainties	-	-	
	<b>Sum (uncertainties)</b>	1.55°C	1.05°C	
	<b>Over/underestimate because of numerical model simplifications</b>			
S1	Representation of canister	-0.7°C	-0.7°C	Canister thermal conductivity 30 W/(m·K) used in numerical programme
S2-	Numerical precision	-0.8°C	-0.8°C	See /Hökmark et al. 2009/
S3	Boundary conditions	0.4°C	0.4°C	10% higher conductivity in one neighbouring tunnels gives 0.2°C in temperature contribution /Hökmark et al. 2009/. The difference between mean thermal conductivity and conductivity around a canister in low conductive rock is typically 10–15% for the domains or subdomains
	<b>Sum (under/overestimates)</b>	-1.1°C	-1.1°C	
	<b>Total <math>T_{wall}</math></b>	0.45°C	-0.05°C	

**Table A-5. Total temperature margin in numerical solution to establish a definitive spacing.**

Uncertainties related to:	Domain RSMM01 and RSMA01	Domain RSMD01
Local solution	3.45°C	3.75°C
Total $T_{wall}$ Numerical solution	0.45°C	-0.05°C
Total Margin	3.9°C	3.7°C

**Table A-6 Thermal conductivities for the 5 m scale for different percentiles and corresponding approximately guess values for the canister spacing based on nomographic chart in Figure A-1 for domain RSMA01, RSMM01 and RSMD01 /Sundberg et al. 2008/.**

	0.1 percentile		1 percentile	
	Thermal conductivity (W/(m·K))	Corresponding guess value for spacing, m	Thermal conductivity (W/(m·K))	Corresponding guess value for spacing, m
RSMD01	2.41	8.5	2.48	8
RSMM01	2.11	11	2.19	10
RSMA01	2.16	10.5	2.27	9.5



**Figure A-1.** Guess values for canister spacing, exemplified for the 0.1 percentile of the thermal conductivity distribution in the different domains, based on nomographic chart in /Hökmark et al. 2009/. To get the absolute upper bound peak temperature value the in situ temperature and the temperature margin established for the analytical solution must be added to the peak buffer temperature. Heat capacity 2.17 MJ/(m<sup>3</sup>·°C).

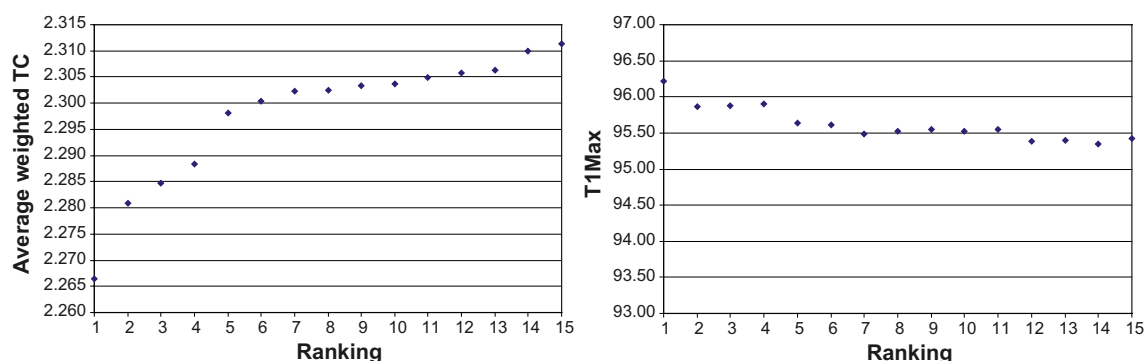
**Table A-7** Maximum bentonite temperature for the canister with the lowest thermal conductivity in each of the 15 lowest ranked realisations for Domain RSMD01, canister cc distance 8.1 m, tunnel cc distance 40 m, start temperature 14.8°C, gradient 0.015°C/m.

Ranking (based on thermal cond.)	Realisation no	Canister no	Min average weighted thermal conductivity W/ (m·K)	Max bentonite temperature without temp. dep. properties °C	Max bentonite temperature with temp. dep. properties °C
1	725	6	2.267	96.21	96.17
2	955	3	2.281	95.87	—
3	318	5	2.285	95.88	—
4	349	7	2.288	95.90	—
5	35	6	2.298	95.64	—
6	873	3	2.300	95.61	—
7	673	6	2.302	95.48	—
8	352	7	2.302	95.52	—
9	689	7	2.303	95.55	—
10	297	6	2.304	95.52	—
11	9	6	2.305	95.55	—
12	138	7	2.306	95.39	—
13	940	7	2.306	95.40	—
14	493	3	2.310	95.35	—
15	687	3	2.311	95.42	—

The results of Table A-7 are presented graphically in Figure A-2. With some exceptions, higher ranking gives a lower bentonite temperature. The peak temperature decreases with increasing ranking. With the ranking procedure it seems possible to find the hottest deposition holes if 5–10 realisations are tested. It can be concluded from the tables that temperature dependent thermal properties have a very small influence on the maximum temperature, as expected. The temperature dependency in the thermal conductivity is small for the actual rock types. The change of the peak bentonite temperature, when using temperature dependent thermal properties, is  $< 0.1^{\circ}\text{C}$  for the actual domain.

### Spacing between canisters – Domain RSMM01

In a similar way as for domain RSMD01, a number of iterative calculations have been made with the numerical model. The guess value based on the 0.1 percentiles is a bit too large. The resulting canister spacing in order to fulfil the temperature threshold ( $96.1^{\circ}\text{C}$ ) is set to 10.6 m. The calculation results in Table A-8 show that the temperature threshold is fulfilled for all canisters when the temperature is rounded off to one decimal. The use of temperature dependent thermal properties increases the maximum bentonite temperature with  $< 0.2^{\circ}\text{C}$  compared to the use of constant thermal properties.



**Figure A-2.** Maximum bentonite temperature for the canister with the lowest thermal conductivity in each of the 15 lowest ranked realisations for Domain RSMD01. Left: Ranking vs. weighted thermal conductivity ( $\text{W}/(\text{m}\cdot\text{K})$ ), Right: Ranking vs. max bentonite temperature ( $^{\circ}\text{C}$ ). Temperature-dependent rock thermal properties are not used (compare Table A-7). Canister cc distance 8.1 m, tunnel cc distance 40 m, start temperature  $14.8^{\circ}\text{C}$ , gradient  $0.015^{\circ}\text{C}/\text{m}$ .

**Table A-8** Maximum bentonite temperature for the canister with the lowest thermal conductivity in each of the 15 lowest ranked realisations for Domain RSMM01, canister cc distance 10.6 m, tunnel cc distance 40 m, start temperature  $14.8^{\circ}\text{C}$ , gradient  $0.015^{\circ}\text{C}/\text{m}$ .

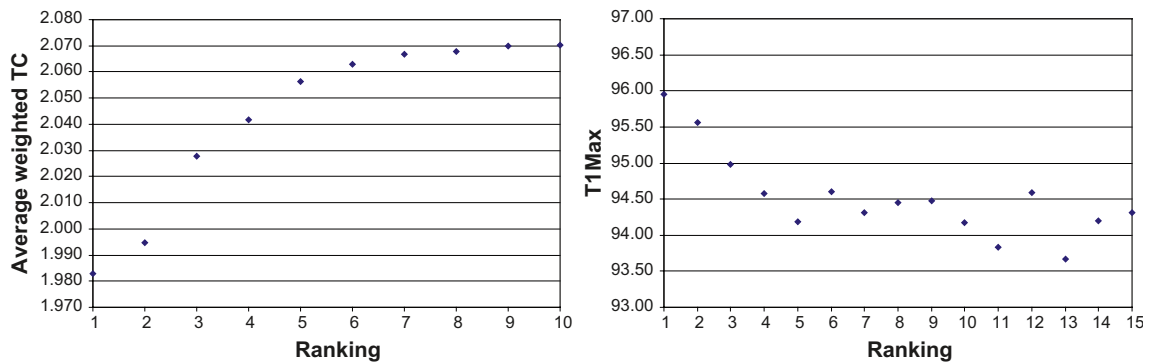
Ranking (based on thermal cond.)	Realisation no	Canister no	Min average weighted TC $\text{W}/(\text{m}\cdot\text{K})$	Max bentonite temperature without temp. dep. properties $^{\circ}\text{C}$	Max bentonite temperature with temp. dep. properties $^{\circ}\text{C}$
1	208	3	1.983	95.96	96.13
2	383	3	1.995	95.56	–
3	274	4	2.028	94.98	–
4	537	5	2.042	94.58	–
5	320	4	2.056	94.19	–
6	637	3	2.063	94.61	–
7	65	6	2.067	94.31	–
8	499	5	2.068	94.45	–
9	350	4	2.070	94.48	–
10	460	4	2.070	94.17	–
11	490	6	2.071	93.83	–
12	209	6	2.073	94.60	–
13	102	7	2.076	93.67	–
14	528	5	2.080	94.20	–
15	79	6	2.081	94.31	–

The results are presented graphically in Figure A-3. In the same way as for domain RSMD01, the weighted thermal conductivity reflects the ranking and increased ranking corresponds in general to lower maximum bentonite temperature.

### Spacing between canisters – Domain RSMA01

The guess values based on both the 0.1 percentile and the 1 percentile for canister spacing are too large. Trough iterative calculations with the numerical model the canister spacing is set to 9 m in order to fulfil the temperature threshold (96.1°C). The calculation results in Table A-9 show that the temperature requirement is fulfilled for all canisters when the temperature is rounded off to one decimal. The results are presented graphically in Figure A-4.

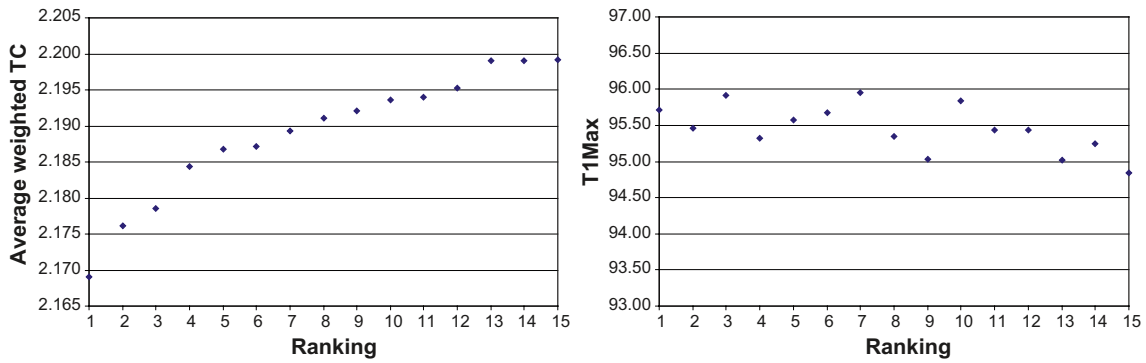
In contrast to domain RSMD01 and RSMM01, the highest temperature is ranked as no 7 instead of no 1. However, the difference between the temperatures is quite small and the overall trend shows that increased ranking reflects lower maximum bentonite temperature. The use of temperature dependent thermal properties increases the maximum bentonite temperature with < 0.2°C compared to the use of constant thermal properties.



**Figure A-3.** Canister with the lowest thermal conductivity in each of the 15 lowest ranked realisations for Domain RSMM01. Left: Ranking vs. weighted thermal conductivity ( $W/(m\cdot K)$ ), Right: Ranking vs. max bentonite temperature ( $^{\circ}C$ ). Temperature-dependent rock thermal properties are not used (compare Table A-8), canister cc distance 10.6 m, tunnel cc distance 40 m, start temperature 14.8°C, gradient 0.015°C/m.

**Table A-9 Maximum bentonite temperature for the canister with the lowest thermal conductivity in each of the 15 lowest ranked realisations for Domain RSMA01, canister cc distance 9.0 m, tunnel cc distance 40 m, start temperature 14.8°C, gradient 0.015°C/m.**

Ranking (based on thermal cond.)	Realisation no	Canister no	Min average weighted TC $W/(m\cdot K)$	Max bentonite temperature without temp. dep. properties $^{\circ}C$	Max bentonite temperature with temp. dep. properties $^{\circ}C$
1	913	6	2.1691	95.72	–
2	490	6	2.1762	95.45	–
3	919	5	2.1786	95.92	96.10
4	759	4	2.1844	95.32	–
5	867	7	2.1868	95.57	–
6	771	4	2.1872	95.67	–
7	893	4	2.1893	95.96	96.13
8	589	4	2.1911	95.35	–
9	443	3	2.1921	95.04	–
10	492	7	2.1936	95.84	–
11	820	3	2.194	95.43	–
12	516	7	2.1952	95.43	–
13	740	6	2.199	95.02	–
14	806	6	2.1991	95.24	–
15	797	6	2.1992	94.84	–



**Figure A-4.** Canister with the lowest thermal conductivity in each of the 15 lowest ranked realisations for Domain RSMA01. Left: Ranking vs. weighted thermal conductivity (W/(m-K)), Right: Ranking vs. max bentonite temperature (°C). Temperature-dependent rock thermal properties are not used (compare Table A-9), canister cc distance 9.0 m, tunnel cc distance 40 m, start temperature 14.8°C, gradient 0.015°C/m.

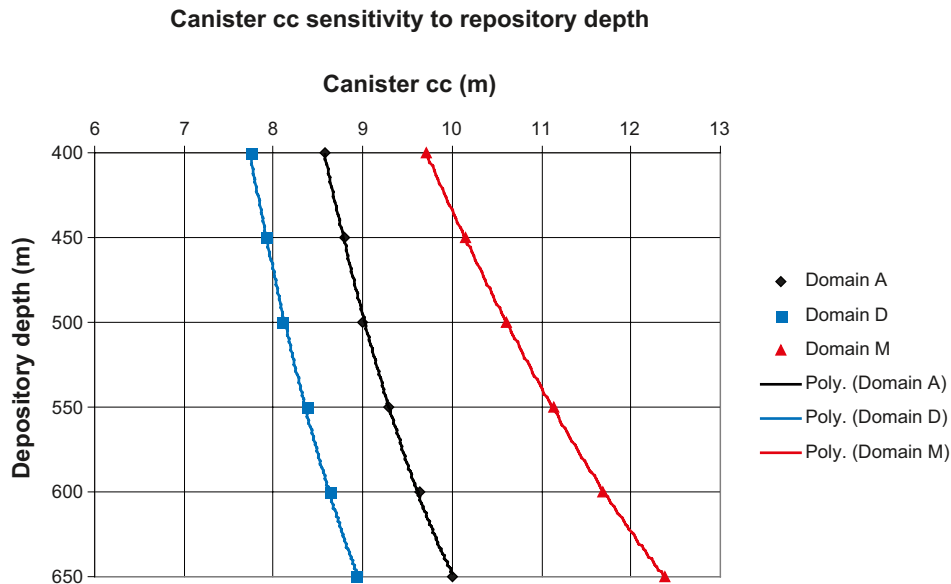
## A.7 Spacing sensitivity

### Sensitivity to repository depth

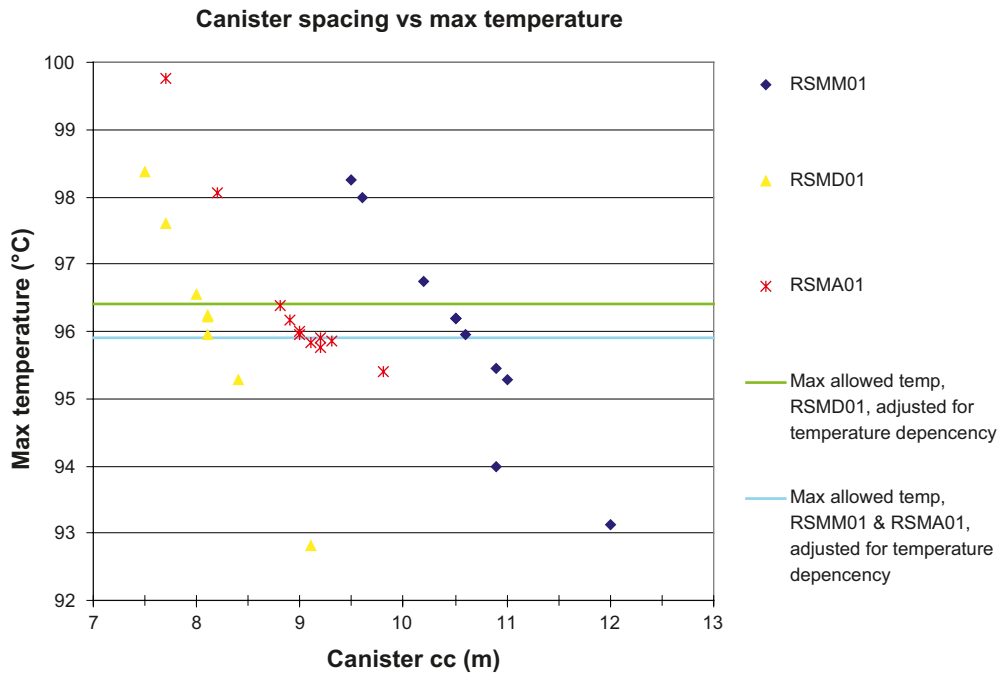
The dimensioning canister spacing has been calculated for 500 m repository depth for the different domains. If the repository depth for some reason is changed, the in-situ temperature will increase or decrease (1.5°C/100 m according to /Sundberg et al. 2008/) and influence the temperature threshold and the canister spacing. In Figure A-5 the sensitivity in canister spacing for the depth is showed. The influence is largest for domain RSMM01.

### Sensitivity for temperature

In Figure A-6 a summary of numerical calculation results is presented. The canister distance versus calculated peak buffer temperature is illustrated.



**Figure A-5.** Canister spacing sensitivity to repository depth. The start temperature increases 1.5°C for every 100 m depth increase.



**Figure A-6.** Summary of numerical program calculation results, temperature dependency of rock thermal properties not included. It is assumed temperature dependency increases with 0.2°C for domain RSMM01 & RSMA01, and decreases it with 0.1°C for domain RSMD01. Therefore the Max allowed temperature lines have been adjusted accordingly to counter this effect.

## A.8 References

SKB's (Svensk Kärnbränslehantering AB) publications can be found at [www.skb.se/publications](http://www.skb.se/publications).

**Hökmark H, Sundberg J, Kristenson O, Lönnqvist M, Hellström G, 2009.** Strategy for thermal dimensioning of the final repository for spent nuclear fuel. SKB R-09-04, Svensk Kärnbränslehantering AB.

**Sundberg J, Wrafter J, Back P-E, Rosén L, 2008.** Thermal properties Laxemar. Site descriptive modelling. SDM-Site Laxemar. SKB R-08-61, Svensk Kärnbränslehantering AB.



### Properties of deformation zones modelled to intersect the local model volume at –400 to –600 m masl

The geological and hydrogeological properties of the thirty seven (37) deformation zones that have been modelled to intersect the Laxemar focused volume between –400 to –600 m elevation are summarised in the tables in this appendix. Six (6) of these zones are gently dipping and thirty-one (31) zones are steeply dipping structures. Eight (8) of the steeply dipping zones have a trace length at the ground surface that is longer than 3,000 m (ZSMNE005A, ZSMNE011A, ZSMNE107A, ZSMNS001C (with the inclusion of Sections A to E), ZSMNS059A, ZSMEW002A, ZSMNW042A and ZSMEW007A (with the inclusion of Section C)). Nineteen (19) zones are devoided of any identified ground surface expression. No local minor deformation zones (trace length of < 1,000 m) are included in the deterministic model.

Transmissivities assigned to the deformation zones are:

*Measured T (sum T(PFL-f))*: Summed-up measured T from PFL-f for individual boreholes intercepting the deformation zone in the given depth interval.

*Model T*: Calibrated T value of zone extracted from the ConnectFlow base case model for the given depth interval.

The tables in this appendix provide basic data concerning the deformation zones intersecting the focused volume. A more comprehensive geological description of all deformation zones intersecting the local model volume can be found in Appendix 14 /Wahlgren et al. 2008/.

## **Contents**

### **Format for zone property descriptions**

#### **NE-SW Striking deformation zones, steeply dipping**

Deformation zone ZSMNE005A  
Deformation zone ZSMNE011A  
Deformation zone ZSMNE063A  
Deformation zone ZSMNE107A  
Deformation zone ZSMNE108A  
Deformation zone ZSMNE942A  
Deformation zone ZSMNE944A

#### **N-S Striking deformation zones, steeply dipping**

Deformation zone ZSMNS001A-E  
Deformation zone ZSMNS046A  
Deformation zone ZSMNS059A  
Deformation zone ZSMNS945A  
Deformation zone ZSMNS947A  
Deformation zone KLX04\_dz6b  
Deformation zone KLX04\_dz6c  
Deformation zone KLX07\_dz13  
Deformation zone KLX21B\_dz10-12  
Deformation zone KLX28\_dz1

#### **E-W to NW-SE striking deformation zones, steep to moderately southward dipping**

Deformation zone ZSMEW002A  
Deformation zone ZSMEW120A  
Deformation zone ZSMEW900A-B  
Deformation zone ZSMNW042A  
Deformation zone ZSMNW119A  
Deformation zone KLX07\_dz7  
Deformation zone KLX08\_dz6  
Deformation zone KLX18\_dz9

#### **E-W to NW-SE striking deformation zones, steep to moderately northward dipping**

Deformation zone ZSMEW007A-C  
Deformation zone KLX07\_dz9  
Deformation zone KLX07\_dz11  
Deformation zone KLX07\_dz12  
Deformation zone KLX10C\_dz3  
Deformation zone KLX10C\_dz7

#### **Gently dipping deformation zones**

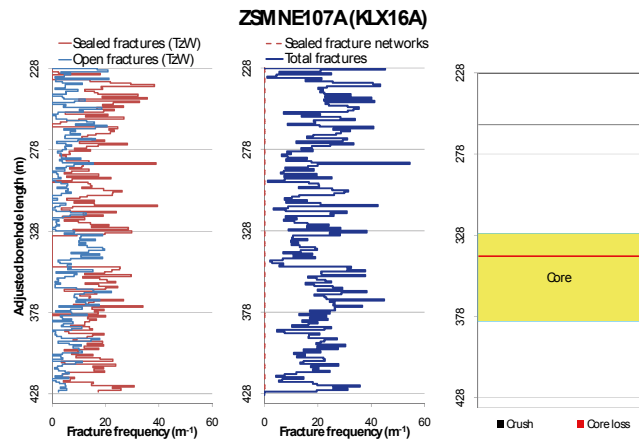
Deformation zone ZSMEW946A  
Deformation zone KLX03\_dz1b  
Deformation zone KLX03\_dz1c  
Deformation zone KLX07\_dz10  
Deformation zone KLX08\_dz10  
Deformation zone KLX11\_dz11

## Format for zone property descriptions

<b>Deformation zone:</b> <i>Zone name</i>	
<p style="text-align: center;"><b>Borehole intersections (metres along borehole)</b></p> <p>Borehole name: <i>intersection depth.</i>            ESHI= <i>Extended Single Hole Interpretation</i>            DZ<sub>x</sub>= <i>Numbered possible deformation zone from ESHI</i></p>	<p><i>Figure showing the location of the zone, relevant boreholes and the local model boundary.</i></p>
<p style="text-align: center;"><b>Deformation style, alteration and geometry</b></p> <p><b>Deformation style:</b> <i>statement of evidence for a ductile and/or brittle zone character.</i></p> <p><b>Alteration:</b> <i>type of alteration.</i></p> <p><b>Strike/dip (right-hand-rule):</b> <i>modelled average zone orientation.</i></p> <p><b>Trace length at ground surface:</b> <i>x.x km, not limited by the model boundary. Sometimes referred to as the 'geological length'.</i></p> <p><b>Model thickness / model thickness span :</b> <i>x m / x-x m</i></p> <p><b>Measured thickness (-400 to -600 m elevation):</b> <i>x m</i></p> <p><b>Comment:</b></p>	
<b>Fractures in the deformation zone</b>	
<p><i>Terzaghi corrected, borehole specific, fracture orientations within the modelled zone boundaries.</i></p>	
<p><b>Elevation:</b> <i>-x to -x m (RHB 70)</i></p>	
<b>Transmissivity (m<sup>2</sup>/s)</b>	
<p><b>General dip of PFL-features, elevation -400 to -600m:</b> <i>x</i>  <b>Measured T (sum T(PFL-f)), elevation -400 to -600m:</b> <i>x</i>  <b>Number of PFL-features, elevation -400 to -600m:</b> <i>x</i>  <b>Model T, elevation -400 to -500m:</b> <i>x.x E-6</i>  <b>Model T, elevation -500 to -600m:</b> <i>x.x E-7</i></p>	

## Deformation zone: *Zone name*

*Terzaghi corrected, selected borehole specific, fracture frequencies within the modelled zone boundaries. Deformation core zone marked in yellow. Position of crush and core-loss, not included in fracture frequency calculations, shown in grey and red respectively. All depths refer to adjusted values after borehole surveying.*



*Fracture frequency, P10 (number of fractures/m), were calculated for 1-m bins, starting from (adjusted) SEC\_UP of the DZ. The lowest bin is constrained by the (adjusted) SEC\_LOW, and may therefore be smaller than 1 m.*

*Example: A DZ defined between 100.5 m to 103.0 m, will be resolved into three bins: 100.5 to 101.5 m, 101.5 to 102.5 m, and 102.5 to 103.0 m.*

*Partly open fractures are included in the data set “open fractures”. The Terzaghi-weighted P10 for a 1-m bin is calculated as*

$$P_{10} = \frac{\sum_n \frac{1}{\sin(\max[\alpha, \alpha_{\min}])}}{L}, \text{ minimum bias angle, } \alpha_{\min} = 15^\circ \Leftrightarrow \text{Max TzW} = 3.86,$$

*Where L = 1 m, and n is the number of fractures inside the bin. The minimum bias angle is used to avoid artificial weights for small angles, where the effects of non-zero borehole radius are not negligible. The Terzaghi weighing is not implemented for sealed networks and crush zones, as TW concerns geometric bias owing to orientation of planar features versus scan line (borehole); the orientation of a sealed nw or crush zone, itself, is generally unclear (even if fractures inside are defined).*

*P10 for a sealed nw or crush zone is calculated by: 1000 [mm/m]/d [mm], where d is the piece-length of rock between fractures, in the unit m. It is superimposed onto the DZ 1-m bins, by fractional section length inside each bin.*

*Example: A crush with piece length 10 mm extends from 99.0 m to 102.0m. The crush has a P10 of 100 [1/m]. The first bin (ex. above) 100.5 to 101.5 m, will have a crush P10 of 100 [1/m], while the second bin, 101.5 to 102.5 m will have a crush P10 of 50 [1/m], as only half of the second bin contains crush.*

*Crush P10 is not shown explicitly, but included in the total frequency = Open (TzW) + Sealed (TzW) + crush + sealed nw.*

*In the third graph, the SEC\_UP/SEC\_LOW is shown for DZ core, crush, and core-loss. These reflect actual lengths – not binned.*

## Deformation zone: *Zone name*

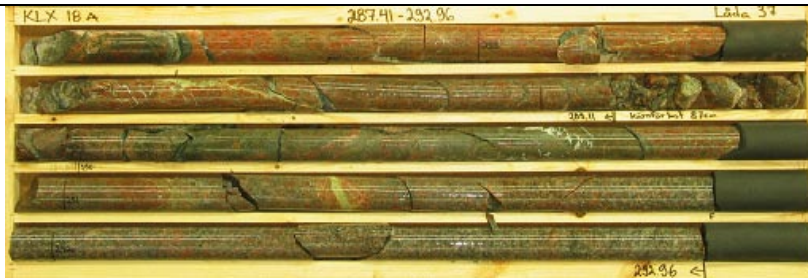


Photo of drill core from part of the deformation zone. Generally part of a core zone if such has been identified. The depth numbers shown at the top of each core box are generally unadjusted measurements (not based on detailed borehole geometry survey) since photography was performed at an early stage prior to the down-hole survey.

### Engineering characteristics

#### Transition part of zone:

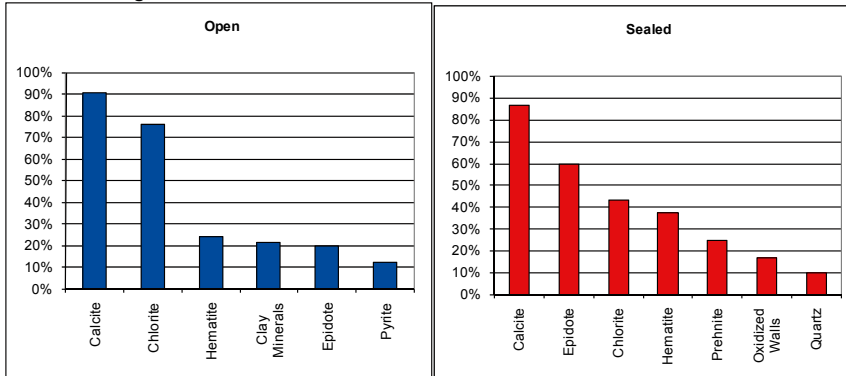
Frequency of open fractures:  $x.x \text{ m}^{-1}$

Std dev:  $x.x$

Frequency of sealed fractures:  $x.x \text{ m}^{-1}$

Std dev:  $x.x$

#### Mineral coatings



#### Fault core:

Percentage of fault core: fault core percentage of DZ/DZs,  $x \%$

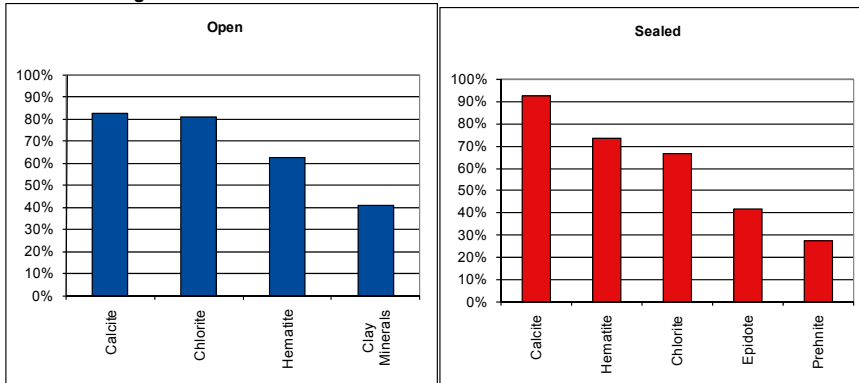
Frequency of open fractures:  $x.x \text{ m}^{-1}$

Std dev:  $x.x$

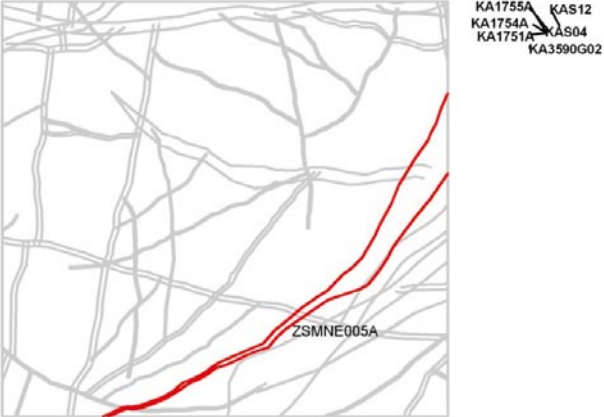
Frequency of sealed fractures:  $x.x \text{ m}^{-1}$

Std dev:  $x.x$



#### Mineral coatings




## NE-SW striking deformation zones, steeply dipping

<b>Deformation zone ZSMNE005A</b>		
<p><b>Borehole intersections (metres along borehole)</b></p> <p>HLX09: no data            HLX16: no data            HLX17: no data            KA1751A: 110-114 m            KA1754A: 90-115 m            KA1755A: 95-140 m            KA3590G02: 19-30 m            KAS04: 131-437 m            KAS12: 19-286 m            KAS17: no data            KA2598A: no data            KA3600F: no data            KA3510A: no data            KA2563A: no data</p>		
<p><b>Deformation style, alteration and geometry</b></p> <p><b>Deformation style:</b> ductile and brittle</p> <p><b>Alteration:</b> red staining. Evidence from bounding outcrops</p> <p><b>Strike/dip (right-hand-rule):</b> 060/90</p> <p><b>Trace length at ground surface:</b> 16 km</p> <p><b>Model thickness / model thickness span :</b> 250 m / 10-300 m</p> <p><b>Measured thickness (-400 to -600 m elevation):</b> no data</p> <p><b>Comment:</b> no data obtained during the current site investigation within the local model volume.</p>		
<b>Fractures in the deformation zone</b>		
<b>KA1751A</b>	<b>KA1754A</b>	<b>KA1755A</b>
<p><b>Elevation:</b> -247 to -247.2 m (RHB 70) no data</p>	<p><b>Elevation:</b> -277 to -288 m (RHB 70) no data</p>	<p><b>Elevation:</b> -269.9 to -285.6 m (RHB 70) no data</p>
<p><b>Transmissivity (m<sup>2</sup>/s)</b></p> <p><b>General dip of PFL-features, elevation -400 to -600m:</b> no data</p> <p><b>Measured T (sum T(PFL-f)), elevation -400 to -600m:</b> no data</p> <p><b>Number of PFL-features, elevation -400 to -600m:</b> no data</p> <p><b>Model T, elevation -400 to -500m:</b> 1.49E-6</p> <p><b>Model T, elevation -500 to -600m:</b> 8.27E-7</p>	<p><b>Transmissivity (m<sup>2</sup>/s)</b></p> <p><b>General dip of PFL-features, elevation -400 to -600m:</b> no data</p> <p><b>Measured T (sum T(PFL-f)), elevation -400 to -600m:</b> no data</p> <p><b>Number of PFL-features, elevation -400 to -600m:</b> no data</p> <p><b>Model T, elevation -400 to -500m:</b> 1.49E-6</p> <p><b>Model T, elevation -500 to -600m:</b> 8.27E-7</p>	<p><b>Transmissivity (m<sup>2</sup>/s)</b></p> <p><b>General dip of PFL-features, elevation -400 to -600m:</b> no data</p> <p><b>Measured T (sum T(PFL-f)), elevation -400 to -600m:</b> no data</p> <p><b>Number of PFL-features, elevation -400 to -600m:</b> no data</p> <p><b>Model T, elevation -400 to -500m:</b> 1.49E-6</p> <p><b>Model T, elevation -500 to -600m:</b> 8.27E-7</p>

<b>Deformation zone ZSMNE005A</b>		
<b>KA3590G02</b>	<b>KAS04</b>	<b>KAS12</b>
<b>Elevation:</b> -461.2 to -468.8 m (RHB 70) no data	<b>Elevation:</b> -100.7 to -357.4 m (RHB 70) no data	<b>Elevation:</b> -13 to -259.6 m (RHB 70) no data
<b>Transmissivity (m<sup>2</sup>/s)</b> <b>General dip of PFL-features, elevation -400 to -600m:</b> no data <b>Measured T (sum T(PFL-f)), elevation -400 to -600m:</b> no data <b>Number of PFL-features, elevation -400 to -600m:</b> no data <b>Model T, elevation -400 to -500m:</b> 1.49E-6 <b>Model T, elevation -500 to -600m:</b> 8.27E-7	<b>Transmissivity (m<sup>2</sup>/s)</b> <b>General dip of PFL-features, elevation -400 to -600m:</b> no data <b>Measured T (sum T(PFL-f)), elevation -400 to -600m:</b> no data <b>Number of PFL-features, elevation -400 to -600m:</b> no data <b>Model T, elevation -400 to -500m:</b> 1.49E-6 <b>Model T, elevation -500 to -600m:</b> 8.27E-7	<b>Transmissivity (m<sup>2</sup>/s)</b> <b>General dip of PFL-features, elevation -400 to -600m:</b> no data <b>Measured T (sum T(PFL-f)), elevation -400 to -600m:</b> no data <b>Number of PFL-features, elevation -400 to -600m:</b> no data <b>Model T, elevation -400 to -500m:</b> 1.49E-6 <b>Model T, elevation -500 to -600m:</b> 8.27E-7
<b>Engineering characteristics</b>		
<p><b>Fracture orientation:</b> 220/85, 110/80, 250/30, 025/20</p> <p><b>Fracture frequency:</b> 9 m<sup>-1</sup> (limited dataset)</p> <p><b>Crush zone:</b> no data</p> <p><b>Fracture filling:</b> Calcite, chlorite, epidote, hematite, quartz</p> <p><b>Percentage of fault core:</b> no data</p>		

<b>Deformation zone ZSMNE011A</b>	
<p><b>Borehole intersections (metres along borehole)</b></p> <p>None</p>	
<p><b>Deformation style, alteration and geometry</b></p> <p><b>Deformation style:</b> brittle and ductile</p> <p><b>Alteration:</b> red staining</p> <p><b>Strike/dip (right-hand-rule):</b> 050/90</p> <p><b>Trace length at ground surface:</b> 10.5 km</p> <p><b>Model thickness / model thickness span :</b> 100 m / 50-150 m</p> <p><b>Measured thickness (-400 to -600 m elevation):</b> no data</p> <p><b>Comment:</b></p>	
<b>Fractures in the deformation zone</b>	
<p>No data</p>	 <p>Outcrop PSM004118 brittle ductile deformation associated with ZSMNE011A.</p>
<b>Transmissivity (m<sup>2</sup>/s)</b>	
<p><b>General dip of PFL-features, elevation -400 to -600m:</b> no data</p> <p><b>Measured T (sum T(PFL-f)), elevation -400 to -600m:</b> no data</p> <p><b>Number of PFL-features, elevation -400 to -600m:</b> no data</p> <p><b>Model T, elevation -400 to -500m:</b> 1.49E-6</p> <p><b>Model T, elevation -500 to -600m:</b> 8.27E-7</p>	
<b>Engineering characteristics</b>	
<p>No borehole intercepts</p>	



<b>Deformation zone ZSMNE063A</b>	
<p style="text-align: center;"><b>Borehole intersections (metres along borehole)</b></p> <p>None</p>	
<p style="text-align: center;"><b>Deformation style, alteration and geometry</b></p> <p><b>Deformation style:</b> brittle and ductile (no direct evidence- inferred association with other NE-SW trending deformation zones)</p> <p><b>Alteration:</b> oxidation</p> <p><b>Strike/dip (right-hand-rule):</b> 040/90</p> <p><b>Trace length at ground surface:</b> 1.1 km</p> <p><b>Model thickness / model thickness span :</b> 10 m / 5-20 m</p> <p><b>Measured thickness (-400 to -600 m elevation):</b> no data</p> <p><b>Comment:</b></p>	
<b>Fractures in the deformation zone</b>	
<p><b>Transmissivity (m<sup>2</sup>/s)</b></p>	
<p><b>General dip of PFL-features, elevation -400 to -600m:</b> no data</p> <p><b>Measured T (sum T(PFL-f)), elevation -400 to -600m:</b> no data</p> <p><b>Number of PFL-features, elevation -400 to -600m:</b> no data</p> <p><b>Model T, elevation -400 to -500m:</b> 2.26E-7</p> <p style="padding-left: 100px;"><b>Model T, elevation -500 to -600m:</b> 1.37E-7</p>	
<b>Engineering characteristics</b>	
<p><b>Fracture orientation:</b> 220/85, 100/65, 250/30, 025/20 (no direct evidence- inferred association with other NE-SW trending deformation zones)</p> <p><b>Fracture frequency:</b> no data</p> <p><b>Crush zone:</b> no data</p> <p><b>Fracture filling:</b> no data</p> <p><b>Fault core:</b> no data</p>	

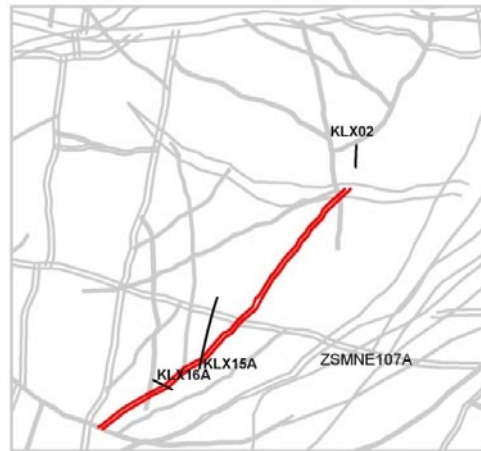
## Deformation zone ZSMNE107A

### Borehole intersections (metres along borehole)

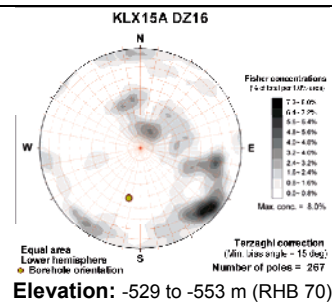
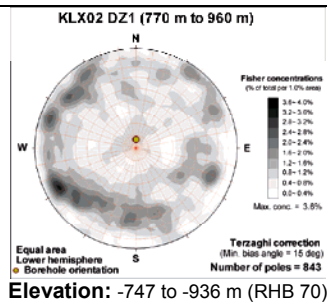
HLX10: - m (no data)  
 KLX02: 770-960 m (ESHI DZ1 770-960 m)  
 KLX15A: 711-744 m (ESHI DZ16 711-744 m)  
 KLX16: 228-434 m (ESHI DZ9 228-231 m, DZ10 252-254 m, DZ11 259-266 m, DZ12 327-434 m)

### Deformation style, alteration and geometry

**Deformation style:** ductile and brittle  
**Alteration:** red staining and saussuritisation.  
**Strike/dip (right-hand-rule):** 225/80  
**Trace length at ground surface:** 3.1 km  
**Model thickness / model thickness span :** 35 m / 10-40 m  
**Measured thickness (-400 to -600 m elevation):** 15 m (KLX15A DZ16)  
**Comment:** length- possible break at ZSMNW042A that would give an interpretation as two separate structures would halve the length.



## Fractures in the deformation zone



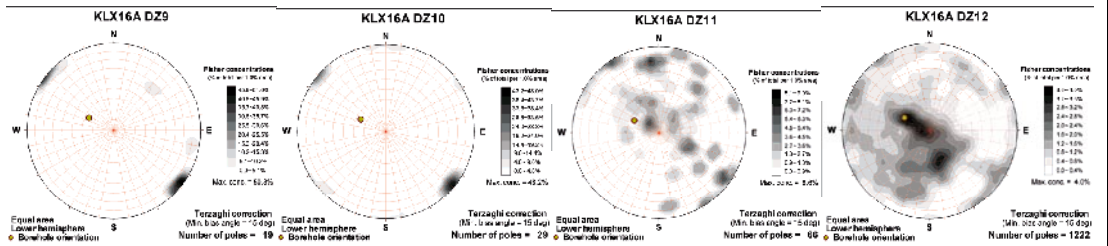
### Transmissivity (m<sup>2</sup>/s)

General dip of PFL-features, elevation -400 to -600m: no data  
 Measured T (sum T(PFL-f)), elevation -400 to -600m: no data  
 Number of PFL-features, elevation -400 to -600m: no data  
 Model T, elevation -400 to -500m: 1.49E-6  
 Model T, elevation -500 to -600m: 8.27E-7

### Transmissivity (m<sup>2</sup>/s)

General dip of PFL-features, elevation -400 to -600m: No PFL-f  
 Measured T (sum T(PFL-f)), elevation -400 to -600m: 0  
 Number of PFL-features, elevation -400 to -600m: 0  
 Model T, elevation -400 to -500m: 1.49E-6  
 Model T, elevation -500 to -600m: 8.27E-7

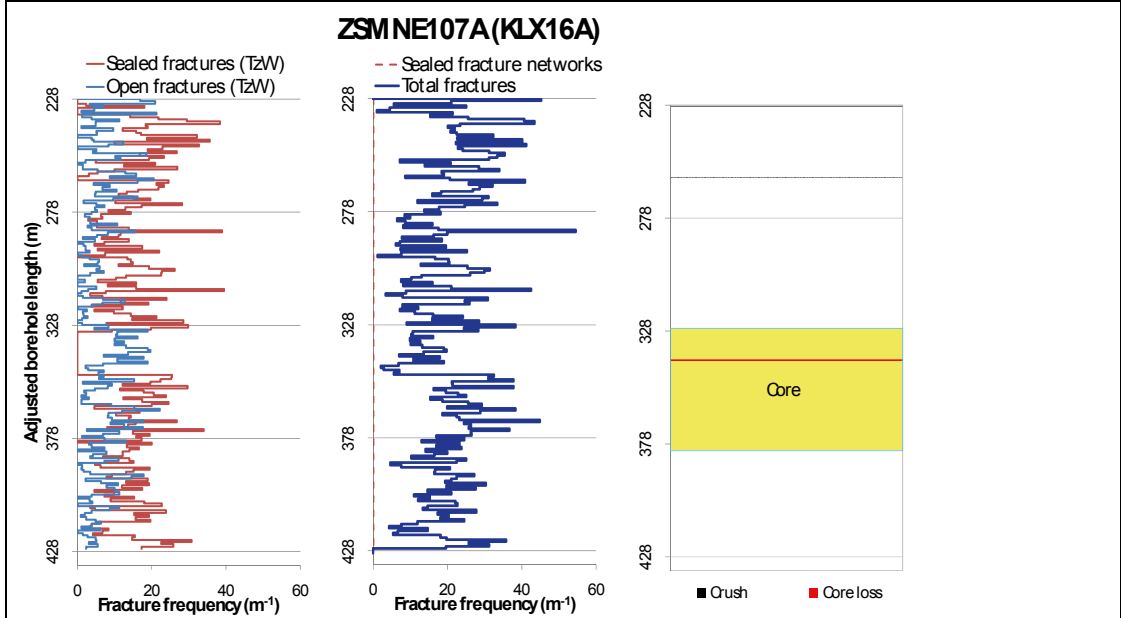
## Deformation zone ZSMNE107A



Elevation: -187.0 to -371.4 m (RHB 70)

### Transmissivity ( $m^2/s$ )

General dip of PFL-features, elevation -400 to -600m: no data  
 Measured T (sum T(PFL-f)), elevation -400 to -600m: no data  
 Number of PFL-features, elevation -400 to -600m: no data  
 Model T, elevation -400 to -500m: 1.49E-6  
 Model T, elevation -500 to -600m: 8.27E-7



## Deformation zone ZSMNE107A



KLX16A 335-345 m borehole length. Part of DZ12 including core zone.

### Engineering characteristics

**Transition part of zone:**

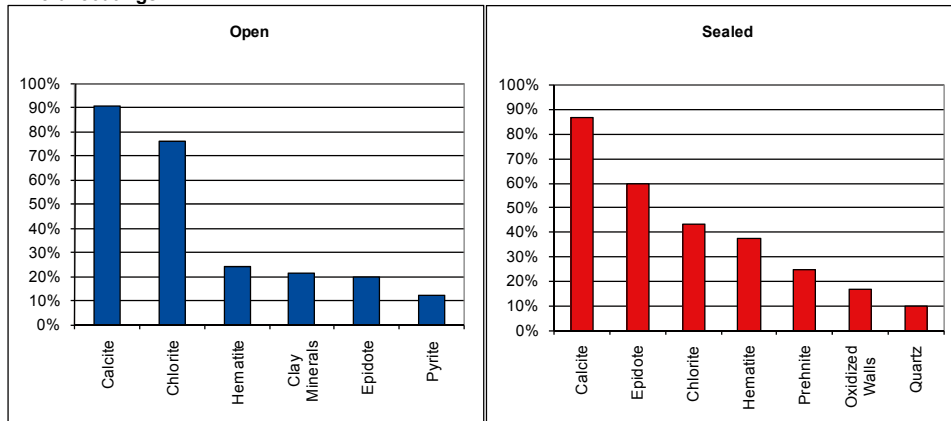
Frequency of open fractures:  $3.2 \text{ m}^{-1}$

Std dev: 0.5

Frequency of sealed fractures:  $24.3 \text{ m}^{-1}$

Std dev: 5.2

**Mineral coatings**



## Deformation zone ZSMNE107A

### Fault core:

Percentage of fault core: 18 %

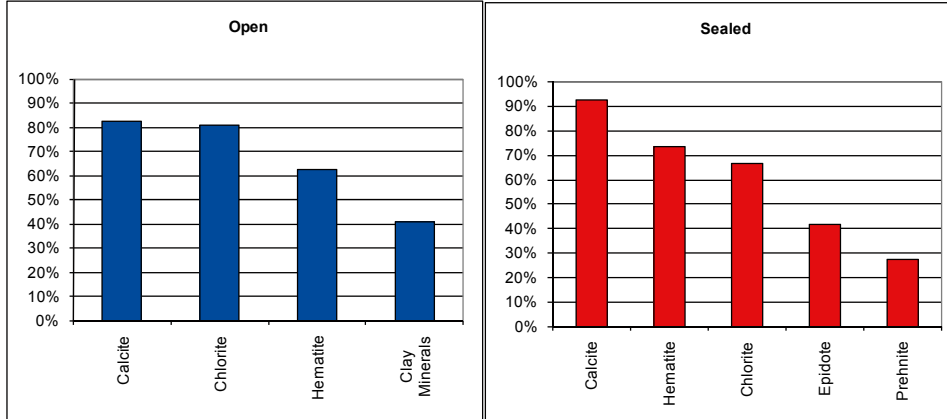
Frequency of open fractures: 6.0 m<sup>-1</sup>


Std dev: 3.0

Frequency of sealed fractures: 55.8 m<sup>-1</sup>

Std dev: 54.3

### Mineral coatings



<b>Deformation zone ZSMNE108A</b>	
<p><b>Borehole intersections (metres along borehole)</b></p> <p>None</p>	
<p><b>Deformation style, alteration and geometry</b></p> <p><b>Deformation style:</b> ductile and brittle</p> <p><b>Alteration:</b> red staining.</p> <p><b>Strike/dip (right-hand-rule):</b> 060/90</p> <p><b>Trace length at ground surface:</b> 1.8 km</p> <p><b>Model thickness / model thickness span :</b> 10 m / 5-50 m</p> <p><b>Measured thickness (-400 to -600 m elevation):</b> no data</p> <p><b>Comment:</b> character and properties are based on other similar trending deformation zones</p>	
<b>Fractures in the deformation zone</b>	
No borehole intercepts	
<p><b>Transmissivity (m<sup>2</sup>/s)</b></p> <p><b>General dip of PFL-features, elevation -400 to -600m:</b> no data</p> <p><b>Measured T (sum T(PFL-f)), elevation -400 to -600m:</b> no data</p> <p><b>Number of PFL-features, elevation -400 to -600m:</b> no data</p> <p><b>Model T, elevation -400 to -500m:</b> 2.26E-7</p> <p><b>Model T, elevation -500 to -600m:</b> 1.37E-7</p>	
<b>Engineering characteristics</b>	
No borehole intercepts	

## Deformation zone ZSMNE942A

### Borehole intersections (metres along borehole)

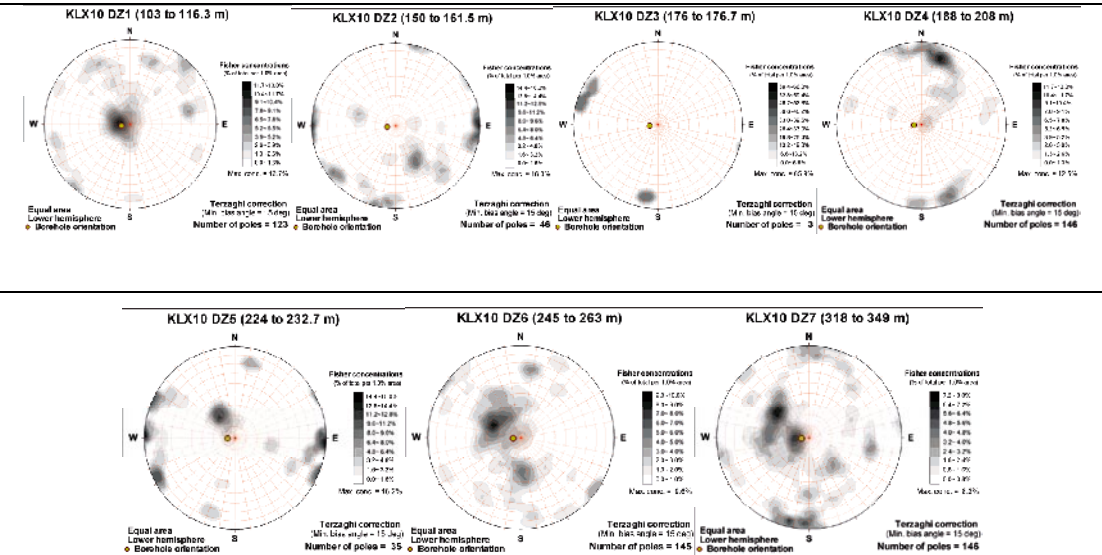
KLX10: 103-349 m (ESHI; DZ1 103-116.3m, DZ2 150-161.5, DZ3 176-176.7m, DZ4 188-208m, DZ5 224-232.7 m, DZ6 245-263 m and DZ7 318-349 m)  
 KLX10B: 0-20 m (ESHI DZ1 10.35-20.35m)  
 KLX19A: 437-464 m (ESHI DZ4 434-464m)



### Deformation style, alteration and geometry

**Deformation style:** brittle and ductile  
**Alteration:** red staining, chloritisation, epidotisation, argillisation  
**Strike/dip (right-hand-rule):** 246/87  
**Trace length at ground surface:** 2.5 km  
**Model thickness / model thickness span :** 15 m / 10-50 m  
**Measured thickness (-400 to -600 m elevation):** no data  
**Comment:**

## Fractures in the deformation zone

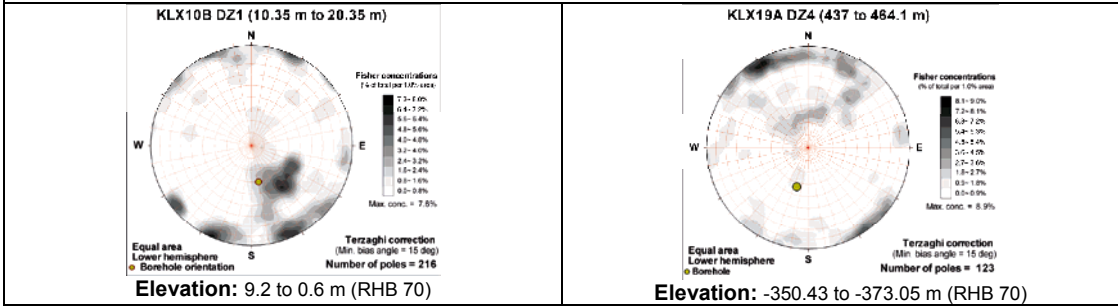


Elevation: -84.0 to 328.0 m (RHB 70)

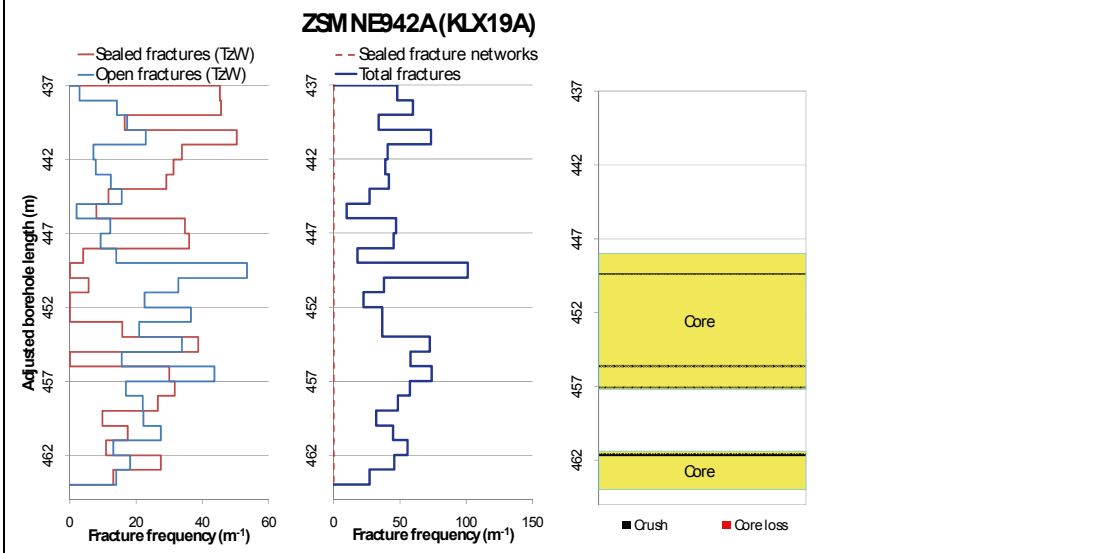
## Transmissivity (m<sup>2</sup>/s)

**General dip of PFL-features, elevation -400 to -600m:** no data  
**Measured T (sum T(PFL-f)), elevation -400 to -600m:** no data  
**Number of PFL-features, elevation -400 to -600m:** no data  
**Model T, elevation -400 to -500m:** 6.85E-7  
**Model T, elevation -500 to -600m:** 3.94E-7

## Deformation zone ZSMNE942A



<p style="text-align: center;"><b>Transmissivity (m<sup>2</sup>/s)</b></p> <p>General dip of PFL-features, elevation -400 to -600m: no data</p> <p>Measured T (sum T(PFL-f)), elevation -400 to -600m: no data</p> <p>Number of PFL-features, elevation -400 to -600m: no data</p> <p>Model T, elevation -400 to -500m: 6.85E-7</p> <p>Model T, elevation -500 to -600m: 3.94E-7</p>	<p style="text-align: center;"><b>Transmissivity (m<sup>2</sup>/s)</b></p> <p>General dip of PFL-features, elevation -400 to -600m: no data</p> <p>Measured T (sum T(PFL-f)), elevation -400 to -600m: no data</p> <p>Number of PFL-features, elevation -400 to -600m: no data</p> <p>Model T, elevation -400 to -500m: 6.85E-7</p> <p>Model T, elevation -500 to -600m: 3.94E-7</p>
--	--





## Deformation zone ZSMNE942A



KLX19A 449-459 m borehole length. Part of DZ4, including part of one (of two) core zone 448.0-457.2 m.

### Engineering characteristics

**Transition part of zone:**

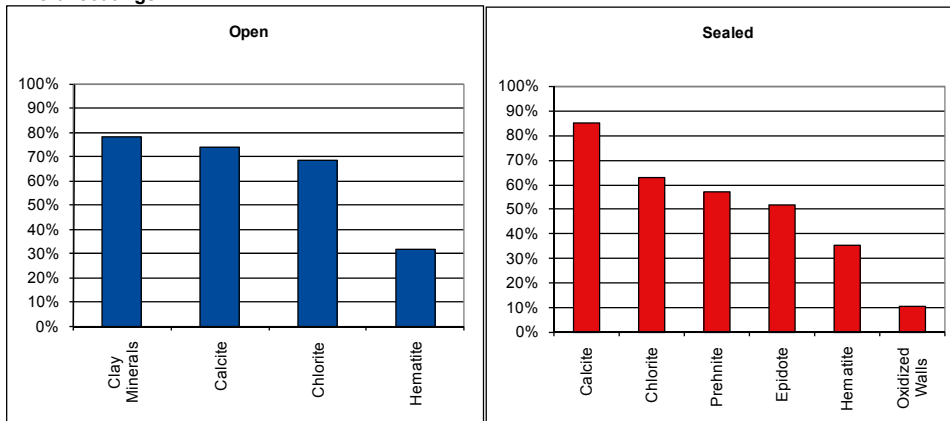
Frequency of open fractures:  $7.9 \text{ m}^{-1}$

Std dev: 4.3

Frequency of sealed fractures:  $26.8 \text{ m}^{-1}$

Std dev: 17.9

**Mineral coatings**



## Deformation zone ZSMNE942A

### **Fault core:**

**Percentage of fault core:** 44 %

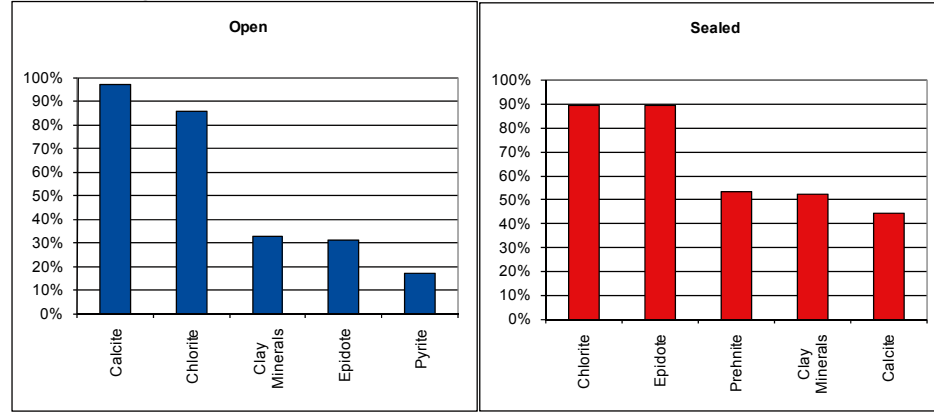
**Frequency of open fractures:** 12.1 m<sup>-1</sup>

**Std dev:** no data

**Frequency of sealed fractures:** 21.3 m<sup>-1</sup>

**Std dev:** no data

### **Mineral coatings**



## Deformation zone ZSMNE944A

### Borehole intersections (metres along borehole)

KLX18A: 284-292 m (ESHI DZ3 284-292 m)



### Deformation style, alteration and geometry

**Deformation style:** brittle and ductile

**Alteration:** red staining, chloritisation

**Strike/dip (right-hand-rule):** 058/75

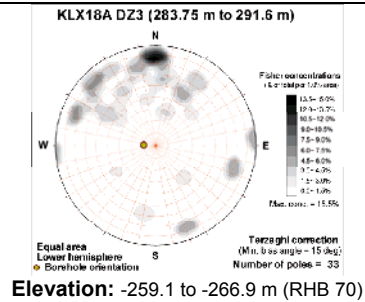
**Trace length at ground surface:** 1.2 km

**Model thickness / model thickness span :** 10 m / 5-20 m

**Measured thickness (-400 to -600 m elevation):** no data

**Comment:**

## Fractures in the deformation zone



## Transmissivity ( $m^2/s$ )

**General dip of PFL-features, elevation -400 to -600m:** no data

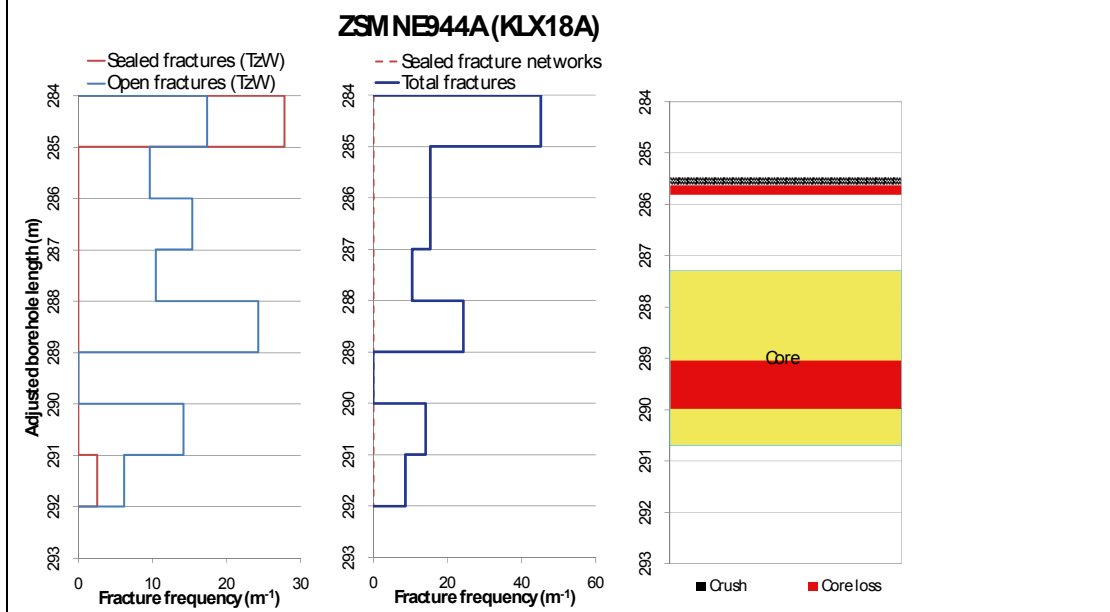
**Measured T (sum T(PFL-f)), elevation -400 to -600m:** no data

**Number of PFL-features, elevation -400 to -600m:** no data

**Model T, elevation -400 to -500m:** 7.54E-8

**Model T, elevation -500 to -600m:** 4.56E-8

## Deformation zone ZSMNE944A



KLX18A 287-293 m borehole length. Part of DZ3, including core zone 287.29-290.70 m.

### Engineering characteristics

**Transition part of zone:**

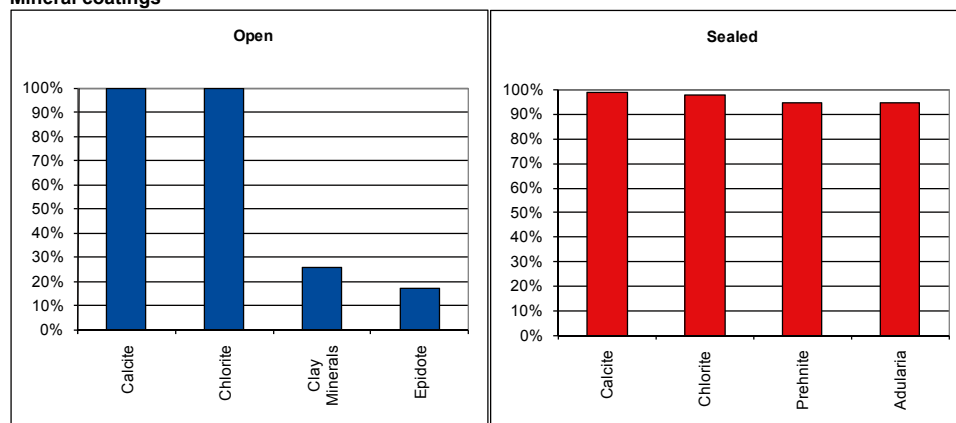
Frequency of open fractures: 7.6 m<sup>-1</sup>

Std dev: no data

Frequency of sealed fractures: 43.6 m<sup>-1</sup>

Std dev: no data

**Mineral coatings**



**Fault core:** note that core loss, crush and fault rocks define the core

Percentage of fault core: 43 %

## Deformation zone ZSMNE944A

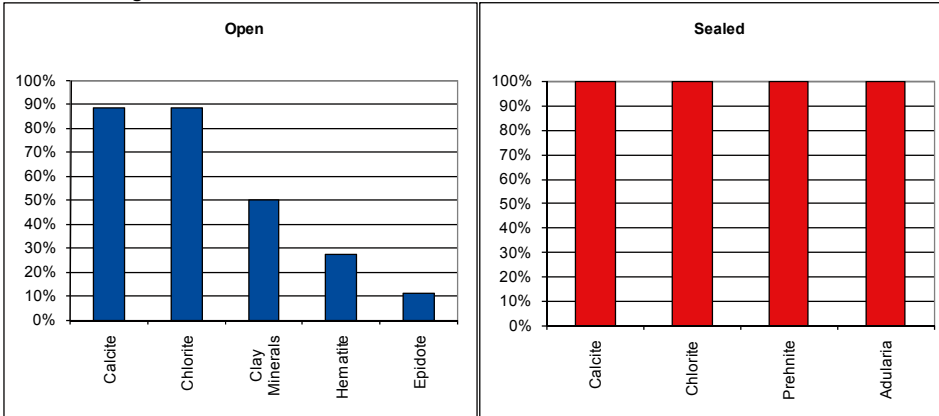
Frequency of open fractures:  $5.3 \text{ m}^{-1}$

Std dev: no data


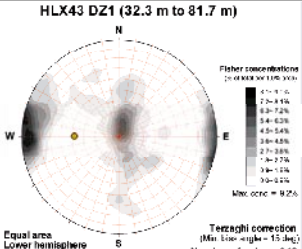
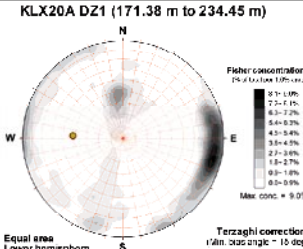
Frequency of sealed fractures:  $66.9 \text{ m}^{-1}$

Std dev: no data

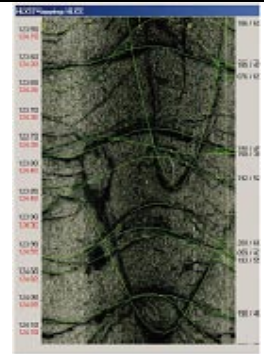
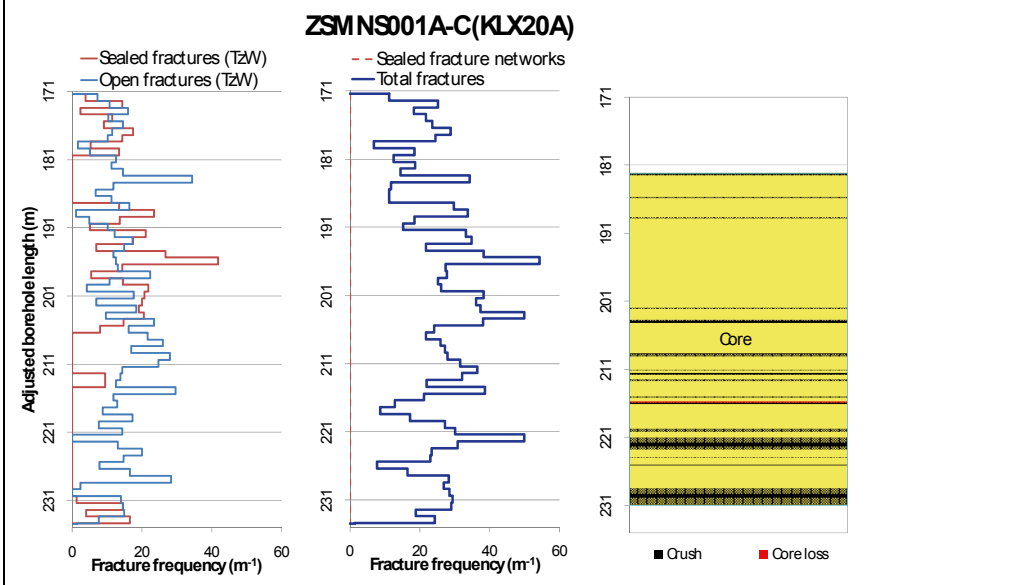
### Mineral coatings



## N-S Striking deformation zones, steeply dipping

<b>Deformation zone ZSMNS001A-E</b>	
<p><b>Borehole intersections (metres along borehole)</b></p> <p>HLX36: 111-191 m (ESHI DZ1 111-191 m)            HLX37: 122-147 m (ESHI DZ1 122-147 m)            HLX43: 32-82 m (ESHI DZ1 32-82 m)            KLX20: 171-234 m (ESHI DZ1 171-234 m)</p>	
<p><b>Deformation style, alteration and geometry</b></p>	
<p><b>Deformation style:</b> brittle and ductile</p> <p><b>Alteration:</b> Weak red staining, saussuritisation and epidotisation</p> <p><b>Strike/dip (right-hand-rule):</b> 187/81</p> <p><b>Trace length at ground surface:</b> 10.9 km</p> <p><b>Model thickness / model thickness span :</b> 45 m / 20-80 m</p> <p><b>Measured thickness (-400 to -600 m elevation):</b> no data</p> <p><b>Comment:</b></p>	
<b>Fractures in the deformation zone</b>	
<p>HLX43 DZ1 (32.3 m to 81.7 m)</p>  <p>Equal area Lower hemisphere Borehole orientation</p> <p>Terzaghi correction (Min. size-angle = 15 deg) Number of poles = 349</p> <p><b>Elevation: -0.9 to -39.8 m (RHB 70)</b></p>	<p>KLX20A DZ1 (171.38 m to 234.45 m)</p>  <p>Equal area Lower hemisphere Borehole orientation</p> <p>Terzaghi correction (Min. size-angle = 15 deg) Number of poles = 459</p> <p><b>Elevation: -104.4 to -151.7 m (RHB 70)</b></p>
<p><b>Transmissivity (m<sup>2</sup>/s)</b></p> <p>General dip of PFL-features, elevation -400 to -600m: no data</p> <p>Measured T (sum T(PFL-f)), elevation -400 to -600m: no data</p> <p>Number of PFL-features, elevation -400 to -600m: no data</p> <p>Model T, elevation -400 to -500m: 5.19E-6</p> <p>Model T, elevation -500 to -600m: 2.98E-6</p>	<p><b>Transmissivity (m<sup>2</sup>/s)</b></p> <p>General dip of PFL-features, elevation -400 to -600m: no data</p> <p>Measured T (sum T(PFL-f)), elevation -400 to -600m: no data</p> <p>Number of PFL-features, elevation -400 to -600m: no data</p> <p>Model T, elevation -400 to -500m: 5.19E-6</p> <p>Model T, elevation -500 to -600m: 2.98E-6</p>

## Deformation zone ZSMNS001A-E



**BIPS-image showing the unaltered, fine- to medium-grained, strongly fractured dolerite. Green lines mark the open fractures.**



**KLX20A 205.71-210.81 m borehole length. Part of DZ1, including part of the dolerite core zone, 182.0-231.0 m.**



**Slickensided fracture surfaces in the dolerite.**

## Deformation zone ZSMNS001A-E

### Engineering characteristics

**Transition part of zone:**

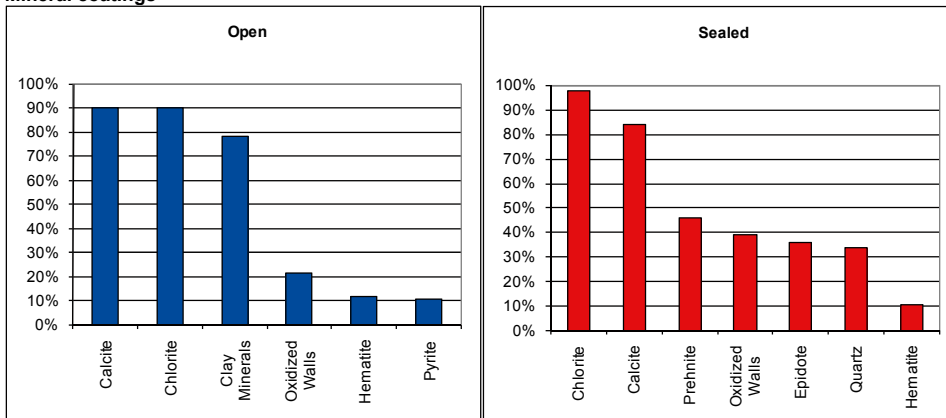
Frequency of open fractures: 5.8 m<sup>-1</sup>

Std dev: no data

Frequency of sealed fractures: 29.2 m<sup>-1</sup>

Std dev: no data

**Mineral coatings**



**Fault core:**

Percentage of fault core: 77 %

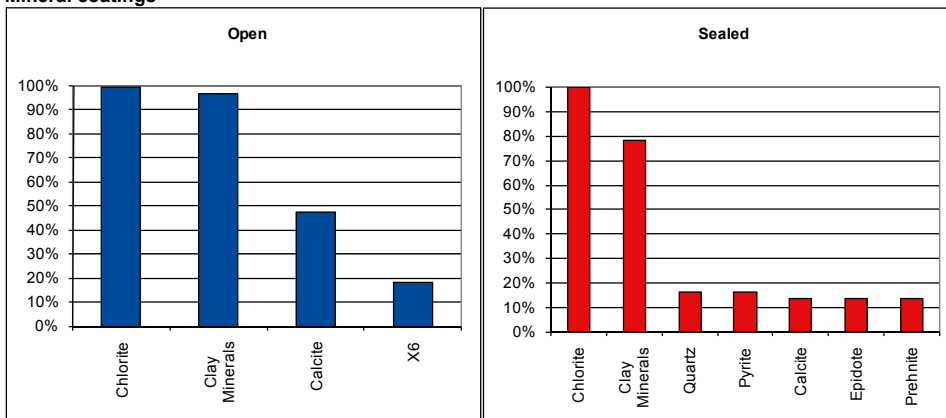
Frequency of open fractures: 14.4 m<sup>-1</sup>

Std dev: no data

Frequency of sealed fractures: 43.4 m<sup>-1</sup>

Std dev: no data

**Mineral coatings**

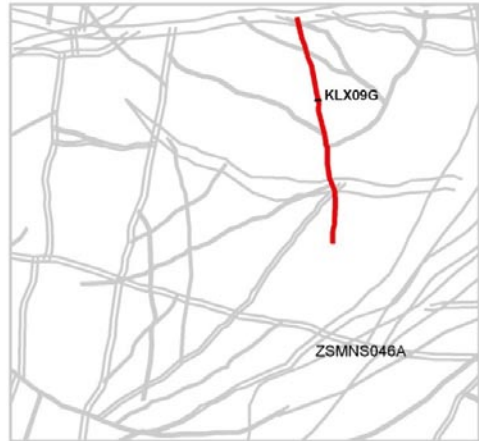




## Deformation zone ZSMNS046A

### Borehole intersections (metres along borehole)

KLX09G: 40-68 m (ESHI DZ1 40-68m)



### Deformation style, alteration and geometry

**Deformation style:** ductile and brittle

**Alteration:** red staining and chloritisation

**Strike/dip (right-hand-rule):** 170/90

**Trace length at ground surface:** 2.1 km

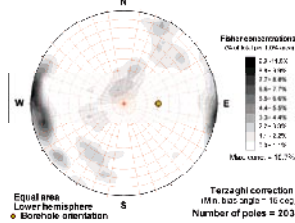
**Model thickness / model thickness span :** 20 m / 10-30 m

**Measured thickness (-400 to -600 m elevation):** no data

**Comment:**

## Fractures in the deformation zone

KLX09G DZ1 (40.02 m to 67.52 m)



**Elevation:** -15.2 to -39 m (RHB 70)

## Transmissivity (m<sup>2</sup>/s)

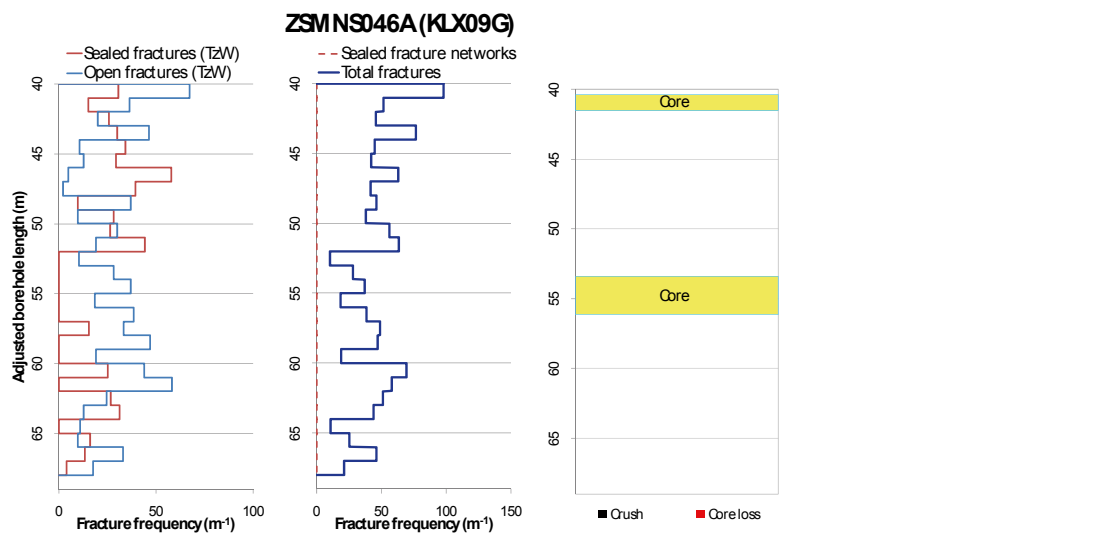
**General dip of PFL-features, elevation -400 to -600m:** no data

**Measured T (sum T(PFL-f)), elevation -400 to -600m:** no data

**Number of PFL-features, elevation -400 to -600m:** no data

**Model T, elevation -400 to -500m:** 1.49E-6

**Model T, elevation -500 to -600m:** 8.27E-7



## Deformation zone ZSMNS046A



KLX09G 38.95-44.25 m borehole length. Part of DZ1 including one (40.38-41.50 m) of two core zones.

### Engineering characteristics

**Transition part of zone:**

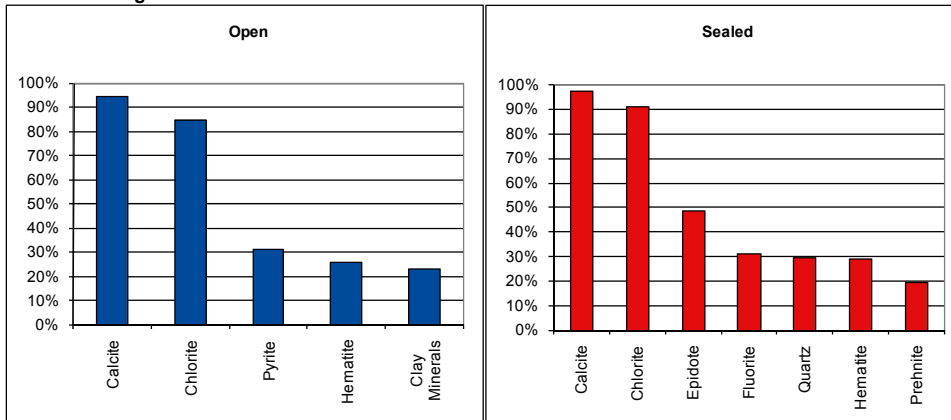
Frequency of open fractures: 6.2 m<sup>-1</sup>

Std dev: no data

Frequency of sealed fractures: 35.7 m<sup>-1</sup>

Std dev: no data

**Mineral coatings**



**Fault core:**

Percentage of fault core: 14 %

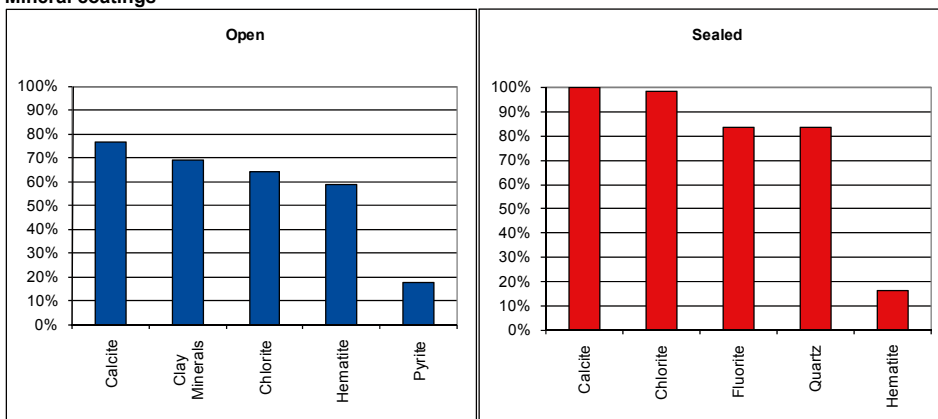
Frequency of open fractures: 10.1 m<sup>-1</sup>

Std dev: no data

Frequency of sealed fractures: 85.5 m<sup>-1</sup>

Std dev: no data

**Mineral coatings**



## Deformation zone ZSMNS059A

### Borehole intersections (metres along borehole)

HLX34: 33-113 m (ESHI DZ1 33-35m; DZ2 52-55m; DZ3 68-73m; DZ4 85-87m; DZ5 111-113m)  
 HLX35: 116-142 m (ESHI DZ1 116-142m)  
 HLX38: 23-67 m (ESHI DZ1 23.4-26.5m; DZ2 30.3-32m; DZ3 64.3-66.8m)  
 KLX14: 75-125 m (ESHI DZ4 75-125 m)



### Deformation style, alteration and geometry

**Deformation style:** brittle and ductile

**Alteration:** Weak red staining and epidotisation

**Strike/dip (right-hand-rule):** 192/88

**Trace length at ground surface:** 4.8 km

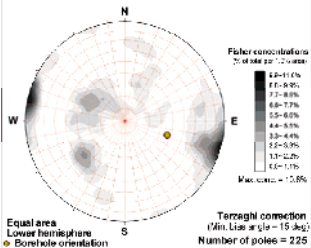
**Model thickness / model thickness span :** 50 m / 20-80 m

**Measured thickness (-400 to -600 m elevation):** no data

**Comment:**

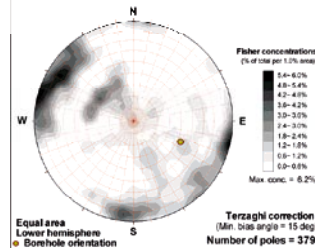
## Fractures in the deformation zone

HLX35 DZ1 (116.0783 to 141.7004 m)



**Elevation:** -83.3 to -104.1 m (RHB 70)

KLX14A DZ4 (74.67 m to 125.35 m)



**Elevation:** -40 to -77 m (RHB 70)

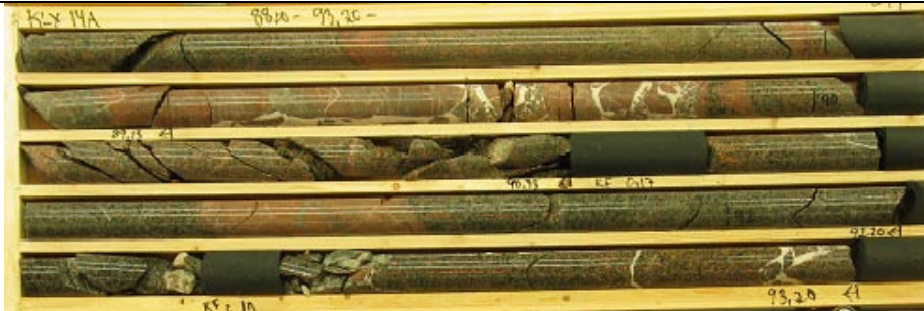
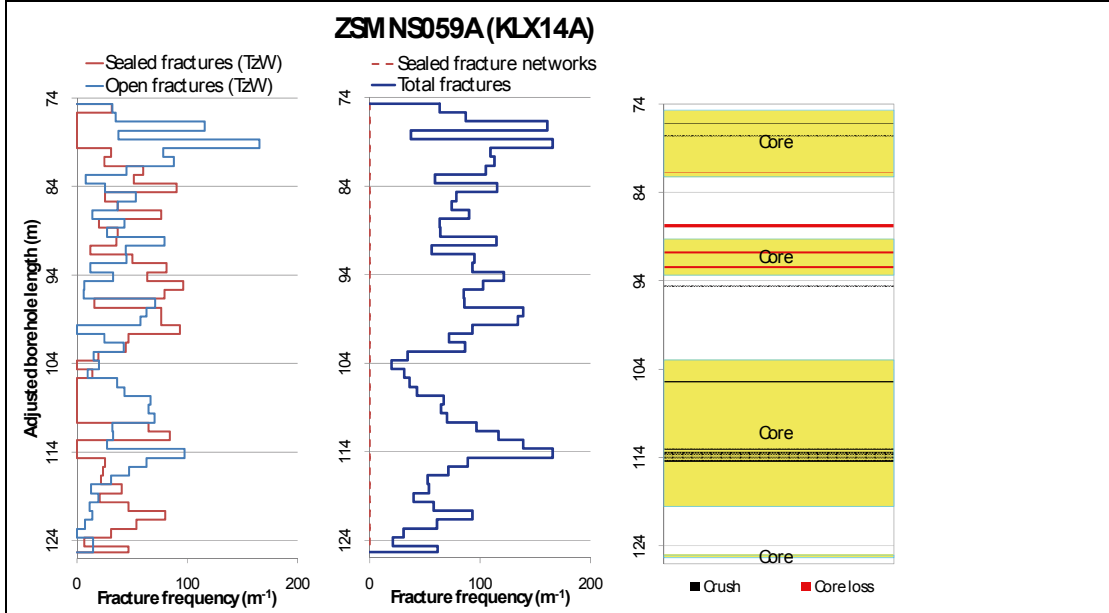
### Transmissivity (m<sup>2</sup>/s)

**General dip of PFL-features, elevation -400 to -600m:** no data  
**Measured T (sum T(PFL-f)), elevation -400 to -600m:** no data  
**Number of PFL-features, elevation -400 to -600m:** no data  
**Model T, elevation -400 to -500m:** 5.53E-6  
**Model T, elevation -500 to -600m:** 3.18E-6

### Transmissivity (m<sup>2</sup>/s)

**General dip of PFL-features, elevation -400 to -600m:** no data  
**Measured T (sum T(PFL-f)), elevation -400 to -600m:** no data  
**Number of PFL-features, elevation -400 to -600m:** no data  
**Model T, elevation -400 to -500m:** 5.53E-6  
**Model T, elevation -500 to -600m:** 3.18E-6

## Deformation zone ZSMNS059A



KLX14A 88-93.20 m borehole length. Part of DZ4, including one (89.25-93.35 m) of multiple core zones.

### Engineering characteristics

**Transition part of zone:**

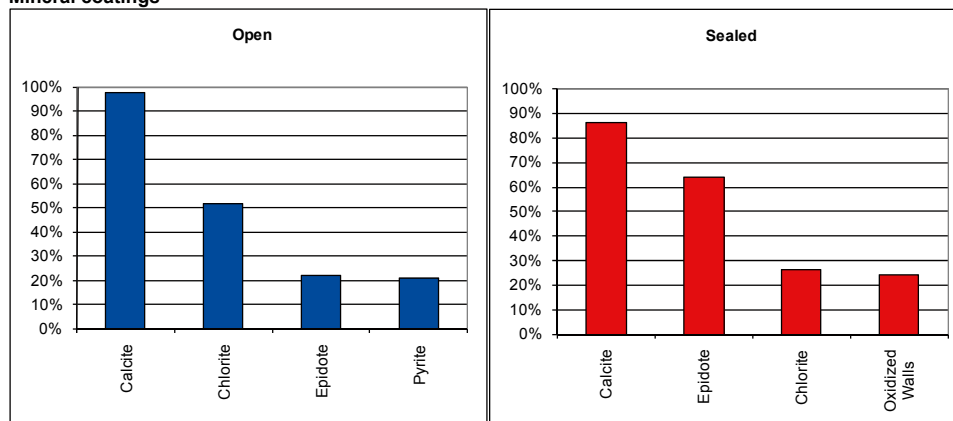
Frequency of open fractures: 4.1 m<sup>-1</sup>

Std dev: no data

Frequency of sealed fractures: 13.1 m<sup>-1</sup>

Std dev: no data

**Mineral coatings**



## Deformation zone ZSMNS059A

### Fault core:

Percentage of fault core: 56 %

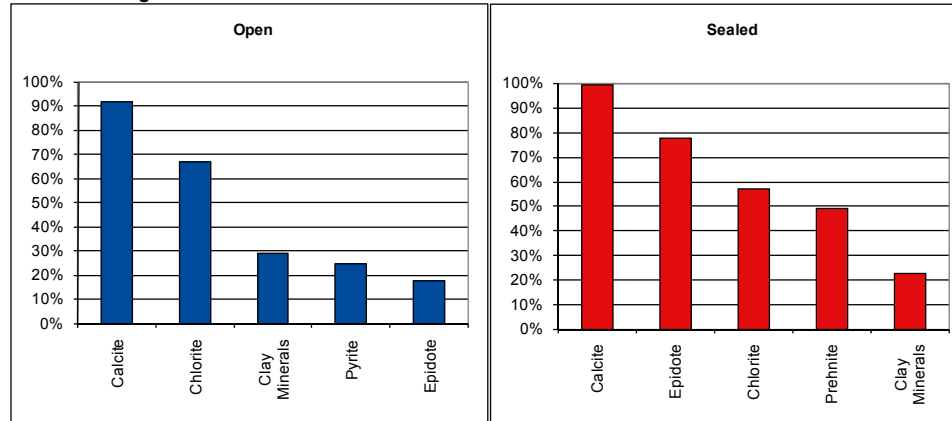
Frequency of open fractures: 10.7 m<sup>-1</sup>


Std dev: no data


Frequency of sealed fractures: 38.1 m<sup>-1</sup>

Std dev: no data

### Mineral coatings



<b>Deformation zone ZSMNS945A</b>	
<p><b>Borehole intersections (metres along borehole)</b></p> <p>None</p>	
<p><b>Deformation style, alteration and geometry</b></p> <p><b>Deformation style:</b> ductile and brittle</p> <p><b>Alteration:</b> red staining. May not be exclusive to this structure</p> <p><b>Strike/dip (right-hand-rule):</b> 176/90</p> <p><b>Trace length at ground surface:</b> 2.0 km</p> <p><b>Model thickness / model thickness span :</b> 10m / 5-25 m</p> <p><b>Percentage of fault core:</b> 5 m / +2 m (thickness)</p> <p><b>Measured thickness (-400 to -600 m elevation):</b> no data</p> <p><b>Comment:</b> General character based on inferred association with ZSMNS059A and ZSMNS046A</p>	
<b>Fractures in the deformation zone</b>	
<p>(No Borehole intercepts. Inferred similar fracture sets to ZSMNS046A)</p>	
<p><b>Transmissivity (m<sup>2</sup>/s)</b></p> <p><b>General dip of PFL-features, elevation -400 to -600m:</b> no data</p> <p><b>Measured T (sum T(PFL-f)), elevation -400 to -600m:</b> no data</p> <p><b>Number of PFL-features, elevation -400 to -600m:</b> no data</p> <p><b>Model T, elevation -400 to -500m:</b> 1.49E-6</p> <p><b>Model T, elevation -500 to -600m:</b> 8.27E-7</p>	
<b>Engineering characteristics</b>	
<p>(No borehole intercepts. Inferred similar characteristics to ZSMNS046A)</p>	

<b>Deformation zone ZSMNS947A</b>	
<p><b>Borehole intersections (metres along borehole)</b></p> <p>HLX42: - m (No ESHI interpreted DZ)</p>	
<p><b>Deformation style, alteration and geometry</b></p> <p>Deformation style: ductile and brittle</p> <p>Alteration: -</p> <p>Strike/dip (right-hand-rule): 178/90</p> <p>Trace length at ground surface: 1.8 km</p> <p>Model thickness / model thickness span : 20 m / 5-25 m</p> <p>Measured thickness (-400 to -600 m elevation): no data</p> <p>Comment:</p>	
<b>Fractures in the deformation zone</b>	
<p>(No Borehole intercepts. Inferred similar fracture sets to ZSMNS046A)</p>	
<b>Transmissivity (m<sup>2</sup>/s)</b>	
<p>General dip of PFL-features, elevation -400 to -600m: no data</p> <p>Measured T (sum T(PFL-f)), elevation -400 to -600m: no data</p> <p>Number of PFL-features, elevation -400 to -600m: no data</p> <p>Model T, elevation -400 to -500m: 2.26E-7</p> <p>Model T, elevation -500 to -600m: 1.37E-7</p>	
<b>Engineering characteristics</b>	
<p>(No borehole intercepts. Inferred similar characteristics to ZSMNS046A)</p>	

## Deformation zone KLX04\_dz6b

### Borehole intersections (metres along borehole)

KLX04: 887-914 m – Note this interval differs from: (ESHI DZ6 873-973 m)



### Deformation style, alteration and geometry

**Deformation style:** brittle

**Alteration:** red staining, epidotisation

**Strike/dip (right-hand-rule):** 156/67

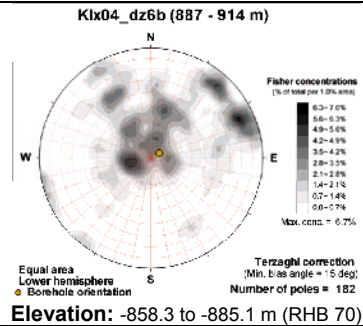
**Trace length at ground surface:** no data

**Model thickness / model thickness span :** 14 m / no data

**Measured thickness (-400 to -600 m elevation):** no data

**Comment:**

## Fractures in the deformation zone



## Transmissivity (m<sup>2</sup>/s)

**General dip of PFL-features, elevation -400 to -600m:** no data

**Measured T (sum T(PFL-f)), elevation -400 to -600m:** no data

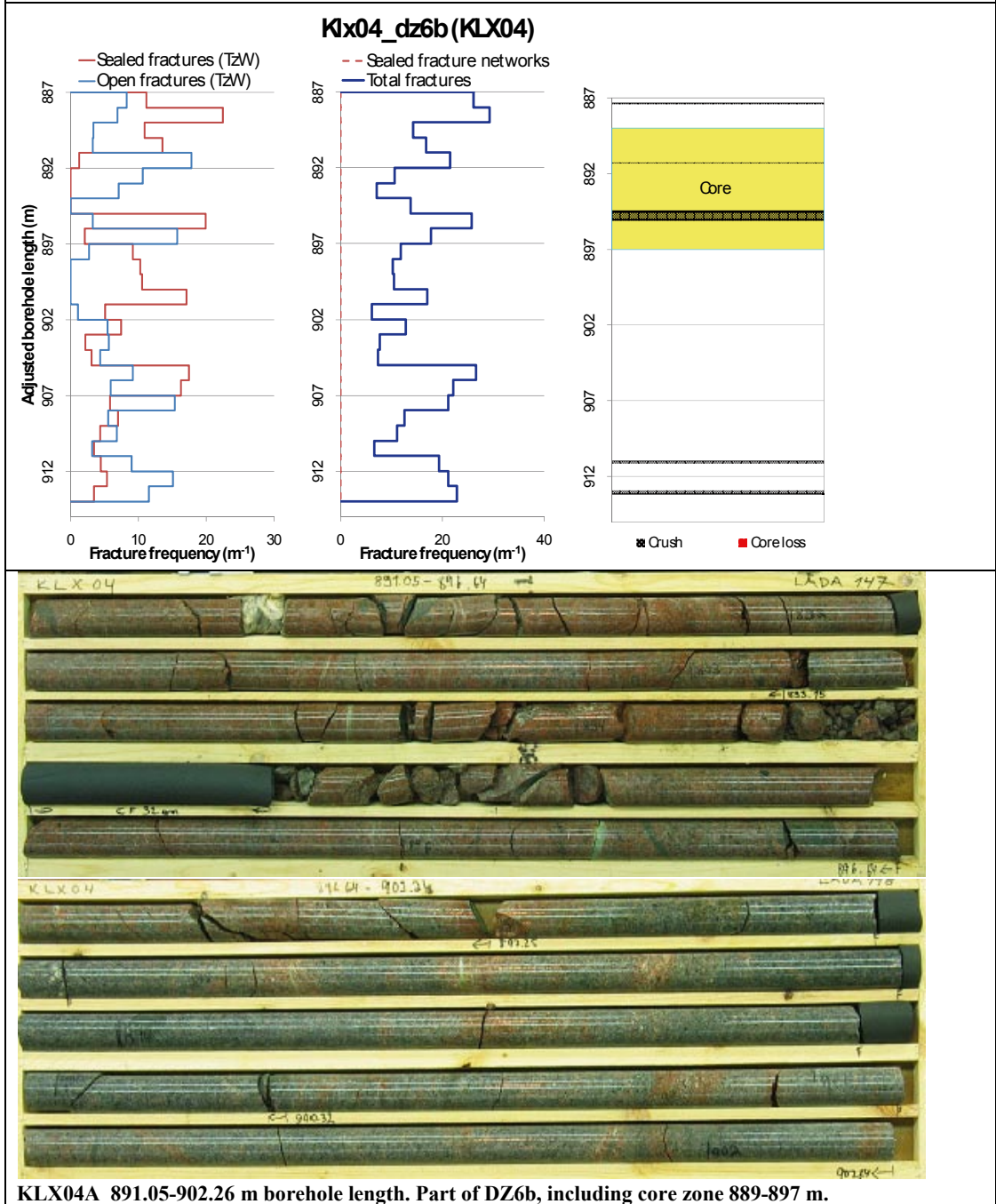
**Number of PFL-features, elevation -400 to -600m:** no data

**Model T, elevation -400 to -500m:** 2.26E-7

**Model T, elevation -500 to -600m:** 1.37E-7



## Deformation zone KLX04\_dz6b



## Deformation zone KLX04\_dz6b

### Engineering characteristics

**Transition part of zone:**

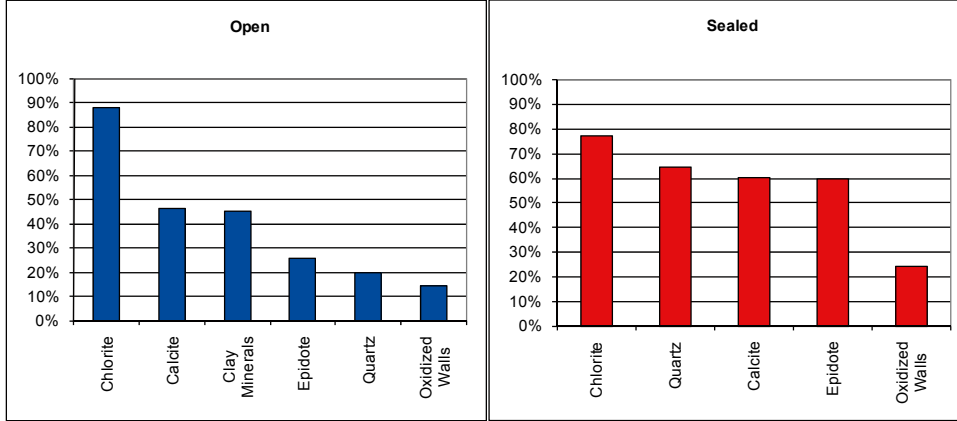
Frequency of open fractures: 5.3 m<sup>-1</sup>

Std dev: no data

Frequency of sealed fractures: 18.6 m<sup>-1</sup>

Std dev: no data

**Mineral coatings**



**Fault core:**

Percentage of fault core: 30 %

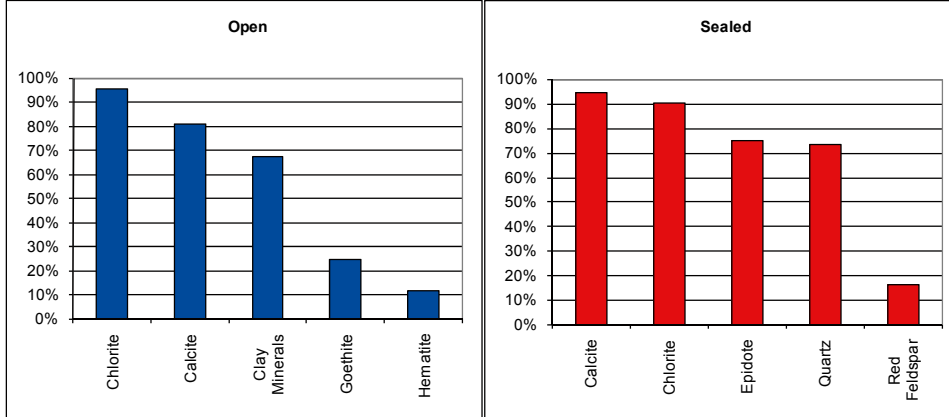
Frequency of open fractures: 8.5 m<sup>-1</sup>

Std dev: no data

Frequency of sealed fractures: 20.8 m<sup>-1</sup>

Std dev: no data

**Mineral coatings**



## Deformation zone KLX04\_dz6c

### Borehole intersections (metres along borehole)

KLX04: 935-972 m (ESHI DZ6 873-973 m)



### Deformation style, alteration and geometry

**Deformation style:** brittle

**Alteration:** red staining, chloritisation, epidotisation, saussuritisation

**Strike/dip (right-hand-rule):** 177/42

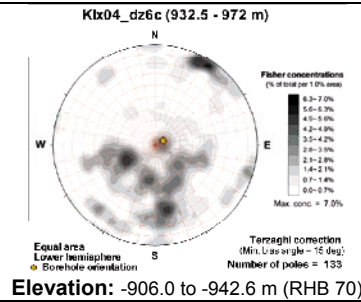
**Trace length at ground surface:** no data

**Model thickness / model thickness span :** 30 m / no data

**Measured thickness (-400 to -600 m elevation):** no data

**Comment:** Zone orientation based on /Viola et al. 2007a/

## Fractures in the deformation zone



## Transmissivity (m<sup>2</sup>/s)

**General dip of PFL-features, elevation -400 to -600m:** no data

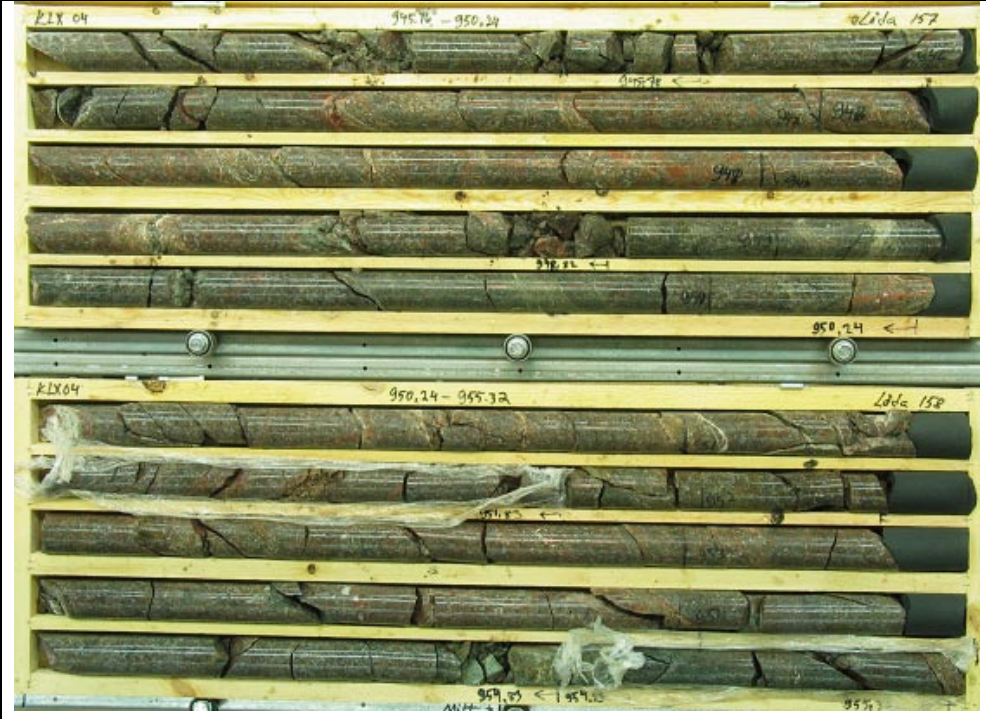
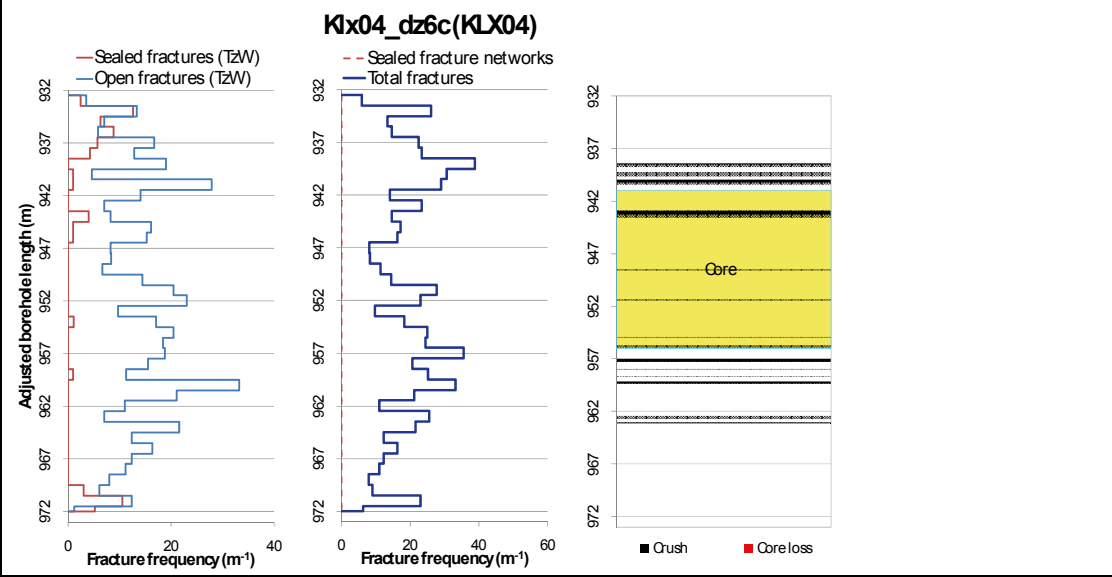
**Measured T (sum T(PFL-f)), elevation -400 to -600m:** no data

**Number of PFL-features, elevation -400 to -600m:** no data

**Model T, elevation -400 to -500m:** 2.26E-7

**Model T, elevation -500 to -600m:** 1.37E-7

## Deformation zone KLX04\_dz6c



## Deformation zone KLX04\_dz6c

### Engineering characteristics

**Transition part of zone:**

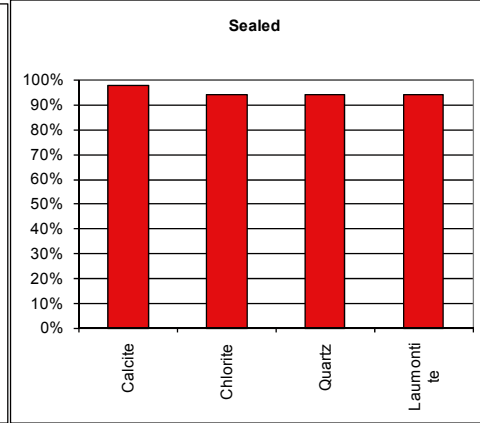
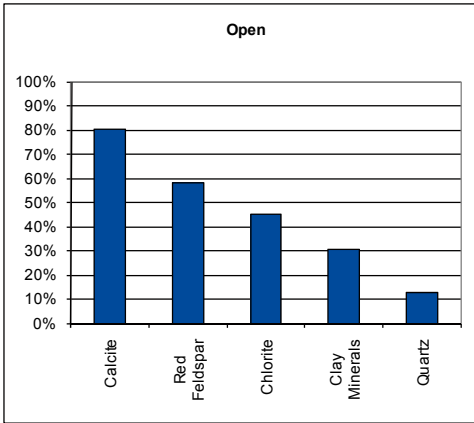
Frequency of open fractures: 14.4 m<sup>-1</sup>

Std dev: no data

Frequency of sealed fractures: 33.6 m<sup>-1</sup>

Std dev: no data

**Mineral coatings**



**Fault core:**

Percentage of fault core: 38 %

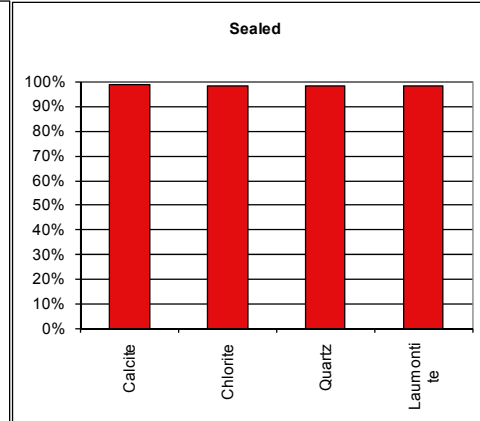
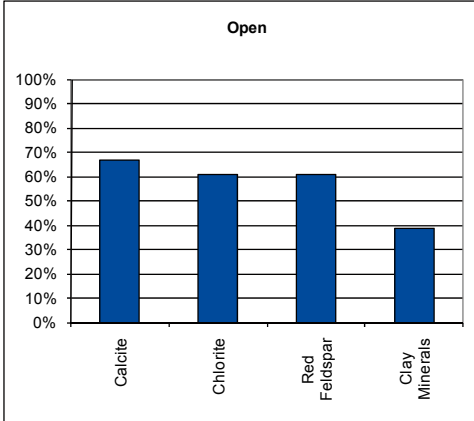
Frequency of open fractures: 13.7 m<sup>-1</sup>

Std dev: no data

Frequency of sealed fractures: 33.9 m<sup>-1</sup>

Std dev: no data

**Mineral coatings**



## Deformation zone KLX07\_dz13

### Borehole intersections (metres along borehole)

KLX07A: 817-836 m (ESHI DZ13 817-836 m)

### Deformation style, alteration and geometry

**Deformation style:** brittle and ductile

**Alteration:** red staining

**Strike/dip (right-hand-rule):** 348/65

**Trace length at ground surface:** 1.0 km

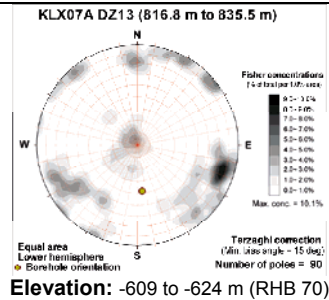
**Model thickness / model thickness span :** 10 m

**Measured thickness (-400 to -600 m elevation):** no data

**Comment:**



## Fractures in the deformation zone



## Transmissivity ( $m^2/s$ )

**General dip of PFL-features, elevation -400 to -600m:** no data

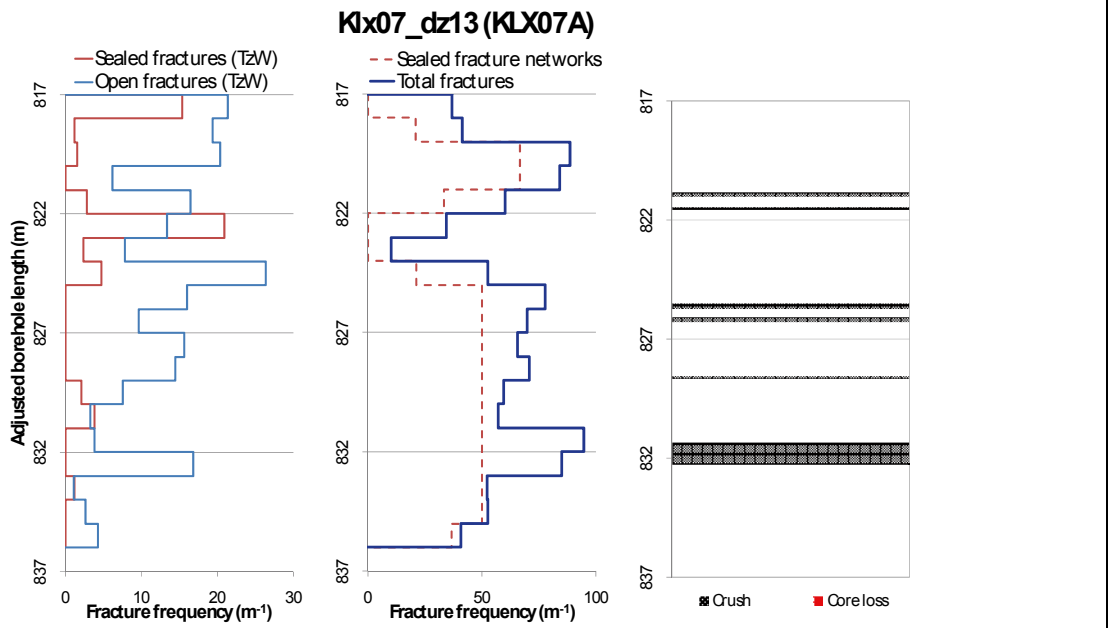
**Measured T (sum T(PFL-f)), elevation -400 to -600m:** no data

**Number of PFL-features, elevation -400 to -600m:** no data

**Model T, elevation -400 to -500m:** 2.26E-7

**Model T, elevation -500 to -600m:** 1.37E-7

## Deformation zone KLX07\_dz13



**KLX07A, 821.83-832.23 m borehole length. Part of DZ13, no defined core zone.**

## Deformation zone KLX07\_dz13

### Engineering characteristics

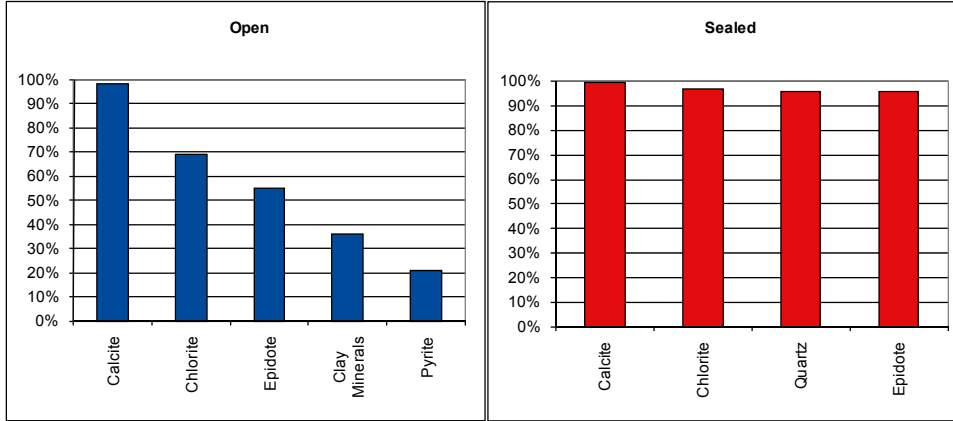
Frequency of open fractures: 12.9 m<sup>-1</sup>

Std dev: no data

Frequency of sealed fractures: 41.1 m<sup>-1</sup>

Std dev: no data

#### Mineral coatings





## Deformation zone KLX21B\_dz10-12

### Borehole intersections (metres along borehole)

KLX21B: 559-707 m (ESHI DZ10 559-572 m, DZ11 577.7- 578 m, DZ12 595-707 m)

### Deformation style, alteration and geometry

**Deformation style:** brittle and ductile

**Alteration:** red staining, epidotisation

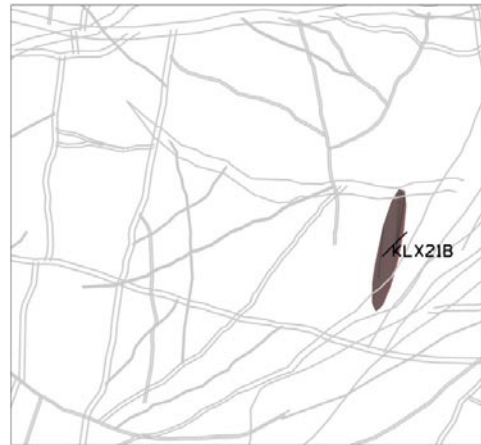
**Strike/dip (right-hand-rule):** 192/80

**Trace length at ground surface:** no data

**Model thickness / model thickness span :** 10 m / no data

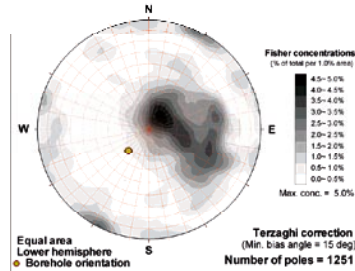
**Measured thickness (-400 to -600 m elevation):** no data

**Comment:**



## Fractures in the deformation zone

Klx21b\_dz10-12 (559 - 707 m)



**Elevation:** -511.1 to -648.5 m (RHB 70)

## Transmissivity (m<sup>2</sup>/s)

**General dip of PFL-features, elevation -400 to -600m:** Moderately to sub-horizontally and Steep

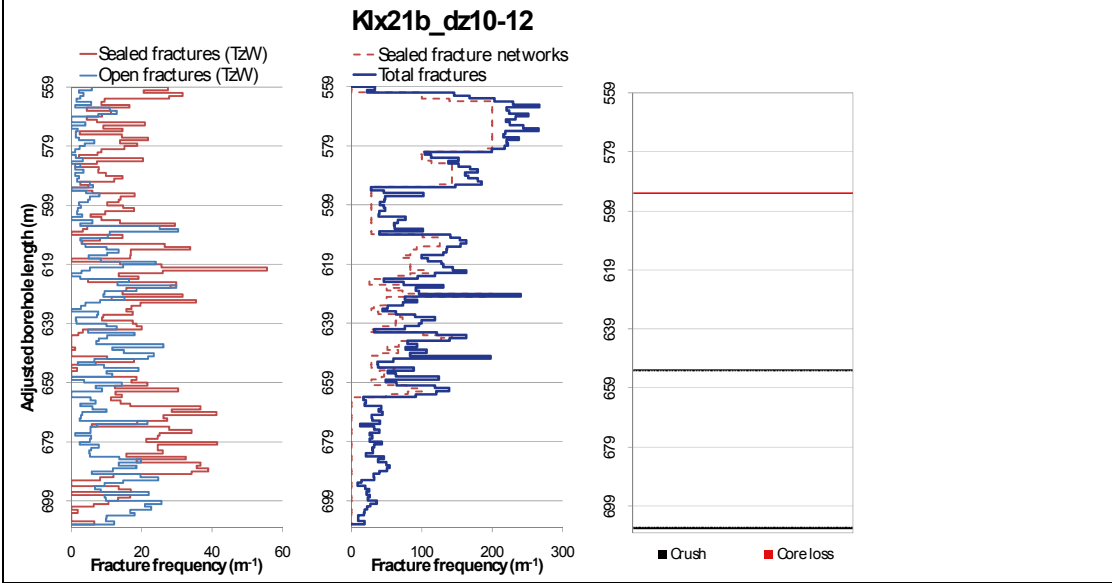
**Measured T (sum T(PFL-f)), elevation -400 to -600m:** 1.72E-5

**Number of PFL-features, elevation -400 to -600m:** 21

**Model T, elevation -400 to -500m:** 2.26E-7

**Model T, elevation -500 to -600m:** 1.37E-7

## Deformation zone KLX21B\_dz10-12



**KLX21B 641.05-645.65 m Borehole length, part of DZ12 (595-707 m Borehole length). Note the zone is interpreted as have an orientation parallel to the Borehole. No defined core zone.**

## Deformation zone KLX21B\_dz10-12

### Engineering characteristics

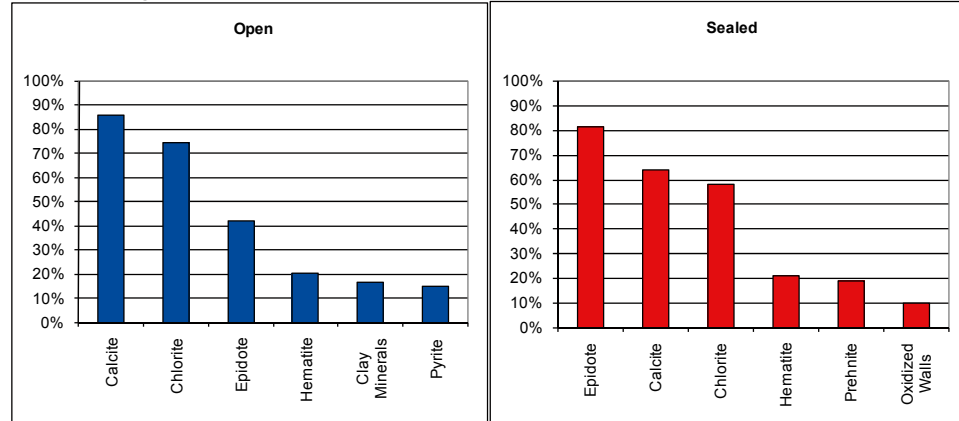
Frequency of open fractures:  $4.9 \text{ m}^{-1}$

Std dev: no data

Frequency of sealed fractures:  $28.0 \text{ m}^{-1}$

Std dev: no data

#### Mineral coatings



## Deformation zone KLX28\_dz1

### Borehole intersections (metres along borehole)

KLX28: 14.4-33.1 m (ESHI DZ1 14.4-33.1m)

### Deformation style, alteration and geometry

**Deformation style:** brittle and ductile

**Alteration:** red staining

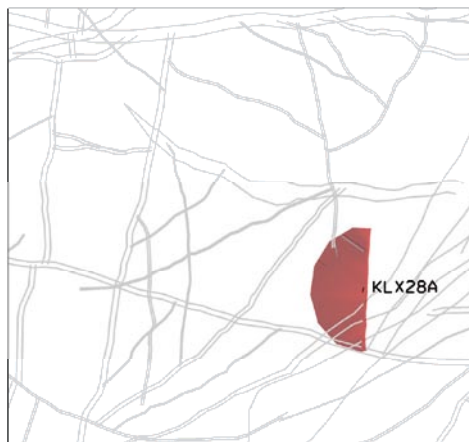
**Strike/dip (right-hand-rule):** 182/33

**Trace length at ground surface:** no data

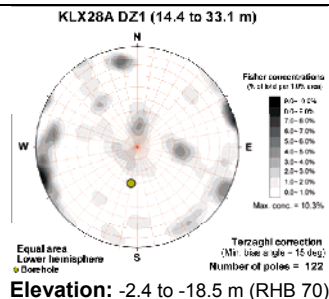
**Model thickness / model thickness span :** 13 m / no data

**Measured thickness (-400 to -600 m elevation):** no data

**Comment:**



## Fractures in the deformation zone



Elevation: -2.4 to -18.5 m (RHB 70)

## Transmissivity (m<sup>2</sup>/s)

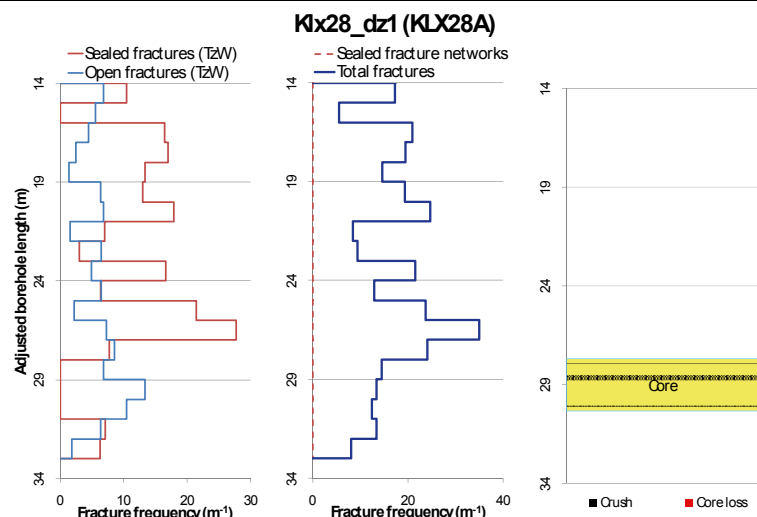
**General dip of PFL-features, elevation -400 to -600m:** no data

**Measured T (sum T(PFL-f)), elevation -400 to -600m:** no data

**Number of PFL-features, elevation -400 to -600m:** no data

**Model T, elevation -400 to -500m:** 2.26E-7

**Model T, elevation -500 to -600m:** 1.37E-7



## Deformation zone KLX28\_dz1



KLX28A 24.62-35.23 m borehole length. Part of DZ1 including core zone (27.7-30.35 m)

### Engineering characteristics

**Transition part of zone:**

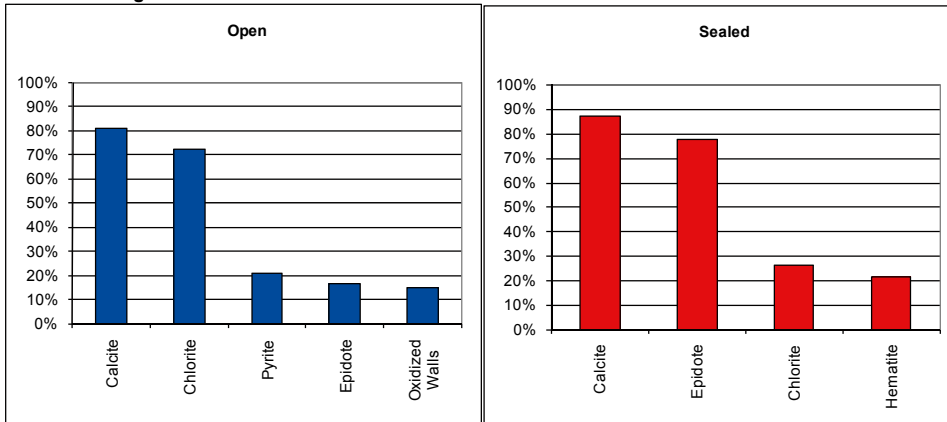
Frequency of open fractures:  $2.9 \text{ m}^{-1}$

Std dev: no data

Frequency of sealed fractures:  $26.7 \text{ m}^{-1}$

Std dev: no data

**Mineral coatings**



## Deformation zone KLX28\_dz1

### **Fault core:**

**Percentage of fault core:** 14 %

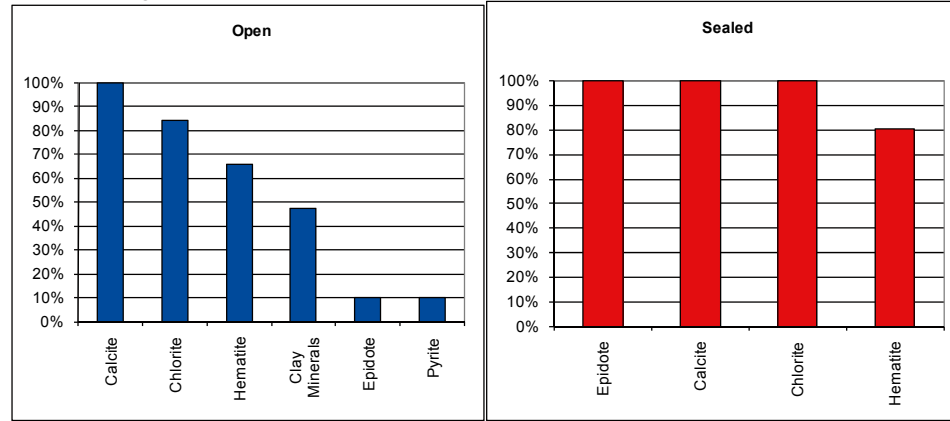
**Frequency of open fractures:** 14.3 m<sup>-1</sup>

**Std dev:** no data

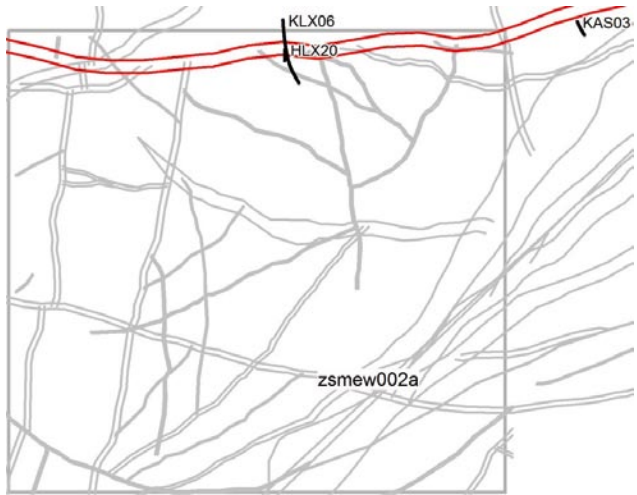
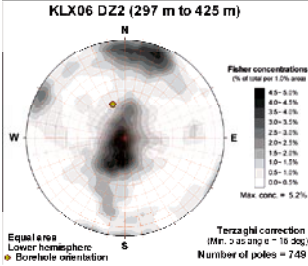
**Frequency of sealed fractures:** 37.0 m<sup>-1</sup>

**Std dev:** no data

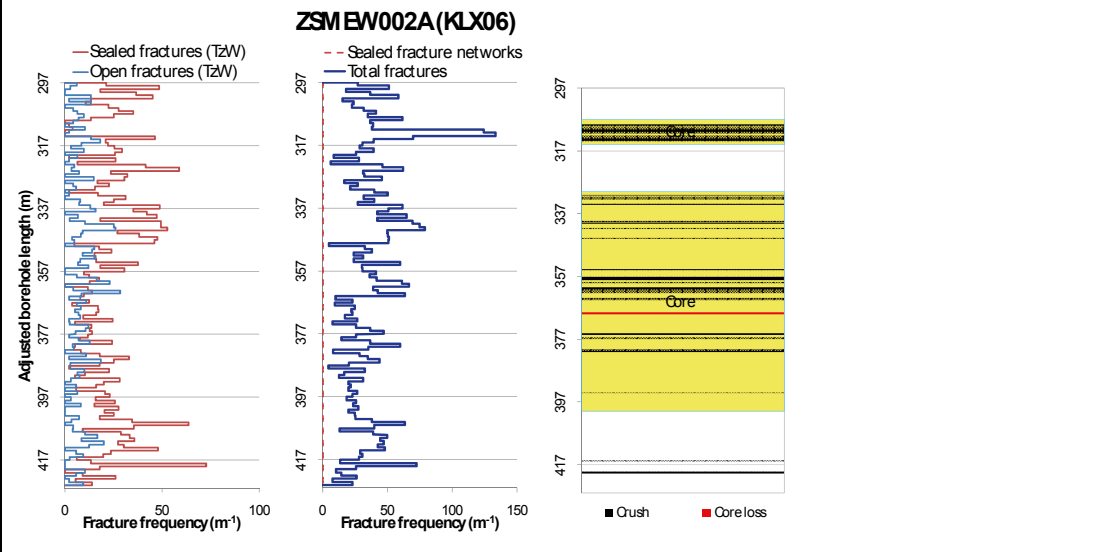
### **Mineral coatings**



**E-W to NW-SE striking deformation zones, steep to moderately southward dipping**

<b>Deformation zone ZSMEW002A</b>	
<p><b>Borehole intersections (metres along borehole)</b></p> <p>HLX20: 90-170m            KLX06: 297-425m (ESHI DZ2 297-425m)            KAS03: 280-480m</p>	
<p><b>Deformation style, alteration and geometry</b></p> <p><b>Deformation style:</b> brittle and ductile</p> <p><b>Alteration:</b> red staining, laumontite, saussuritisation and clay alteration,</p> <p><b>Strike/dip (right-hand-rule):</b> 090/65</p> <p><b>Trace length at ground surface:</b> 17.9 km</p> <p><b>Model thickness / model thickness span :</b> 100 m / 20-200 m</p> <p><b>Measured thickness (-400 to -600 m elevation):</b> no data</p> <p><b>Comment:</b></p>	
<b>Fractures in the deformation zone</b>	
 <p><b>KLX06 DZ2 (297 m to 425 m)</b></p> <p><b>Elevation:</b> -249.1 to -360.5 m (RHB 70)</p>	
<b>Transmissivity (m<sup>2</sup>/s)</b>	
<p><b>General dip of PFL-features, elevation -400 to -600m:</b> no data</p> <p><b>Measured T (sum T(PFL-f)), elevation -400 to -600m:</b> no data</p> <p><b>Number of PFL-features, elevation -400 to -600m:</b> no data</p> <p><b>Model T, elevation -400 to -500m:</b> 3.74E-6</p> <p><b>Model T, elevation -500 to -600m:</b> 2.42E-6</p>	

## Deformation zone ZSMEW002A



**KLX06 357.5 -368.37 m borehole length. Central part of one core zone.**



## Deformation zone ZSMEW002A

### Engineering characteristics

**Transition part of zone:**

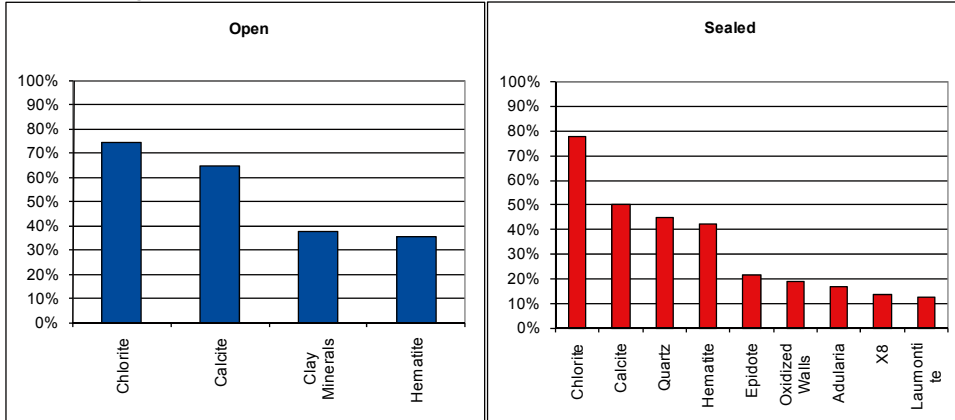
Frequency of open fractures: 2.1 m<sup>-1</sup>

Std dev: no data

Frequency of sealed fractures: 24.1 m<sup>-1</sup>

Std dev: no data

**Mineral coatings**



**Fault core:**

Percentage of fault core: 61%

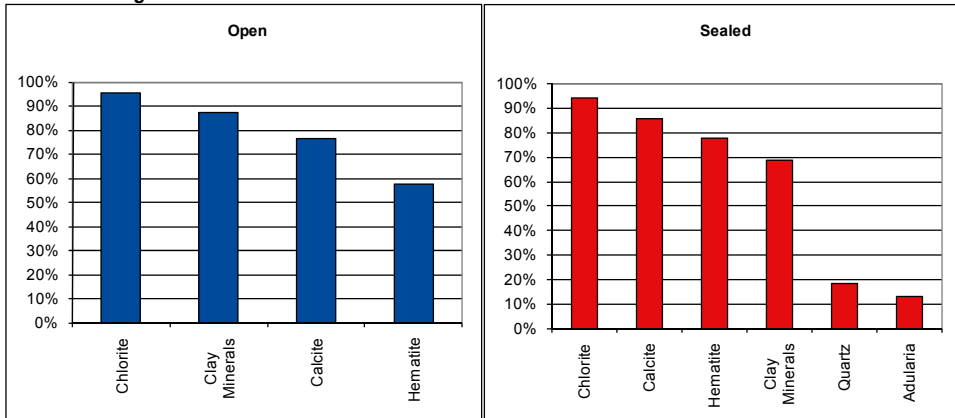
Frequency of open fractures: 8.4 m<sup>-1</sup>

Std dev: no data

Frequency of sealed fractures: 44.2 m<sup>-1</sup>

Std dev: no data

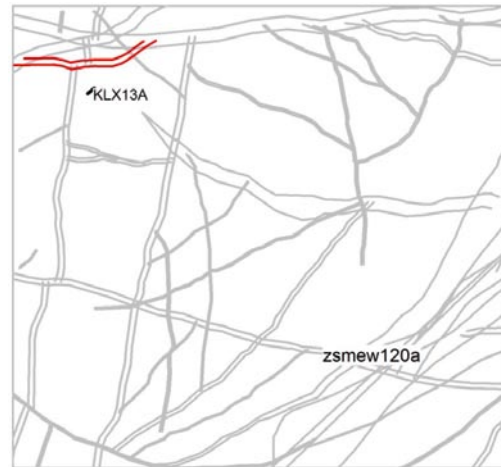
**Mineral coatings**



## Deformation zone ZSMEW120A

### Borehole intersections (metres along borehole)

KLX13A: 488- 593m (ESHI DZ7 488-593m)



### Deformation style, alteration and geometry

**Deformation style:** brittle and ductile

**Alteration:** red staining

**Strike/dip (right-hand-rule):** 080/64

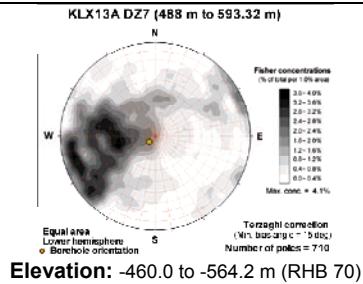
**Trace length at ground surface:** 1.2 km

**Model thickness / model thickness span :** 50 m / 30->60 m

**Measured thickness (-400 to -600 m elevation):** >50 m

**Comment:** KLX13A does not penetrate the full thickness of the zone

## Fractures in the deformation zone



## Transmissivity ( $m^2/s$ )

**General dip of PFL-features, elevation -400 to -600m:** Moderately to sub-horizontally

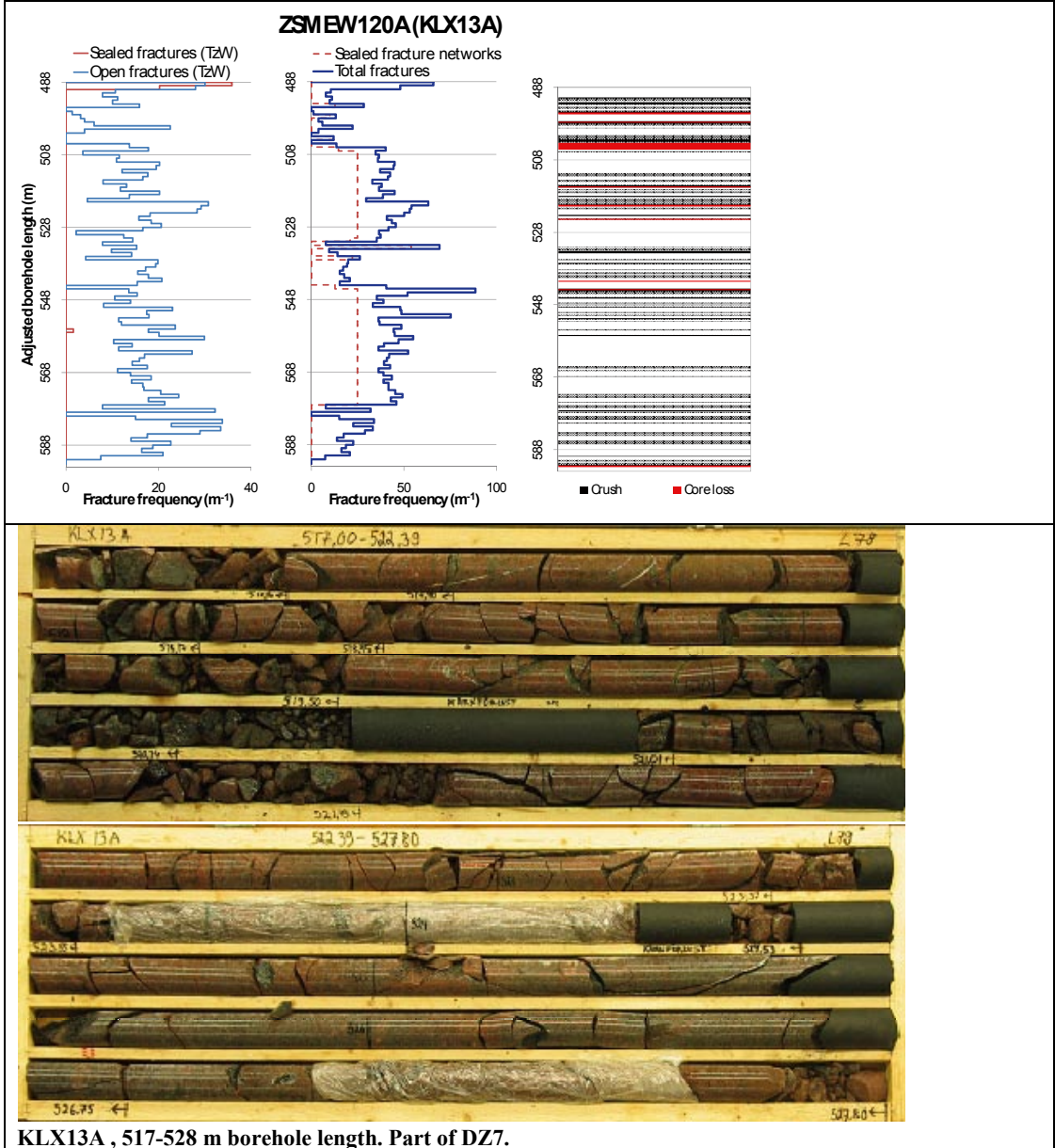
**Measured T (sum T(PFL-f)), elevation -400 to -600m:**  $9.0E-7$

**Number of PFL-features, elevation -400 to -600m:** 39

**Model T, elevation -400 to -500m:**  $4.23E-7$

**Model T, elevation -500 to -600m:**  $2.62E-7$

## Deformation zone ZSMEW120A



## Deformation zone ZSMEW120A

### Engineering characteristics

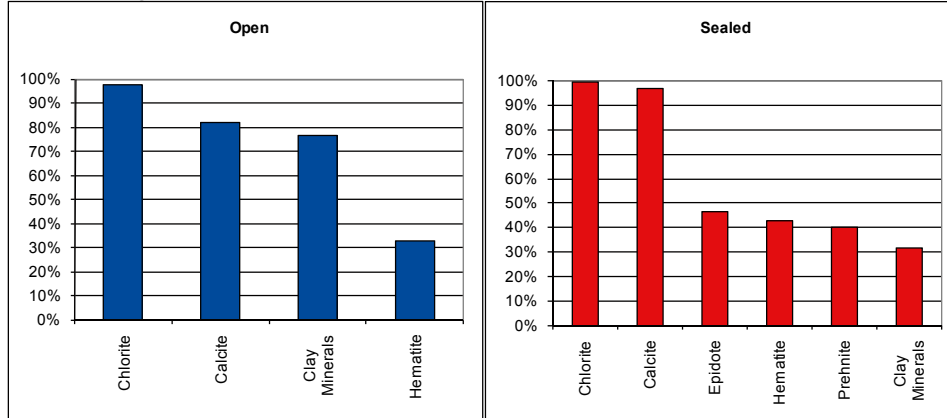
Frequency of open fractures: 22.8 m<sup>-1</sup>

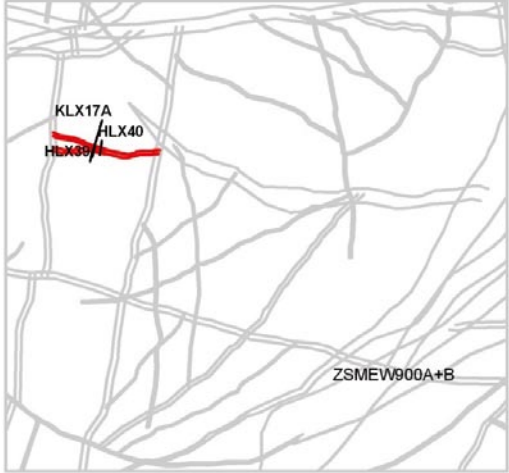
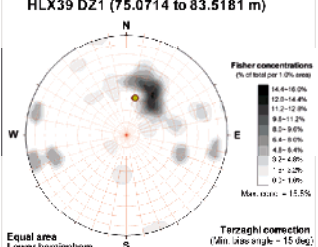
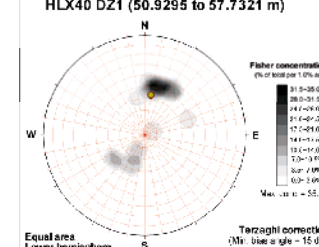
Std dev: no data

Frequency of sealed fractures: 90.4 m<sup>-1</sup>

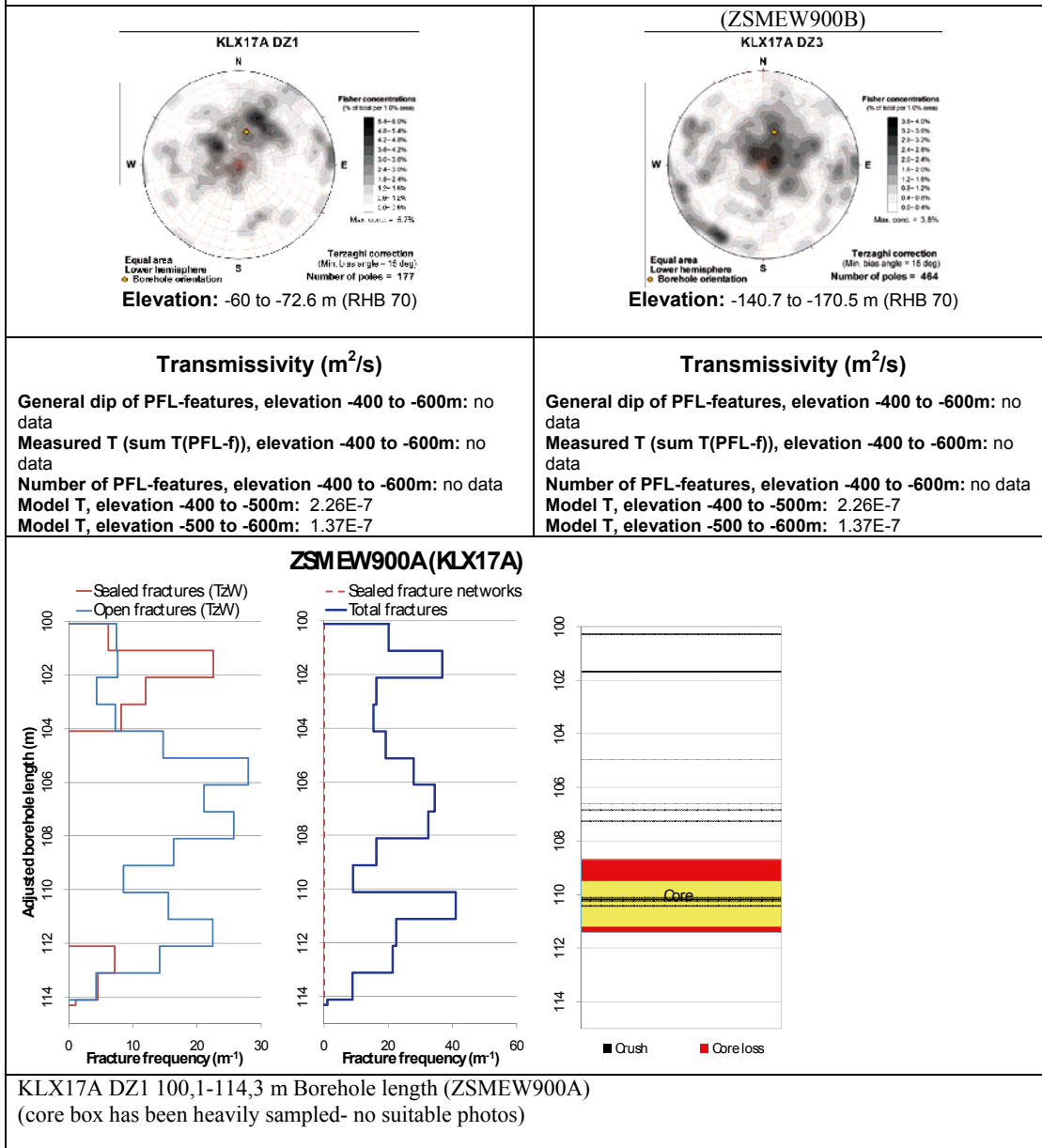
Std dev: no data

#### Mineral coatings



<b>Deformation zone ZSMEW900A-B</b>	
<p><b>Borehole intersections (metres along borehole)</b></p> <p>HLX39: 75-85m (ESHI DZ1 75-85m)            HLX40: 49.8-59.6m (ESHI DZ1 49.8-59.6m)            KLX17: 100.1-114.3m (ESHI DZ1 100.1-114.3m)            KLX17: 192.7-227 m (ESHI DZ3 192.7-227m) (ZSMEW900B)</p>	
<p><b>Deformation style, alteration and geometry</b></p> <p><b>Deformation style:</b> brittle and ductile  <b>Alteration:</b> red staining, epidotisation and saussuritisation,  <b>Strike/dip (right-hand-rule):</b> 092/57  <b>Trace length at ground surface:</b> 0.9 km  <b>Model thickness / model thickness span :</b> 25 m / 10-30 m  <b>Measured thickness (-400 to -600 m elevation):</b> no data  <b>Comment:</b></p>	
<b>Fractures in the deformation zone</b>	
<p style="text-align: center;">HLX39 DZ1 (75.0714 to 83.5181 m)</p>  <p style="text-align: center;"><b>Elevation:</b> -39 to -45.5 m (RHB 70)</p>	<p style="text-align: center;">HLX40 DZ1 (50.9295 to 57.7321 m)</p>  <p style="text-align: center;"><b>Elevation:</b> -16.7 to -24.9 m (RHB 70)</p>
<p style="text-align: center;"><b>Transmissivity (m<sup>2</sup>/s)</b></p> <p><b>General dip of PFL-features, elevation -400 to -600m:</b> no data  <b>Measured T (sum T(PFL-f)), elevation -400 to -600m:</b> no data  <b>Number of PFL-features, elevation -400 to -600m:</b> no data  <b>Model T, elevation -400 to -500m:</b> 2.26E-7  <b>Model T, elevation -500 to -600m:</b> 1.37E-7</p>	<p style="text-align: center;"><b>Transmissivity (m<sup>2</sup>/s)</b></p> <p><b>General dip of PFL-features, elevation -400 to -600m:</b> no data  <b>Measured T (sum T(PFL-f)), elevation -400 to -600m:</b> no data  <b>Number of PFL-features, elevation -400 to -600m:</b> no data  <b>Model T, elevation -400 to -500m:</b> 2.26E-7  <b>Model T, elevation -500 to -600m:</b> 1.37E-7</p>

## Deformation zone ZSMEW900A-B



## Deformation zone ZSMEW900A-B

### Engineering characteristics

**Transition part of zone:**

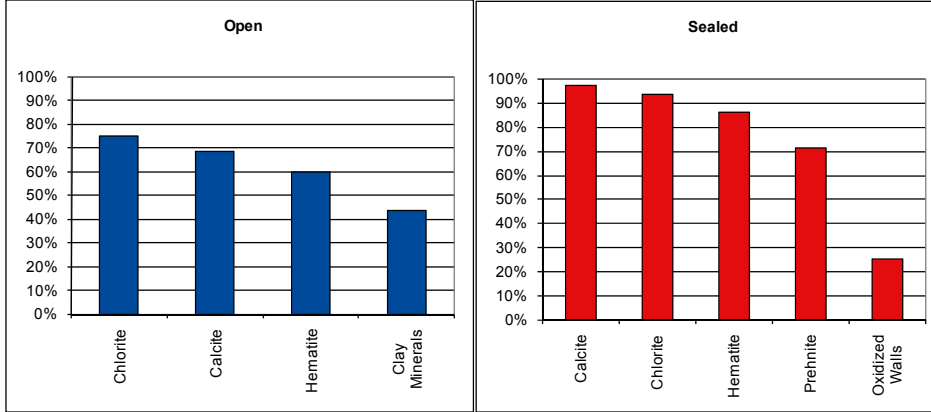
Frequency of open fractures: 14.6 m<sup>-1</sup>

Std dev: no data

Frequency of sealed fractures: 42.6 m<sup>-1</sup>

Std dev: no data

**Mineral coatings**



**Fault core:**

Percentage of fault core: 15 %

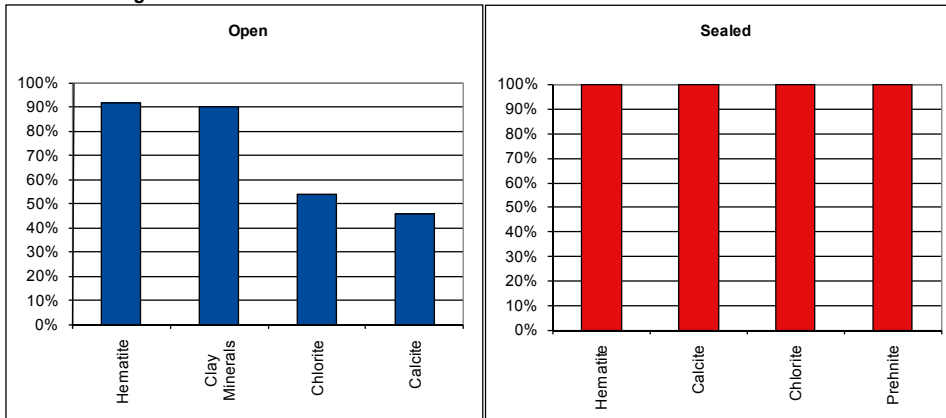
Frequency of open fractures: 18.5 m<sup>-1</sup>

Std dev: no data

Frequency of sealed fractures: 67.0 m<sup>-1</sup>

Std dev: no data

**Mineral coatings**



## Deformation zone ZSMNW042A

### Borehole intersections (metres along borehole)

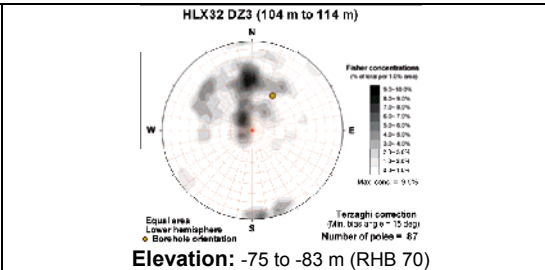
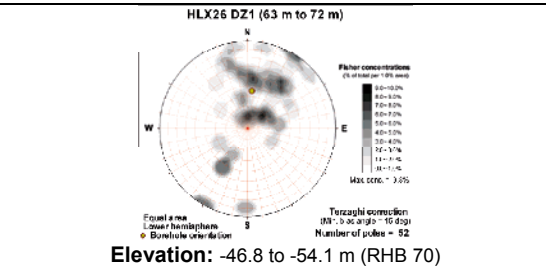
HLX26: 50-80 m (ESHI DZ1 63-72m)  
 HLX32: 20-130 m (ESHI DZ3 104-114m)  
 KLX15A: 977-1000,4+ m (ESHI 978-1000m)  
 KLX27A : 209-255 m (ESHI DZ3 208.5-255.0 m)



### Deformation style, alteration and geometry

**Deformation style:** ductile and brittle  
**Alteration:** oxidation, chloritisation, epidotisation  
**Strike/dip (right-hand-rule):** 105/55  
**Trace length at ground surface:** 8.3 km  
**Model thickness / model thickness span :** 40 m / 20-50 m  
**Measured thickness (-400 to -600 m elevation):** no data  
**Comment:**

## Fractures in the deformation zone

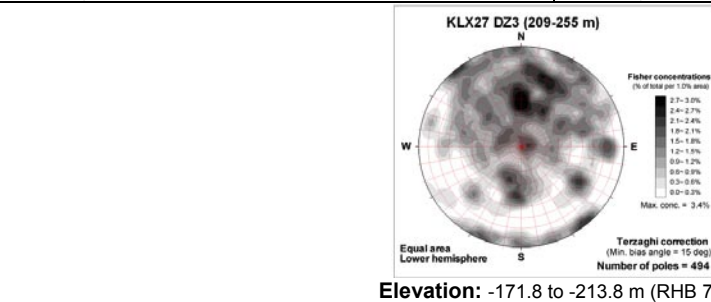


### Transmissivity (m<sup>2</sup>/s)

**General dip of PFL-features, elevation -400 to -600m:** no data  
**Measured T (sum T(PFL-f)), elevation -400 to -600m:** no data  
**Number of PFL-features, elevation -400 to -600m:** no data  
**Model T, elevation -400 to -500m:** 1.49E-6  
**Model T, elevation -500 to -600m:** 8.27E-7

### Transmissivity (m<sup>2</sup>/s)

**General dip of PFL-features, elevation -400 to -600m:** no data  
**Measured T (sum T(PFL-f)), elevation -400 to -600m:** no data  
**Number of PFL-features, elevation -400 to -600m:** no data  
**Model T, elevation -400 to -500m:** 1.49E-6  
**Model T, elevation -500 to -600m:** 8.27E-7

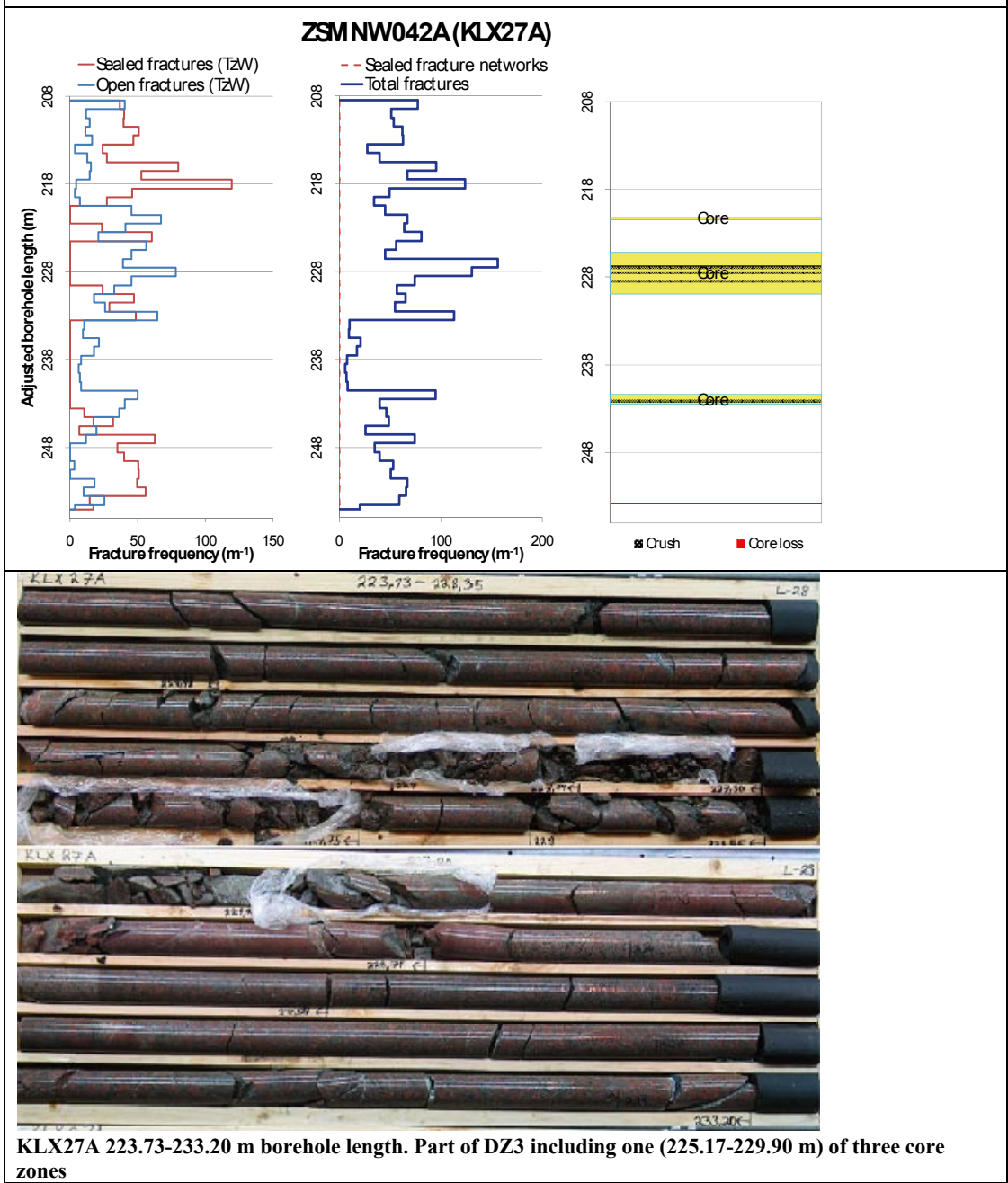


### Transmissivity (m<sup>2</sup>/s)

**General dip of PFL-features, elevation -400 to -600m:** no data  
**Measured T (sum T(PFL-f)), elevation -400 to -600m:** no data  
**Number of PFL-features, elevation -400 to -600m:** no data  
**Model T, elevation -400 to -500m:** 1.49E-6  
**Model T, elevation -500 to -600m:** 8.27E-7



## Deformation zone ZSMNW042A



## Deformation zone ZSMNW042A

### Engineering characteristics

**Transition part of zone:**

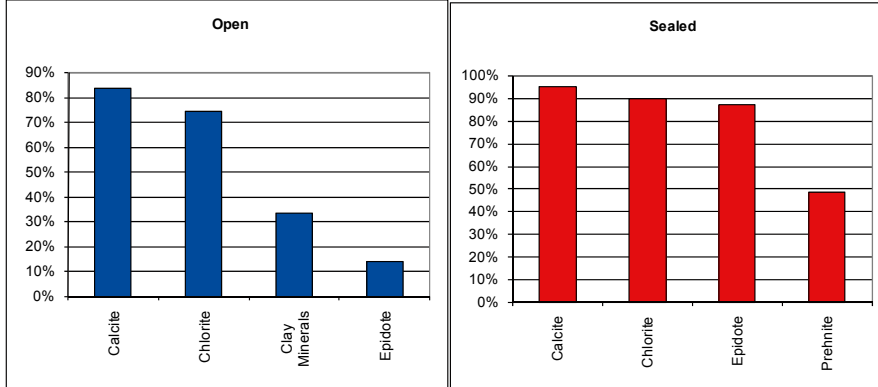
Frequency of open fractures: 4.5 m<sup>-1</sup>

Std dev: no data

Frequency of sealed fractures: 48.9 m<sup>-1</sup>

Std dev: no data

**Mineral coatings**



**Fault core:**

Percentage of fault core: 13 %

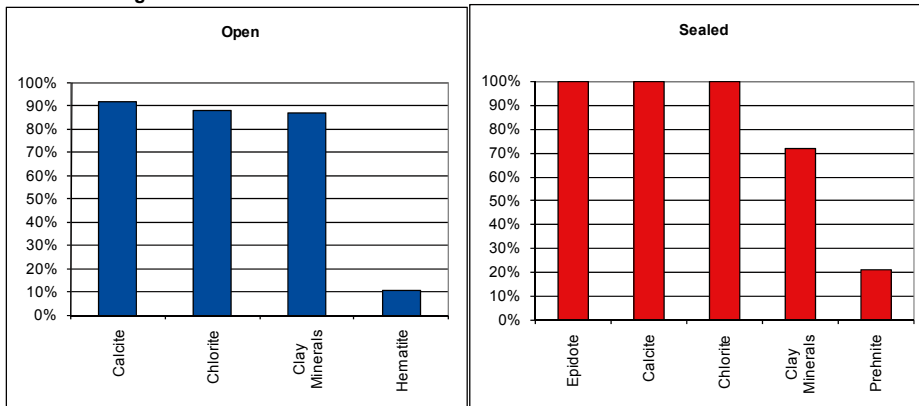
Frequency of open fractures: 24.3 m<sup>-1</sup>


Std dev: no data

Frequency of sealed fractures: 70.5 m<sup>-1</sup>

Std dev: no data

**Mineral coatings**



<b>Deformation zone ZSMNW119A</b>	
<p><b>Borehole intersections (metres along borehole)</b></p> <p>no data</p>	
<p><b>Deformation style, alteration and geometry</b></p> <p><b>Deformation style:</b> brittle and ductile</p> <p><b>Alteration:</b> red staining</p> <p><b>Strike/dip (right-hand-rule):</b> 130/90</p> <p><b>Trace length at ground surface:</b> 2.0 km</p> <p><b>Model thickness / model thickness span :</b> 10 m / 5-20 m</p> <p><b>Measured thickness (-400 to -600 m elevation):</b> no data</p> <p><b>Comment:</b></p>	
<b>Fractures in the deformation zone</b>	
No Borehole intercepts	
<b>Transmissivity (m<sup>2</sup>/s)</b>	
<p><b>General dip of PFL-features, elevation -400 to -600m:</b> no data</p> <p><b>Measured T (sum T(PFL-f)), elevation -400 to -600m:</b> no data</p> <p><b>Number of PFL-features, elevation -400 to -600m:</b> no data</p> <p><b>Model T, elevation -400 to -500m:</b> 1.49E-6</p> <p><b>Model T, elevation -500 to -600m:</b> 8.27E-7</p>	
<b>Engineering characteristics</b>	
No Borehole intercepts	

## Deformation zone KLX07\_dz7

### Borehole intersections (metres along borehole)

KLX07A: 347-388 m (Eshi DZ7 347-388 m)  
 HLX21: 20-71 m (Eshi DZ1 18-24m)  
 HLX24: 27-40 m (Eshi DZ1 27-40 m)

### Deformation style, alteration and geometry

**Deformation style:** brittle and ductile

**Alteration:** oxidation, chloritisation, epidotisation

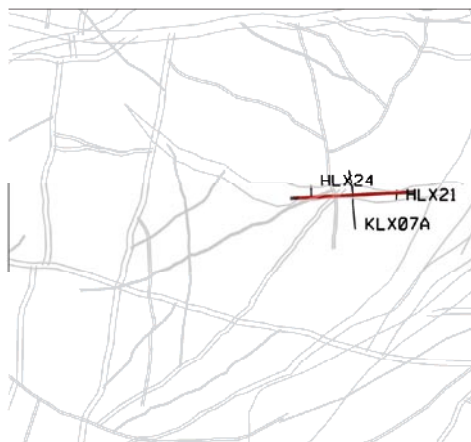
**Strike/dip (right-hand-rule):** 267/90

**Trace length at ground surface:** no data

**Model thickness / model thickness span :** 30 m / no data

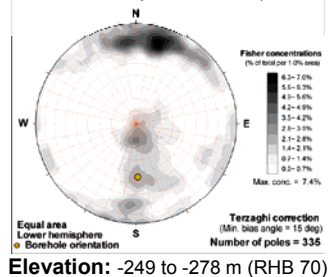
**Measured thickness (-400 to -600 m elevation):** no data

**Comment:** The modelled geometry generates theoretical intercepts in HLX21, HLX22, HLX23 and HLX24. While fracture data weakly supports possible correlation with HLX21 and HLX24 no correlation with HLX22 or HLX23 exists. It should be noted that all four hammer holes lie within the complex ZSMEW007A deformation belt.

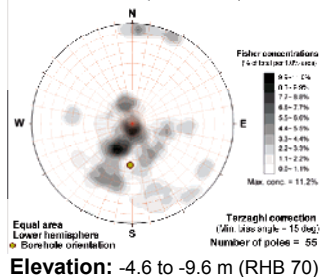


## Fractures in the deformation zone

KLX07A DZ7 (347 m to 387.5 m)



HLX21 DZ1 (18 m to 24 m)



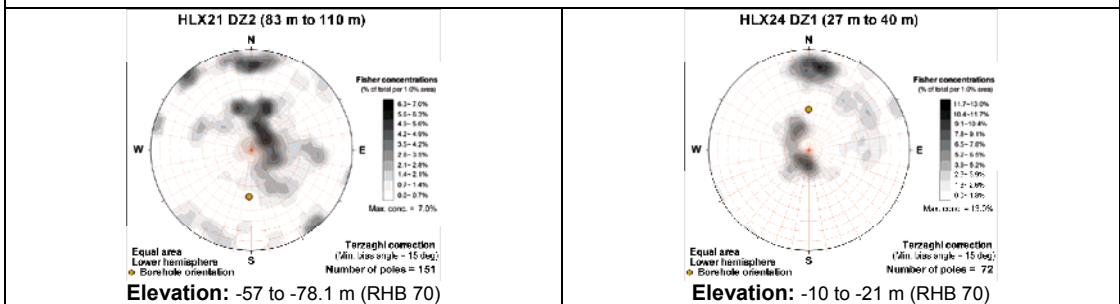
### Transmissivity ( $m^2/s$ )

**General dip of PFL-features, elevation -400 to -600m:** no data  
**Measured T (sum T(PFL-f)), elevation -400 to -600m:** no data  
**Number of PFL-features, elevation -400 to -600m:** no data  
**Model T, elevation -400 to -500m:** 2.26E-7  
**Model T, elevation -500 to -600m:** 1.37E-7

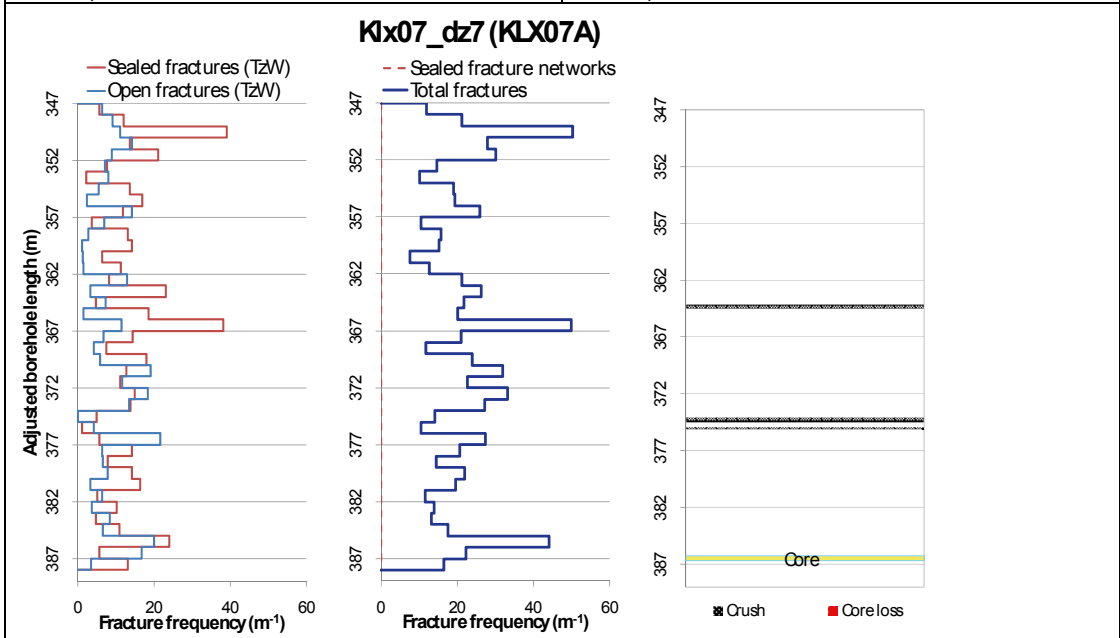
### Transmissivity ( $m^2/s$ )

**General dip of PFL-features, elevation -400 to -600m:** no data  
**Measured T (sum T(PFL-f)), elevation -400 to -600m:** no data  
**Number of PFL-features, elevation -400 to -600m:** no data  
**Model T, elevation -400 to -500m:** 2.26E-7  
**Model T, elevation -500 to -600m:** 1.37E-7

## Deformation zone KLX07\_dz7



<p><b>Transmissivity (m<sup>2</sup>/s)</b></p> <p>General dip of PFL-features, elevation -400 to -600m: no data          Measured T (sum T(PFL-f)), elevation -400 to -600m: no data          Number of PFL-features, elevation -400 to -600m: no data          Model T, elevation -400 to -500m: 2.26E-7          Model T, elevation -500 to -600m: 1.37E-7</p>	<p><b>Transmissivity (m<sup>2</sup>/s)</b></p> <p>General dip of PFL-features, elevation -400 to -600m: no data          Measured T (sum T(PFL-f)), elevation -400 to -600m: no data          Number of PFL-features, elevation -400 to -600m: no data          Model T, elevation -400 to -500m: 2.26E-7          Model T, elevation -500 to -600m: 1.37E-7</p>
--	--



**KLX07A 385.03-390.57 m borehole length. Part of DZ7, including core zone 386.3-386.7 m.**

## Deformation zone KLX07\_dz7

### Engineering characteristics

**Transition part of zone:**

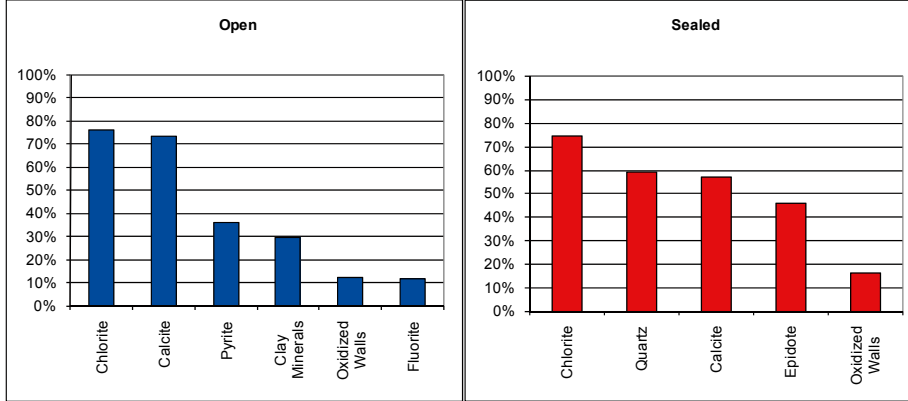
Frequency of open fractures: 5.7 m<sup>-1</sup>

Std dev: no data

Frequency of sealed fractures: 16.2 m<sup>-1</sup>

Std dev: no data

**Mineral coatings**



**Fault core:**

Percentage of fault core: 1 %

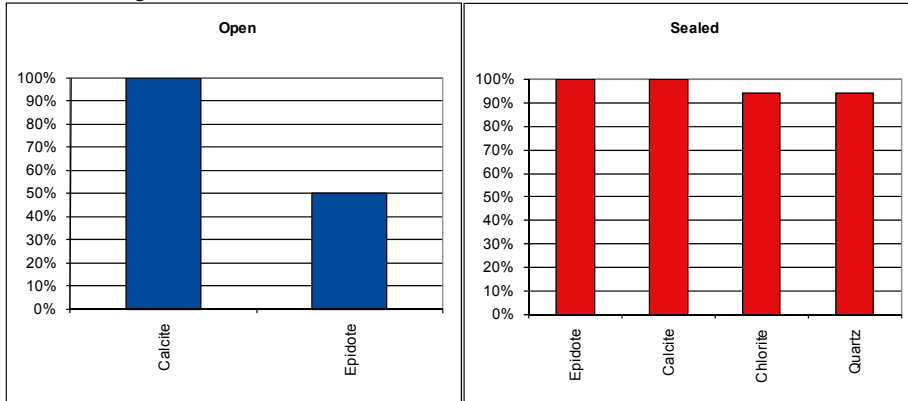
Frequency of open fractures: 10.0 m<sup>-1</sup>

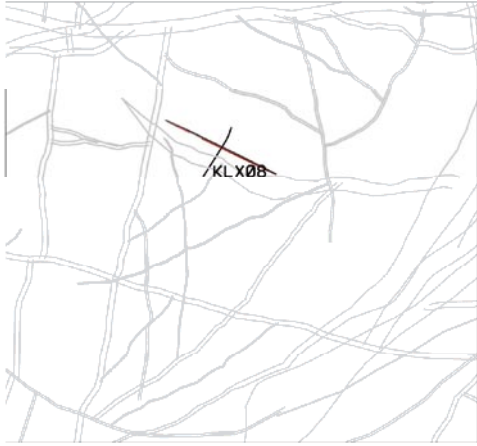
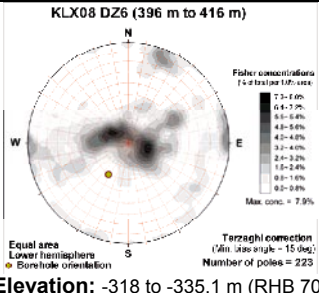
Std dev: no data

Frequency of sealed fractures: 45.0 m<sup>-1</sup>

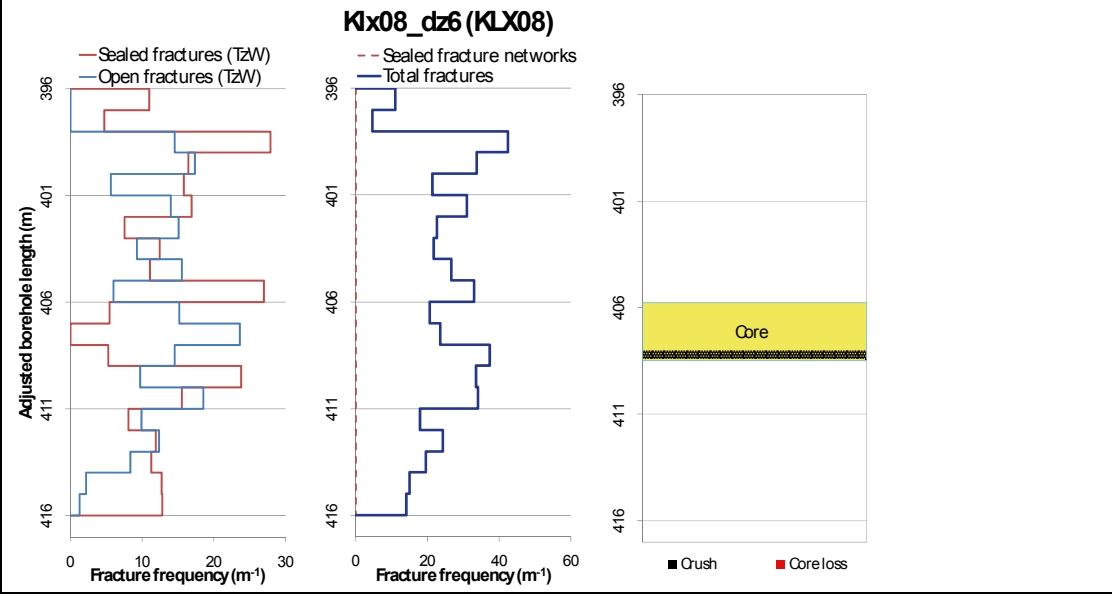
Std dev: no data

**Mineral coatings**



<b>Deformation zone KLX08_dz6</b>	
<p><b>Borehole intersections (metres along borehole)</b></p> <p>KLX08A: 396-416 (Eshi DZ6 396-416 m)</p>	
<p><b>Deformation style, alteration and geometry</b></p> <p><b>Deformation style:</b> brittle</p> <p><b>Alteration:</b> red staining, epidotisation, saussuritization</p> <p><b>Strike/dip (right-hand-rule):</b> 296/89</p> <p><b>Trace length at ground surface:</b> no data</p> <p><b>Model thickness / model thickness span :</b> 10 m / no data</p> <p><b>Measured thickness (-400 to -600 m elevation):</b> no data</p> <p><b>Comment:</b></p>	
<b>Fractures in the deformation zone</b>	
	
<b>Transmissivity (m<sup>2</sup>/s)</b>	
<p><b>General dip of PFL-features, elevation -400 to -600m:</b> no data</p> <p><b>Measured T (sum T(PFL-f)), elevation -400 to -600m:</b> no data</p> <p><b>Number of PFL-features, elevation -400 to -600m:</b> no data</p> <p><b>Model T, elevation -400 to -500m:</b> 2.26E-7</p> <p><b>Model T, elevation -500 to -600m:</b> 1.37E-7</p>	

## Deformation zone KLX08\_dz6



**KLX08A 406.24-415.99 m borehole length. Part of DZ6, including core zone (405.77- 408.50 m)**



## Deformation zone KLX08\_dz6

### Engineering characteristics

**Transition part of zone:**

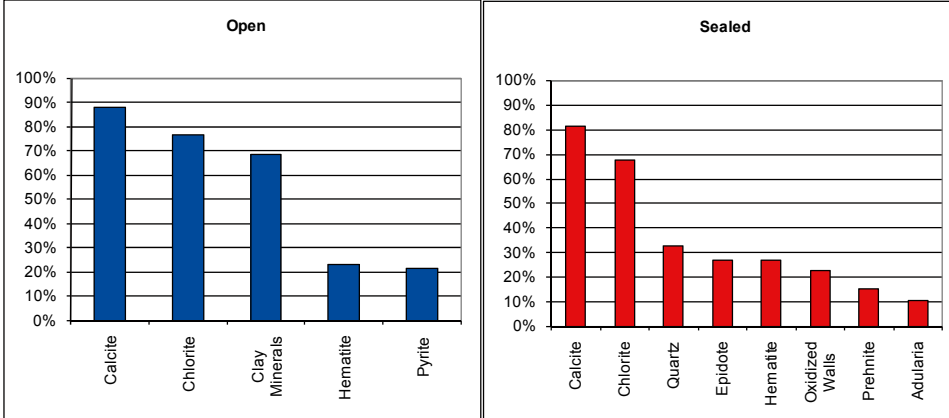
Frequency of open fractures: 6.4 m<sup>-1</sup>

Std dev: no data

Frequency of sealed fractures: 17.3 m<sup>-1</sup>

Std dev: no data

**Mineral coatings**



**Fault core:**

Percentage of fault core: 14 %

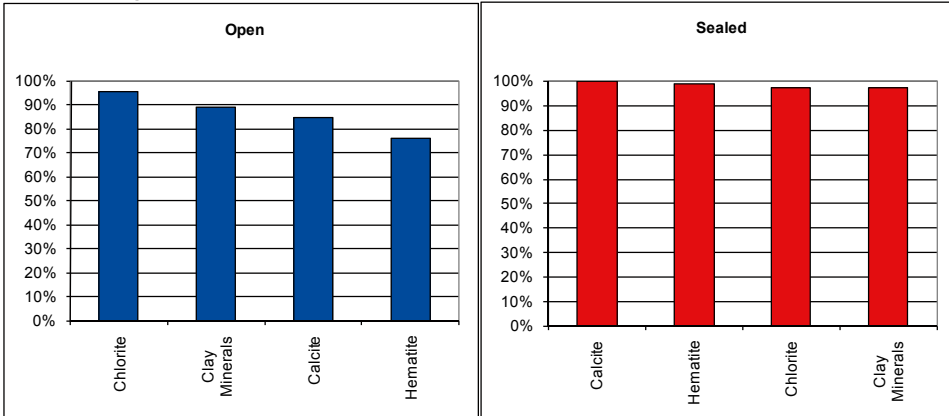
Frequency of open fractures: 16.9 m<sup>-1</sup>

Std dev: no data

Frequency of sealed fractures: 59.0 m<sup>-1</sup>

Std dev: no data

**Mineral coatings**



## Deformation zone KLX18\_dz9

### Borehole intersections (metres along borehole)

KLX18A: 347-388 m (Eshi DZ9 472-489 m)  
 HLX30: None (Eshi DZ2 60-68 m)

### Deformation style, alteration and geometry

**Deformation style:** brittle and ductile

**Alteration:** oxidation, chloritisation, epidotisation

**Strike/dip (right-hand-rule):** 095/50

**Trace length at ground surface:** no data

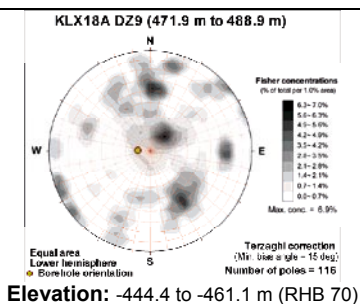
**Model thickness / model thickness span :** 10 m / no data

**Measured thickness (-400 to -600 m elevation):** 10m

**Comment:** orientation is based on detailed mapping of the zone core /Viola et al. 2007a/. An interception at the outer edge of the modelled geometry coincides with Eshi HLX30 DZ2 though no clear correlation is established.



## Fractures in the deformation zone



### Transmissivity ( $m^2/s$ )

**General dip of PFL-features, elevation -400 to -600m:** Moderately to sub-horizontally

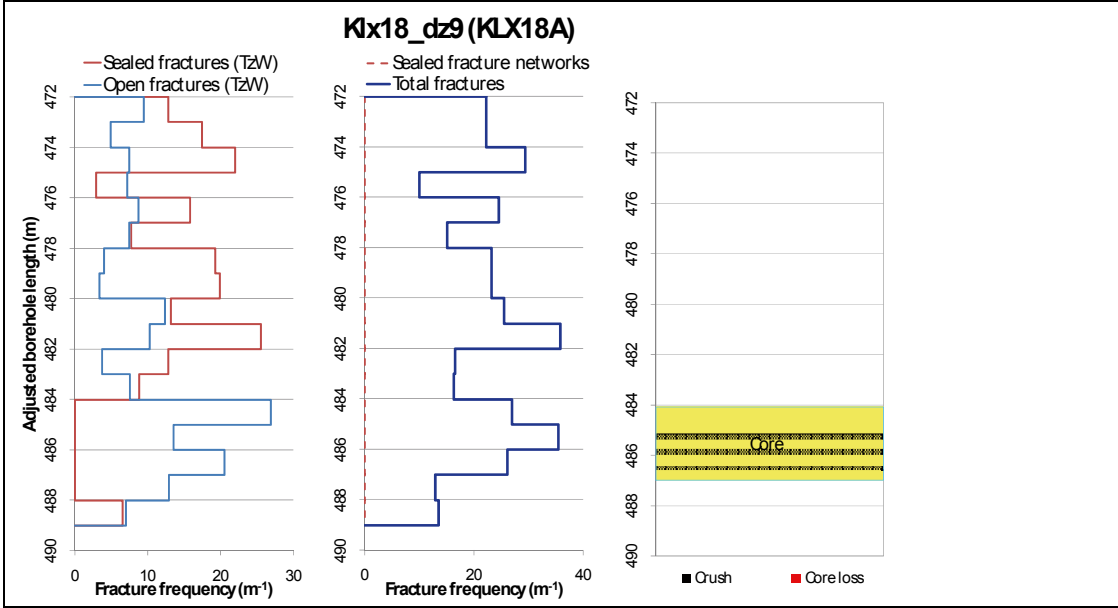
**Measured T (sum T(PFL-f)), elevation -400 to -600m:** 5.44E-8

**Number of PFL-features, elevation -400 to -600m:** 9

**Model T, elevation -400 to -500m:** 2.26E-7

**Model T, elevation -500 to -600m:** 1.37E-7

### Deformation zone KLX18\_dz9



KLX18A 478.18-489.10 m borehole length. Part of DZ9, including core zone 484.1-487.0 m.

## Deformation zone KLX18\_dz9

### Engineering characteristics

**Transition part of zone:**

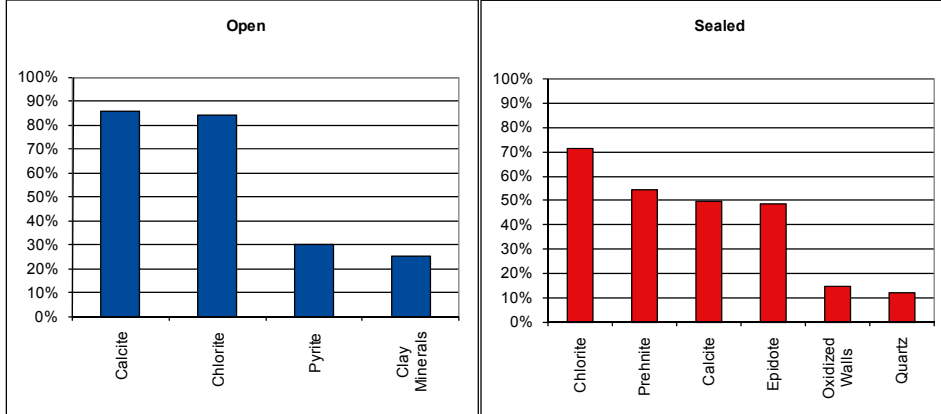
Frequency of open fractures: 4.5 m<sup>-1</sup>

Std dev: no data

Frequency of sealed fractures: 16.0 m<sup>-1</sup>

Std dev: no data

**Mineral coatings**



**Fault core:**

Percentage of fault core: 17 %

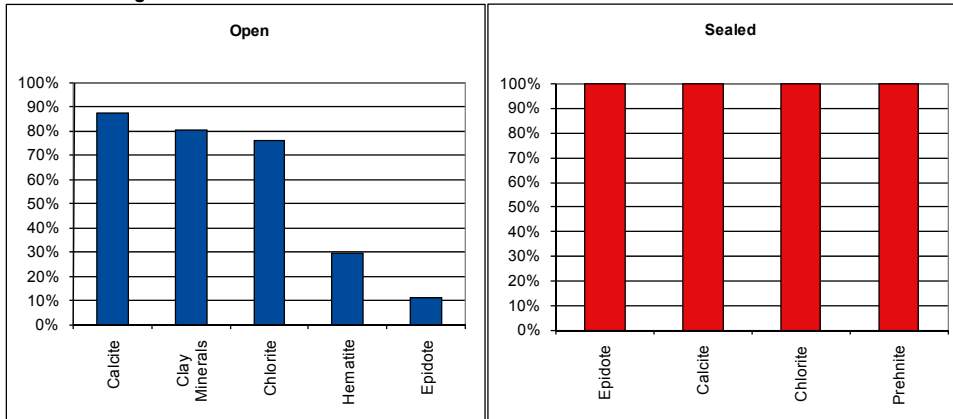
Frequency of open fractures: 24.5 m<sup>-1</sup>

Std dev: no data

Frequency of sealed fractures: 50.0 m<sup>-1</sup>

Std dev: no data

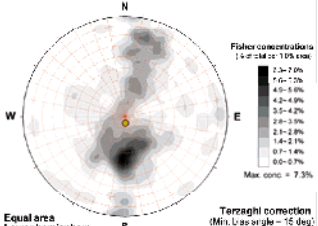
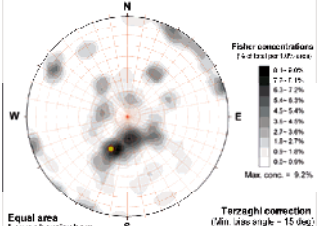
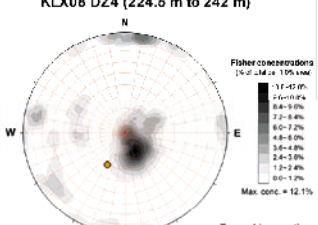
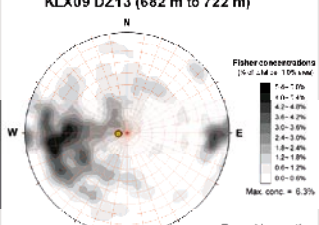
**Mineral coatings**



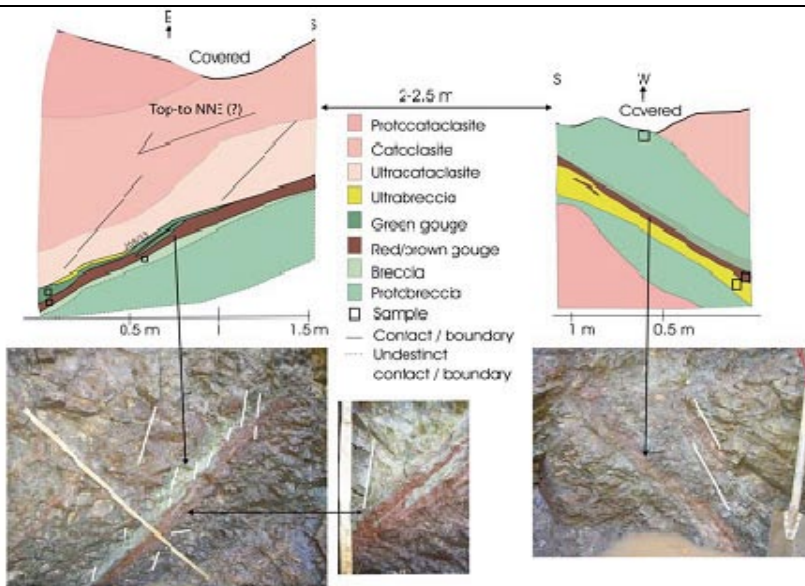
**E-W to NW-SE striking deformation zones, steep to moderately northward dipping**

<b>Deformation zone ZSMEW007A-C</b>	
<p><b>Borehole intersections (metres along borehole)</b></p> <p>HLX10: - m            HLX11: - m            HLX13: 29-103 m (ESHI DZ1 75-108m)            HLX14: - m            HLX21: 18-95 m (ESHI DZ1 18-24m)            HLX22: 0-163 m (ESHI DZ1 116-119m)            HLX23: 0-80 m (ESHI DZ1 47-54m; DZ2 62-67m; DZ3 77-82m)            HLX24: 0-150 m (ESHI DZ1 27-40m; DZ2 58-64m, DZ3 137-145m)            HLX25: 0-80 m (ESHI DZ1 47-52)            HLX30: 0-80 m (ESHI DZ1 10-42m; DZ2 66-74m)            HLX31: 50-100 m (ESHI DZ1 60-67m)            HLX33: 0-70 m (ESHI DZ1 12-28 m)            KLX01: 1000-1020 m (ESHI DZ1 1000-1020m)            KLX02: 180-200 m (no ESHI data)            KLX04: 310-385 m (ESHI DZ4 325-326m; DZ5 346-355m; DZ11 363.25-363.6m)            KLX07A: 105-147 m (ESHI DZ1 105-147m)            KLX07B: 124-172 m (ESHI DZ3 124-172m)            KLX08: 211-300 m (ESHI DZ3 211,5-220m; DZ4 224,5-242m; DZ5 291-302m)            KLX09: 682-722 m (ESHI DZ13 682-722m)</p>	
<p><b>Deformation style, alteration and geometry</b></p> <p><b>Deformation style:</b> brittle</p> <p><b>Alteration:</b> dominated by red staining, but also sections of epidotisation and saussuritisation,</p> <p><b>Strike/dip (right-hand-rule):</b> 281/44</p> <p><b>Trace length at ground surface:</b> 3.3 km</p> <p><b>Model thickness / model thickness span :</b> 80 m / 20-80 m</p> <p><b>Measured thickness (-400 to -600 m elevation):</b> no data</p> <p><b>Comment:</b></p>	
<b>Fractures in the deformation zone</b>	
<p style="text-align: center;"><b>KLX04 DZ5 (346 m to 355 m)</b></p> <p style="text-align: center;"><b>Elevation: -320.2 to -329.1 m (RHB 70)</b></p>	<p style="text-align: center;"><b>KLX07A DZ1 (105 m to 147 m)</b></p> <p style="text-align: center;"><b>Elevation: -67.4 to -99.3 m (RHB 70)</b></p>
<p style="text-align: center;"><b>Transmissivity (m<sup>2</sup>/s)</b></p> <p><b>General dip of PFL-features, elevation -400 to -600m:</b> no data</p> <p><b>Measured T (sum T(PFL-f)), elevation -400 to -600m:</b> no data</p> <p><b>Number of PFL-features, elevation -400 to -600m:</b> no data</p> <p><b>Model T, elevation -400 to -500m:</b> A: 1.08E-5, C: 4.23E-7</p> <p><b>Model T, elevation -500 to -600m:</b> A: 6.56E-6, C: 2.62E-7</p>	<p style="text-align: center;"><b>Transmissivity (m<sup>2</sup>/s)</b></p> <p><b>General dip of PFL-features, elevation -400 to -600m:</b> no data</p> <p><b>Measured T (sum T(PFL-f)), elevation -400 to -600m:</b> no data</p> <p><b>Number of PFL-features, elevation -400 to -600m:</b> no data</p> <p><b>Model T, elevation -400 to -500m:</b> A: 1.08E-5, C: 4.23E-7</p> <p><b>Model T, elevation -500 to -600m:</b> A: 6.56E-6, C: 2.62E-7</p>

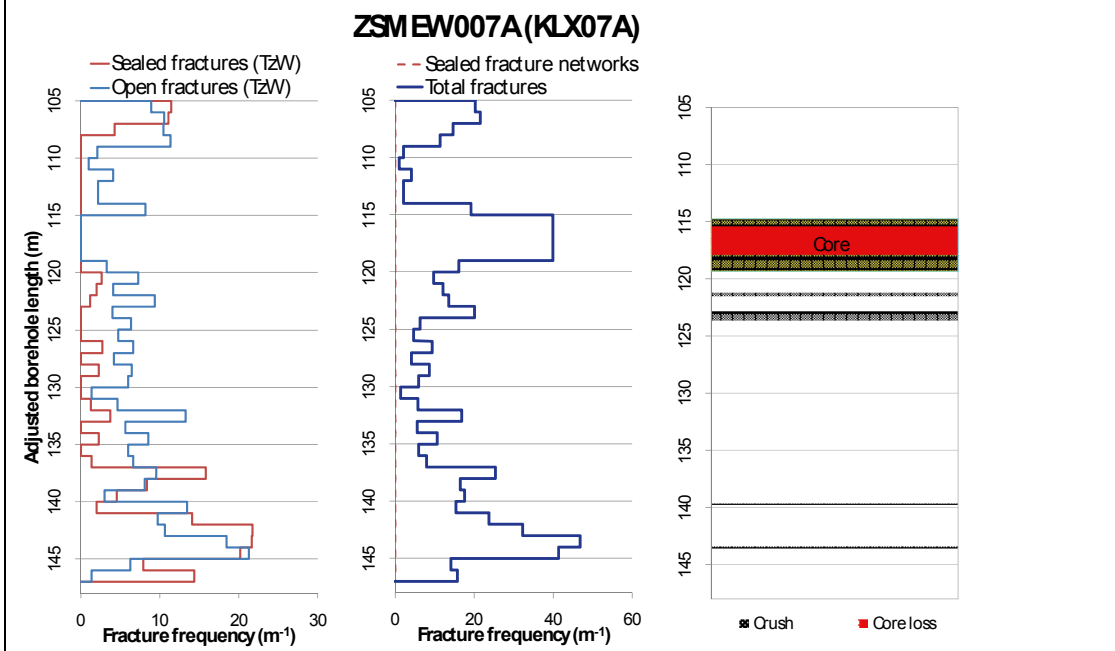
## Deformation zone ZSMEW007A-C

<p style="text-align: center;"><b>KLX07B DZ3 (124 m to 172 m)</b></p>  <p style="text-align: center;">Elevation: -105.2 to -153.0 m (RHB 70)</p>	<p style="text-align: center;"><b>KLX08 DZ3 (211.5 m to 220 m)</b></p>  <p style="text-align: center;">Elevation: -158.8 to -166.2 m (RHB 70)</p>
<p style="text-align: center;"><b>Transmissivity (m<sup>2</sup>/s)</b></p> <p>General dip of PFL-features, elevation -400 to -600m: no data</p> <p>Measured T (sum T(PFL-f)), elevation -400 to -600m: no data</p> <p>Number of PFL-features, elevation -400 to -600m: no data</p> <p>Model T, elevation -400 to -500m: A: 1.08E-5, C: 4.23E-7</p> <p>Model T, elevation -500 to -600m: A: 6.56E-6, C: 2.62E-7</p>	<p style="text-align: center;"><b>Transmissivity (m<sup>2</sup>/s)</b></p> <p>General dip of PFL-features, elevation -400 to -600m: no data</p> <p>Measured T (sum T(PFL-f)), elevation -400 to -600m: no data</p> <p>Number of PFL-features, elevation -400 to -600m: no data</p> <p>Model T, elevation -400 to -500m: A: 1.08E-5, C: 4.23E-7</p> <p>Model T, elevation -500 to -600m: A: 6.56E-6, C: 2.62E-7</p>
<p style="text-align: center;"><b>KLX08 DZ4 (224.5 m to 242 m)</b></p>  <p style="text-align: center;">Elevation: -170.1 to -185.3 m (RHB 70)</p>	<p style="text-align: center;"><b>KLX09 DZ13 (682 m to 722 m)</b></p>  <p style="text-align: center;">Elevation: -653.6 to -693.4 m (RHB 70)</p>
<p style="text-align: center;"><b>Transmissivity (m<sup>2</sup>/s)</b></p> <p>General dip of PFL-features, elevation -400 to -600m: no data</p> <p>Measured T (sum T(PFL-f)), elevation -400 to -600m: no data</p> <p>Number of PFL-features, elevation -400 to -600m: no data</p> <p>Model T, elevation -400 to -500m: A: 1.08E-5, C: 4.23E-7</p> <p>Model T, elevation -500 to -600m: A: 6.56E-6, C: 2.62E-7</p>	<p style="text-align: center;"><b>Transmissivity (m<sup>2</sup>/s)</b></p> <p>General dip of PFL-features, elevation -400 to -600m: no data</p> <p>Measured T (sum T(PFL-f)), elevation -400 to -600m: no data</p> <p>Number of PFL-features, elevation -400 to -600m: no data</p> <p>Model T, elevation -400 to -500m: A: 1.08E-5, C: 4.23E-7</p> <p>Model T, elevation -500 to -600m: A: 6.56E-6, C: 2.62E-7</p>

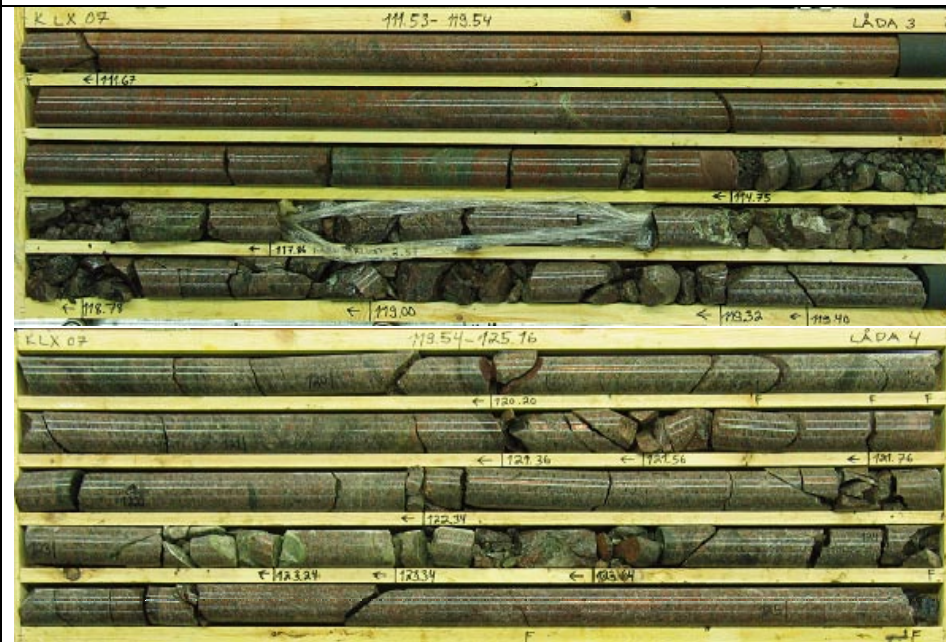
## Deformation zone ZSMEW007A-C



Sketch and photographs of trench walls with exposed fault rocks. As exposed in the trench located along profile LSM000280. /Viola and Ganerod, 2006/



## Deformation zone ZSMEW007A-C



**KLX07A 111,50-125 m borehole length. Part of DZ1 including core zone 114,75-119.40 m.**

### Engineering characteristics

**Transition part of zone:**

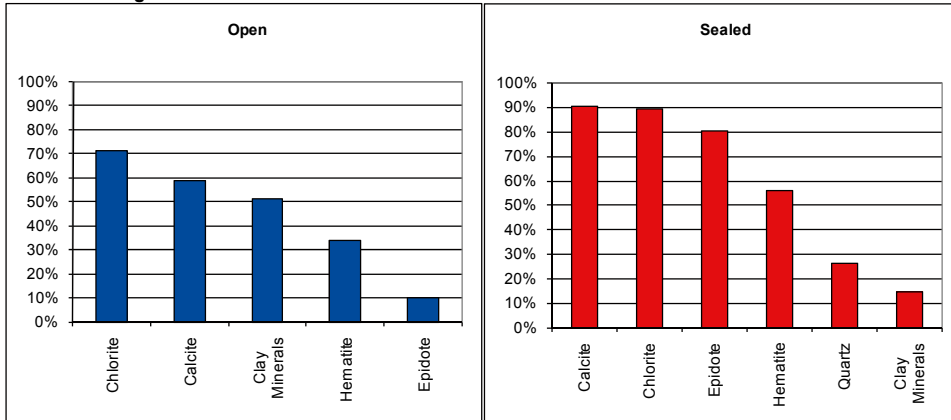
Frequency of open fractures:  $5.5 \text{ m}^{-1}$

Std dev: 1.0

Frequency of sealed fractures:  $32.5 \text{ m}^{-1}$

Std dev: 13.6

**Mineral coatings**





## Deformation zone ZSMEW007A-C

### Fault core:

Percentage of fault core: 10 %

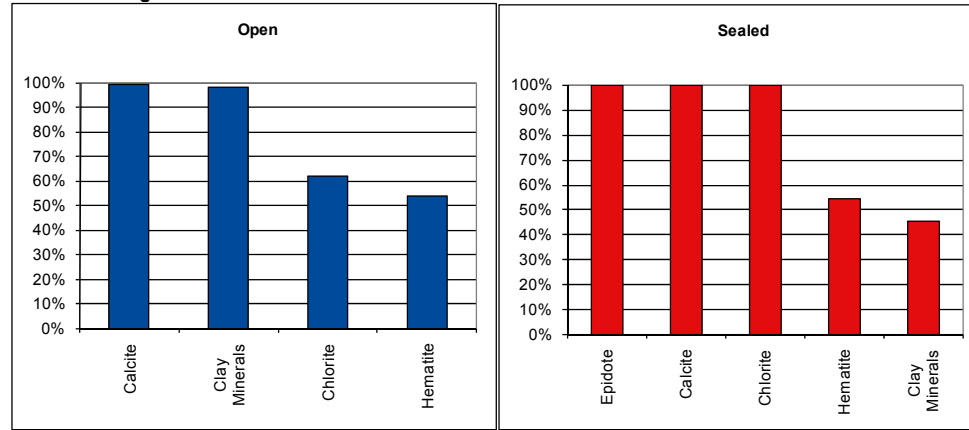
Frequency of open fractures: 40.0 m<sup>-1</sup>

Std dev: 1.0

Frequency of sealed fractures: 50.2 m<sup>-1</sup>

Std dev: 0.1

### Mineral coatings



## Deformation zone KLX07\_dz9

### Borehole intersections (metres along borehole)

KLX07A: 448-459 m (ESHI DZ9 448-459)

### Deformation style, alteration and geometry

**Deformation style:** brittle and ductile

**Alteration:** red staining

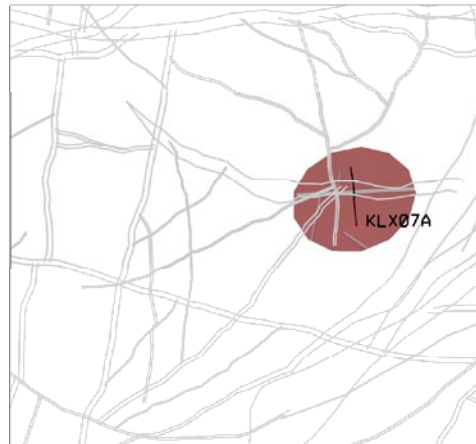
**Strike/dip (right-hand-rule):** 253/35

**Trace length at ground surface:** no data

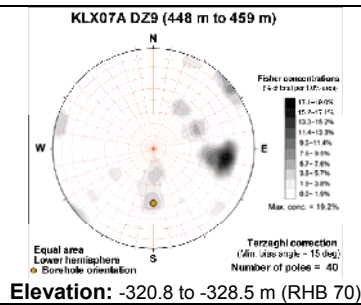
**Model thickness / model thickness span :** 10 m / no data

**Measured thickness (-400 to -600 m elevation):** no data

**Comment:** orientation is based on seismic reflector 'D' /Juhlin 2004/, generally supported by mylonite ca. 250/50; crush 270/45 and fracture orientation concentration. Towards the edge of the modelled geometry there is a theoretical intercept with KLX02 but no evidence of likely correlation.



## Fractures in the deformation zone



### Transmissivity ( $m^2/s$ )

**General dip of PFL-features, elevation -400 to -600m:** no data

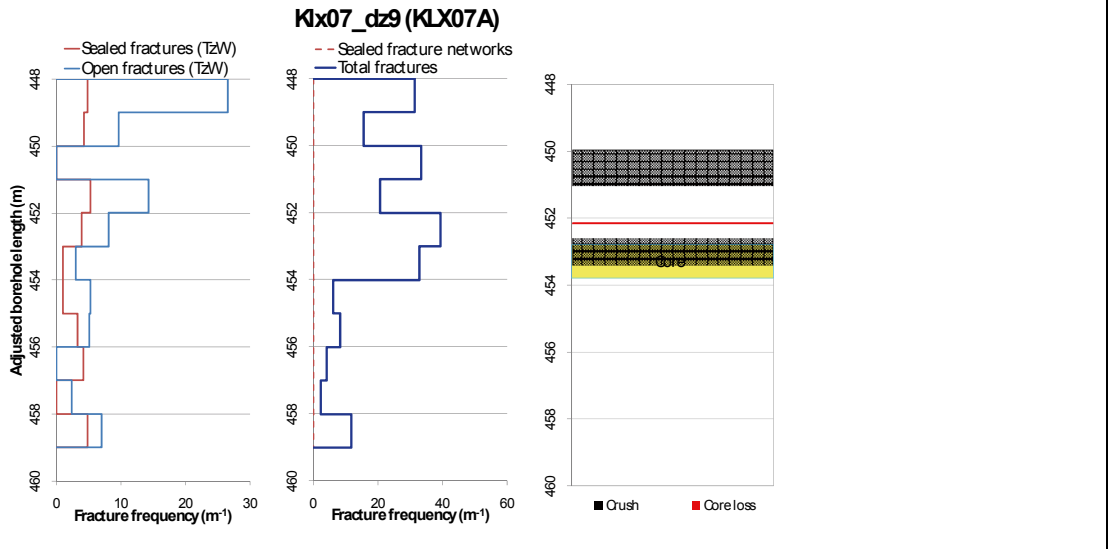
**Measured T (sum T(PFL-f)), elevation -400 to -600m:** no data

**Number of PFL-features, elevation -400 to -600m:** no data

**Model T, elevation -400 to -500m:** 2.26E-7

**Model T, elevation -500 to -600m:** 1.37E-7

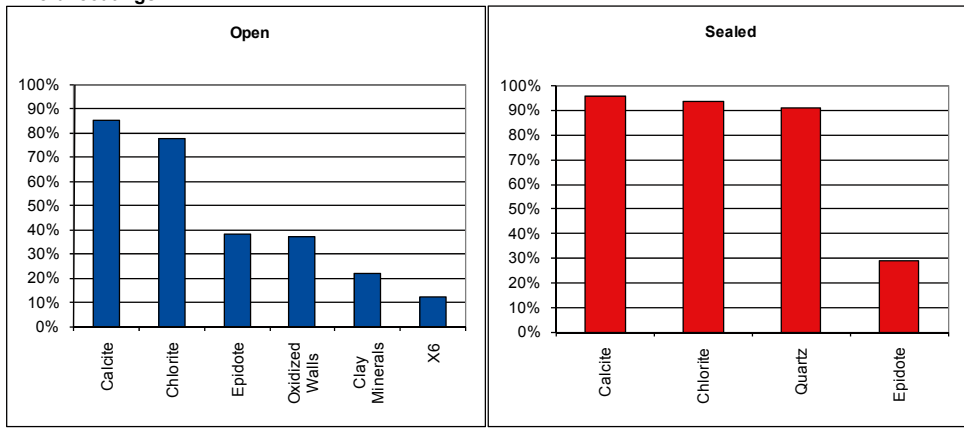
## Deformation zone KLX07\_dz9



KLX07 451.14- 456.93 m borehole length. Part of DZ9 including core zone 452.80-453.8 m.

### Engineering characteristics

**Transition part of zone:**  
 Frequency of open fractures: 10.4 m<sup>-1</sup>  
 Std dev: no data  
 Frequency of sealed fractures: 19.1 m<sup>-1</sup>  
 Std dev: no data  
**Mineral coatings**



## Deformation zone KLX07\_dz9

### **Fault core:**

Percentage of fault core: 9 %

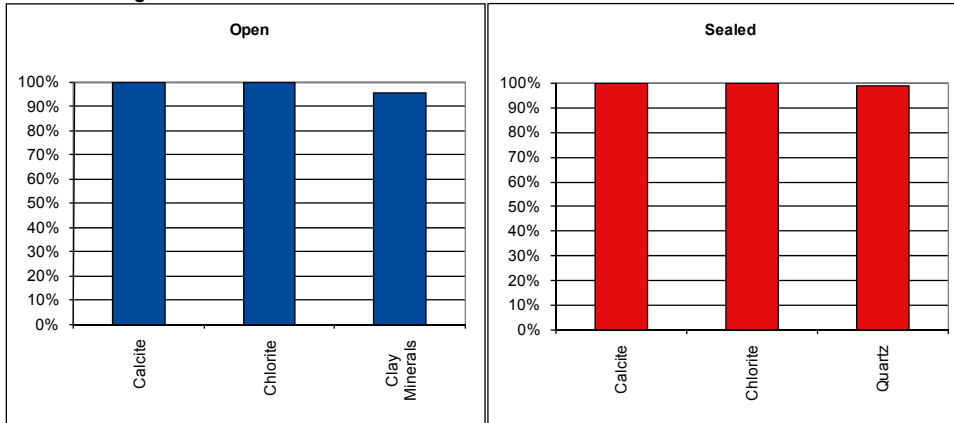
Frequency of open fractures: 45.0 m<sup>-1</sup>

Std dev: no data

Frequency of sealed fractures: 102.0 m<sup>-1</sup>

Std dev: no data

### **Mineral coatings**



## Deformation zone KLX07\_dz11

### Borehole intersections (metres along borehole)

KLX07A: 693-724 m (ESHI DZ11 693-724 m)

### Deformation style, alteration and geometry

**Deformation style:** brittle

**Alteration:** oxidation, chloritisation, epidotisation

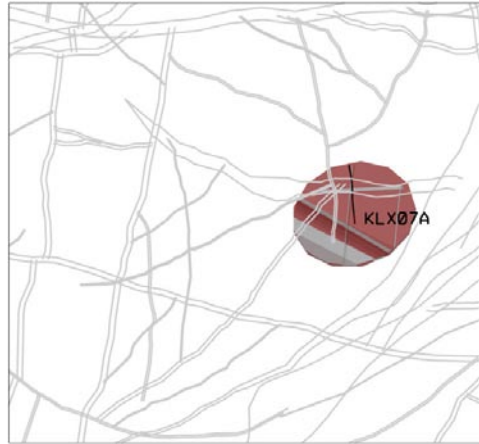
**Strike/dip (right-hand-rule):** 253/35

**Trace length at ground surface:** no data

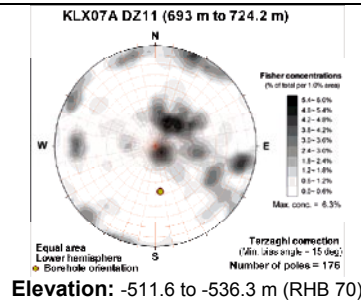
**Model thickness / model thickness span :** 30 m / no data

**Measured thickness (-400 to -600 m elevation):** 30 m

**Comment:**



## Fractures in the deformation zone



## Transmissivity (m<sup>2</sup>/s)

**General dip of PFL-features, elevation -400 to -600m:** Moderately to sub-horizontally and steep

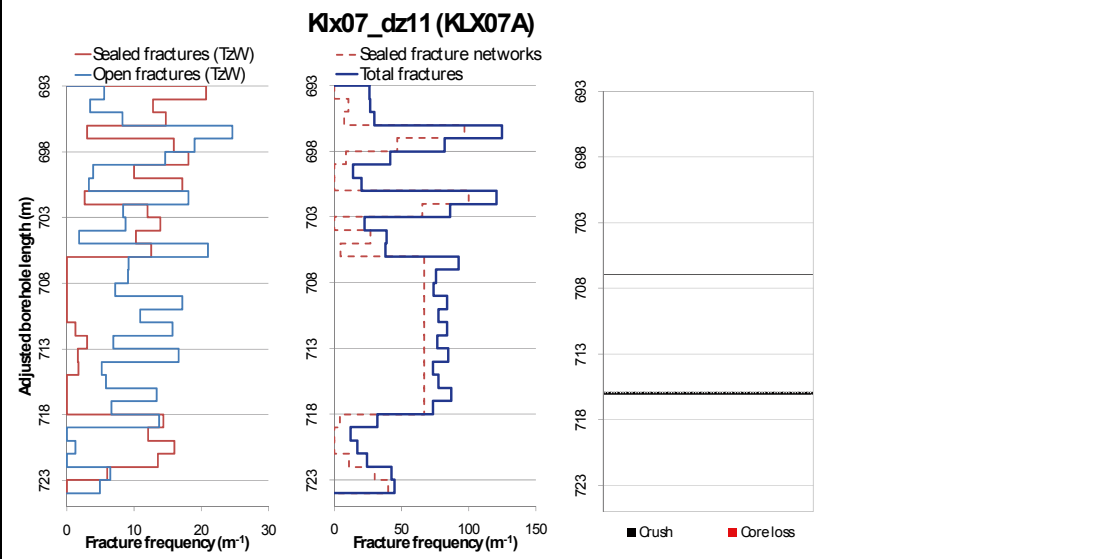
**Measured T (sum T(PFL-f)), elevation -400 to -600m:** 7.06E-7

**Number of PFL-features, elevation -400 to -600m:** 8

**Model T, elevation -400 to -500m:** 2.26E-7

**Model T, elevation -500 to -600m:** 1.37E-7

## Deformation zone KLX07\_dz11



**KLX07A 702.82-713.53 m borehole length. Part of DZ11 (no defined core zone)**

## Deformation zone KLX07\_dz11

### Engineering characteristics

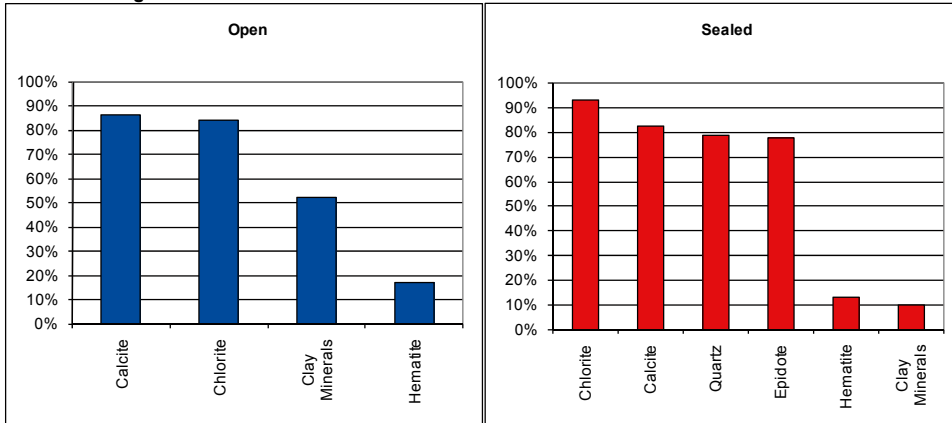
Frequency of open fractures:  $6.2 \text{ m}^{-1}$

Std dev: no data

Frequency of sealed fractures:  $44.7 \text{ m}^{-1}$

Std dev: no data

### Mineral coatings



## Deformation zone KLX07\_dz12

### Borehole intersections (metres along borehole)

KLX07A: 738-785 m (ESHI DZ12 738-785 m)

### Deformation style, alteration and geometry

**Deformation style:** brittle

**Alteration:** red staining, epidotisation

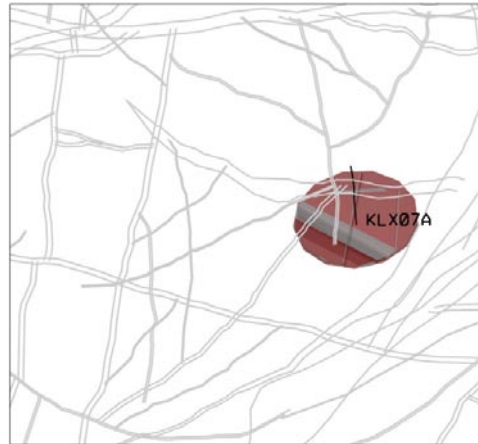
**Strike/dip (right-hand-rule):** 263/41

**Trace length at ground surface:** no data

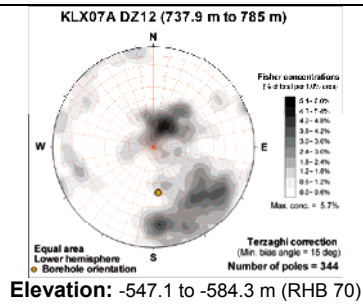
**Model thickness / model thickness span :** 47 m / no data

**Measured thickness (-400 to -600 m elevation):** 47 m

**Comment:**



## Fractures in the deformation zone



## Transmissivity ( $m^2/s$ )

**General dip of PFL-features, elevation -400 to -600m:** moderately to sub-horizontally and steep

**Measured T (sum T(PFL-f)), elevation -400 to -600m:**  $9.47E-6$

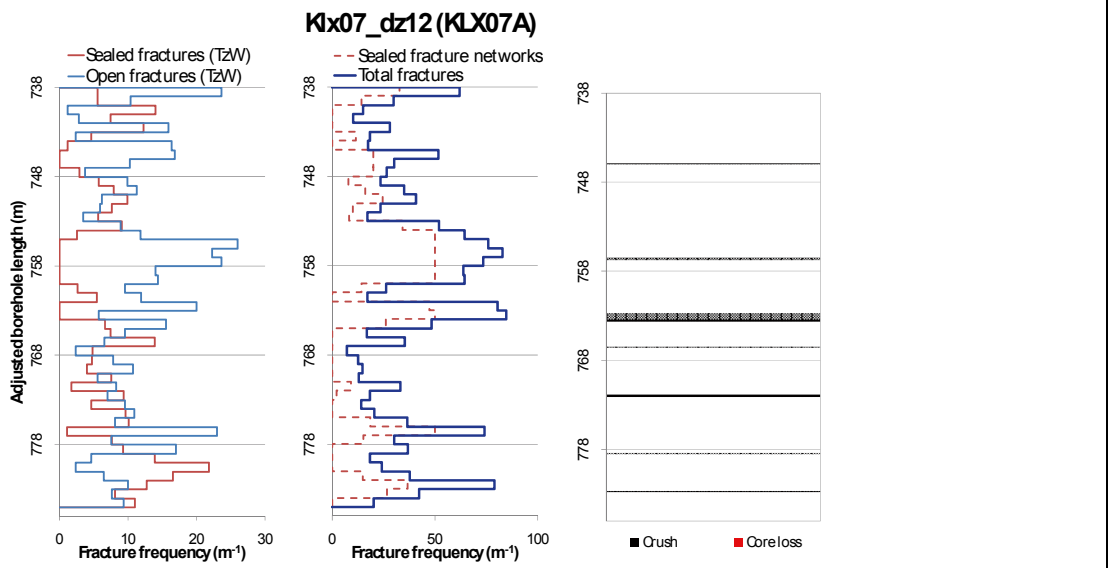
**Number of PFL-features, elevation -400 to -600m:** 21

**Model T, elevation -400 to -500m:**  $2.26E-7$

**Model T, elevation -500 to -600m:**  $1.37E-7$



## Deformation zone KLX07\_dz12



**KLX07A 745.89-756.90 borehole length. Part of DZ12, no defined core zone.**

## Deformation zone KLX07\_dz12

### Engineering characteristics

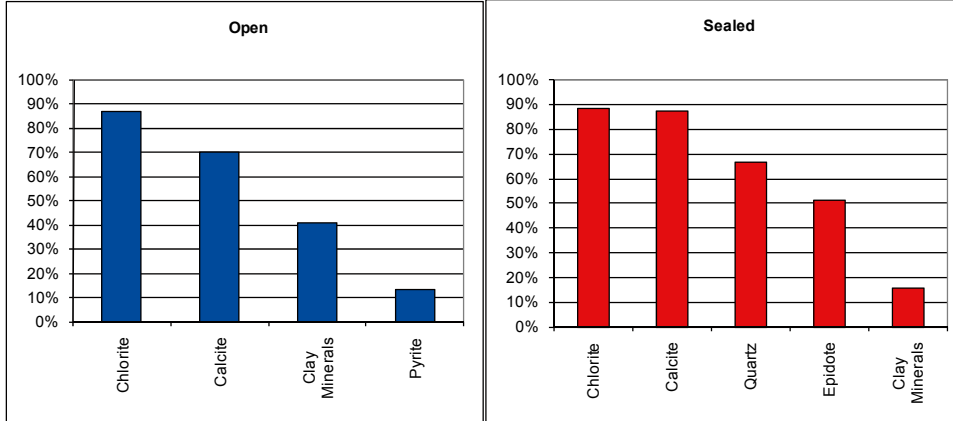
Frequency of open fractures:  $10.2 \text{ m}^{-1}$

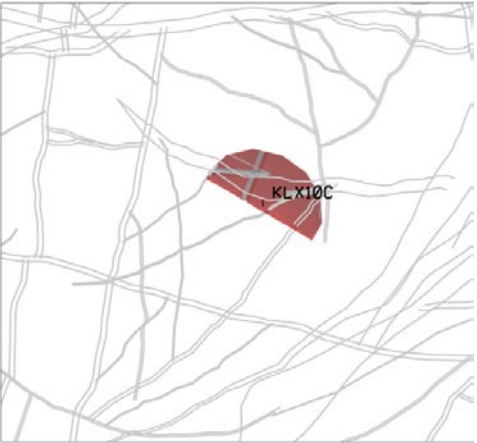
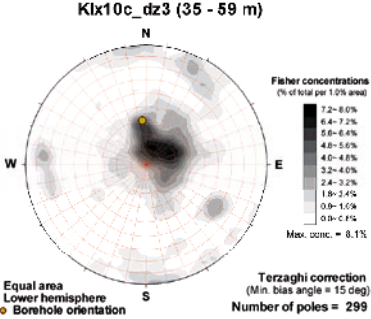
Std dev: no data

Frequency of sealed fractures:  $21.4 \text{ m}^{-1}$

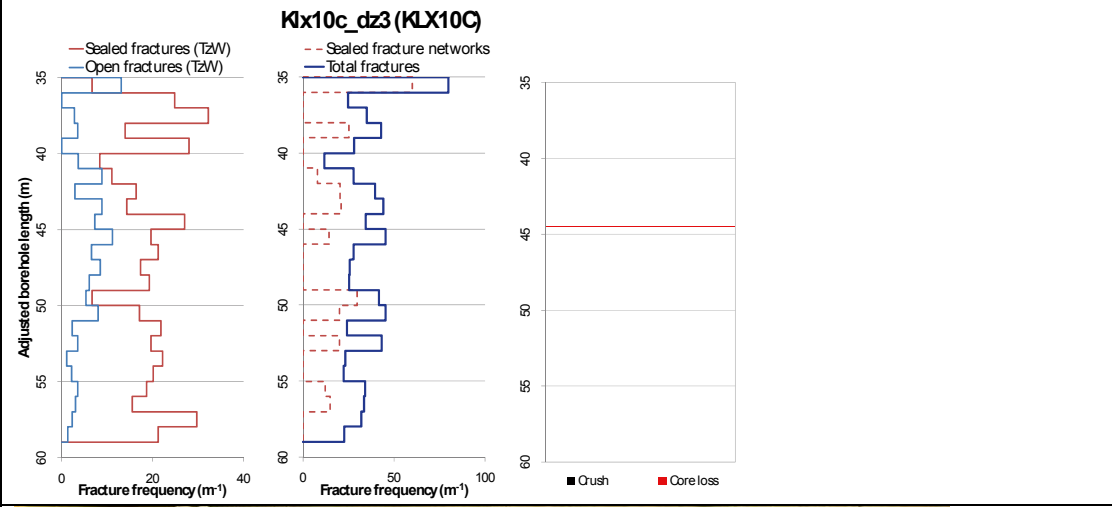
Std dev: no data

#### Mineral coatings



<b>Deformation zone KLX10C_dz3</b>	
<p><b>Borehole intersections (metres along borehole)</b></p> <p>KLX10C: 35-59 m (ESHI DZ3 35-59 m)</p>	
<p><b>Deformation style, alteration and geometry</b></p> <p><b>Deformation style:</b> brittle and ductile</p> <p><b>Alteration:</b> red staining, epidotisation, saussuritisation.</p> <p><b>Strike/dip (right-hand-rule):</b> 300/35</p> <p><b>Trace length at ground surface:</b> no data</p> <p><b>Model thickness / model thickness span :</b> 10 m / no data</p> <p><b>Measured thickness (-400 to -600 m elevation):</b> no data</p> <p><b>Comment:</b> orientation is based on ductile-brittle zones mapped in the drill core. The modelled geometry generates theoretical intercepts in KLX10, KLX10B, HLX31 and HLX33. KLX10 and KLX10B were not cored at this position. HLX31 and HLX33 lack clear correlation but it should be noted both holes lie in the complex ZSMEW007A belt.</p>	
<b>Fractures in the deformation zone</b>	
<p>Klx10c_dz3 (35 - 59 m)</p>  <p><b>Elevation:</b> -13.3 to -34.3 m (RHB 70)</p>	
<b>Transmissivity (m<sup>2</sup>/s)</b>	
<p><b>General dip of PFL-features, elevation -400 to -600m:</b> no data</p> <p><b>Measured T (sum T(PFL-f)), elevation -400 to -600m:</b> no data</p> <p><b>Number of PFL-features, elevation -400 to -600m:</b> no data</p> <p><b>Model T, elevation -400 to -500m:</b> 2.26E-7</p> <p><b>Model T, elevation -500 to -600m:</b> 1.37E-7</p>	

## Deformation zone KLX10C\_dz3



**KLX10C 39.17-50.46 m borehole length. Part of DZ3**

## Deformation zone KLX10C\_dz3

### Engineering characteristics

#### Transition part of zone:

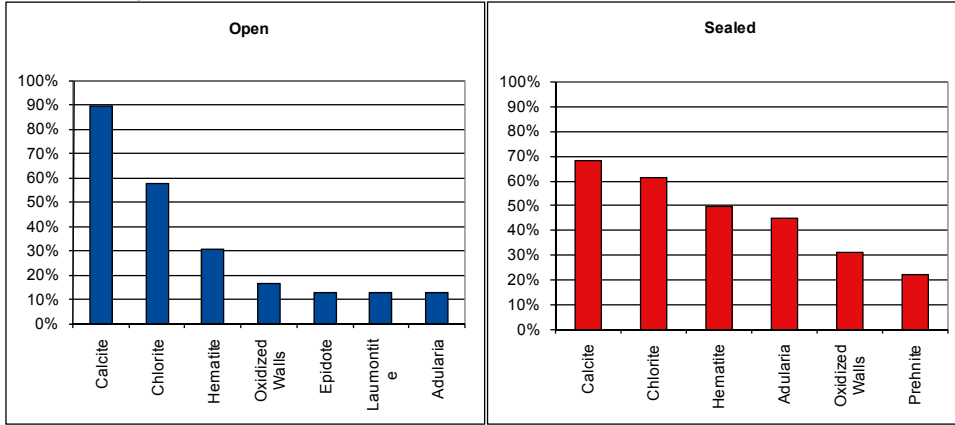
Frequency of open fractures:  $3.3 \text{ m}^{-1}$

Std dev: no data

Frequency of sealed fractures:  $23.0 \text{ m}^{-1}$

Std dev: no data

#### Mineral coatings



## Deformation zone KLX10C\_dz7

### Borehole intersections (metres along borehole)

KLX10C: 121-140 m (ESHI DZ7 121-140 m)

### Deformation style, alteration and geometry

**Deformation style:** brittle and ductile

**Alteration:** red staining

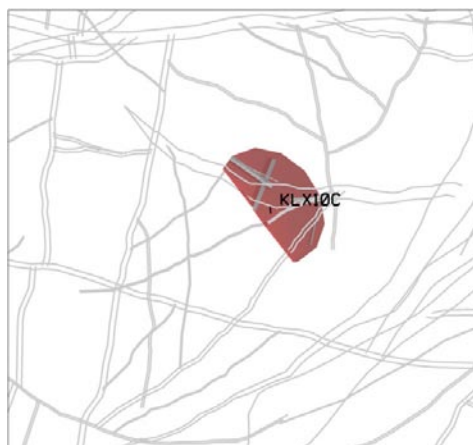
**Strike/dip (right-hand-rule):** 323/39

**Trace length at ground surface:** no data

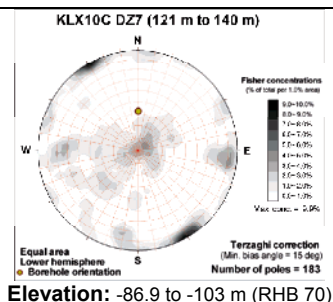
**Model thickness / model thickness span :** 10 m / no data

**Measured thickness (-400 to -600 m elevation):** no data

**Comment:** orientation is based on mapped brittle- ductile indicators in the drill core. The modelled geometry results in theoretical intercepts in KLX10 and HLX31. KLX10 is not cored in this position. No clear correlation with HLX31 has been identified. However, the HLX31 intercept is towards the edge of the modelled zone geometry and this hole lies within the complex ZSMEW007A zone belt.



## Fractures in the deformation zone



### Transmissivity ( $m^2/s$ )

**General dip of PFL-features, elevation -400 to -600m:** no data

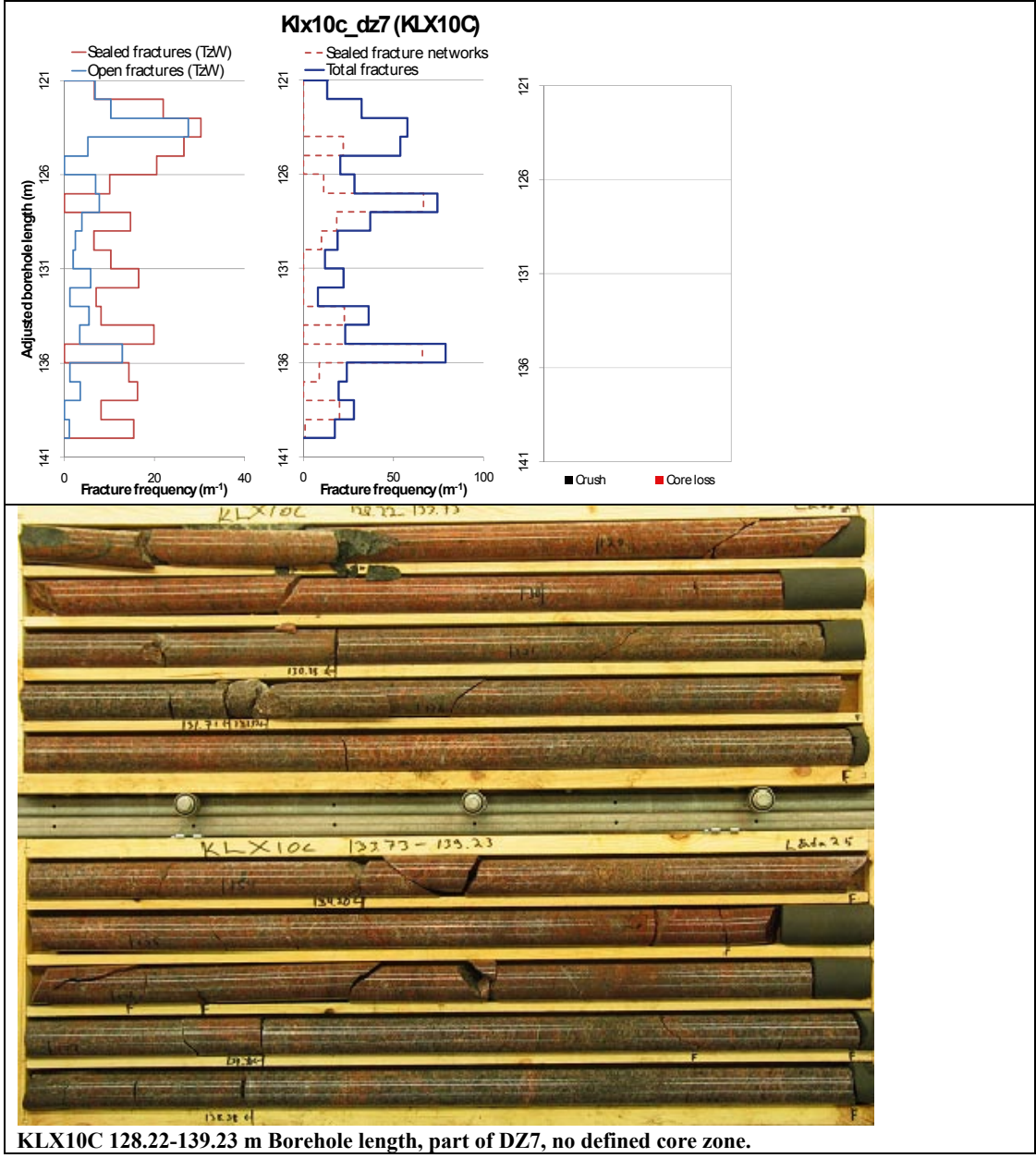
**Measured T (sum T(PFL-f)), elevation -400 to -600m:** no data

**Number of PFL-features, elevation -400 to -600m:** no data

**Model T, elevation -400 to -500m:** 2.26E-7

**Model T, elevation -500 to -600m:** 1.37E-7

## Deformation zone KLX10C\_dz7



## Deformation zone KLX10C\_dz7

### Engineering characteristics

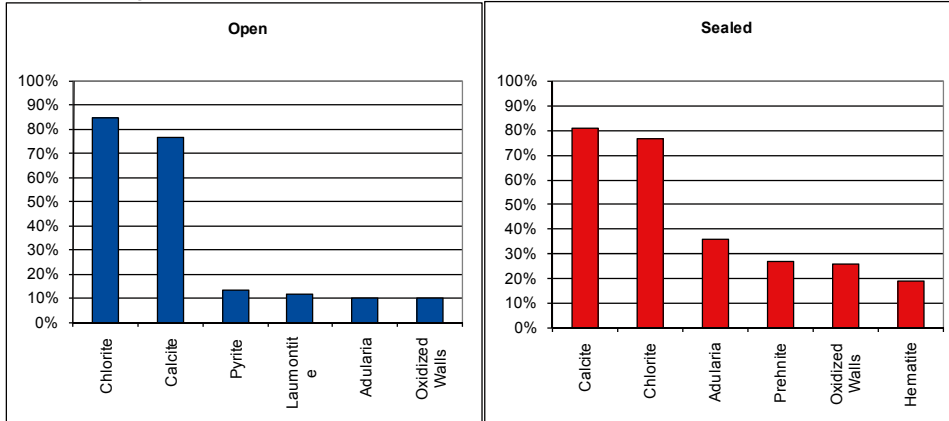
Frequency of open fractures:  $3.2 \text{ m}^{-1}$

Std dev: no data

Frequency of sealed fractures:  $20.6 \text{ m}^{-1}$


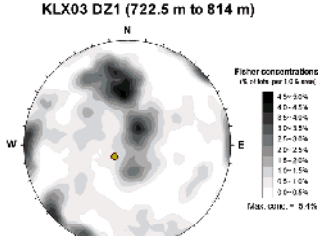
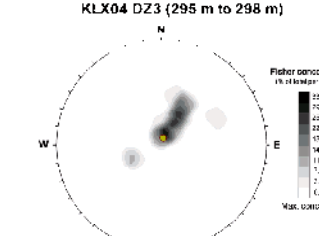
Std dev: no data

#### Mineral coatings

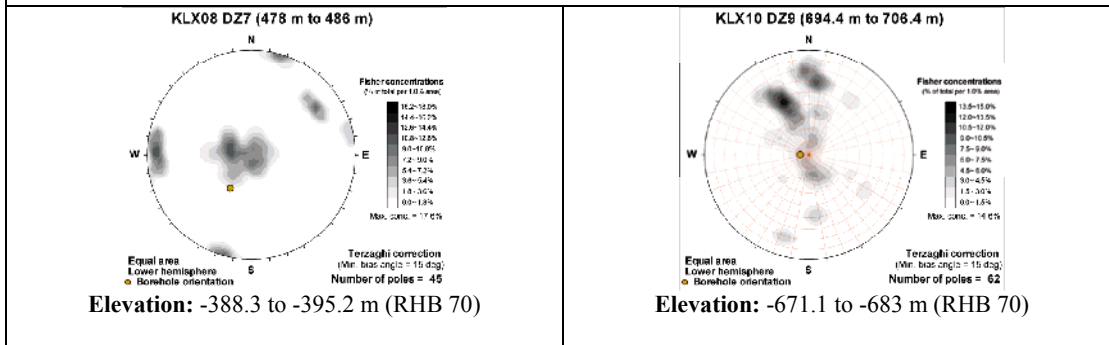




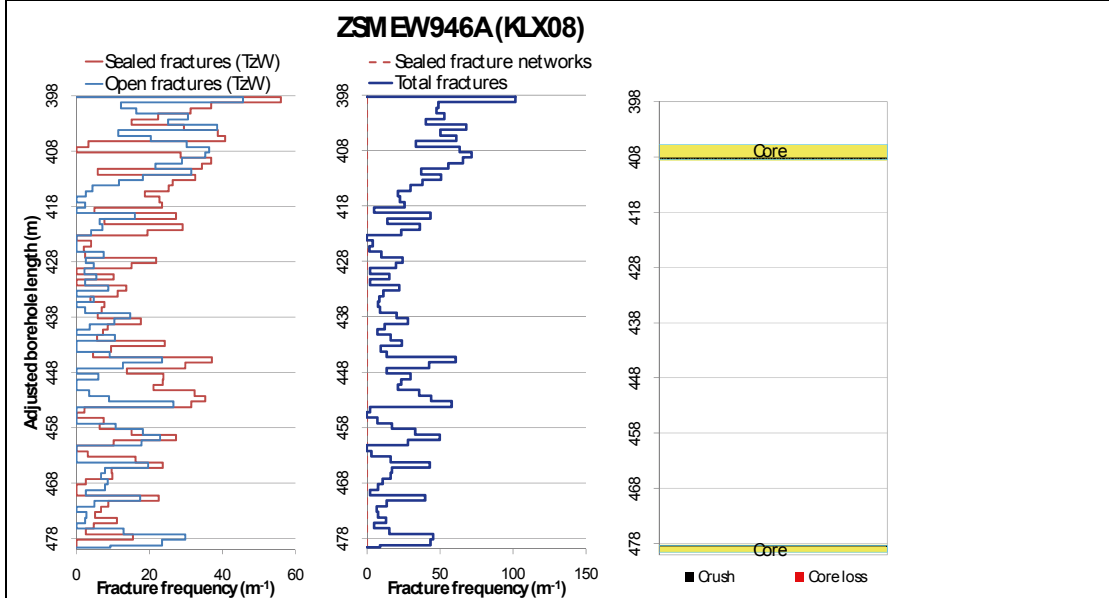
## Gently dipping deformation zones

<b>Deformation zone ZSMEW946A</b>	
<p><b>Borehole intersections (metres along borehole)</b></p> <p>KLX03: 723-743 m (ESHI DZ1, 722.5-814m)            KLX04: 295-298 m (ESHI DZ3 295-298 m). <i>Other potential members of the M1 series are ESHI DZ2 254-258m and ESHI DZ4 325-326m)</i>            KLX08: 478-486 m (ESHI DZ7 478-486m). <i>Other potential members of the M1 series: ESHI DZ6 396-416m)</i>            KLX10: 698-705 m (ESHI DZ 9 690m to 706m)            KLX18: 580 m  <i>Other potential members of the M1 series are KLX11 DZ11: 486-513m and DZ13: 577.90-586.16 m)</i></p>	
<p><b>Deformation style, alteration and geometry</b></p> <p><b>Deformation style:</b> ductile and brittle</p> <p><b>Alteration:</b> red staining and saussuritisation</p> <p><b>Strike/dip (right-hand-rule):</b> 080/23</p> <p><b>Trace length at ground surface:</b> no data</p> <p><b>Model thickness / model thickness span :</b> 10 m / 5-20 m</p> <p><b>Measured thickness (-400 to -600 m elevation):</b></p> <p><b>Comment:</b> ZSMEW946A marks the upper boundary of a much thicker sequence of similarly oriented MDZs and mafic intrusions. The fracture information given here can be taken to be typical of structures in this series.</p>	
<b>Fractures in the deformation zone</b>	
<p style="text-align: center;"><b>KLX03 DZ1 (722.5 m to 814 m)</b></p>  <p style="text-align: center;">(Borehole length KLX03 723-743 m)  <b>Elevation: -682.3 to -701.8 m (RHB 70)</b></p>	<p style="text-align: center;"><b>KLX04 DZ3 (295 m to 298 m)</b></p>  <p style="text-align: center;"><b>Elevation: -269.4 to -272.4 m (RHB 70)</b></p>
<p style="text-align: center;"><b>Transmissivity (m<sup>2</sup>/s)</b></p> <p><b>General dip of PFL-features, elevation -400 to -600m:</b> no data</p> <p><b>Measured T (sum T(PFL-f)), elevation -400 to -600m:</b> no data</p> <p><b>Number of PFL-features, elevation -400 to -600m:</b> no data</p> <p><b>Model T, elevation -400 to -500m:</b> 1.51E-7</p> <p><b>Model T, elevation -500 to -600m:</b> 5.20E-8</p>	<p style="text-align: center;"><b>Transmissivity (m<sup>2</sup>/s)</b></p> <p><b>General dip of PFL-features, elevation -400 to -600m:</b> no data</p> <p><b>Measured T (sum T(PFL-f)), elevation -400 to -600m:</b> no data</p> <p><b>Number of PFL-features, elevation -400 to -600m:</b> no data</p> <p><b>Model T, elevation -400 to -500m:</b> 1.51E-7</p> <p><b>Model T, elevation -500 to -600m:</b> 5.20E-8</p>

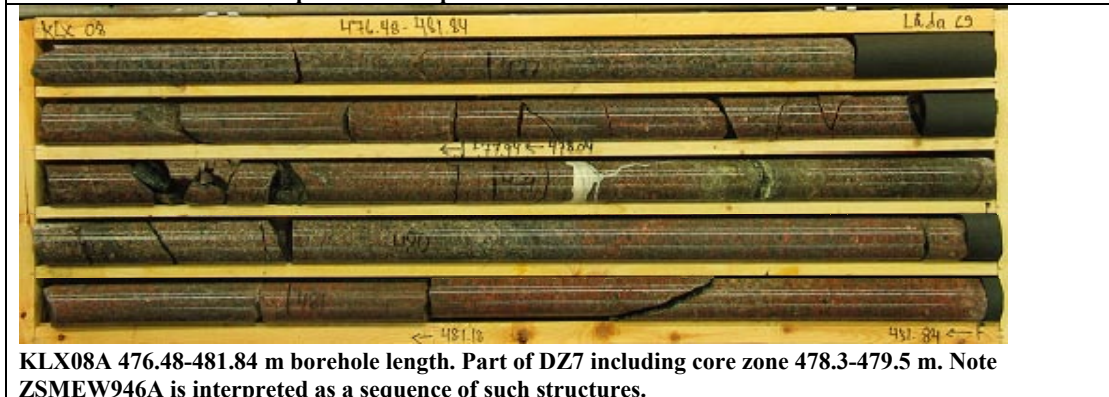
## Deformation zone ZSMEW946A



<p style="text-align: center;"><b>Transmissivity (m<sup>2</sup>/s)</b></p> <p>General dip of PFL-features, elevation -400 to -600m: no data</p> <p>Measured T (sum T(PFL-f)), elevation -400 to -600m: no data</p> <p>Number of PFL-features, elevation -400 to -600m: no data</p> <p>Model T, elevation -400 to -500m: 1.51E-7</p> <p>Model T, elevation -500 to -600m: 5.20E-8</p>	<p style="text-align: center;"><b>Transmissivity (m<sup>2</sup>/s)</b></p> <p>General dip of PFL-features, elevation -400 to -600m: no data</p> <p>Measured T (sum T(PFL-f)), elevation -400 to -600m: no data</p> <p>Number of PFL-features, elevation -400 to -600m: no data</p> <p>Model T, elevation -400 to -500m: 1.51E-7</p> <p>Model T, elevation -500 to -600m: 5.20E-8</p>
--	--



Note ZSMEW946A is interpreted as a sequence of such structures.



## Deformation zone ZSMEW946A

### Engineering characteristics

**Transition part of zone:**

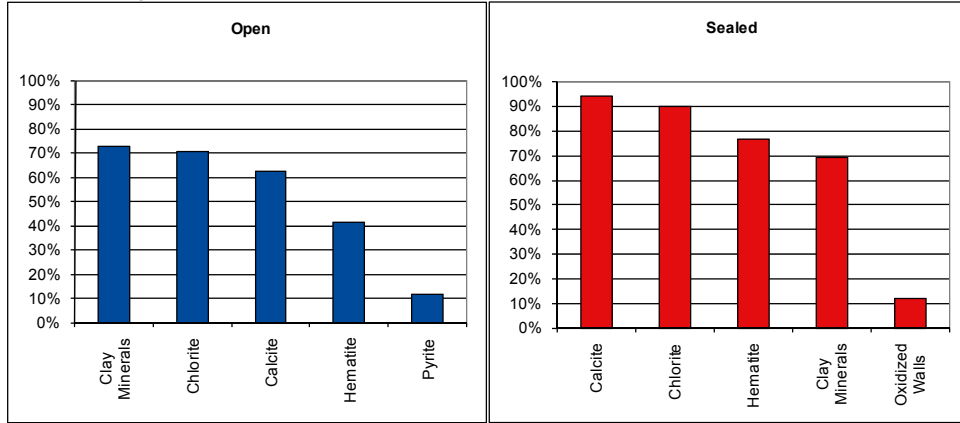
Frequency of open fractures: 9.1 m<sup>-1</sup>

Std dev: 4.3

Frequency of sealed fractures: 41.7 m<sup>-1</sup>

Std dev: 51.9

**Mineral coatings**



**Fault core:**

Percentage of fault core: 29 %

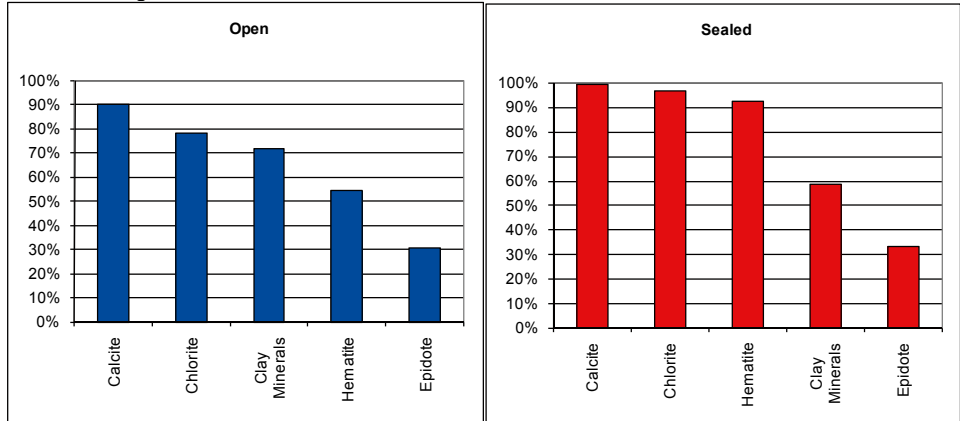
Frequency of open fractures: 19.5 m<sup>-1</sup>

Std dev: 17.2

Frequency of sealed fractures: 46.5 m<sup>-1</sup>

Std dev: 31.4

**Mineral coatings**



## Deformation zone KLX03\_dz1b

### Borehole intersections (metres along borehole)

KLX03: 759-777 m (a part of ESHI DZ1 722-814 m)

### Deformation style, alteration and geometry

**Deformation style:** brittle

**Alteration:** epidotisation

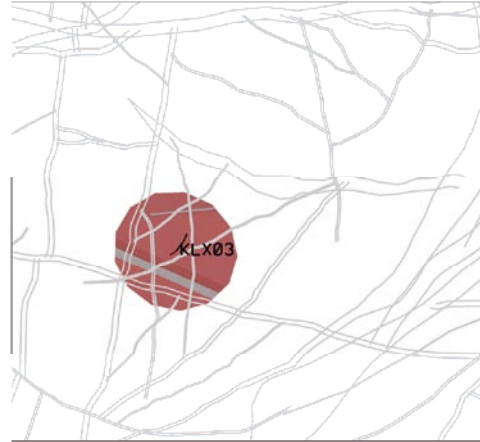
**Strike/dip (right-hand-rule):** 121/20

**Trace length at ground surface:** no data

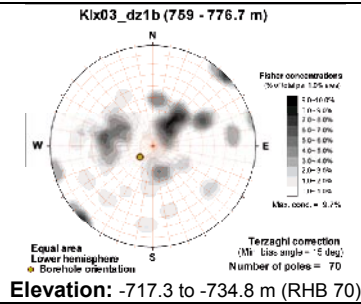
**Model thickness / model thickness span :** 10 m / no data

**Measured thickness (-400 to -600 m elevation):** no data

**Comment:**



## Fractures in the deformation zone



## Transmissivity (m<sup>2</sup>/s)

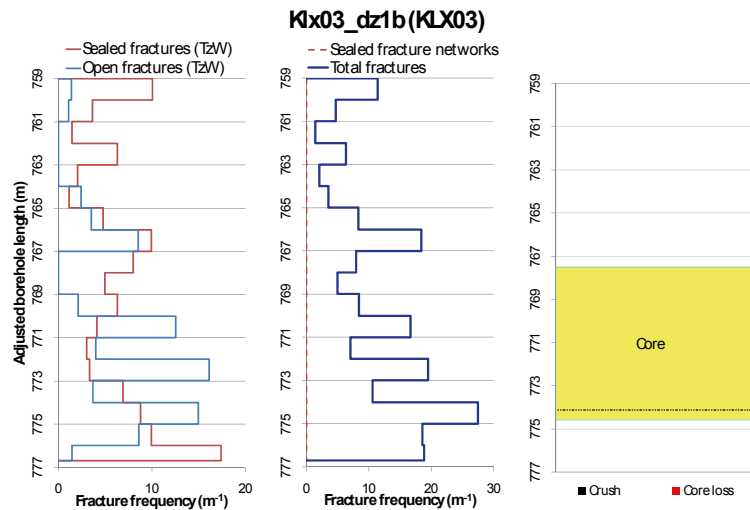
**General dip of PFL-features, elevation -400 to -600m:** no data

**Measured T (sum T(PFL-f)), elevation -400 to -600m:** no data

**Number of PFL-features, elevation -400 to -600m:** no data

**Model T, elevation -400 to -500m:** 2.26E-7

**Model T, elevation -500 to -600m:** 1.37E-7



## Deformation zone KLX03\_dz1b



KLX03A 769.39-774.83 m borehole length. Part of DZ1b including part of core zone 767.50-774.60 m.

### Engineering characteristics

**Transition part of zone:**

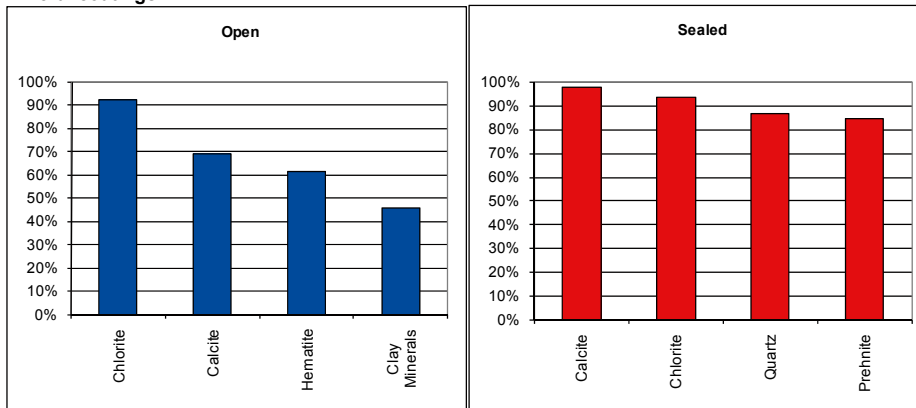
Frequency of open fractures: 2.5 m<sup>-1</sup>

Std dev: no data

Frequency of sealed fractures: 34.7 m<sup>-1</sup>

Std dev: no data

**Mineral coatings**



**Fault core:**

Percentage of fault core: 40 %

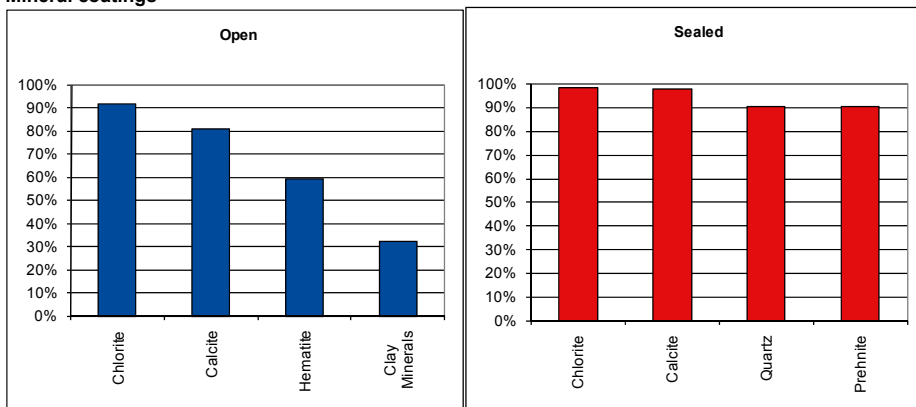
Frequency of open fractures: 5.2 m<sup>-1</sup>

Std dev: no data

Frequency of sealed fractures: 36.9 m<sup>-1</sup>

Std dev: no data

**Mineral coatings**



## Deformation zone KLX03\_dz1c

### Borehole intersections (metres along borehole)

KLX03: 789-801 m (a part of ESHI DZ1 722-814 m)

### Deformation style, alteration and geometry

**Deformation style:** brittle and ductile

**Alteration:** red staining and saussuritisation

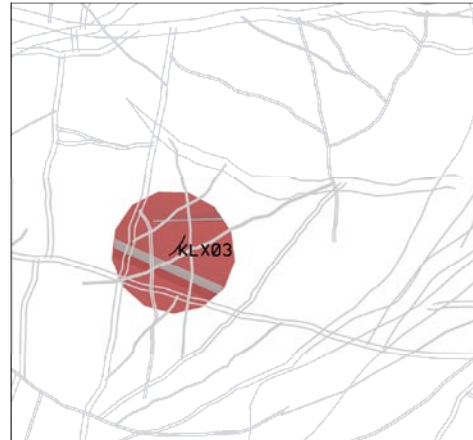
**Strike/dip (right-hand-rule):** 125/13

**Trace length at ground surface:** no data

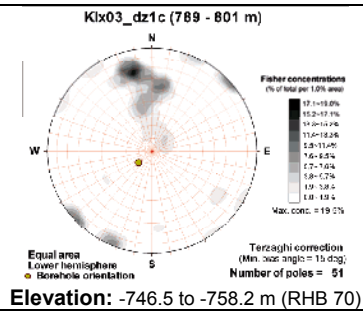
**Model thickness / model thickness span :** 10 m /no data

**Measured thickness (-400 to -600 m elevation):** no data

**Comment:**



## Fractures in the deformation zone



### Transmissivity ( $m^2/s$ )

**General dip of PFL-features, elevation -400 to -600m:** no data

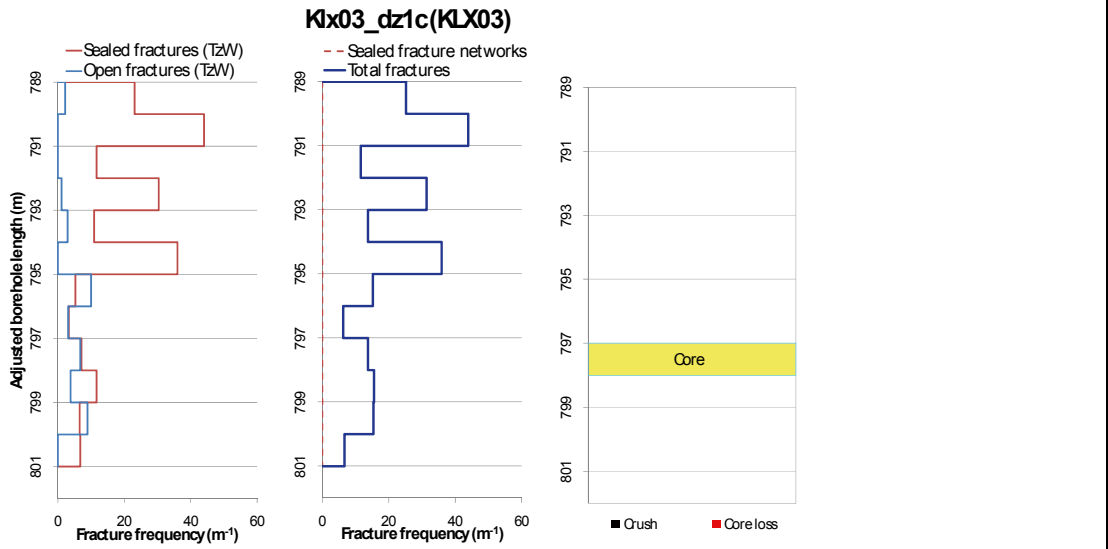
**Measured T (sum T(PFL-f)), elevation -400 to -600m:** no data

**Number of PFL-features, elevation -400 to -600m:** no data

**Model T, elevation -400 to -500m:** 2.26E-7

**Model T, elevation -500 to -600m:** 1.37E-7

## Deformation zone KLX03\_dz1c



**KLX03A 796.6-801.9 m borehole length. Part of DZ1c, including core zone 797-798 m.**

### Engineering characteristics

**Transition part of zone:**

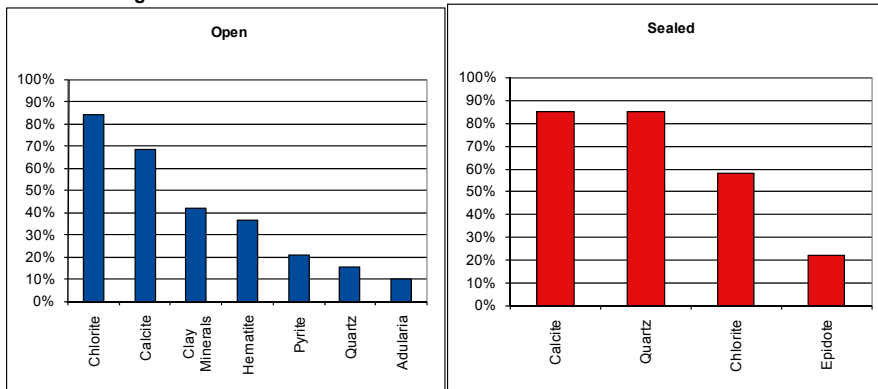
Frequency of open fractures: 1.7 m<sup>-1</sup>

Std dev: no data

Frequency of sealed fractures: 27.3

Std dev: no data

**Mineral coatings**



## Deformation zone KLX03\_dz1c

### **Fault core:**

Percentage of fault core: 8 %

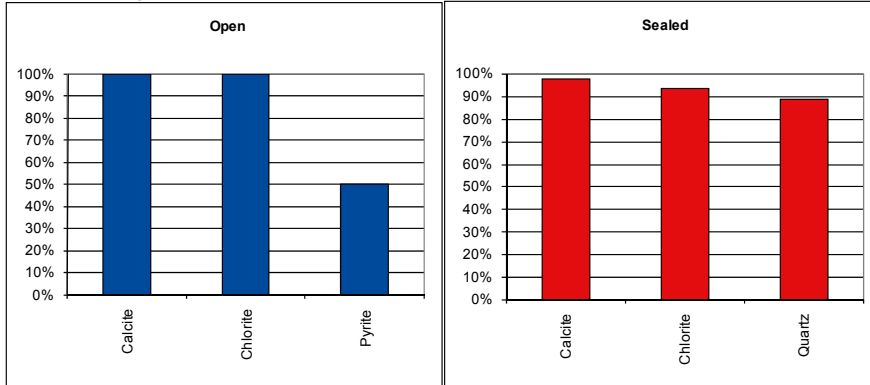
Frequency of open fractures: 4 m<sup>-1</sup>

Std dev: no data

Frequency of sealed fractures: 46 m<sup>-1</sup>

Std dev: no data

### **Mineral coatings**





## Deformation zone KLX07\_dz10

### Borehole intersections (metres along borehole)

KLX07A: 645-655 m (part of ESHI DZ10 604-655 m)

### Deformation style, alteration and geometry

**Deformation style:** brittle and ductile

**Alteration:** red staining

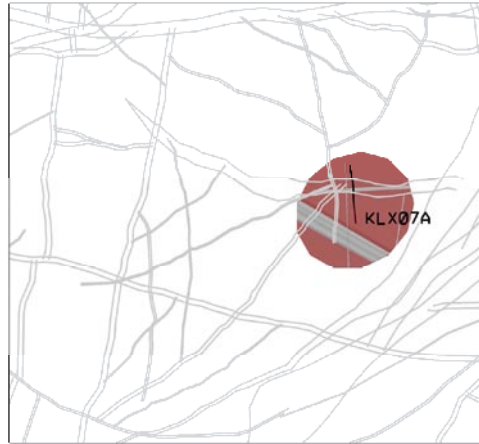
**Strike/dip (right-hand-rule):** 225/28

**Trace length at ground surface:** no data

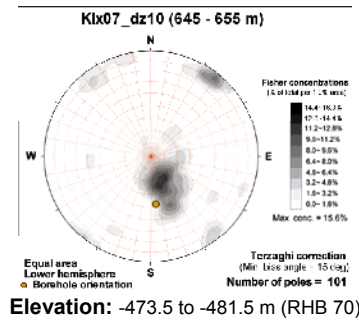
**Model thickness / model thickness span :** 10 m / no data

**Measured thickness (-400 to -600 m elevation):** 10 m

**Comment:** The modelled extent results in intersections at the very outer limits with KLX02 and KLX21B. Neither borehole shows correlation and can superficially be taken to confirm the general limits of the zone.



## Fractures in the deformation zone



## Transmissivity (m<sup>2</sup>/s)

**General dip of PFL-features, elevation -400 to -600m:** Moderately to sub-horizontally

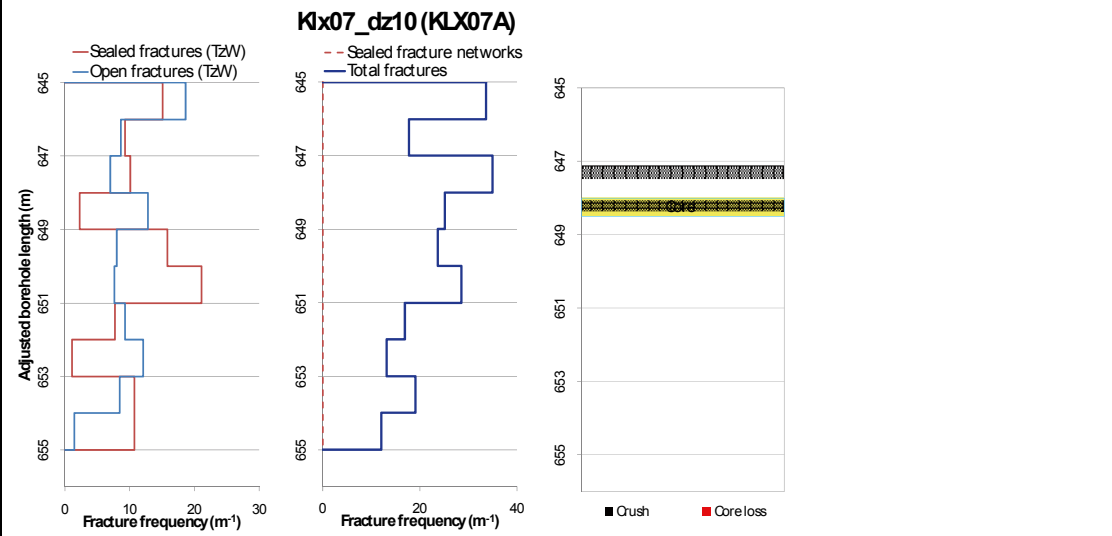
**Measured T (sum T(PFL-f)), elevation -400 to -600m:** 3.12E-6

**Number of PFL-features, elevation -400 to -600m:** 11

**Model T, elevation -400 to -500m:** 2.26E-7

**Model T, elevation -500 to -600m:** 1.37E-7

## Deformation zone KLX07\_dz10



**KLX07A ,942.53-653.39 borehole length. Part of DZ10, including core zone 648.0-648.55 m.**

## Deformation zone KLX07\_dz10

### Engineering characteristics

**Transition part of zone:**

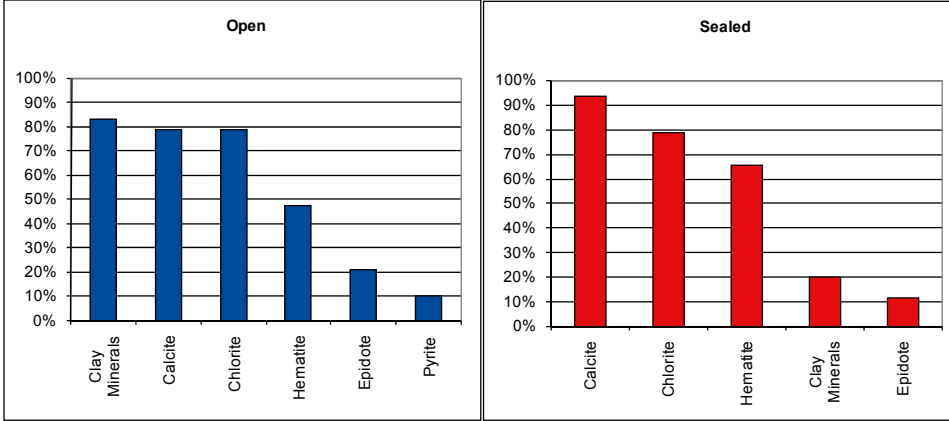
Frequency of open fractures: 9.5 m<sup>-1</sup>

Std dev: no data

Frequency of sealed fractures: 22.2 m<sup>-1</sup>

Std dev: no data

**Mineral coatings**



**Fault core:**

Percentage of fault core: 5 %

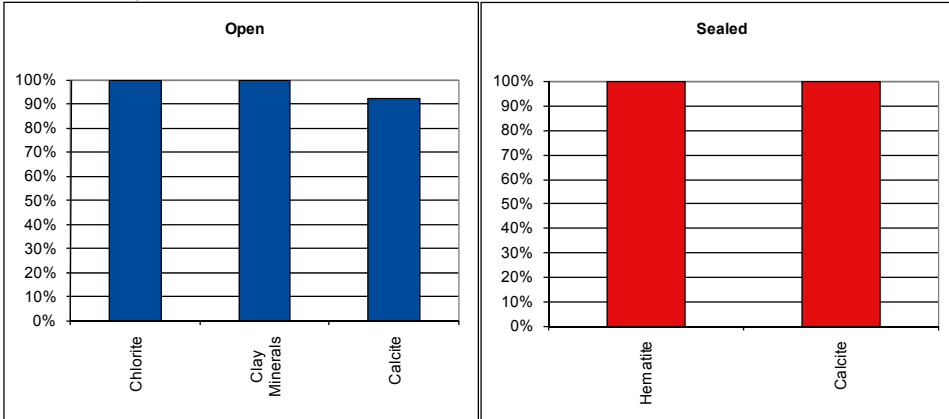
Frequency of open fractures: 26.0 m<sup>-1</sup>

Std dev: no data

Frequency of sealed fractures: 2.0 m<sup>-1</sup>

Std dev: no data

**Mineral coatings**



## Deformation zone KLX08\_dz10

### Borehole intersections (metres along borehole)

KLX08A: 925-940 m (ESHI DZ10 925-940 m)

### Deformation style, alteration and geometry

**Deformation style:** brittle

**Alteration:** red staining, epidotisation, saussuritization

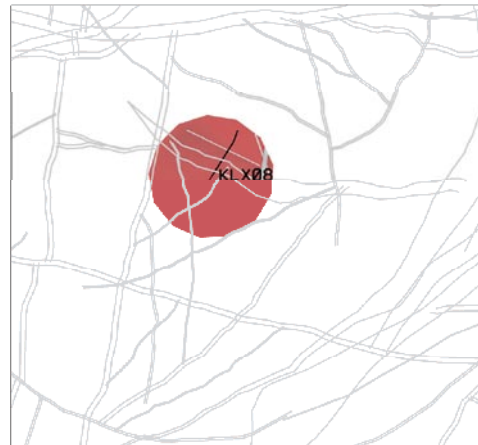
**Strike/dip (right-hand-rule):** 079/11

**Trace length at ground surface:** no data

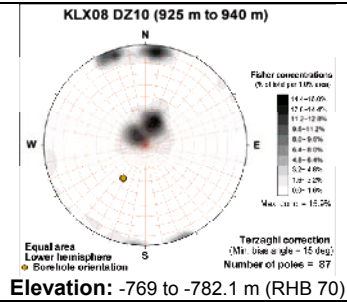
**Model thickness / model thickness span :** 11 m / no data

**Measured thickness (-400 to -600 m elevation):** no data

**Comment:**



## Fractures in the deformation zone



### Transmissivity ( $m^2/s$ )

**General dip of PFL-features, elevation -400 to -600m:** no data

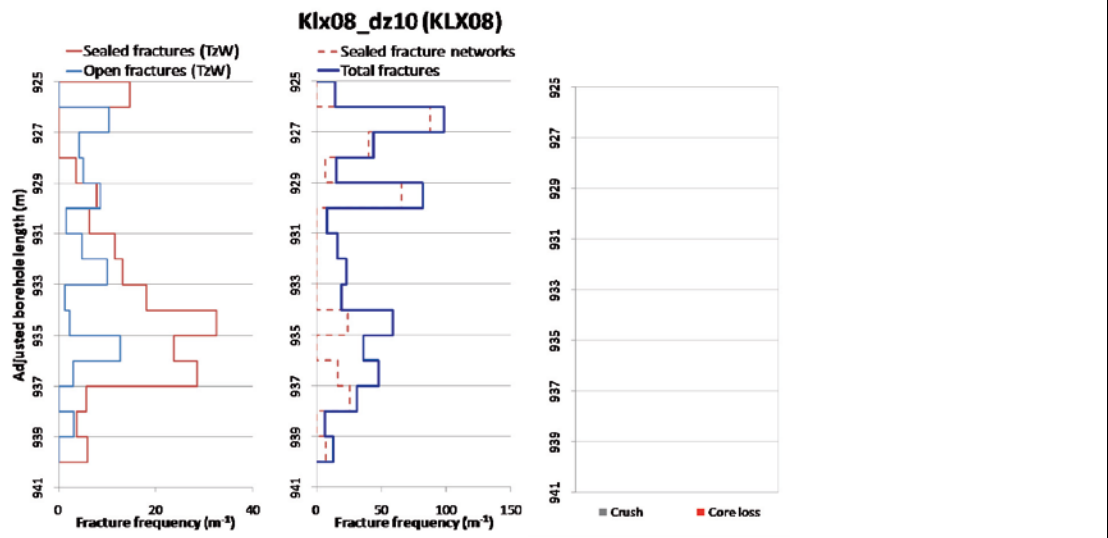
**Measured T (sum T(PFL-f)), elevation -400 to -600m:** no data

**Number of PFL-features, elevation -400 to -600m:** no data

**Model T, elevation -400 to -500m:** 2.26E-7

**Model T, elevation -500 to -600m:** 1.37E-7

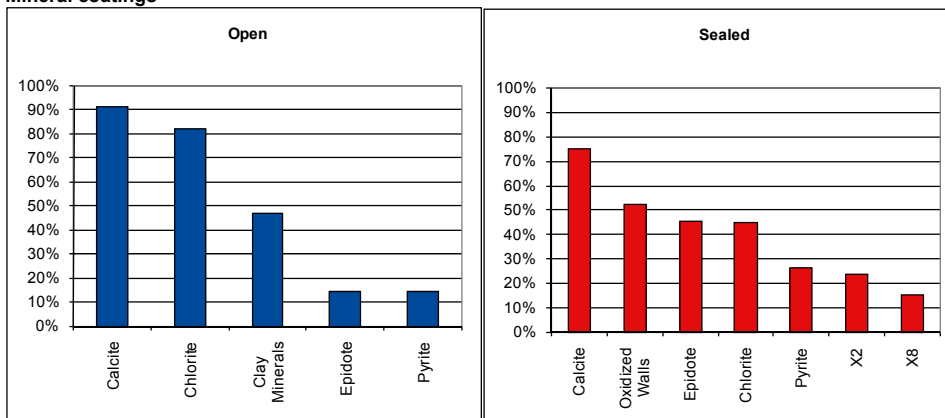
## Deformation zone KLX08\_dz10



KLX08 925.5-931.91 m Borehole length, part of DZ10, no defined core zone.

### Engineering characteristics

Frequency of open fractures: 2.3 m<sup>-1</sup>  
 Std dev: no data  
 Frequency of sealed fractures: 25.6 m<sup>-1</sup>  
 Std dev: no data  
**Mineral coatings**



## Deformation zone KLX11\_dz11

### Borehole intersections (metres along borehole)

KLX11A: 486-513 m (ESHI DZ11 486-513 m)

### Deformation style, alteration and geometry

**Deformation style:** brittle

**Alteration:** red staining, epidotisation

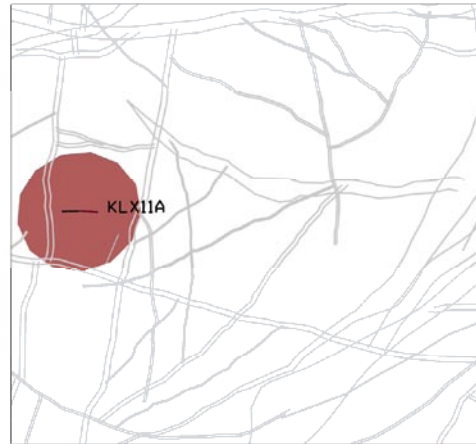
**Strike/dip (right-hand-rule):** 065/20

**Trace length at ground surface:** no data

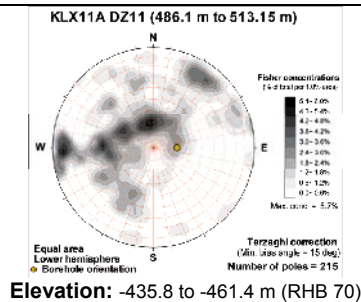
**Model thickness / model thickness span :** 20 m / no data

**Measured thickness (-400 to -600 m elevation):** 20 m

**Comment:** orientation is based on crush and fracture concentration orientations along with kinematic mapping by Viola et al. 2007a. Orientation and elevation makes this zone potentially a western extension of the M1 minor deformation zone series.



## Fractures in the deformation zone



### Transmissivity (m<sup>2</sup>/s)

**General dip of PFL-features, elevation -400 to -600m:** moderately to sub-horizontally

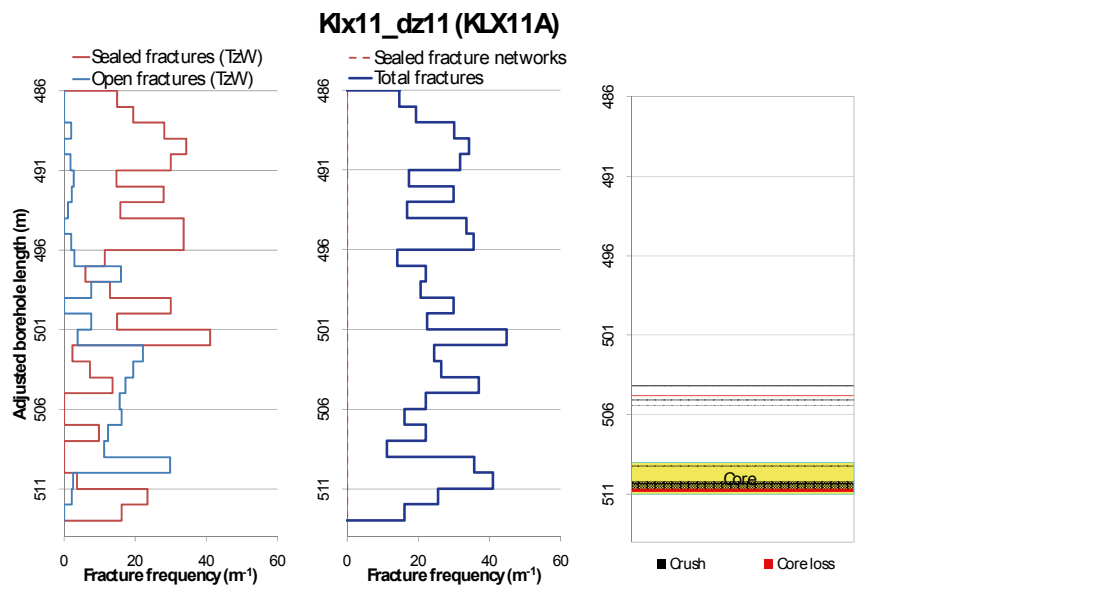
**Measured T (sum T(PFL-f)), elevation -400 to -600m:** 2.11E-8

**Number of PFL-features, elevation -400 to -600m:** 6

**Model T, elevation -400 to -500m:** 2.26E-7

**Model T, elevation -500 to -600m:** 1.37E-7

## Deformation zone KLX11\_dz11



**KLX11A 501.57-511.90 m borehole length. Part of DZ11 including core zone 509.0-511.0 m.**

## Deformation zone KLX11\_dz11

### Engineering characteristics

**Transition part of zone:**

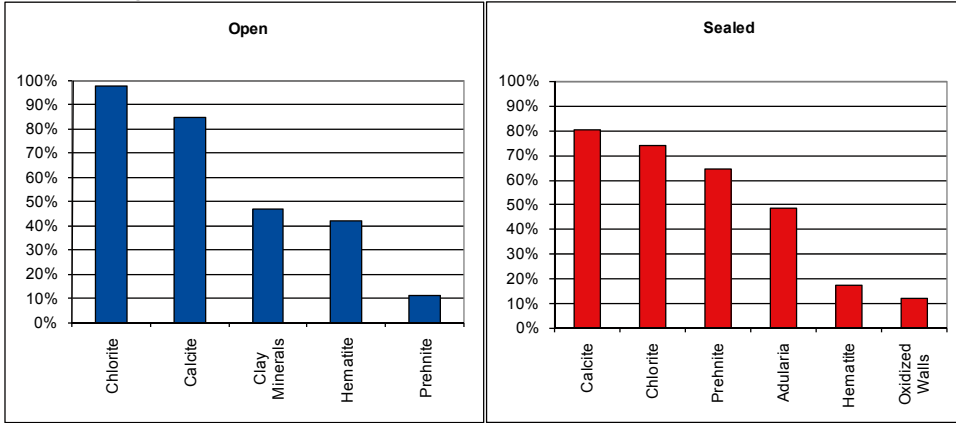
Frequency of open fractures: 6.6 m<sup>-1</sup>

Std dev: no data

Frequency of sealed fractures: 22.1 m<sup>-1</sup>

Std dev: no data

**Mineral coatings**



**Fault core:**

Percentage of fault core: 7 %

Frequency of open fractures: 30.5 m<sup>-1</sup>

Std dev: no data

Frequency of sealed fractures: 44.5 m<sup>-1</sup>

Std dev: no data

**Mineral coatings**

